Oxidative Medicine and Cellular Longevity

# Cellular and Molecular Mechanisms of Oxidative Stress in Nerve Injury

Lead Guest Editor: Wei Zhao
Guest Editors: Zhengyuan Xia, Jingping Wang, and Shi-Yuan Xu

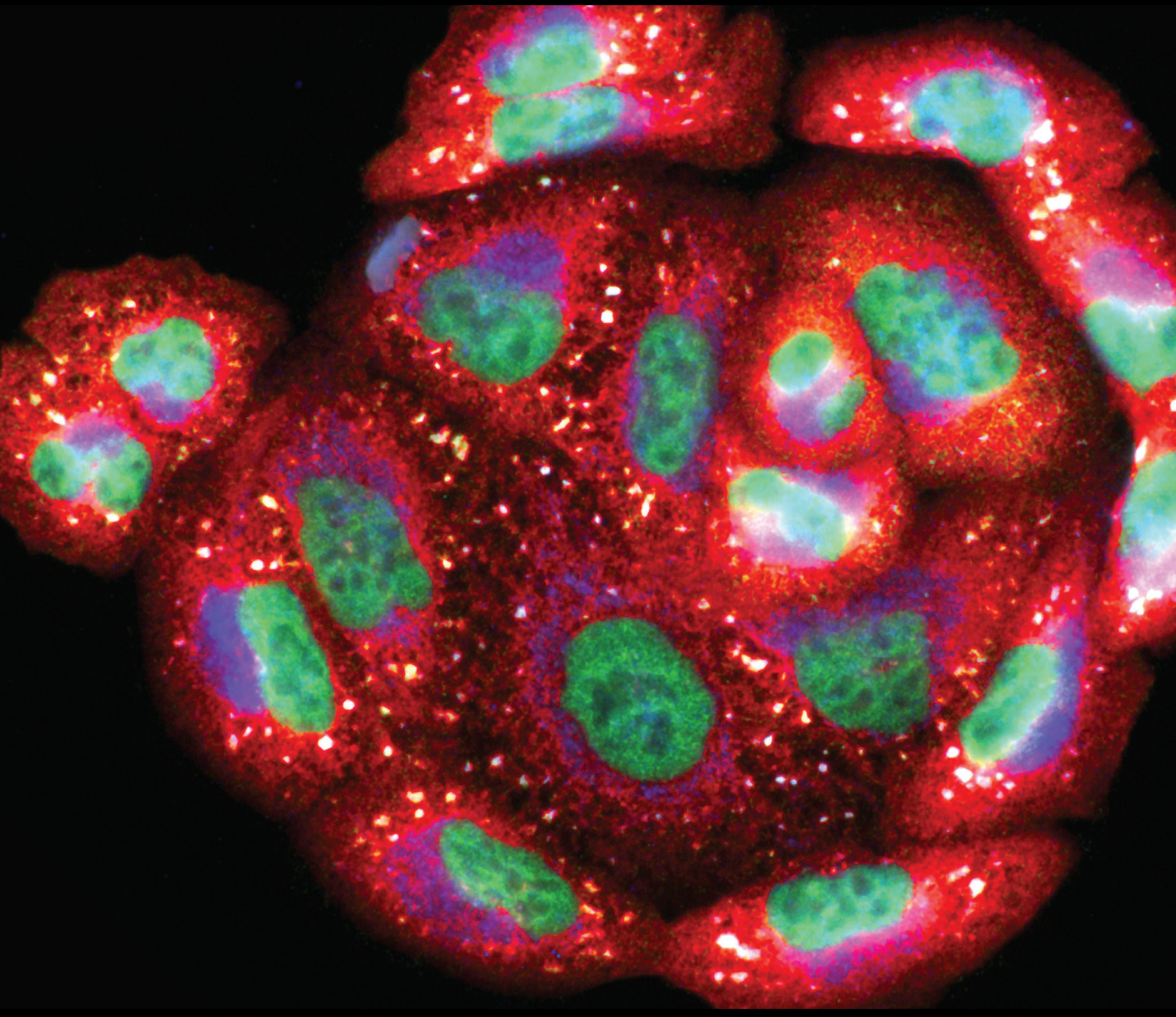

# Cellular and Molecular Mechanisms of Oxidative Stress in Nerve Injury

Oxidative Medicine and Cellular Longevity

# Cellular and Molecular Mechanisms of Oxidative Stress in Nerve Injury

Lead Guest Editor: Wei Zhao
Guest Editors: Zhengyuan Xia, Jingping Wang, and Shi-Yuan Xu

# Contents

**RiPerC Attenuates Cerebral Ischemia Injury through Regulation of miR-98/PIK3IP1/PI3K/AKT Signaling Pathway**
Dengwen Zhang, Li Mei, Ruichun Long, Can Cui, Yi Sun, Sheng Wang, and Zhengyuan Xia
Research Article (12 pages), Article ID 6454281, Volume 2020 (2020)

**Network Pharmacology Analysis and Molecular Characterization of the Herbal Medicine Formulation Qi-Fu-Yin for the Inhibition of the Neuroinflammatory Biomarker iNOS in Microglial BV-2 Cells: Implication for the Treatment of Alzheimer's Disease**
Fung Yin Ngo, Weiwei Wang, Qilei Chen, Jia Zhao, Hubiao Chen, Jin-Ming Gao, and Jianhui Rong
Research Article (15 pages), Article ID 5780703, Volume 2020 (2020)

**Understanding Diabetic Neuropathy: Focus on Oxidative Stress**
Lei Pang, Xin Lian, Huanqiu Liu, Yuan Zhang, Qian Li, Yin Cai, Haichun Ma, and Xin Yu
Review Article (13 pages), Article ID 9524635, Volume 2020 (2020)

Hindawi
Oxidative Medicine and Cellular Longevity
Volume 2021, Article ID 6643382, 13 pages
https://doi.org/10.1155/2021/6643382

*Review Article*

# Crosstalk between Oxidative Stress and Ferroptosis/Oxytosis in Ischemic Stroke: Possible Targets and Molecular Mechanisms

**Jia-Xin Ren,[1,2] Chao Li,[1,2] Xiu-Li Yan,[1,2] Yang Qu,[1,2] Yi Yang,[1,2,3] and Zhen-Ni Guo[1,2,3]**

[1]*Stroke Center & Clinical Trial and Research Center for Stroke, Department of Neurology, The First Hospital of Jilin University, No. 1 Xinmin Street, Changchun 130021, China*
[2]*China National Comprehensive Stroke Center, No. 1 Xinmin Street, Changchun 130021, China*
[3]*Jilin Provincial Key Laboratory of Cerebrovascular Disease, No. 1 Xinmin Street, Changchun 130021, China*

Correspondence should be addressed to Yi Yang; doctoryangyi@163.com and Zhen-Ni Guo; zhen1ni2@163.com

Received 12 November 2020; Accepted 23 April 2021; Published 12 May 2021

Academic Editor: Wei Zhao



Oxidative stress is a key cause of ischemic stroke and an initiator of neuronal dysfunction and death, mainly through the overproduction of peroxides and the depletion of antioxidants. Ferroptosis/oxytosis is a unique, oxidative stress-induced cell death pathway characterized by lipid peroxidation and glutathione depletion. Both oxidative stress and ferroptosis/oxytosis have common molecular pathways. This review summarizes the possible targets and the mechanisms underlying the crosstalk between oxidative stress and ferroptosis/oxytosis in ischemic stroke. This knowledge might help to further understand the pathophysiology of ischemic stroke and open new perspectives for the treatment of ischemic stroke.

## 1. Introduction

Stroke is one of the leading causes of death and disability worldwide [1]. According to the 2020 American Heart Association statistics, approximately 795,000 people experience a new or recurrent stroke each year, with an average of one person having a stroke every 40 seconds in the United States [2]. Ischemic stroke accounts for 87% of all strokes [2]. This type of stroke begins with cerebral artery occlusion, which reduces blood flow to the brain, leading to insufficient blood glucose and oxygen, which causes metabolic changes, cell death, and brain damage [3]. Ischemia-damaged brain tissue can be divided in two areas: the ischemic core and the penumbra [4]. The ischemic core has minimal blood flow, with rapid and severe damage, and neuronal death is transient and necrotic [5]. The penumbra is a hypoperfused area at the periphery of the core that comprises half of the total lesion volume [6]. Neurons in the penumbra are fragile and respond to stress by releasing substances, activating signaling pathways, and undergoing complex dynamic changes [7], which allow the neurons to survive for hours or even days, until they ultimately die [8]. Oxidative stress, caused by an imbalance between oxidants and antioxidants [4], is a major initiator and propagator of neuronal dysfunction and death [9–11] and a key deleterious factor in cerebral ischemia [12]. In ischemic stroke, increased production of reactive oxygen species (ROS) in neuronal cells depletes the antioxidant system, thereby disrupting the balance between ROS production and consumption. An excess of ROS induces lipid peroxidation and oxidation of proteins, DNA, and RNA, which lead to neuronal dysfunction and death [13–15].

Ferroptosis is a type of iron-dependent, oxidative stress-induced cell death that has been shown to play an important role in ischemic stroke [16–20]. Ferroptosis is induced by erastin, RAS-selective lethal 3 (RSL3), and their related compounds, and it has been defined by Dixon et al. using pharmacological methods in 2012 [21, 22]. Different from apoptosis, necrosis, and autophagy in morphological, biochemical, and genetic terms, ferroptosis does not have characteristics such as chromatin condensation, nuclear atrophy, and cellular swelling. The distinctive morphological characteristics of ferroptosis are mitochondrial atrophy and changes in the structure of the mitochondrial cristae [21, 23, 24]. At a molecular level, ferroptosis is characterized by

glutathione (GSH) depletion and lipid peroxidation, particularly oxidation of phosphatidylethanolamine (PE) containing arachidonic and adrenal acids [25]. It is noteworthy that ferroptosis is significantly similar to oxytosis, which is a distinctive oxidative stress-induced programmed cell death pathway [26]. However, after a detailed comparison of the roles of ferroptosis and oxytosis in the central nervous system, Fricker et al. suggested that ferroptosis and oxytosis should be considered for the same cell death pathway [24, 26–29].

The cellular processes and molecular machinery of cell death (and their association) in the brain of patients with ischemic stroke remain unclear [30–32]. However, it is known that, after ischemic stroke, a series of molecular events induced by oxidative stress overlap with the process of ferroptosis/oxytosis and that there are common molecular targets, such as lipid peroxidation and GSH depletion [33–35]. The widely used oxidative stress stimulant tert-butyl hydroperoxide was found to induce neuronal cell death that can be blocked by ferroptosis inhibitors, thus implying a crosstalk between the initial oxidative damage and ferroptosis [36]. Exploring the association between oxidative stress and ferroptosis/oxytosis might help to further understand the pathophysiology of ischemic stroke [27]. This review provides an overview of the key molecules involved in oxidative stress-induced peroxide production and antioxidant depletion after ischemic stroke, describes their role in ferroptosis/oxytosis, and summarizes the molecular mechanisms underlying the crosstalk between oxidative stress and ferroptosis/oxytosis.

## 2. Summary of Classic Pathways

### *2.1. Classic Pathways of Ferroptosis in Ischemic Stroke*

*2.1.1. Free Iron Accumulation.* Ferroptosis is dependent on excessive iron accumulation, which is an important component of lipid oxidation [37]. Under normal central nervous system conditions, iron is primarily bound to ferritin and neuromelanin. Iron is a crucial cofactor in the central nervous system [38], and it is involved in several important processes including oxygen transport, oxidative phosphorylation, myelin production, and neurotransmitter synthesis and metabolism [39]. Through the transferrin-transferrin receptor 1 system, iron is released into the cytoplasm after crossing the blood-brain barrier. The inactive form ($Fe^{3+}$) is recognized by transferrin and moved into the cell by transferrin receptor 1. Subsequently, $Fe^{3+}$ is converted to free iron ($Fe^{2+}$) by 6-transmembrane epithelial antigen of the prostate 3. Free iron is partly transferred by ferritin and can be partly stored in the labile iron pool and is thus involved in lipid ROS production [40, 41]. $Fe^{2+}$ is considered to be a cofactor for several metalloenzymes in oxidative reactions, such as lipoxygenase (LOX) and hypoxia-inducible factor prolyl-hydroxylase [42–44]. In this process, protein-bound iron is safe, whereas abnormal iron homeostasis and excess $Fe^{2+}$ produce excess lipid peroxidation via Fenton reactions [40, 41]. Studies have observed increased total iron content and increased expression of iron and iron regulatory proteins in ischemic areas after permanent or transient ischemic strokes [45, 46]. Deferoxamine and iron chelators prevent free radical production and delay neuronal death [46].

*2.1.2. Lipid Peroxidation.* Lipid peroxidation is the main consequence of ROS-mediated brain injury [4] and the key driving force of ferroptosis [23]. Lipid peroxide production occurs in three steps. First, the acyl-CoA synthetase long-chain family member 4, which exists mainly in the endoplasmic reticulum and the outer mitochondrial membrane, acts as a key regulator to catalyze the formation of arachidonic acid or other polyunsaturated fatty acids (PUFAs) to form PUFA acetyl coenzyme A [47]. Second, PE-PUFA is produced by the action of lysophosphatidylcholine acyltransferase 3. Third, under the action of iron ions, oxygen, and LOX, PE-PUFA is oxidized to PUFA hydroperoxide [25], which is eventually degraded into toxic 4-hydroxynonenal and malondialdehyde [48]. It is hypothesized that there are two main sources of lipid peroxidation: one is the endoplasmic reticulum, where PUFAs form lipid peroxides through the three above-mentioned steps, and the other is the mitochondrial ROS, which is indirectly involved [27, 49].

*2.1.3. GSH Consumption.* Ferroptosis can be triggered by small molecules or conditions that inhibit GSH biosynthesis or the GSH-dependent antioxidant enzyme GSH peroxidase 4 (GPX4). Studies using the ferroptosis inducer erastin have shown that system $X_C^-$ plays an important role in ferroptosis [21]. System $X_C^-$ promotes the synthesis of cysteine-dependent GSH. First, the ferroptosis inducer erastin inhibits systemic $X_C^-$ and competitively inhibits cystine uptake, which leads to depletion of cysteine (a rate-limiting precursor of GSH synthesis). This subsequently leads to GSH depletion, resulting in an imbalance of cellular oxidants and antioxidants, which leads to cell death [50]. GSH depletion is a key feature of ferroptosis [37, 51, 52]. In an animal model of ischemic stroke, peptides containing selenocysteine inhibit ferroptosis by driving GPX4 expression, thus exerting a protective effect on neurons and reducing ischemic core [19, 53].

*2.2. Classic Pathways of Oxidative Stress in Ischemic Stroke.* Oxidative stress refers to the relative excess of ROS caused by excessive production of ROS and/or impaired degradation of ROS, which plays a key role in the pathological mechanism of ischemic stroke. After cerebral ischemia, a significant increase in the number of cellular calcium ions ($Ca^{2+}$) is observed, followed by excessive accumulation of extracellular glutamate and an increased level of arachidonic acid. Further progression follows with increased ROS production and depletion of ROS scavengers, which deactivates the antioxidant system. The balance between ROS production and depletion is disrupted, ultimately leading to excessive ROS accumulation. Excess ROS leads to cellular dysfunction and cell death through lipid peroxidation and oxidation of proteins, DNA, and RNA, resulting in brain tissue damage [13–15]. Lipid peroxidation is one of the major consequences of ROS-mediated brain injury and ultimately leads to the production of conjugated diene hydroperoxides, 4-hydroxynonenal, which are toxic to neurons and white matter and can induce cell death [54]. Excess ROS production in

ischemic stroke through oxidative stress activates the nuclear factor erythroid 2-related factor (Nrf2) [55], which induces the expression of Nrf2-targeted genes. Additionally, activating transcription factor 4 (ATF4) is found to be a progenitor transcription factor induced by oxidative stress in in vivo and in vitro experiments. Increased ATF4 mRNA levels and translation levels after oxidative stress make ATF4 overexpression sufficient to induce cell death [56].

## 3. Molecular Players in Peroxide Production (Table 1)

*3.1. Glutamate.* Glutamate is the most abundant neurotransmitter in the brain and one of the most abundant free amino acids. However, excessively high concentrations of extracellular glutamate are toxic to neurons [26]. Glutamate plays a key role in cerebral ischemia [57], with excessive accumulation of extracellular glutamate being a major factor contributing to neuronal cell death in the penumbra [58–60]. The reasons for an increase in extracellular glutamate include the following: (1) the concentrations of free glutamate and glutamine in the central nervous system are 5-10 mM and 2-4 mM, respectively [61]; (2) glutaminase in nerve cells converts extracellular glutamine into glutamate during cell lysis [62]; and (3) oxidative stress during ischemia shuts down the high-affinity glutamate transporters that usually remove extracellular glutamate [63] in nerve and glial cells.

Cell death pathways activated by glutamate in the nervous system include excitotoxicity and oxidative glutamate toxicity [24]. Excitatory toxicity is initiated by the activation of N-methyl-D-aspartic acid receptors [57, 64], which causes neuronal damage and oxidative stress after ischemia. However, most clinical trials assessing the effectiveness of N-methyl-D-aspartic acid receptor in patients with stroke have reported the ineffectiveness of this receptor [65–67]. In addition to the short time window for the treatment of stroke, another reason for the ineffectiveness of N-methyl-D-aspartic acid receptor inhibitors is that excitotoxicity might not be the single or main mechanism of neuronal death in stroke [24]. Oxidative glutamate toxicity is also thought to play an essential role [68].

Glutamate-induced HT22 hippocampal cell death is an established model system to study ferroptosis/oxytosis and has been widely used to clarify the mechanisms leading to cell death [69]. In glutamate-exposed HT22 hippocampal cells, oxidative glutamate toxicity does not induce nuclear fragmentation and chromatin condensation typical of apoptosis. The most evident damage caused by oxidative glutamate toxicity is mitochondrial swelling and loss of cristae. Similar phenomena have been observed in the developing nervous system [70] and ischemia models [71]. Morphological and biochemical data have revealed that oxidative glutamate toxicity also differs from the classical apoptotic pathway [72–74] in that it appears to depend on oxidative stress and ROS generation. Therefore, in 2001, Tan et al. have named oxidative glutamate toxicity as oxytosis [26].

Oxidative glutamate toxicity inhibits amino acid uptake by inhibiting the cystine/glutamate $X_C^-$ antiporter system (described below in more detail) [75]. When glutamate or other conditions deplete GSH by more than 80% for several hours, cell death might occur. As mentioned above, ferroptosis is consistent with oxytosis [76]. High concentrations of extracellular glutamate inhibit the $X_C^-$ system and induces ferroptosis [18]. The accumulation of extracellular glutamate can be a natural trigger for ferroptosis/oxytosis [51].

*3.2. ROS Generation.* ROS are by-products of oxygen metabolism and include oxygen ions, free radicals, and peroxides. ROS are highly reactive because of the presence of unpaired electrons. During oxidative stress, ROS can accumulate to toxic levels, leading to cell damage and functional impairment [77]. ROS are produced abundantly after ischemic stroke [4], and a biphasic pattern of free radical production by the pyramidal neurons in the hippocampal CA1 region of rats has been reported after transient forebrain ischemia. Biphasic ROS production can be inhibited by antioxidants and iron-chelating neuroprotectants [46]. This biphasic production of ROS has been confirmed in glutamate-exposed HT22 hippocampal cells [28]: within 0-6 hours after the addition of glutamate, the production of ROS increases linearly to approximately 10% of its maximum value; after 6 hours, ROS accumulation increases exponentially to 100-200 times that observed in untreated cells [26].

The mechanism of ROS generation is complex, which involves the interruption of mitochondrial respiratory chain oxidative phosphorylation, anaerobic glycolysis, $Ca^{2+}$ influx, and activation of nitric oxide synthase. There are two main reasons for the production of ROS related to ferroptosis/oxytosis during ischemia: (1) Excessive intracellular ferrous ion ($Fe^{2+}$) levels induce the production of a large number of reactive oxygen free radicals, which further attack and oxidize cell membrane lipids to trigger ferroptosis [47]. This is because the total iron content in the ischemic area increases significantly after an ischemic stroke [45], and the levels of transferrin receptor and transferrin, both of which are involved with iron metabolism, also increase [19, 46, 78–80]. Magnetic resonance imaging revealed increased iron deposition in severely hypoxic-ischemic brain tissue [81]. There are three reasons for the increase in ROS caused by excessive iron levels. First, the Haber-Weiss chemical reaction converts superoxide and hydrogen peroxide into highly reactive and toxic hydroxyl radicals [82]. Second, iron acts as a catalyst in lipid oxidation. Third, iron is an important component of the catalytic subunit of the enzyme LOX, the key target enzyme that catalyzes lipid peroxidation (described below in more detail) [83]. (2) Mitochondria are the center of ROS production and cell death, and free radicals generate superoxide anion radicals during the electron transfer step of oxidative respiration [4]. The most likely source of the late exponential burst of ROS (6 hours after glutamate exposure) is the reverse electron transfer of the flavin mononucleotide group of mitochondrial electron transfer chain complex I [84, 85]. The mitochondrial electron transport uncoupler disperses the mitochondrial membrane potential; blocks the second exponential phase of ROS generation, but not the first [85]; and prevents cell death. The same experiment has confirmed that mitochondrion-triggered ROS production is essential for erastin-induced ferroptosis [86].

Table 1: Summary of molecular targets.

| Molecular targets | | Changes in ischemic stroke | Role in crosstalk between oxidative stress and ferroptosis/oxytosis | Clinical implications | References |
|---|---|---|---|---|---|
| Molecular players in peroxide production | Glutamate | Extracellular glutamate accumulation | A natural trigger which inhibits the cystine/glutamate $X_C^-$ antiporter system and promotes oxidative stress and ROS production | Glutamate-induced HT22 hippocampal cell death is an established model system to study ferroptosis/oxytosis | [18, 24, 26, 51, 57, 69, 75] |
| | $Fe^{2+}$ | Excessive intracellular $Fe^{2+}$ | $Fe^{2+}$ induces the increase of ROS by three ways: the Haber-Weiss chemical reaction, catalyzing lipid peroxidation, and important component of the catalytic subunit of LOX | Iron chelators deferoxamine can prevent ROS production and delay neuronal death | [38, 39, 46, 47, 82, 83, 146] |
| | ROS generation | Excessive ROS generation | The key molecular which leads to the production of lipid peroxidation | The target of antioxidants | [4, 26, 28, 77, 82, 84–86] |
| | $Ca^{2+}$ | Intracellular $Ca^{2+}$ increase | $Ca^{2+}$ is associated with ROS production and lipid peroxidation | Compounds that reduce $Ca^{2+}$ influx can protect cell erastin-induced ferroptosis | [3, 27, 85, 87, 88, 90] |
| | Lipid peroxidation and LOX | Significant increase of lipid peroxidation | Lipid peroxidation is the main consequence of ROS-mediated brain injury and the key driving force of ferroptosis. LOX is a very important enzyme in the production of lipid peroxides | LOX inhibitors block glutamate toxicity and reduce neuronal ferroptosis and infarct size | [17, 23, 92, 93, 96, 97, 99] |
| | ATF4 | ATF4 overexpression | ATF4, as a predecessor transcription factor of oxidative stress in neurons, drives the expression of presumed ferroptotic genes, including Chac1, Trb3, Chop, CARS, and the xCT cystine antiporter | ATF4 knockdown protects adult rats from stroke-induced injury | [53, 56, 120–124] |
| Molecular players in antioxidant depletion | $X_C^-$, GSH, GPX4 | GPX4 and $X_C^-$ inhibition, GSH depletion | Ultimately resulting in lipid peroxide accumulation and ferroptosis | TAT SelPep (a peptide containing selenocysteine) inducing GPX4 expression reduces the size of focal postischemic infarcts | [19, 26, 35, 102, 103, 105–107] |
| | Nrf2 | Nrf2 activation | Nrf2 induces the transcription of proteins and enzymes, which are responsible for preventing lipid peroxidation and ferroptosis | Taraxasterol protects hippocampal neurons from damage due to oxygen glucose deprivation by activating the Nrf2 signaling pathway | [52, 130–132, 135–137, 139] |

*3.3. Intracellular Calcium Ions ($Ca^{2+}$).* The entry of $Ca^{2+}$ into cells is a necessary step for oxidative glutamate toxicity, ultimately leading to cell death. Glutamate induces a large increase in intracellular $Ca^{2+}$ [3, 87]. Experiments have shown that after adding glutamate, intracellular $Ca^{2+}$ increases by 30-50 times, roughly parallel to the increase in ROS, but with a delay of 30-60 minutes. Certainly, $Ca^{2+}$ influx and mitochondrial ROS production are tightly coupled [87]. Ruthenium red, an effective single transporter inhibitor of mitochondrial $Ca^{2+}$ uptake, can prevent late ROS production and cell death. Therefore, mitochondrial $Ca^{2+}$ influx is likely to be essential for maximum ROS production [85]. The mechanism underlying harmful calcium influx caused by oxidative stress during ischemia is mediated by the ORAI calcium release-activated calcium modulator 1 (ORAI1) $Ca^{2+}$ channel and store-operated calcium entry (SOCE) [27, 88]. In the process of glutamate-induced oxidative stress, inositol triphosphate receptors are activated because of GSH depletion or other reasons, thereby depleting endoplasmic reticulum calcium stores and triggering the activation of ORAI1, which in turn activates SOCE to further increase the intracellular $Ca^{2+}$ influx. The above-mentioned mechanism has been proven using inhibitors of corresponding molecules and gene knockout experiments [88]. In addition, $Ca^{2+}$ influx is also blocked by soluble guanylate cyclase inhibitors [74] and stimulated by cyclic guanosine monophosphate (cGMP) [89]. $Ca^{2+}$ entry is likely to occur through cGMP-gated $Ca^{2+}$ channels [26]. Although the role of $Ca^{2+}$ in ferroptosis has not received much attention [90], compounds that reduce $Ca^{2+}$ influx, such as cobalt chloride and apomorphine, can protect erastin- and RSL3-induced ferroptosis [85]. Therefore, although $Ca^{2+}$ cannot directly induce ferroptosis, it is coupled with ROS production and lipid peroxidation and is also affected by GSH depletion.

*3.4. Lipid Peroxidation and LOX.* In humans, the brain is the organ with the highest content of PUFAs; it is also rich in lipid peroxidation precursors [91]. The brain is highly sensitive to hypoxia-ischemia and free radical reactions [36]. Experiments using a rat ischemia model have shown that

occlusion of the common carotid artery for 30 minutes and reperfusion for 1 hour lead to a significant increase in the production of ROS and the final products of lipid peroxidation [92, 93].

LOX is a very important enzyme in the pathophysiological process underlying ischemic stroke and the production of lipid peroxides leading to ferroptosis [94]. LOX binds molecular oxygen to specific positions of PUFAs and is classified as 5-LOX, 12-LOX, or 15-LOX according to the oxygen insertion position. In the central nervous system, 12-LOX predominates and produces 12- and 15-hydroxyeicosatetraenoic acids [95]. Germline deletion of *12/15-LOX* genes can reduce the infarct size after stroke [96, 97]. An increase in 12/15-LOX can be observed in neurons after ischemia [98]. In transient cerebral ischemia models, the inhibition of 12/15-LOX by baicalein can protect nerve cells from ischemia/reperfusion injury [34], and its degree of protection is similar to that of 12/15-LOX knockout mice [99]. Similarly, *LOX* gene depletion can prevent erastin-induced ferroptosis [100]. Experiments have confirmed that PE-binding protein 1 (PEBP1), the backbone protein inhibitor of protein kinases, forms a complex with 15-LOX to produce hydrogen peroxide. Therefore, PEBP1/15-LOX complex can be used as the main regulator of ferroptosis [101]. Similarly, 12/15-LOX plays an important role in oxidative glutamate toxicity and oxidative stress. Experiments with primary cultures of HT22 hippocampal neurons and the cerebral cortex have shown that glutamate activates LOX to produce 12-hydroxyeicosatetraenoic acid, and LOX inhibitors block glutamate toxicity [87]. Six hours after the addition of glutamate, the enzyme activity of 12-LOX increases significantly at the time point when the level of GSH is close to zero. This shows that GSH depletion causes LOX activation to precede the second stage of ROS production, and it is necessary for the exponential accumulation of ROS [26]. Additionally, 12-LOX metabolites can activate soluble guanylate cyclase to further produce cGMP. cGMP activates ORAI1 and SOCE to promote $Ca^{2+}$ influx into cells [27, 74].

## 4. Molecular Players in Antioxidant Depletion (Table 1)

*4.1. $X_C^-$, GSH, and GPX4.* Another important consequence of oxidative stress in cerebral ischemia is the depletion of the antioxidant system, which is manifested primarily by the inhibition of cystine uptake by glutamate resulting in the loss of intracellular GSH [26, 102]. Lipid peroxidation due to GSH depletion is a key feature of ferroptosis [24]. Glutamate acts by inhibiting cystine deprivation at the site of the membrane cysteine/glutamate reverse exchange transporter (the $X_C^-$ system) [47, 75]. $X_C^-$ is a dimer composed of a light-chain subunit (xCT, SLC7A11) and a heavy-chain subunit (CD98hc, SLC3A2) [75]. The main function of the $X_C^-$ system is to mediate the exchange of extracellular cystine and intracellular glutamate across the cellular plasma membrane, and the newly imported cystine is used in the synthesis of GSH [59]. Reduced GSH is an essential intracellular antioxidant that serves as an important defense against oxidative stress [103] and is synthesized from glutamate, cysteine, and glycine in a two-step process via two ATP-dependent cytoplasmic enzymes: glutamate-cysteine ligase and GSH synthetase [104]. GPX4 is the only GSH peroxidase that accepts membrane phospholipid hydroperoxides as oxidation substrates [105–107] to protect biological membranes from peroxidative degradation [108]. Selenium serves as an essential key regulator of GPX4 biosynthesis [109]. In HT22 hippocampal cells, the intracellular GSH level becomes almost zero after 6 hours of glutamate addition [26], and cell death occurs when glutamate or other conditions deplete GSH beyond 80% for several hours. GSH is the cellular metabolite whose levels decrease the most during erastin-induced ferroptosis [35]. Intraperitoneal injection of TAT SelPep (a peptide containing selenocysteine) to induce GPX4 expression reduces the size of focal postischemic infarcts. Additionally, in a mouse model of ischemia, TAT SelPep can drive transcriptional responses resistant to reactive lipogenesis and cell death [19]. In summary, it is hypothesized that in cerebral ischemia, oxidative stress leads to glutamate accumulation, which inhibits the $X_C^-$ system and the import of cysteine [21]. Reduced intracellular cysteine levels lead to GSH depletion, loss of cellular antioxidant capacity, and inhibition of GPX4 [107], ultimately resulting in lipid peroxide accumulation and ferroptosis [110, 111].

## 5. Crosstalk between Oxidative Stress and Ferroptosis/Oxytosis in Ischemic Stroke (Figures 1 and 2)

*5.1. GSH-12/15-LOX-ROS-$Ca^{2+}$-Lipid Peroxidation-Ferroptosis.* In ischemic stroke, oxidative stress leads to excessive glutamate accumulation and an increase in ROS via the Fenton chemical reaction. Glutamate inhibits $X_C^-$, leading to inactivation of GSH-depleted GPX4, which subsequently activates 12/15-LOX. Consequently, the activated 12/15-LOX induces lipid peroxidation. Additionally, LOX activates soluble guanylate cyclase and cGMP, resulting in a large increase in intracellular $Ca^{2+}$ levels mediated through the ORAI1 and SOCE, thereby promoting maximal ROS production. Elevated 12/15-LOX stimulates mitochondrial production, further amplifying the oxidative stress caused by glutamate accumulation and GSH loss [112]. Finally, accumulation of toxic lipid peroxide products leads to ferroptosis [28, 113].

*5.2. GSH-ATF4-Ferroptosis.* ATF4 is a member of the ATF/-CREB family of transcription factors [114]. Both erastin and RSL3 (ferroptosis inducers) activate leucine zipper transcription factor ATF4 proteins in primary neurons [53, 56]. Knockdown of the ATF4 homologous gene was found to protect the adult mouse brain from stroke-induced injury and disability [56]. The brains of $ATF4^{-/-}$ mice are resistant to oxidative stress-induced cell death, and overexpression of ATF4 is sufficient to restore sensitivity to cell death induced by GSH depletion and to induce cell death on its own [115]. After GSH depletion, an increase in the mRNA levels of *ATF4* and an upregulation of translation efficiency in neurons lead to ATF4 overexpression and cell death [56].

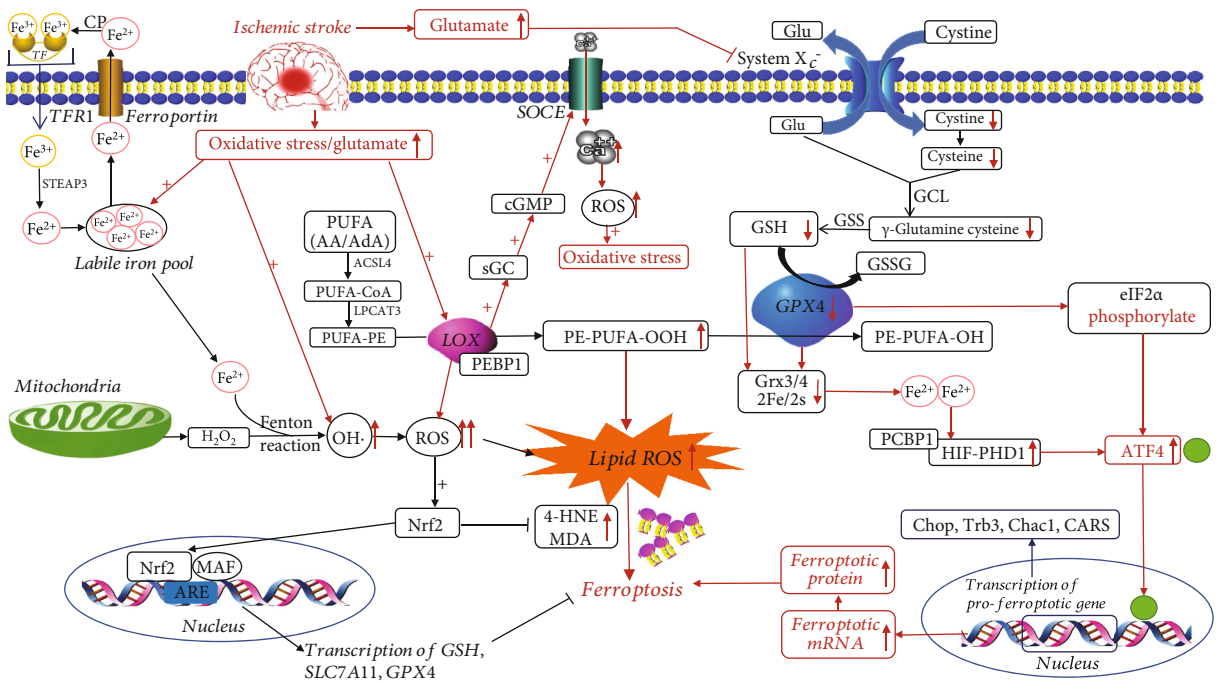


Figure 1: Possible targets and molecular mechanisms of the crosstalk between oxidative stress and ferroptosis/oxytosis in ischemic stroke. Red boxes and spikes indicate potential mechanisms after ischemic stroke, with upward spikes indicating an increase and downward spikes indicating a decrease. *Abbreviations*: AA: arachidonic acid; AdA: adrenic acid; ACSL4: acyl-CoA synthetase long-chain family member 4; ARE: antioxidant response element; CP: ceruloplasmin; GCL: glutamate cysteine ligase; Glu: glutamate; GSS: glutathione synthetase; GSSG: oxidized GSH; HIF-PHD 1: hypoxia-inducible factor prolyl-hydroxylase 1; $H_2O_2$: hydrogen peroxide; 4-HNE: 4-hydroxynonenal; LPCAT3: lysophosphatidylcholine acyltransferase 3; MAF: muscle tendon fibrosarcoma protein; MDA: malondialdehyde; OH·: hydroxyl radical; sGC: soluble guanylate cyclase; STEAP3: six-transmembrane epithelial antigen of the prostate 3.

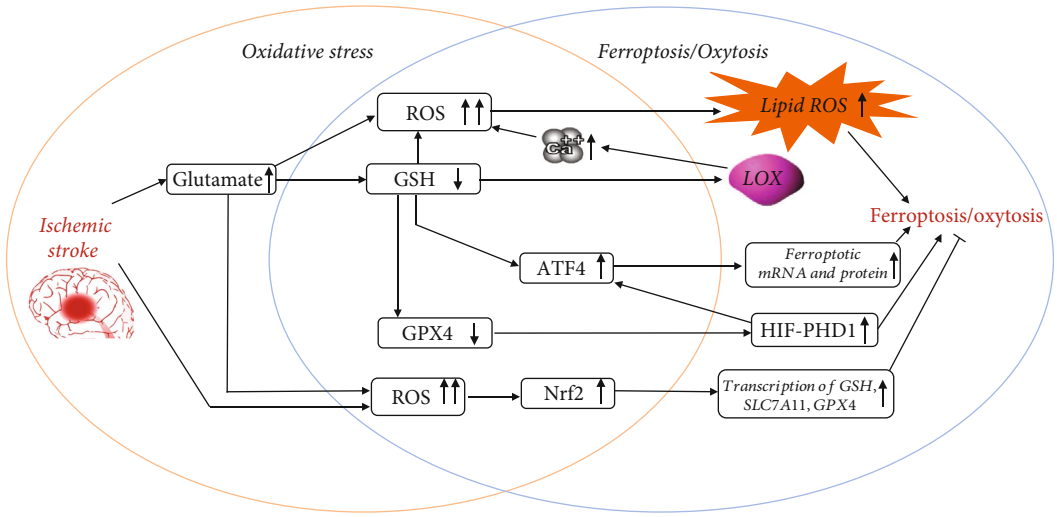


Figure 2: Highlight of the potential crosstalk between ferroptosis and oxidative stress. The orange circle indicates the classical pathways of oxidative stress in the process of ischemic stroke. The blue circle indicates the classical pathways of ferroptosis in the process of ischemic stroke. The intersection of the two circles indicates the potential crosstalk between ferroptosis and oxidative stress.

Therefore, ATF4 is not only a stress-response protein but also a redox-regulated protein that affects the threshold of oxidative stress-induced neuronal death. Further investigation of the ATF4-mediated mechanism of cell death revealed that ATF4 activates $X_C^-$ [116] through the induction of xCT [117]. In glutamate-induced HT22 hippocampal cells, deprivation of eukaryotic translation initiation factor 2 alpha (eIF2$\alpha$) inhibits the activation of eIF2$\alpha$ kinase general control nonderepressible 2 and the formation of eIF2$\alpha$-GTP, greatly reducing the number of ternary translation initiation complexes, which prevents aberrant ATF4 translation. In summary, it is hypothesized that the ATF4-mediated pathway

may be caused by cysteine deprivation, GSH depletion, and GCN2 activation mechanisms in the endoplasmic reticulum [118, 119], which may lead to eIF2$\alpha$ phosphorylation and formation of the ternary translation complex. These changes would promote ATF4 activation and ferroptosis through ATF4-mediated transcriptional stimulation of probable upstream ferroptotic genes [120]. Using a transcriptional repressor (actinomycin D) and a translation inhibitor (cycloheximide), ATF4 has been found to drive the expression of presumed ferroptotic genes, including Chac1 [121], Trb3 [122], Chop [123], CARS [124], and the xCT cystine antiporter [53]. Another mechanism mediated by ATF is the destruction of the Grx3/Grx4-2Fe/2S cluster complex upon GSH depletion. Thereafter, iron may be absorbed by the hypoxia-inducible factor prolyl-hydroxylases and by other enzymes that partner with iron, such as PCB1, and subsequently drive the expression of the ATF4 gene, eventually causing ferroptosis [111].

*5.3. Keap1-Nrf2-GSH.* Nrf2 is a stress-induced transcription factor that is maintained under nonstress conditions primarily by Kelch-like ECH-associated protein 1- (Keap1-) mediated degradation of the proteasome. Following oxidative stress, Keap1 degrades and dissociates from Nrf2, allowing Nrf2 to translocate into the nucleus; heterologously dimerize with proteins such as the small muscle tendon fibrosarcoma protein, which recognizes the appropriate antioxidant response element sequence [125–128]; and initiate transcription [129–131]. Many of the proteins and enzymes responsible for preventing lipid peroxidation and thereby triggering ferroptosis are Nrf2 target genes [130, 132]. *GPX4* and *SLC7A11* are two such Nrf2 target genes: activated Nrf2 protects cells from hydrogen peroxide and ferroptosis by directly upregulating the transcription of *GPX4* and *SLC7A11* [133, 134]. Notably, Nrf2 probably plays an important role in protecting brain cells from ischemic injury. Loss of Nrf2 function increases the extent of cerebral infarction and neurological deficits developing after ischemic events [135, 136]. In a mouse model of transient middle cerebral artery occlusion, Nrf2 expression was found to increase from 2 hours, peaking at 8 hours, and then declining at 24-72 hours [137]. Nrf2 levels were significantly higher in the penumbra than in the core region [138], which may be explained by higher oxidative stress in the former [137]. The Nrf2 activator tert-butylhydroquinone has been shown to enhance Nrf2 signaling activity and protect different brain cells from oxidative stress in vitro [135, 136, 139]. Thus, Nrf2 activation is induced by excessive ROS production after stroke, and Nrf2 protects the brain against ischemia/reperfusion injury primarily by inducing its target antioxidant genes to counteract excessive ROS production [135]. In summary, it is hypothesized that upon ischemic oxidative stress, Keap1 degrades and dissociates from Nrf2, allowing Nrf2 to translocate into the nucleus. Nrf2 heterodimerizes with the muscle tendon fibrosarcoma protein to recognize the appropriate antioxidant response element sequence and initiate transcription of genes such as GPX4, thereby inhibiting ferroptosis. The Keap1-Nrf2-GPX4 signaling pathway plays an important role in mediating lipid peroxidation and ferroptosis [130]. In addition, many of the proteins involved in the Nrf2 signaling pathway are also direct targets of lipid oxidation, and 4-hydroxynonenal has been shown to bind to the negative regulator of Nrf2, Keap1, to activate the expression of Nrf2 target genes [140]. Nrf2 also plays a role in preventing the formation of reactive lipid intermediates.

*5.4. Clinical Studies.* Although there is no complete cellular, animal, or clinical evidence for the possible crosstalk mechanism postulated above, there are studies that confirm the mechanism as a possible target for clinical treatment and encourage further exploration. First, edaravone, a free radical scavenger that has been clinically approved for the treatment of acute ischemic stroke, resists ferroptosis induced by various conditions, particularly under cystine deprivation. Similarly, edaravone inhibits ferroptosis induced in cells by the use of xCT or GPX4 inhibitors. It was confirmed that edaravone inhibits the metabolic features normally observed in ferroptosis, which concludes $Fe^{2+}$ accumulation and increased lipid peroxidation [141]. Second, taraxasterol protects hippocampal neurons from damage due to oxygen glucose deprivation by activating the Nrf2 signaling pathway. Taraxasterol ameliorates the decrease in cell viability of hippocampal neurons induced by oxygen glucose deprivation. Notably, by inducing Nrf2 nuclear accumulation and GPX4 expression, taraxerol significantly inhibits ROS and malondialdehyde production in hippocampal neurons induced by oxyglucose deprivation/reperfusion. Therefore, it can be hypothesized that taraxerol protects hippocampal neurons from oxidative stress and ferroptosis by regulating the Nrf2 signaling pathway in ischemia [52]. Third, the Nrf2 activator octreotide protects the brain from cerebral ischemic injury by activating the Nrf2/ARE pathway [142].

*5.5. Research and Clinical Implications.* There are several implications of the crosstalk between oxidative stress and ferroptosis/oxytosis. First, salvage of the penumbra is an important target for stroke therapy [24]. Although the mechanisms of cell death in the penumbra are diverse and complex [31], the potential targets and molecular mechanisms of ferroptosis/oxytosis summarized herein provide new insights into the exploration of stroke therapeutics. Second, the study of oxidative stress has been plagued by the use of excessive micromolar-to-millimolar concentration peroxide models, which cannot be fully realized in intact cells [143]. Thus, the massive depletion of endogenous antioxidants in ferroptosis/oxytosis models provides new ideas for studying the mechanisms of oxidative stress [111]. Third, it is only in the last decade that ferroptosis has been gradually recognized and explored for its role in neurological diseases [21]. Most studies on ferroptosis have focused on experimental models induced by various chemical inhibitors. More basic experiments, including ferroptosis-related gene knockouts and cellular and animal experiments, are still needed to fully validate and explore these potential targets and molecular mechanisms. The association between oxidative stress and the molecules involved in the development of ferroptosis is still to be explored in greater depth to provide more convincing conclusions with a causal association. In addition, this review

focuses on the analysis of oxidative stress-induced ferroptosis/oxytosis. Moreover, it was also found that the molecules involved in ferroptosis/oxytosis amplify oxidative stress [26, 144]; therefore, whether and how ferroptosis/oxytosis contributes further to oxidative stress need to be further explored.

## 6. Conclusions

Oxidative stress is an established mediator of neuronal loss in cerebral ischemia [145] and an initiator and propagator of neuronal dysfunction and death [9–11], which are key causative factors of cerebral ischemia [12]. Ferroptosis/oxytosis is a unique, oxidative stress-induced cell death pathway that has expanded our understanding of the role of oxidative stress in ischemic stroke [111]. Starting off from the excessive production of peroxides and the depletion of antioxidants in neurons following oxidative stress, we described the triggers of ferroptosis/oxytosis: glutamate and its oxidative toxicity, ROS generation, increased intracellular calcium levels, lipid peroxidation, and GSH depletion. Next, we provided a summary of the interactions between these molecules targets and how they amplify oxidative stress and lead to ferroptosis/oxytosis. Exploring the crosstalk between possible targets and molecular mechanisms shared by oxidative stress and ferroptosis/oxytosis has important theoretical and clinical implications for ischemic stroke pathology. This knowledge might open new perspectives for the treatment of ischemic stroke.

## Abbreviations

| | |
|---|---|
| cGMP: | Cyclic guanosine monophosphate |
| GPX4: | Glutathione peroxidase-4 |
| GSH: | Glutathione |
| 12/15-LOX: | 12/15-Lipoxygenases |
| PEs: | Phosphatidylethanolamines |
| PHDs: | Prolyl-hydroxylases |
| PUFA: | Polyunsaturated fatty acid |
| ROS: | Reactive oxygen species |
| TF: | Transferrin |
| TFR1: | Transferrin receptor 1. |

## Conflicts of Interest

The authors declare that they have no conflicts of interest.

## Authors' Contributions

Jia-Xin Ren and Chao Li contributed equally to this work.

## Acknowledgments

We would like to thank Editage for English language editing. This work was supported by the National Natural Science Foundation of China to Yi Yang (Grant No. 82071291), the Program for Jilin University Science and Technology Innovative Research Team (2017TD-12), and the Jilin Provincial Key Laboratory (20190901005JC) to Yi Yang.

## References

[1] P. Lipton, "Ischemic cell death in brain neurons," *Physiological Reviews*, vol. 79, no. 4, pp. 1431–1568, 1999.

[2] S. S. Virani, A. Alonso, E. J. Benjamin et al., "Heart disease and stroke statistics-2020 update: a report from the American Heart Association," *Circulation*, vol. 141, no. 9, pp. e139–e596, 2020.

[3] D. Radak, I. Resanovic, and E. R. Isenovic, "Link between oxidative stress and acute brain ischemia," *Angiology*, vol. 65, no. 8, pp. 667–676, 2014.

[4] C. L. Allen and U. Bayraktutan, "Oxidative stress and its role in the pathogenesis of ischaemic stroke," *International Journal of Stroke*, vol. 4, no. 6, pp. 461–470, 2009.

[5] M. A. Moskowitz, E. H. Lo, and C. Iadecola, "The science of stroke: mechanisms in search of treatments," *Neuron*, vol. 67, no. 2, pp. 181–198, 2010.

[6] B. R. Broughton, D. C. Reutens, and C. G. Sobey, "Apoptotic mechanisms after cerebral ischemia," *Stroke*, vol. 40, no. 5, pp. e331–e339, 2009.

[7] T. G. Phan, P. M. Wright, R. Markus, D. W. Howells, S. M. Davis, and G. A. Donnan, "Salvaging the ischaemic penumbra: more than just reperfusion?," *Clinical and Experimental Pharmacology & Physiology*, vol. 29, no. 1-2, pp. 1–10, 2002.

[8] T. Back, "Pathophysiology of the ischemic penumbra–revision of a concept," *Cellular and Molecular Neurobiology*, vol. 18, no. 6, pp. 621–638, 1998.

[9] M. F. Beal, "Oxidative metabolism," *Annals of the New York Academy of Sciences*, vol. 924, pp. 164–169, 2000.

[10] M. T. Lin and M. F. Beal, "Mitochondrial dysfunction and oxidative stress in neurodegenerative diseases," *Nature*, vol. 443, no. 7113, pp. 787–795, 2006.

[11] X. Y. Kong, J. Guan, and R. Z. Wang, "Molecular biological roles of oxidative stress in acute brain ischemia," *Zhongguo Yi Xue Ke Xue Yuan Xue Bao*, vol. 38, no. 2, pp. 222–227, 2016.

[12] S. Manzanero, T. Santro, and T. V. Arumugam, "Neuronal oxidative stress in acute ischemic stroke: sources and contribution to cell injury," *Neurochemistry International*, vol. 62, no. 5, pp. 712–718, 2013.

[13] Y. B. Ouyang, C. M. Stary, R. E. White, and R. G. Giffard, "The use of microRNAs to modulate redox and immune response to stroke," *Antioxidants & Redox Signaling*, vol. 22, no. 2, pp. 187–202, 2015.

[14] H. Chen, H. Yoshioka, G. S. Kim et al., "Oxidative stress in ischemic brain damage: mechanisms of cell death and potential molecular targets for neuroprotection," *Antioxidants & Redox Signaling*, vol. 14, no. 8, pp. 1505–1517, 2011.

[15] P. H. Chan, "Reactive oxygen radicals in signaling and damage in the ischemic brain," *Journal of Cerebral Blood Flow and Metabolism*, vol. 21, no. 1, pp. 2–14, 2001.

[16] W. Tonnus and A. Linkermann, "The in vivo evidence for regulated necrosis," *Immunological Reviews*, vol. 277, no. 1, pp. 128–149, 2017.

[17] K. Yigitkanli, A. Pekcec, H. Karatas et al., "Inhibition of 12/15-lipoxygenase as therapeutic strategy to treat stroke," *Annals of Neurology*, vol. 73, no. 1, pp. 129–135, 2013.

[18] R. E. Speer, S. S. Karuppagounder, M. Basso et al., "Hypoxia-inducible factor prolyl hydroxylases as targets for neuroprotection by "antioxidant" metal chelators: from ferroptosis to stroke," *Free Radical Biology & Medicine*, vol. 62, pp. 26–36, 2013.

[19] I. Alim, J. T. Caulfield, Y. Chen et al., "Selenium drives a transcriptional adaptive program to block ferroptosis and treat stroke," *Cell*, vol. 177, no. 5, pp. 1262–1279.e25, 2019.

[20] Q. Li, X. Han, X. Lan et al., "Inhibition of neuronal ferroptosis protects hemorrhagic brain," *JCI Insight*, vol. 2, no. 7, article e90777, 2017.

[21] S. J. Dixon, K. M. Lemberg, M. R. Lamprecht et al., "Ferroptosis: an iron-dependent form of nonapoptotic cell death," *Cell*, vol. 149, no. 5, pp. 1060–1072, 2012.

[22] Y. Xie, W. Hou, X. Song et al., "Ferroptosis: process and function," *Cell Death and Differentiation*, vol. 23, no. 3, pp. 369–379, 2016.

[23] J. X. Ren, X. Sun, X. L. Yan, Z. N. Guo, and Y. Yang, "Ferroptosis in neurological diseases," *Frontiers in Cellular Neuroscience*, vol. 14, p. 218, 2020.

[24] M. Fricker, A. M. Tolkovsky, V. Borutaite, M. Coleman, and G. C. Brown, "Neuronal cell death," *Physiological Reviews*, vol. 98, no. 2, pp. 813–880, 2018.

[25] K. D'herde and D. V. Krysko, "Oxidized PEs trigger death," *Nature Chemical Biology*, vol. 13, no. 1, pp. 4-5, 2017.

[26] S. Tan, D. Schubert, and P. Maher, "Oxytosis: a novel form of programmed cell death," *Current Topics in Medicinal Chemistry*, vol. 1, no. 6, pp. 497–506, 2001.

[27] J. Lewerenz, G. Ates, A. Methner, M. Conrad, and P. Maher, "Oxytosis/ferroptosis-(Re-) emerging roles for oxidative stress-dependent non-apoptotic cell death in diseases of the central nervous system," *Frontiers in Neuroscience*, vol. 12, p. 214, 2018.

[28] P. Maher, K. van Leyen, P. N. Dey, B. Honrath, A. Dolga, and A. Methner, "The role of $Ca^{2+}$ in cell death caused by oxidative glutamate toxicity and ferroptosis," *Cell Calcium*, vol. 70, pp. 47–55, 2018.

[29] D. Schubert and D. Piasecki, "Oxidative glutamate toxicity can be a component of the excitotoxicity cascade," *The Journal of Neuroscience*, vol. 21, no. 19, pp. 7455–7462, 2001.

[30] A. Rami, J. Sims, G. Botez, and J. Winckler, "Spatial resolution of phospholipid scramblase 1 (PLSCR1), caspase-3 activation and DNA-fragmentation in the human hippocampus after cerebral ischemia," *Neurochemistry International*, vol. 43, no. 1, pp. 79–87, 2003.

[31] J. Puyal, V. Ginet, and P. G. Clarke, "Multiple interacting cell death mechanisms in the mediation of excitotoxicity and ischemic brain damage: a challenge for neuroprotection," *Progress in Neurobiology*, vol. 105, pp. 24–48, 2013.

[32] C. Culmsee, V. Junker, W. Kremers, S. Thal, N. Plesnila, and J. Krieglstein, "Combination therapy in ischemic stroke: synergistic neuroprotective effects of memantine and clenbuterol," *Stroke*, vol. 35, no. 5, pp. 1197–1202, 2004.

[33] I. Y. Choi, J. H. Lim, C. Kim, H. Y. Song, C. Ju, and W. K. Kim, "4-Hydroxy-2(E)-nonenal facilitates NMDA-induced neurotoxicity via triggering mitochondrial permeability transition pore opening and mitochondrial calcium overload," *Experimental Neurobiology*, vol. 22, no. 3, pp. 200–207, 2013.

[34] A. Seiler, M. Schneider, H. Förster et al., "Glutathione peroxidase 4 senses and translates oxidative stress into 12/15-lipoxygenase dependent- and AIF-mediated cell death," *Cell Metabolism*, vol. 8, no. 3, pp. 237–248, 2008.

[35] W. S. Yang, R. SriRamaratnam, M. E. Welsch et al., "Regulation of ferroptotic cancer cell death by GPX4," *Cell*, vol. 156, no. 1-2, pp. 317–331, 2014.

[36] N. Degregorio-Rocasolano, O. Martí-Sistac, and T. Gasull, "Deciphering the iron side of stroke: neurodegeneration at the crossroads between iron dyshomeostasis, excitotoxicity, and ferroptosis," *Frontiers in Neuroscience*, vol. 13, p. 85, 2019.

[37] J. Y. Cao and S. J. Dixon, "Mechanisms of ferroptosis," *Cellular and Molecular Life Sciences*, vol. 73, no. 11-12, pp. 2195–2209, 2016.

[38] C. Moreau, J. A. Duce, O. Rascol et al., "Iron as a therapeutic target for Parkinson's disease," *Movement Disorders*, vol. 33, no. 4, pp. 568–574, 2018.

[39] R. J. Ward, F. A. Zucca, J. H. Duyn, R. R. Crichton, and L. Zecca, "The role of iron in brain ageing and neurodegenerative disorders," *Lancet Neurology*, vol. 13, no. 10, pp. 1045–1060, 2014.

[40] Y. Wu, J. Song, Y. Wang, X. Wang, C. Culmsee, and C. Zhu, "The potential role of ferroptosis in neonatal brain injury," *Frontiers in Neuroscience*, vol. 13, p. 115, 2019.

[41] Y. Ke and Z. M. Qian, "Brain iron metabolism: neurobiology and neurochemistry," *Progress in Neurobiology*, vol. 83, no. 3, pp. 149–173, 2007.

[42] N. Yan and J. J. Zhang, "The emerging roles of ferroptosis in vascular cognitive impairment," *Frontiers in Neuroscience*, vol. 13, p. 811, 2019.

[43] V. E. Kagan, G. Mao, F. Qu et al., "Oxidized arachidonic and adrenic PEs navigate cells to ferroptosis," *Nature Chemical Biology*, vol. 13, no. 1, pp. 81–90, 2017.

[44] S. S. Karuppagounder and R. R. Ratan, "Hypoxia-inducible factor prolyl hydroxylase inhibition: robust new target or another big bust for stroke therapeutics?," *Journal of Cerebral Blood Flow and Metabolism*, vol. 32, no. 7, pp. 1347–1361, 2012.

[45] Q. Z. Tuo, P. Lei, K. A. Jackman et al., "Tau-mediated iron export prevents ferroptotic damage after ischemic stroke," *Molecular Psychiatry*, vol. 22, no. 11, pp. 1520–1530, 2017.

[46] U. J. Park, Y. A. Lee, S. M. Won et al., "Blood-derived iron mediates free radical production and neuronal death in the hippocampal CA1 area following transient forebrain ischemia in rat," *Acta Neuropathologica*, vol. 121, no. 4, pp. 459–473, 2011.

[47] K. Hadian and B. R. Stockwell, "SnapShot: Ferroptosis," *Cell*, vol. 181, no. 5, pp. 1188–1188.e1, 2020.

[48] C. Schneider, N. A. Porter, and A. R. Brash, "Routes to 4-hydroxynonenal: fundamental issues in the mechanisms of lipid peroxidation," *The Journal of Biological Chemistry*, vol. 283, no. 23, pp. 15539–15543, 2008.

[49] A. Higdon, A. R. Diers, J. Y. Oh, A. Landar, and V. M. Darley-Usmar, "Cell signalling by reactive lipid species: new concepts and molecular mechanisms," *The Biochemical Journal*, vol. 442, no. 3, pp. 453–464, 2012.

[50] A. Siddiq, I. A. Ayoub, J. C. Chavez et al., "Hypoxia-inducible factor prolyl 4-hydroxylase inhibition:," *The Journal of Biological Chemistry*, vol. 280, no. 50, pp. 41732–41743, 2005.

[51] M. Gao, P. Monian, N. Quadri, R. Ramasamy, and X. Jiang, "Glutaminolysis and transferrin regulate ferroptosis," *Molecular Cell*, vol. 59, no. 2, pp. 298–308, 2015.

[52] L. J. Su, J. H. Zhang, H. Gomez et al., "Reactive oxygen species-induced lipid peroxidation in apoptosis, autophagy, and ferroptosis," *Oxidative Medicine and Cellular Longevity*, vol. 2019, Article ID 5080843, 13 pages, 2019.

[53] S. S. Karuppagounder, I. Alim, S. J. Khim et al., "Therapeutic targeting of oxygen-sensing prolyl hydroxylases abrogates ATF4-dependent neuronal death and improves outcomes after brain hemorrhage in several rodent models," *Science Translational Medicine*, vol. 8, no. 328, p. 328ra29, 2016.

[54] E. McCracken, V. Valeriani, C. Simpson, T. Jover, J. McCulloch, and D. Dewar, "The lipid peroxidation by-product 4-hydroxynonenal is toxic to axons and oligodendrocytes," *Journal of Cerebral Blood Flow and Metabolism*, vol. 20, no. 11, pp. 1529–1536, 2000.

[55] R. Zhang, M. Xu, Y. Wang, F. Xie, G. Zhang, and X. Qin, "Nrf2-a promising therapeutic target for defensing against oxidative stress in stroke," *Molecular Neurobiology*, vol. 54, no. 8, pp. 6006–6017, 2017.

[56] P. S. Lange, J. C. Chavez, J. T. Pinto et al., "ATF4 is an oxidative stress-inducible, prodeath transcription factor in neurons in vitro and in vivo," *The Journal of Experimental Medicine*, vol. 205, no. 5, pp. 1227–1242, 2008.

[57] S. M. Rothman and J. W. Olney, "Glutamate and the pathophysiology of hypoxic–ischemic brain damage," *Annals of Neurology*, vol. 19, no. 2, pp. 105–111, 1986.

[58] C. Iadecola and J. Anrather, "The immunology of stroke: from mechanisms to translation," *Nature Medicine*, vol. 17, no. 7, pp. 796–808, 2011.

[59] G. Y. Xu, D. J. McAdoo, M. G. Hughes, G. Robak, and R. de Castro Jr., "Considerations in the determination by microdialysis of resting extracellular amino acid concentrations and release upon spinal cord injury," *Neuroscience*, vol. 86, no. 3, pp. 1011–1021, 1998.

[60] D. J. McAdoo, G. Y. Xu, G. Robak, and M. G. Hughes, "Changes in amino acid concentrations over time and space around an impact injury and their diffusion through the rat spinal cord," *Experimental Neurology*, vol. 159, no. 2, pp. 538–544, 1999.

[61] K. Matsumoto, E. H. Lo, A. R. Pierce, E. F. Halpern, and R. Newcomb, "Secondary elevation of extracellular neurotransmitter amino acids in the reperfusion phase following focal cerebral ischemia," *Journal of Cerebral Blood Flow and Metabolism*, vol. 16, no. 1, pp. 114–124, 1996.

[62] R. Newcomb, X. Sun, L. Taylor, N. Curthoys, and R. G. Giffard, "Increased Production of Extracellular Glutamate by the Mitochondrial Glutaminase following Neuronal Death," *The Journal of Biological Chemistry*, vol. 272, no. 17, pp. 11276–11282, 1997.

[63] D. Trotti, N. C. Danbolt, and A. Volterra, "Glutamate transporters are oxidant-vulnerable: a molecular link between oxidative and excitotoxic neurodegeneration?," *Trends in Pharmacological Sciences*, vol. 19, no. 8, pp. 328–334, 1998.

[64] S. M. Rothman, "The neurotoxicity of excitatory amino acids is produced by passive chloride influx," *The Journal of Neuroscience*, vol. 5, no. 6, pp. 1483–1489, 1985.

[65] G. F. Morris, R. Bullock, S. B. Marshall et al., "Failure of the competitive N-methyl-D-aspartate antagonist Selfotel (CGS 19755) in the treatment of severe head injury: results of two phase III clinical trials," *Journal of Neurosurgery*, vol. 91, no. 5, pp. 737–743, 1999.

[66] K. R. Lees, K. Asplund, A. Carolei et al., "Glycine antagonist (gavestinel) in neuroprotection (GAIN International) in patients with acute stroke: a randomised controlled trial," *Lancet (North American ed)*, vol. 355, no. 9219, pp. 1949–1954, 2000.

[67] R. L. Sacco, J. T. DeRosa, E. C. Haley, Jr et al., "Glycine antagonist in neuroprotection for patients with acute stroke: GAIN Americas: a randomized controlled trial," *JAMA*, vol. 285, no. 13, pp. 1719–1728, 2001.

[68] T. H. Murphy, M. Miyamoto, A. Sastre, R. L. Schnaar, and J. T. Coyle, "Glutamate toxicity in a neuronal cell line involves inhibition of cystine transport leading to oxidative stress," *Neuron*, vol. 2, no. 6, pp. 1547–1558, 1989.

[69] P. Albrecht, J. Lewerenz, S. Dittmer, R. Noack, P. Maher, and A. Methner, "Mechanisms of oxidative glutamate toxicity: the glutamate/cystine antiporter system xc- as a neuroprotective drug target," *CNS & Neurological Disorders Drug Targets*, vol. 9, no. 3, pp. 373–382, 2010.

[70] P. G. Clarke, "Developmental cell death: morphological diversity and multiple mechanisms," *Anatomy and Embryology*, vol. 181, no. 3, pp. 195–213, 1990.

[71] C. Portera-Cailliau, D. L. Price, and L. J. Martin, "Non-NMDA and NMDA receptor-mediated excitotoxic neuronal deaths in adult brain are morphologically distinct: further evidence for an apoptosis-necrosis continuum," *The Journal of Comparative Neurology*, vol. 378, no. 1, pp. 88–104, 1997.

[72] N. Shibata and M. Kobayashi, "The role for oxidative stress in neurodegenerative diseases," *Brain and Nerve*, vol. 60, no. 2, pp. 157–170, 2008.

[73] S. Tan, M. Wood, and P. Maher, "Oxidative stress induces a form of programmed cell death with characteristics of both apoptosis and necrosis in neuronal cells," *Journal of Neurochemistry*, vol. 71, no. 1, pp. 95–105, 1998.

[74] Y. Li, P. Maher, and D. Schubert, "Requirement for cGMP in nerve cell death caused by glutathione depletion," *The Journal of Cell Biology*, vol. 139, no. 5, pp. 1317–1324, 1997.

[75] H. Sato, M. Tamba, T. Ishii, and S. Bannai, "Cloning and expression of a plasma membrane cystine/glutamate exchange transporter composed of two distinct proteins," *The Journal of Biological Chemistry*, vol. 274, no. 17, pp. 11455–11458, 1999.

[76] C. Descloux, V. Ginet, P. G. Clarke, J. Puyal, and A. C. Truttmann, "Neuronal death after perinatal cerebral hypoxia-ischemia: focus on autophagy-mediated cell death," *International Journal of Developmental Neuroscience*, vol. 45, no. 1, pp. 75–85, 2015.

[77] L. Bergendi, L. Beneš, Z. Ďuračková, and M. Ferenčik, "Chemistry, physiology and pathology of free radicals," *Life Sciences*, vol. 65, no. 18-19, pp. 1865–1874, 1999.

[78] N. DeGregorio-Rocasolano, O. Martí-Sistac, J. Ponce et al., "Iron-loaded transferrin (Tf) is detrimental whereas iron-free Tf confers protection against brain ischemia by modifying blood Tf saturation and subsequent neuronal damage," *Redox Biology*, vol. 15, pp. 143–158, 2018.

[79] X. Guan, X. Li, X. Yang et al., "The neuroprotective effects of carvacrol on ischemia/reperfusion-induced hippocampal neuronal impairment by ferroptosis mitigation," *Life Sciences*, vol. 235, article 116795, 2019.

[80] A. Datta, D. Sarmah, L. Mounica et al., "Cell death pathways in ischemic stroke and targeted pharmacotherapy," *Translational Stroke Research*, vol. 11, no. 6, pp. 1185–1202, 2020.

[81] R. B. Dietrich and W. G. Bradley Jr., "Iron accumulation in the basal ganglia following severe ischemic-anoxic insults in children," *Radiology*, vol. 168, no. 1, pp. 203–206, 1988.

[82] J. P. Kehrer, "The Haber-Weiss reaction and mechanisms of toxicity," *Toxicology*, vol. 149, no. 1, pp. 43–50, 2000.

[83] S. J. Dixon, G. E. Winter, L. S. Musavi et al., "Human haploid cell genetics reveals roles for lipid metabolism genes in non-apoptotic cell death," *ACS Chemical Biology*, vol. 10, no. 7, pp. 1604–1609, 2015.

[84] Y. Liu and D. R. Schubert, "The specificity of neuroprotection by antioxidants," *Journal of Biomedical Science*, vol. 16, no. 1, p. 98, 2009.

[85] S. Tan, Y. Sagara, Y. Liu, P. Maher, and D. Schubert, "The regulation of reactive oxygen species production during programmed cell death," *The Journal of Cell Biology*, vol. 141, no. 6, pp. 1423–1432, 1998.

[86] N. Yagoda, M. von Rechenberg, E. Zaganjor et al., "RAS-RAF-MEK-dependent oxidative cell death involving voltage-dependent anion channels," *Nature*, vol. 447, no. 7146, pp. 864–868, 2007.

[87] Y. Li, P. Maher, and D. Schubert, "A role for 12-lipoxygenase in nerve cell death caused by glutathione depletion," *Neuron*, vol. 19, no. 2, pp. 453–463, 1997.

[88] N. Henke, P. Albrecht, I. Bouchachia et al., "The plasma membrane channel ORAI1 mediates detrimental calcium influx caused by endogenous oxidative stress," *Cell Death & Disease*, vol. 4, no. 1, p. e470, 2013.

[89] K. Ishige, Q. Chen, Y. Sagara, and D. Schubert, "The activation of dopamine D4 receptors inhibits oxidative stress-induced nerve cell death," *The Journal of Neuroscience*, vol. 21, no. 16, pp. 6069–6076, 2001.

[90] A. J. Wolpaw, K. Shimada, R. Skouta et al., "Modulatory profiling identifies mechanisms of small molecule-induced cell death," *Proceedings of the National Academy of Sciences of the United States of America*, vol. 108, no. 39, pp. E771–E780, 2011.

[91] R. P. Bazinet and S. Layé, "Polyunsaturated fatty acids and their metabolites in brain function and disease," *Nature Reviews. Neuroscience*, vol. 15, no. 12, pp. 771–785, 2014.

[92] A. Sakamoto, S. Tsuyoshi Ohnishi, T. Ohnishi, and R. Ogawa, "Relationship between free radical production and lipid peroxidation during ischemia-reperfusion injury in the rat brain," *Brain Research*, vol. 554, no. 1-2, pp. 186–192, 1991.

[93] B. D. Watson, R. Busto, W. J. Goldberg, M. Santiso, S. Yoshida, and M. D. Ginsberg, "Lipid peroxidation in vivo induced by reversible global ischemia in rat brain," *Journal of Neurochemistry*, vol. 42, no. 1, pp. 268–274, 1984.

[94] J. R. Wu, Q. Z. Tuo, and P. Lei, "Ferroptosis, a recent defined form of critical cell death in neurological disorders," *Journal of Molecular Neuroscience*, vol. 66, no. 2, pp. 197–206, 2018.

[95] R. Shintoku, Y. Takigawa, K. Yamada et al., "Lipoxygenase-mediated generation of lipid peroxides enhances ferroptosis induced by erastin and RSL3," *Cancer Science*, vol. 108, no. 11, pp. 2187–2194, 2017.

[96] M. Conrad, V. E. Kagan, H. Bayir et al., "Regulation of lipid peroxidation and ferroptosis in diverse species," *Genes & Development*, vol. 32, no. 9-10, pp. 602–619, 2018.

[97] H. Karatas, J. Eun Jung, E. H. Lo, and K. van Leyen, "Inhibiting 12/15-lipoxygenase to treat acute stroke in permanent and tPA induced thrombolysis models," *Brain Research*, vol. 1678, pp. 123–128, 2018.

[98] Y. Zheng, Y. Liu, H. Karatas, K. Yigitkanli, T. R. Holman, and K. van Leyen, "Contributions of 12/15-Lipoxygenase to bleeding in the brain following ischemic stroke," *Advances in Experimental Medicine and Biology*, vol. 1161, pp. 125–131, 2019.

[99] K. van Leyen, H. Y. Kim, S. R. Lee, G. Jin, K. Arai, and E. H. Lo, "Baicalein and 12/15-lipoxygenase in the ischemic brain," *Stroke*, vol. 37, no. 12, pp. 3014–3018, 2006.

[100] W. S. Yang and B. R. Stockwell, "Ferroptosis: Death by Lipid Peroxidation," *Trends in Cell Biology*, vol. 26, no. 3, pp. 165–176, 2016.

[101] S. E. Wenzel, Y. Y. Tyurina, J. Zhao et al., "PEBP1 wardens ferroptosis by enabling lipoxygenase generation of lipid death signals," *Cell*, vol. 171, no. 3, pp. 628–641.e26, 2017.

[102] S. J. Dixon and B. R. Stockwell, "The role of iron and reactive oxygen species in cell death," *Nature Chemical Biology*, vol. 10, no. 1, pp. 9–17, 2014.

[103] J. B. Schulz, J. Lindenau, J. Seyfried, and J. Dichgans, "Glutathione, oxidative stress and neurodegeneration," *European Journal of Biochemistry*, vol. 267, no. 16, pp. 4904–4911, 2000.

[104] B. R. Stockwell, J. P. Friedmann Angeli, H. Bayir et al., "Ferroptosis: a regulated cell death nexus linking metabolism, redox biology, and disease," *Cell*, vol. 171, no. 2, pp. 273–285, 2017.

[105] A. Roveri, M. Maiorino, C. Nisii, and F. Ursini, "Purification and characterization of phospholipid hydroperoxide glutathione peroxidase from rat testis mitochondrial membranes," *Biochimica et Biophysica Acta*, vol. 1208, no. 2, pp. 211–221, 1994.

[106] K. Schnurr, J. Belkner, F. Ursini, T. Schewe, and H. Kühn, "The Selenoenzyme Phospholipid Hydroperoxide Glutathione Peroxidase Controls the Activity of the 15-Lipoxygenase with Complex Substrates and Preserves the Specificity of the Oxygenation Products (∗)," *The Journal of Biological Chemistry*, vol. 271, no. 9, pp. 4653–4658, 1996.

[107] R. Brigelius-Flohé and M. Maiorino, "Glutathione peroxidases," *Biochimica et Biophysica Acta*, vol. 1830, no. 5, pp. 3289–3303, 2013.

[108] F. Ursini, M. Maiorino, M. Valente, L. Ferri, and C. Gregolin, "Purification from pig liver of a protein which protects liposomes and biomembranes from peroxidative degradation and exhibits glutathione peroxidase activity on phosphatidylcholine hydroperoxides," *Biochimica et Biophysica Acta*, vol. 710, no. 2, pp. 197–211, 1982.

[109] B. R. Cardoso, D. J. Hare, A. I. Bush, and B. R. Roberts, "Glutathione peroxidase 4: a new player in neurodegeneration?," *Molecular Psychiatry*, vol. 22, no. 3, pp. 328–335, 2017.

[110] J. P. Friedmann Angeli, M. Schneider, B. Proneth et al., "Inactivation of the ferroptosis regulator Gpx4 triggers acute renal failure in mice," *Nature Cell Biology*, vol. 16, no. 12, pp. 1180–1191, 2014.

[111] R. R. Ratan, "The chemical biology of ferroptosis in the central nervous system," *Cell Chemical Biology*, vol. 27, no. 5, pp. 479–498, 2020.

[112] S. Pallast, K. Arai, X. Wang, E. H. Lo, and K. van Leyen, "12/15-Lipoxygenase targets neuronal mitochondria under oxidative stress," *Journal of Neurochemistry*, vol. 111, no. 3, pp. 882–889, 2009.

[113] J. Julien, C. Vital, J. Rivel et al., "Primary meningeal B lymphoma presenting as a subacute ascending polyradiculoneuropathy," *Journal of Neurology, Neurosurgery, and Psychiatry*, vol. 54, no. 7, pp. 610–613, 1991.

[114] K. Ameri and A. L. Harris, "Activating transcription factor 4," *The International Journal of Biochemistry & Cell Biology*, vol. 40, no. 1, pp. 14–21, 2008.

[115] J. Lewerenz, H. Sato, P. Albrecht et al., "Mutation of ATF4 mediates resistance of neuronal cell lines against oxidative

stress by inducing xCT expression," *Cell Death and Differentiation*, vol. 19, no. 5, pp. 847–858, 2012.

[116] H. P. Harding, Y. Zhang, H. Zeng et al., "An integrated stress response regulates amino acid metabolism and resistance to oxidative stress," *Molecular Cell*, vol. 11, no. 3, pp. 619–633, 2003.

[117] J. Lewerenz and P. Maher, "Basal levels of eIF2$\alpha$ phosphorylation determine cellular antioxidant status by regulating ATF4 and xCT expression," *The Journal of Biological Chemistry*, vol. 284, no. 2, pp. 1106–1115, 2009.

[118] K. M. Mazor and M. H. Stipanuk, "GCN2- and eIF2$\alpha$-phosphorylation-independent, but ATF4-dependent, induction of CARE-containing genes in methionine-deficient cells," *Amino Acids*, vol. 48, no. 12, pp. 2831–2842, 2016.

[119] D. Wanders, K. P. Stone, L. A. Forney et al., "Role of GCN2-independent signaling through a noncanonical PERK/NRF2 pathway in the physiological responses to dietary methionine restriction," *Diabetes*, vol. 65, no. 6, pp. 1499–1510, 2016.

[120] S. S. Pathak, D. Liu, T. Li et al., "The eIF2$\alpha$ Kinase GCN2 Modulates Period and Rhythmicity of the Circadian Clock by Translational Control of *Atf4*," *Neuron*, vol. 104, no. 4, pp. 724–735.e6, 2019.

[121] M. S. Chen, S. F. Wang, C. Y. Hsu et al., "CHAC1 degradation of glutathione enhances cystine-starvation-induced necroptosis and ferroptosis in human triple negative breast cancer cells via the GCN2-eIF2$\alpha$-ATF4 pathway," *Oncotarget*, vol. 8, no. 70, pp. 114588–114602, 2017.

[122] N. Ohoka, S. Yoshii, T. Hattori, K. Onozaki, and H. Hayashi, "TRB3, a novel ER stress-inducible gene, is induced via ATF4-CHOP pathway and is involved in cell death," *The EMBO Journal*, vol. 24, no. 6, pp. 1243–1255, 2005.

[123] M. Matsumoto, M. Minami, K. Takeda, Y. Sakao, and S. Akira, "Ectopic expression of CHOP (GADD153) induces apoptosis in M1 myeloblastic leukemia cells," *FEBS Letters*, vol. 395, no. 2-3, pp. 143–147, 1996.

[124] M. Hayano, W. S. Yang, C. K. Corn, N. C. Pagano, and B. R. Stockwell, "Loss of cysteinyl-tRNA synthetase (CARS) induces the transsulfuration pathway and inhibits ferroptosis induced by cystine deprivation," *Cell Death and Differentiation*, vol. 23, no. 2, pp. 270–278, 2016.

[125] S. K. Niture, R. Khatri, and A. K. Jaiswal, "Regulation of Nrf2–an update," *Free Radical Biology & Medicine*, vol. 66, pp. 36–44, 2014.

[126] B. Chen, Y. Lu, Y. Chen, and J. Cheng, "The role of Nrf2 in oxidative stress-induced endothelial injuries," *The Journal of Endocrinology*, vol. 225, no. 3, pp. R83–R99, 2015.

[127] K. Itoh, T. Chiba, S. Takahashi et al., "An Nrf2/small Maf heterodimer mediates the induction of phase II detoxifying enzyme genes through antioxidant response elements," *Biochemical and Biophysical Research Communications*, vol. 236, no. 2, pp. 313–322, 1997.

[128] Y. Hirotsu, F. Katsuoka, R. Funayama et al., "Nrf2-MafG heterodimers contribute globally to antioxidant and metabolic networks," *Nucleic Acids Research*, vol. 40, no. 20, pp. 10228–10239, 2012.

[129] X. Sun, Z. Ou, R. Chen et al., "Activation of the p62-Keap1-NRF2 pathway protects against ferroptosis in hepatocellular carcinoma cells," *Hepatology*, vol. 63, no. 1, pp. 173–184, 2016.

[130] M. Dodson, R. Castro-Portuguez, and D. Zhang, "NRF2 plays a critical role in mitigating lipid peroxidation and ferroptosis," *Redox Biology*, vol. 23, article 101107, 2019.

[131] N. Kajarabille and G. O. Latunde-Dada, "Programmed cell-death by ferroptosis: antioxidants as mitigators," *International Journal of Molecular Sciences*, vol. 20, no. 19, p. 4968, 2019.

[132] M. Dodson, M. R. de la Vega, A. B. Cholanians, C. J. Schmidlin, E. Chapman, and D. D. Zhang, "Modulating NRF2 in disease: timing is everything," *Annual Review of Pharmacology and Toxicology*, vol. 59, no. 1, pp. 555–575, 2019.

[133] M. K. Kwak, K. Itoh, M. Yamamoto, and T. W. Kensler, "Enhanced expression of the transcription factor Nrf2 by cancer chemopreventive agents: role of antioxidant response element-like sequences in the nrf2 promoter," *Molecular and Cellular Biology*, vol. 22, no. 9, pp. 2883–2892, 2002.

[134] W. O. Osburn, N. Wakabayashi, V. Misra et al., "Nrf2 regulates an adaptive response protecting against oxidative damage following diquat-mediated formation of superoxide anion," *Archives of Biochemistry and Biophysics*, vol. 454, no. 1, pp. 7–15, 2006.

[135] Z. A. Shah, R. C. Li, R. K. Thimmulappa et al., "Role of reactive oxygen species in modulation of Nrf2 following ischemic reperfusion injury," *Neuroscience*, vol. 147, no. 1, pp. 53–59, 2007.

[136] A. Y. Shih, P. Li, and T. H. Murphy, "A small-molecule-inducible Nrf2-mediated antioxidant response provides effective prophylaxis against cerebral ischemia in vivo," *The Journal of Neuroscience*, vol. 25, no. 44, pp. 10321–10335, 2005.

[137] N. Tanaka, Y. Ikeda, Y. Ohta et al., "Expression of Keap1-Nrf2 system and antioxidative proteins in mouse brain after transient middle cerebral artery occlusion," *Brain Research*, vol. 1370, pp. 246–253, 2011.

[138] S. Srivastava, A. Alfieri, R. C. Siow, G. E. Mann, and P. A. Fraser, "Temporal and spatial distribution of Nrf2 in rat brain following stroke: quantification of nuclear to cytoplasmic Nrf2 content using a novel immunohistochemical technique," *The Journal of Physiology*, vol. 591, no. 14, pp. 3525–3538, 2013.

[139] J. Sun, X. Ren, and J. W. Simpkins, "Sequential upregulation of superoxide dismutase 2 and heme oxygenase 1 by tert-butylhydroquinone protects mitochondria during oxidative stress," *Molecular Pharmacology*, vol. 88, no. 3, pp. 437–449, 2015.

[140] A. L. Levonen, A. Landar, A. Ramachandran et al., "Cellular mechanisms of redox cell signalling: role of cysteine modification in controlling antioxidant defences in response to electrophilic lipid oxidation products," *The Biochemical Journal*, vol. 378, no. 2, pp. 373–382, 2004.

[141] T. Homma, S. Kobayashi, H. Sato, and J. Fujii, "Edaravone, a free radical scavenger, protects against ferroptotic cell death in vitro," *Experimental Cell Research*, vol. 384, no. 1, article ???, 2019.

[142] L. Chen, L. Wang, X. Zhang et al., "The protection by Octreotide against experimental ischemic stroke: Up- regulated transcription factor Nrf2, HO-1 and down-regulated NF-$\kappa$B expression," *Brain Research*, vol. 1475, pp. 80–87, 2012.

[143] R. E. Haskew-Layton, J. B. Payappilly, N. A. Smirnova et al., "Controlled enzymatic production of astrocytic hydrogen peroxide protects neurons from oxidative stress via an Nrf2-independent pathway," *Proceedings of the National Academy of Sciences of the United States of America*, vol. 107, no. 40, pp. 17385–17390, 2010.

[144] L. Fan, "Mapping the human brain: what is the next frontier?," *The Innovation*, vol. 2, no. 1, p. 100073, 2021.

[145] T. Hayashi, A. Saito, S. Okuno, M. Ferrand-Drake, R. L. Dodd, and P. H. Chan, "Damage to the endoplasmic reticulum and activation of apoptotic machinery by oxidative stress in ischemic neurons," *Journal of Cerebral Blood Flow and Metabolism*, vol. 25, no. 1, pp. 41–53, 2005.

[146] M. Zille, S. S. Karuppagounder, Y. Chen et al., "Neuronal death after hemorrhagic stroke in vitro and in vivo shares features of ferroptosis and necroptosis," *Stroke*, vol. 48, no. 4, pp. 1033–1043, 2017.

Hindawi
Oxidative Medicine and Cellular Longevity
Volume 2021, Article ID 6657944, 12 pages
https://doi.org/10.1155/2021/6657944

*Review Article*

# Studies on the Regulatory Roles and Related Mechanisms of lncRNAs in the Nervous System

**Zijian Zhou**,[1] **Dake Qi**,[2] **Quan Gan**,[1] **Fang Wang**,[3] **Bengang Qin**,[4] **Jiachun Li**,[1] **Honggang Wang**,[4] **and Dong Wang**[1]

[1]*The Seventh Affiliated Hospital of Sun Yat-sen University, Shenzhen, Guangdong, China*
[2]*Memorial University of Newfoundland School of Medicine, Newfoundland and Labrador, Canada*
[3]*Union Hospital of Huazhong University of Science and Technology Shenzhen Hospital, Shenzhen, Guangdong, China*
[4]*The First Affiliated Hospital of Sun Yat-sen University, Guangzhou, Guangdong, China*

Correspondence should be addressed to Honggang Wang; docwhg@sohu.com and Dong Wang; david74429@126.com

Received 20 October 2020; Revised 19 December 2020; Accepted 15 February 2021; Published 15 March 2021

Academic Editor: Wei Zhao



Long noncoding RNAs (lncRNAs) have attracted extensive attention due to their regulatory role in various cellular processes. Emerging studies have indicated that lncRNAs are expressed to varying degrees after the growth and development of the nervous system as well as injury and degeneration, thus affecting various physiological processes of the nervous system. In this review, we have compiled various reported lncRNAs related to the growth and development of central and peripheral nerves and pathophysiology (including advanced nerve centers, spinal cord, and peripheral nervous system) and explained how these lncRNAs play regulatory roles through their interactions with target-coding genes. We believe that a full understanding of the regulatory function of lncRNAs in the nervous system will contribute to understand the molecular mechanism of changes after nerve injury and will contribute to discover new diagnostic markers and therapeutic targets for nerve injury diseases.

## 1. Main Text

Long noncoding RNAs (lncRNAs) are noncoding RNAs (ncRNAs) with a lack of significant open reading frames (ORFs) and length more than 200 nt. lncRNAs not only play a role in the growth and development of nervous system but also play a significant role in the process of nervous system injury and subsequent repair. lncRNAs affect the growth and development of the nervous system in time order and space by regulating the expression of some significant coding genes and also participate in the functional execution of the nervous system. At the same time, the expression of lncRNAs is closely related to the process of nervous system regeneration. Studies have indicated that lncRNAs are involved in the growth, development, and repair of the central and peripheral nervous systems. As a result, in-depth study of lncRNA function and mechanism of action in the nervous system will greatly enhance our understanding of nervous system development, function, and the mechanism of disease occurrence and also provide new ideas for the treatment of some diseases. This review will describe in detail the relevant research progress on the role of lncRNAs in the nervous system.

## 2. Types and Basic Functions of lncRNAs

As human genome sequence has been leaked in 2001, although there are about 90% in eukaryotic genomes transcribed, only about 1% to 2% of the genes are encoding proteins. This indicates that a large number of RNA molecules are ncRNAs [1]. The rest of the noncoding part has been considered useless transcriptional noise in the past. However, in recent decades with the development of high-throughput technology as well as the human genome sequencing, various non-protein-coding DNAs and noncoding RNAs were rediscovered. Okazaki et al. first described the existence of lncRNAs on the length of the mouse cDNA library in the process of the large-scale sequencing [2]. Subsequent

researches have shown lncRNA morphological diversity, including the length of the long chain which is more than 10 KB lncRNAs and shows cricoid circRNAs. lncRNAs exist in a variety of species, including animal plant yeast prokaryotes, even virus. However, lncRNAs between species are less conservative and usually have low expression [3]. Lots of evidence show that lncRNAs play a vital role in various significant biological processes [4]. Therefore, the functional and biological characteristics of lncRNAs make it an interesting and significant research subject.

*2.1. Types of lncRNAs.* With the progress of transcriptome gene sequencing, the gene sequences and mechanism of action of various lncRNAs are constantly revealed, and there are also many classification methods for lncRNAs from different perspectives. For example, lncRNAs are classified according to their positions relative to protein-coding genes, according to their positions in specific DNA regulatory elements and loci, and according to their subcellular location or origin [5]. In this review, we mainly introduce in detail the classification based on the association of lncRNAs with specific biological processes.

*2.1.1. Hypoxic Induction-Related lncRNAs.* Studies have indicated that a large number of lncRNAs are involved in cell damage resistance and ischemia/hypoxia/reperfusion injury [6]. For example, in the hypoxia environment, the expression of lncRNA-H19, the gene product of H19, is upregulated in response to the increased activity of hypoxia induction factor (HIF), which promotes the production of oxygen free radicals and further damages cells [4, 7], while lncRNA-ROR alleviates hypoxia-triggered damage by downregulating miRNA-145 in H9c2 cells [8].

*2.1.2. Senescence-Related lncRNAs.* In the process of cellular senescence regulation, a large number of lncRNAs are expressed, which play a role in both promoting senescence and delaying senescence [9]. lncRNA HOTAIR upregulates autophagy to promote apoptosis and senescence of nucleus pulposus cells [10]. lncRNAs RP11-670E13.6 interact with hnRNPH and delay cell senescence by sponging microRNA-663a [11].

*2.1.3. Stress-Induced Related lncRNAs.* Cells in the oxidative stress state will reduce the number of normal mRNA transcription, but out of a large number of transcription lncRNAs and si-lncRNAs and abundant accumulation in the cells to adapt to the stress state of cellular [12]. FILNC1 (FoxO-induced long noncoding RNA1) in renal cancer cells is an lncRNA induced by energy stress of FoxO transcription factor, and its deletion reduces the apoptosis induced by energy stress, significantly promoting the development of renal tumor [13].

*2.1.4. Nonannotated Stem Cells Transcribe lncRNAs.* lncRNAs play a significant role in pluripotent state maintenance, especially in transcripts derived from nuclear transcription and reverse transcription transposons. L1s and solitary long terminal repeat- (LTR-) derived transcription constitutes the complexity of the stem cell nuclear transcriptome [14]. Some LTR-derived transcripts are associated with enhancers and may be involved in pluripotent maintenance [15]. Studies indicated that deep sequencing transcriptome analysis of mammalian stem cells has determined that unannotated stem cell transcripts (NAST) are significant for maintaining the pluripotency of stem cells [15].

*2.1.5. Disease-Specific Transcripts.* With the development of clinical and diagnostic studies, more and more disease-specific lncRNAs have been detected, and the disease-related specificity of these lncRNAs is used to observe the development status and prognosis of diseases. For example, prostate cancer-related transcription (PCAT) PCAT1 has been proved to play a significant role in the biological function of prostate cancer [16].

*2.2. The Basic Functions of lncRNAs.* lncRNAs influence the transcriptional splicing, translation output, import, and stability of mRNA. Previous studies have indicated that lncRNAs play a recruitment role of transcription factors, act as transcriptional coactivators, or serve as protein scaffoldings through their interactions with transcription initiation sites [17].

lncRNAs may also act as bait to trap transcription factors, thus limiting their binding ability to DNA binding sites [18].

lncRNAs have been indicated to participate in the formation and function of chromatin-circulating nucleosomes [19].

lncRNAs also regulate mRNA processing maturity and stability by regulating mRNA splicing, inhibiting translation, or inhibiting miRNA binding sites on mRNAs by sponge action [18]. According to the definition of lncRNA, we consider circRNA as a kind of lncRNA with special structure. circRNAs are formed by reverse splicing of upstream $3'$ end and downstream $5'$ end, which is highly stable in cells and resistant to exogenous degradation [20]. They bind to a large number of miRNA binding sites through endogenous competition, inhibit the activity of corresponding miRNA, and elevate the expression of its downstream molecules [21]. It is highly consistent with the mechanism of lncRNA acting on miRNA.

Some lncRNAs also encode small peptides. These lncRNAs are used as bifunctional transcripts, that is, as lncRNAs or as protein translation templates [22, 23].

lncRNAs regulate protein and transcript transport and shuttling. The result of this process is that lncRNAs are associated with many biological processes, including cell cycle regulation of pluripotent retrotransposon silencing and telomere elongation in stem cells [24].

## 3. The Regulatory Role of lncRNAs in the Growth, Development, and Various Diseases of the Advanced Central Nervous System

lncRNAs' role in central nervous cell life has gained wide attention and research; many results showed that lncRNAs could regulate various cell pathways involved in the differentiation, development, and pathology of central nerve cells (including hypoxia ischemia change tumor regression). Different from the peripheral nerve injury, the central nerve

is difficult to regenerate and be repaired after injury; thus, related lncRNAs also received special attention in the process of repairment and regeneration of the central nerve after injury.

*3.1. The Regulatory Role of lncRNAs in the Growth and Development of the Advanced Central Nervous System.* In recent years, the mechanisms of lncRNAs in neural development have been gradually revealed; many studies have confirmed the involvement of lncRNAs in the differentiation of neural stem cells or the development of central nerve cells. For example, Pnky is an 825 nt lncRNA. It is expressed in vitro and in vivo in neural stem cells (NSCs) and transregulate the development of the neocortex [25]. PTPB is a splicing factor that plays a key role in normal development and brain tumor. During the differentiation of neurons, the expression of PTBP1 reduced and the expression of PTBP2 increased [26]. Pnky interacts with PTBP1 and regulates the neurogenesis of embryonic and postnatal brain neural stem cells, and there is no evidence for specific interactions between Pnky and PTPB2 or other nuclear RNA binding proteins such as HNRNPK and ELAVL1 [27].

Researches have indicated that lncRNA-Evf2 is the key to promote the differentiation of the GABAergic cells. Evf2 recruits transcription factors DLX and MECP2 into key DNA regulatory elements in the intergenomic region of DLX 5/6, regulating the expression of Dlx5, Dlx6, and GAD67 [28]. Studies have indicated that the expression level of GAD67 protein in mice with Evf2 dysfunction is reduced and the number of GABA-mediated neurons in the early hippocampus and dentate gyrus decreases after birth [29]. Levels of GABA intermediate neurons and GAD67 RNA in the hippocampus of Evf2 returned to normal in adults, but failed to improve symptoms of reduced synaptic inhibition [30].

In addition to participating in the growth and differentiation of various neurons in the brain, lncRNAs are also significant for the formation and function of nerve cells in various receptors, including various nerve cells such as optic nerve and olfaction nerve. lncRNA Tug1 regulates the growth and development of retinal photoreceptor cells and regulates retinal pigment cells [31]. Tug1 deletion may result in loss or malformation of the extracellular segment of the photoreceptor [32]. lncRNA Six3OS is expressed together with the homologous domain factor Six3, which plays a key role in the development of mammalian eyes and regulates the cells of the retina at the early stage of eye formation [33]. However, Six3OS does not regulate the expression level of Six3; instead, Six3OS directly combines known transcription-assisted regulators of Six3 and histone-modifying enzymes, thus playing a role as an RNA-based transcription scaffold [34]. KAP1 is a significant epigenetic regulatory protein that interacts with chromatin-binding proteins to control the formation of heterochromatin and inhibits gene expression at autosomal sites. Pavlaki et al.'s study has indicated that lncRNAs Paupar and KAP1 are both regulators of olfactory bulb neurogenesis in vivo [35, 36]. lncRNA Paupar forms ribonucleoprotein complexes containing KAP1 and PAX6 transcription factors, which, if dysfunctional, will destroy the olfactory bulb neurogenesis [35, 37]. Pax6 plays a key role in the generation of retinal neonate neurons and in the control of the differentiation of various late neuron cell types [38].

*3.2. The Regulatory Role of lncRNAs in Advanced Central Nervous System Diseases.* The role of lncRNAs is not only reflected in the growth and development of nerve cells, but more and more studies have revealed the importance of lncRNAs in various central nervous system diseases. NRON is an lncRNA that mediates the cytoplasmic to nuclear transport of NFAT transcription factors [39]. In animal models, when NRON was removed from the regulation of DSCR1 and DYRK1A genes on chromosome 21, the expressions of DSCR1 and DYRK1A were upregulated, leading to the decrease of NFATc activity, which eventually resulted in characteristics of Down syndrome (DS) [40]. This process indicated that there was a potential link between NRON activity and the pathophysiology of DS.

lncRNA BACE1 is used as a potential biomarker for the diagnosis of Alzheimer's disease (AD). BACE1 contains 9 exons and is a candidate gene for sporadic AD [41]. Studies have indicated that the single nucleotide polymorphism of exon 5 of BACE1 gene is related to the occurrence of AD, and the improvement of BACE1 activity leads to the occurrence of AD. However, its specific potential mechanism is not yet clear [42].

In addition, the coexpression module of lncRNA DGCR5 has been confirmed to be associated with schizophrenia (SCZ). Studies have indicated that DGCR5 expression in the brain tissue of SCZ patients is significantly reduced compared with that of normal individuals [43]. DGCR5 was found to be the only CNV lncRNAs in the coexpression module of neurons downregulated in the postmortem brain tissue of SCZ autism and bipolar disorder patients [44]. These findings suggest that DGCR5 may increase the risk of SCZ through its regulatory effect on coexpressed SCZ-related genes.

Parkinson's disease is one of the most common diseases of the nervous system. A study demonstrated the functional relevance of the HOX transcript antisense intergenic RNA (HOTAIR)/microRNA-221-3 (miR-221-3p)/neuronal pentraxin II (NPTX2) axis in the process of dopaminergic neuron autophagy [45]. HOTAIR binds to miR-221-3P and improves the expression of NPTX2, thus reducing cell activity and enhancing the autophagy ability of dopaminergic neurons, while silenced HOTAIR may save the death of dopaminergic neurons by downregulating the NPTX2 gene mediated by miR-221-3p by inhibiting the autophagy of dopaminergic neurons in the substantia nigra dense region of mice [45, 46].

lncRNA is also confirmed to be widely involved in the process of traumatic brain injury (TBI). The five lncRNAs that were most significantly upregulated in TBI were N333955, n332943, N335470, ENST00000384390, and N341115. Tcons_00018733-xloc_008489, OTTHUMT00000076953, NR029967, ENST00000433249, and N381234 are the five most significantly downregulated lncRNAs [47, 48].

Brain tumors have received more attention in recent years. As a common malignant tumor of the nervous system, glioma is gradually attached importance to the association

with lncRNAs. Studies have demonstrated that during the occurrence of gliomas, significant changes in the expression levels of many lncRNAs are observed, such as HOTAIR1, BDNF-ASBDNF-AS, CCAT2, CRNDE, MALAT1, TUG1, and PART1 [49–52]. Therefore, it demonstrates that the mechanism research of lncRNAs will be critical in the occurrence of gliomas and new targets for subsequent treatment. Among them, BDNF-AS is a naturally conserved lncRNA that inhibits the expression of BDNF by reducing the mRNA level of BDNF and its opposite function to BDNF [53]. BDNF-AS is downregulated in glioblastoma tissues and cells and interacts and stabilizes with the poly-adenosine-binding protein cytoplasm 1 (PABPC1) [54]. The overexpression of BDNF-AS inhibits the proliferation, migration, and invasion of glioblastoma cells and induces their apoptosis, while the effect of BDNF-AS knockout is opposite [55, 56].

As a research hotspot this year, lncRNA H19 has been proved to have a variety of biological functions, including regulating cell proliferation, differentiation, and metabolism [57]. It is also indirectly associated with the development of a number of other neurologic tumors, including medulloblastoma meningiomas and gliomas. In glioma cells, previous studies have demonstrated that lncRNA H19 is upregulated and promotes proliferation, migration, invasion, and angiogenesis through the miRNA-138/HIF-1 axis as ceRNA [58]. Meanwhile, both H19 and SOX4 are targets of miRNA-130a-3p. miRNA-130a is a carcinogenic miRNA that targets phosphatase and tensin homolog deleted on chromosome 10 (PTEN) to drive malignant cell survival and tumor growth [59]. Studies have demonstrated that SOX4 may lead to the occurrence of tumors and promote their epithelial-to-mesenchymal transition (EMT) [60]. There is a positive correlation between H19 and SOX4. In addition, SOX4 expression was significantly inhibited after H19 level was reduced [61]. The overexpression of H19 can significantly reduce the inhibitory effect of miRNA-130a-3P on SOX4.

The following table summarizes the CNS regulatory lncRNAs mentioned in this article (Table 1).

## 4. The Role of lncRNAs in Spinal Cord Nerve Injury Repair

Spinal cord injury (SCI) is a common traumatic disease, which often leads to permanent neurological defects. However, due to the limited understanding of the pathogenesis of SCI, there is still no effective treatment for this permanent neurological defect. In recent years, with the continuous recognition of lncRNAs by the scientific community, the regulatory role of lncRNAs in SCI has received more and more attention. Studies have demonstrated the role of lncRNAs in SCI pathogenesis, including neuronal loss of astrocyte proliferation and activation of microglia to activate inflammatory response [62].

Neuronal apoptosis is the main pathological feature of neuronal loss after spinal cord injury; neuronal autophagy can inhibit the apoptosis after spinal cord injury in rats to improve neuronal injury. Studies have demonstrated that TCTN2 overexpression in SCI rat models can reduce neuronal apoptosis by inducing autophagy, and it has been observed that TCTN2 negatively regulates miRNA-216b. Moreover, the miRNA-216b/Beclin-1 pathway can promote autophagy and inhibit cell apoptosis, thus alleviating spinal cord injury [63, 64]. In addition, lncRNA-Map 2k4 can also promote neuronal proliferation and inhibit neuronal apoptosis through the miRNA-199a/FGF1 pathway [65]. On the other hand, the study has demonstrated that inhibiting tumor regulatory factor lncRNA-IGF2AS can reverse the upward movement of IGF2 and increase the secretion of neurotrophic factors BDNF and NT3, promoting the growth of neurons [66].

Apoptosis of oligodendrocytes (OLs) and demyelination of surviving axons are significant components of SCI cascade secondary events, leading to nerve conduction failure [67]. Therefore, the promotion of remyelination is one of the significant factors to promote functional recovery after spinal cord injury. The overexpression of lncRNA OL1 promotes the differentiation of developing precocious oligocytes, while inactivation of lncRNA OL1 may lead to defects in the central nervous system myelin and remyelin after injury [68]. lncRNA OL1 promotes the maturation of oligos by binding to Suz12 as a complex [69].

Reactive astrocyte proliferation and glial hyperplasia are typical characteristics after spinal cord injury and can lead to the formation of glial scar, resulting in physical and biochemical impairments in plasticity and regeneration and ultimately inhibiting functional recovery [70]. However, reactive astrocytes are also beneficial factors for spinal cord injury, including endogenous neuroprotection and secretion of growth-promoting neurotrophic factor [71]. It was found that the downregulation of lncRNA SCIR1 may promote the proliferation and migration of astrocytes in vitro and may play an adverse role in the pathophysiology of SCI. In the model of acute contusion spinal cord injury, the downregulation of lncRNA SCIR1 was closely related to the decrease/increase of WNT3/BMP7 expression and the promotion of astrocyte proliferation and migration [72], suggesting that lncSCIR1 may be a beneficial factor for traumatic spinal cord injury [71]. Therefore, local overexpression of lncSCIR1 may help to neutralize the inhibitory environment around the lesion site and promote functional recovery. Another study showed that lncRNA Gm4419 can promote the apoptosis of trauma-induced astrocytes by upregulating the expression of inflammatory cytokine tumor necrosis factor-$\alpha$ (TNF-$\alpha$), while the upregulation of TNF-$\alpha$ may be achieved by competitive binding of miRNA-466 [73].

Microglial inflammation is a significant biological process in response to injury, infection, and trauma suffered by cells or tissues. Activated microglia release a number of proinflammatory molecules such as interleukin-1 (IL-1B), TNF-reactive oxygen species, and nitric oxide [74]. After spinal cord injury, microglia cells experience significant changes in cell molecules and functions, and the activation of microglia cells is often used to represent neuronal inflammation in the secondary stage of spinal cord injury [62]. Studies have demonstrated that KLF4 is involved in the spinal cord injury process and can regulate the activation of microglia cells and subsequent neuroinflammation [75]. In SCI rat model, lncRNAs SNHG5 and KLF4 are highly

Table 1: lncRNAs which regulate CNS mentioned in this article.

| lncRNA | Effection | Mechanism |
|---|---|---|
| Pnky [26] | Regulates the neurogenesis of embryonic and postnatal brain neural stem cells | Pnky interacts with PTBP1 and regulates the neurogenesis of embryonic and postnatal brain neural stem cells. |
| Evf2 [28] | Participates in the differentiation of GABA cells | Evf2 recruits DLX and MECP2 transcription factors and controls the expression of D1x5, D1x6, and GAD67. |
| Six30S [34] | Regulates early eye formation and postnatal retinal cells | Six30S can directly combine known Six3 transcription-assisted regulators and histone-modifying enzymes and act as an RNA-based transcription scaffold. |
| Paupar [35, 37] | The generation of retinal neurons and the control of the differentiation of a variety of late neuron cell types | By forming ribonucleoprotein complexes containing KAP1 and PAX6 transcription factors. |
| NRON [40] | Involved in the development of certain disorders of DS | DSCR1 and DYRK1A expression was upregulated and NFATc activity was decreased. |
| BACE1 [42] | Participates in the occurrence of AD | The mechanism is unclear. |
| DGCRS [44] | Increases the risk of SCZ through its regulatory effect on coexpressed SCZ-related genes | The mechanism is unclear. |
| HOTAIR [45, 46] | Participates in the autophagy of dopaminergic neurons in the dense region of the substantia nigra | HOTAIR can bind to miRNA-221-3P and improve the expression of NPTX2, thus reducing cell activity and enhancing the autophagy ability of dopaminergic neurons. |
| n333955, n332943, n335470, ENST00000384390, and n341115 [47, 48] | The downregulation is significant in TBI | The mechanism is unclear. |
| TCONS 00018733-XLOC 008489, 0TTHUMT00000076953, NR029967, ENST00000433249, and n381234 [47, 48] | The upregulation was significant in TBI | The mechanism is unclear. |
| BDNF-AS [54] | Inhibits the proliferation, migration, and invasion of glioblastoma cells | Reduces mRNA level of BDNF and inhibits the expression of BDNF |
| H19 [59] | Drives the survival of malignant cells, the growth of tumor, and the transformation of dermal stroma | miRNA-130a-3p was upregulated. PTEN was targeted, and the inhibitory effect of miRNA-130a-3P on SOX4 was weakened. |

expressed during SCI, which proves that KLF4 is the direct target of SNHG5 and is positively regulated by SNHG5. The study also proved that SNHG5 can enhance the activity of astrocytes and microglia cells and promote the process of spinal cord injury by upregulating KLF4 [76]. On the other hand, the overexpression of lncRNA TUSC7 has been demonstrated to inhibit microglial activation and inflammatory cytokine expression by regulating the expression of peroxisome proliferator-activated receptor (PPAR-) by miRNA-449a [77]. Meanwhile, as an epigenetic regulator of microglia cell polarization, lncRNA GAS5 can inhibit microglia cell M2 polarization [78]. Therefore, GAS5 is considered as a promising target for the treatment of demyelination diseases.

The release of a large number of inflammatory factors after spinal cord injury is also a common pathophysiological process of spinal cord injury [79]. It was found that the expression of TLR4 and leucine-rich repeats (TRIL) could be inhibited by downregulating lncRNA TUG1.TRIL is a receptor-assisted protein of TLR4 and plays a significant role in regulating the activity of TLR4 and its downstream inflammatory cytokine IL-1 [80]. Therefore, inhibition of lncRNAs TUG1 and further reduction of TLR4 expression reduce the release of inflammatory cytokines after spinal cord injury, especially after ischemia-reperfusion [81]. lncRNA LINC00341 is one of the most abundant lncRNAs in endothelial cells. Studies have demonstrated that lncRNA LINC00341 can inhibit the expression of vascular cell adhesion molecule 1 (VCAM1), inhibit mononuclear cell adhesion, and play an anti-inflammatory effect [82].

The following table summarizes the SCI regulatory lncRNAs mentioned in this article (Table 2).

## 5. The Role of lncRNAs in the Repair of Peripheral Nerve Injury

Peripheral nerve injury is a common neurological disease. The peripheral nervous system (PNS) differs from the central nervous system in that nerve regeneration is activated after peripheral neuron injury. Although the peripheral nervous system is capable of axonal regeneration, PNS often shows incomplete functional recovery after nerve injury. After peripheral nerve injury, a series of pathophysiological changes will occur at the site of injury, including the

Table 2: lncRNAs which regulate SCI mentioned in this article.

| lncRNA | Effection | Mechanism |
|---|---|---|
| TCTN2 [63, 64] | Induction of autophagy reduces neuronal apoptosis | Negative regulation of miR-216b, promoted autophagy and inhibited apoptosis |
| Map2k4 [65] | Promotes neuronal proliferation and inhibits neuronal apoptosis | The miR-199a/FGF1 pathway promoted neuronal proliferation and inhibited neuronal apoptosis. |
| IGF2AS [66] | Promotes neuronal growth | Upregulate IGF2 and increase the secretion of neurotrophic factors BDNF and NT3 |
| Inc0L1 [68] | Promotes the differentiation of developing precocious oligodendrocytes | The mechanism is unclear. |
| SCIR1 [72] | Participates in the proliferation and migration of astrocytes in vitro | The downregulation of IncSCIR1 decreased/increased WNT3/BMP7 expression and promoted the proliferation and migration of astrocytes. |
| Gm4419 [73] | Participates in the apoptosis of astrocytes | Upregulation of inflammatory cytokines tumor necrosis factor-$\alpha$ (TNF-$\alpha$) by competitive binding of miR-466 |
| SNHG5 [76] | Regulates microglia cell activation and subsequent neuroinflammation | By upregulating KLF4, the activity of astrocytes and microglia cells was increased and the progression of spinal cord injury was promoted. |
| TUSC7 [77] | Inhibition of microglia activation and inflammatory cytokines expression | The expression of peroxisome proliferator-activated receptor $\gamma$(PPAR-$\gamma$) was regulated by miR-449a |
| GAS5 [78] | Inhibits M2 polarization of microglia cells | The mechanism is unclear. |
| TUG1 [80] | Involved the release of inflammatory cytokines after spinal cord injury, especially after ischemia-reperfusion | Inhibits lncRNA TUG1 and decreases TLR4 expression and its downstream inflammatory cytokine IL-1 |
| LINC00341 [82] | Anti-inflammatory effects | Inhibits vascular cell adhesion molecule 1 (VCAM1) expression |

proliferation and migration of axial mutant Schwann cells (SCs) to form Büngner band, thus providing a suitable microenvironment and promoting axonal regeneration [83]. However, although peripheral neurons have the ability to regenerate, the molecular mechanisms of nerve regeneration in PNS have not been fully elucidated. So far, there is still no effective treatment for peripheral nerve injury. Therefore, it is significant to develop new and effective treatment methods to promote regeneration of peripheral nerve after injury. In recent years, many studies have found that ncRNAs, especially lncRNAs, are differentially expressed in peripheral nerve injury, which plays a significant regulatory role in nerve injury and regeneration.

Yu and Zhou indicated that in the rat model of sciatic nerve injury, according to the results of chip analysis and quantitative polymerase chain reaction verification, there were significant differences in the expression levels of various lncRNAs, among which Bc088327 indicated the highest upregulation. In addition, the knockout of lncRNA Bc088327 inhibits the SC vitality, inducing cell apoptosis and S-phase cell cycle arrest [84]. Therefore, lncRNA Bc088327 can be used as both a biomarker to detect the degree of nerve injury and a new therapeutic target to promote nerve repair.

Dorsal root ganglion (DRG) neurons, on the other hand, act as connections between peripheral tissue and the spinal cord. Transcriptional plasticity of DRG sensory neurons contributes to nerve repair after peripheral nerve injury, but also leads to maladaptive plasticity, including the development of neuropathic pain [85, 86]. Studies have demonstrated that lncRNA MRAK009713 is significantly upregulated in DRG induced by chronic sciatic nerve injury (CCI) in rats and participates in CCI-induced neuropathic pain by regulating the expression and function of DRG P2X3 receptor [86]. Meanwhile, lncRNA BC089918 inhibits the growth of DRG neuronal processes, and BC089918 can promote the growth of DRG neuronal processes in primary culture by siRNA knockout, while Fam57b Kcns1 and Cacng2 are potential targets of BC089918 [87].

The majority of peripheral nerve injury distal cells are Schwann cells whose dedifferentiation, proliferation, migration, and myelin removal are significantly associated with successful nerve regeneration. Blocking Schwann cell proliferation and migration may reduce axonal regeneration in transected nerves [88, 89].

The study has demonstrated that silencing lncRNA Tnax-PS1 can promote Schwann cell migration, and further study has demonstrated that TNXA-PS1 may reduce the inhibitory effect of dual-specificity phosphatase 1 (DUSP1) mediated by miRNA-24-3p/miRNA125-3P by sponging miRNA-24-3p/miRNA-125-3p [90]. After peripheral nerve injury, the expression of DUSP1 was decreased due to the downregulation of TNXA-PS1, which ultimately promoted the migration of Schwann cells. MEG3 is a tumor suppressor gene, which is downregulated in a variety of malignant tumors. Peripheral nerve injury is often accompanied by ischemia and inflammation, leading to the accumulation of reactive oxygen species (ROS) [91], leading to MEG3

upregulation [61]. Downregulation of lncRNA MEG3 promotes proliferation and migration of SCs through the PTEN/PI3K/AKT pathway, while silencing lncRNA MEG3 promotes the migration of SCs and the growth of axons and promotes nerve regeneration and functional recovery [92]. Studies have demonstrated that lncRNA BC088259 can interact with vimentin to regulate Schwann cell migration after compression injury of the sciatic nerve. Vimentin is a major intermediate filament protein involved in the developmental attachment and migration of cells. Silencing vimentin expression in Schwann cells significantly inhibited migration of Schwann cells [93]. In Pan and Shi's studies, the mRNA and protein levels of Ctrc1, Wnt5a, ROR2, Rac1, JNK, and ROCK were significantly upregulated, confirming that lncRNA NONMMUG014387 can promote proliferation of Schwann cells around the damaged site by targeting Ctrc1 and activating the Wnt/PCP pathway [94].

## 6. Regulatory Effect of lncRNAs on Neural-Like Differentiation of Stem Cells

Although more and more attention has been paid to the multidirectional differentiation of stem cell, the molecular regulation mechanism and influencing factors on the differentiation are still not clear. In recent years, with the continuous research and exploration of lncRNA, many lncRNAs have been found to play a significant regulatory role in the process of neural-like differentiation of stem cells.

Adipocyte differentiation-associated lncRNA (ADNCR) and TCF3 expression levels were decreased during the induction of differentiation of neural stem cells into nerve cells and astrocytes [95, 96]. However, the expression of miRNA-204-5p increased over time during the differentiation of neural stem cells into nerve cells and astrocytes [97]. As ceRNA of miRNA-204-5p, ADNCR overexpression inhibited the expression of NSC miRNA-204-5p and enhanced the expression of TCF3. Ectopic expression of ADNCR induces proliferation of NSCs and inhibits neuronal differentiation of NSCs, partly by regulating the expression of miRNA-204-5p/TCF3 [98].

Winzi et al. demonstrated that lncRNA lncR492 can inhibit the differentiation of embryonic stem cells (ESC) into neurons [99]. lncR492 was located in the first intron of the protein-coding gene Srrm4, but the downregulation and overexpression of lncRNA did not affect the expression of Srrm4 [100]. Both lncR492 and HUR are involved in the maintenance of Wnt signaling, as the downregulation and overexpression of these two genes lead to the decrease and increase of Wnt signaling, respectively [99]. In vitro studies of ESC have demonstrated that members of the downstream effector Tcf/Lef protein family of Wnt signaling are significant in the differentiation process (Figure 1) [101, 102].

Glioma stem cells (GSCs) have been demonstrated to be associated with glioma invasion, angiogenesis, immune evasion, and therapeutic resistance [103]. lincRNA-p21, a novel regulator of cell proliferation, apoptosis, and DNA damage, is downregulated in several types of tumors [104]. Studies have

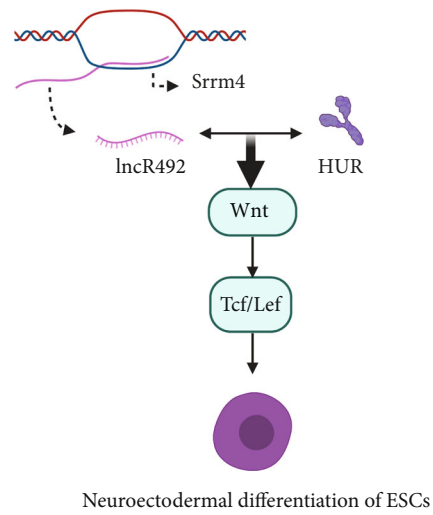


Figure 1: lncR492 interacts with HUR and participates in the maintenance of Wnt signaling, thus affecting the neuroectodermal differentiation of ESCs.

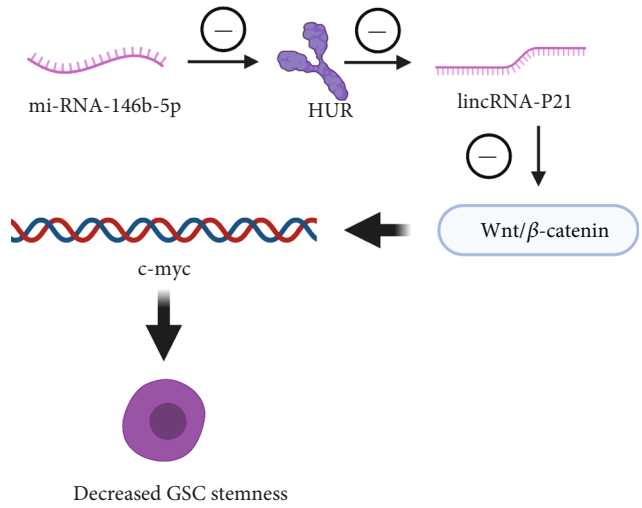


Figure 2: The downregulation of miRNA-146b-5p in GSCs leads to the upregulation of Hu antigen R (HUR) expression and then the downregulation of lincRNA-P21 expression and the upregulation of $\beta$-catenin expression, thus decreasing the stemness of GSCs.

demonstrated that the downregulation of miRNA-146b-5p in GSCs leads to the upregulation of Hu antigen R (HUR) expression and then the downregulation of lincRNA-P21 expression and the upregulation of $\beta$-catenin expression. miRNA-146b-5p inhibit the proliferation of gliomas and thus promote the apoptosis of gliomas [105]. Overexpression of miRNA-146b-5p also increases the apoptosis and radiosensitivity of GSCs, reduces the expression of cell viability, neurogenesis, and stem cell markers, and induces the differentiation of GSCs [106]. In addition, downregulation of lincRNA-P21 or the overexpression of HUR and $\beta$-catenin saves the phenotypic changes induced by the overexpression of miRNA-146b-5p (Figure 2) [105]. These results suggest

Table 3: lncRNAs which regulate PNS and stem cells mentioned in this article.

| lncRNA | Effection | Mechanism |
|---|---|---|
| BC088327 [84] | As a biomarker to detect the degree of nerve damage | Inhibits SC cell vitality, induces apoptosis and S-phase cell cycle arrest |
| MRAK009713 [86] | Participates in ccl-induced neuropathic pain | Regulating the expression and function of DRG P2X3 receptor participates in ccl-induced neuropathic pain |
| BC089918 [87] | Inhibits the growth of DRG neuronal processes | The mechanism is unclear. |
| TNAX-PS1 [90] | Regulates Schwann cell migration | Sponging miR-24-3p/miR-125-3p attenuated the inhibition of bispecific phosphatase 1 (DUSP1) mediated by miR-24-3p/miR-125-3p |
| MEG3 [92] | Promotes SC proliferation and migration | Silencing lncRNA MEG3, promotes SC migration and axonal growth through the PTEN/P13K/AKT pathway |
| BC088259 [93] | Regulates migration of Schwann cells | Interacts with vimentin |
| N0NMMUG0148387 [94] | Promotes the proliferation of Schwann cells around the damaged site | Targeted regulation of Ctrc1 and activation of the Wnt/PCP pathway |
| ADNCR [98] | Participates in the differentiation of NSCs into neurons | Overexpression of ANDCR inhibited the expression of NSC miR-204-5p and enhanced the expression of TCF3. |
| lncR492 [99] | Inhibits the differentiation of embryonic stem cells (ESC) into neurons | The expression level of lncR492 regulates the Wnt signaling pathway and members of its downstream effector Tcf/Lef protein family. |
| lincRNA-p21 [105] | Participates in the proliferation and apoptosis of glioma | Involved in the regulation of the miR-146b-5p/HUR/lincRNA-P21/-catenin signaling pathway |

that targeting the miRNA-146b-5p/HUR/lincRNA-p21/-catenin signaling pathway may be a valuable treatment strategy for glioma.

The following table summarizes the PNS and stem cell regulatory lncRNAs mentioned in this article (Table 3).

## 7. Concluding Remarks

This paper mainly describes the regulatory role of lncRNAs in various nervous systems and in neural differentiation of stem cells in various physiological or pathological processes. lncRNA is significant and cannot be ignored in molecular mechanisms of growth, development, and injury repair. In the process of writing this article, we also found that, at present, most research senior lncRNA focus on growth and development of the central nervous system, brain, neurodegenerative diseases, and spinal cord injury, although there are relatively few studies of the peripheral nervous system injury and differentiation of neural stem cells, so in the future study, lncRNA system around nerve injury, rehabilitation, and neural stem cells differentiating the regulating mechanism in the process will be the research foreground and research value. In addition, most of the existing studies have not described in detail the regulatory mechanism of lncRNA, so it is also a significant research direction to explore the specific mechanism of lncRNA in regulating the activity of the nervous system.

In general, more and more studies have revealed the key role and related mechanism of lncRNAs in the development, growth, and regeneration of nervous systems. With more studies and discoveries, lncRNAs are likely to become a significant therapeutic target for the treatment of various neurological diseases in the future.

## Data Availability

The reference data supporting this systematic review are from previously reported studies and datasets, which have been cited. The processed data are available at PubMed.

## Conflicts of Interest

There is no conflict of interest regarding the publication of this article.

## Authors' Contributions

Zijian Zhou and Dake Qi contributed equally to this work.

## Acknowledgments

This work was supported by the National Natural Science Foundation of China (grant number 81372041) and the Natural Science Foundation of Guangdong Province (grant number 2019A1515012057).

## References

[1] R. Li, H. Zhu, and Y. Luo, "Understanding the functions of long non-coding RNAs through their higher-order structures," *International Journal of Molecular Sciences*, vol. 17, no. 5, p. 702, 2016.

[2] Y. Okazaki, M. Furuno, T. Kasukawa et al., "Analysis of the mouse transcriptome based on functional annotation of 60, 770 full-length cDNAs," *Nature*, vol. 420, no. 6915, pp. 563–573, 2002.

[3] L. Ma, V. B. Bajic, and Z. Zhang, "On the classification of long non-coding RNAs," *RNA Biology*, vol. 10, no. 6, pp. 925–933, 2013.

[4] J. T. Kung, D. Colognori, and J. T. Lee, "Long noncoding RNAs: past, present, and future," *Genetics*, vol. 193, no. 3, pp. 651–669, 2013.

[5] G. St Laurent, "The landscape of long noncoding RNA classification," *Trends in Genetics*, vol. 31, no. 5, pp. 239–251, 2015.

[6] Y. Zhang, H. Zhang, Z. Zhang et al., "LncRNA MALAT1 cessation antagonizes hypoxia/reoxygenation injury in hepatocytes by inhibiting apoptosis and inflammation via the HMGB1-TLR4 axis," *Molecular Immunology*, vol. 112, pp. 22–29, 2019.

[7] Z. Xiao, Y. Qiu, Y. Lin et al., "Blocking lncRNA H19-miR-19a-Id2 axis attenuates hypoxia/ischemia induced neuronal injury," *Aging (Albany NY)*, vol. 11, no. 11, pp. 3585–3600, 2019.

[8] P. Wang and Y. Yuan, "LncRNA-ROR alleviates hypoxia-triggered damages by downregulating miR-145 in rat cardiomyocytes H9c2 cells," *Journal of Cellular Physiology*, vol. 234, no. 12, pp. 23695–23704, 2019.

[9] L. Li, P. C. van Breugel, F. Loayza-Puch et al., "LncRNA-OIS1 regulates DPP4 activation to modulate senescence induced by RAS," *Nucleic Acids Research*, vol. 46, no. 8, pp. 4213–4227, 2018.

[10] S. Zhan, K. Wang, Q. Xiang et al., "lncRNA HOTAIR upregulates autophagy to promote apoptosis and senescence of nucleus pulposus cells," *Journal of Cellular Physiology*, vol. 235, no. 3, pp. 2195–2208, 2020.

[11] M. Li, L. Li, X. Zhang et al., "LncRNA RP11-670E13.6, interacted with hnRNPH, delays cellular senescence by sponging microRNA-663a in UVB damaged dermal fibroblasts," *Aging*, vol. 11, no. 16, pp. 5992–6013, 2019.

[12] S. J. Deng, H. Y. Chen, Z. Zeng et al., "Nutrient stress-dysregulated antisense lncRNA GLS-AS impairs GLS-mediated metabolism and represses pancreatic cancer progression," *Cancer Research*, vol. 79, no. 7, pp. 1398–1412, 2019.

[13] Z. D. Xiao, L. Han, H. Lee et al., "Energy stress-induced lncRNA FILNC1 represses c-Myc-mediated energy metabolism and inhibits renal tumor development," *Nature Communications*, vol. 8, no. 1, p. 783, 2017.

[14] T. Hu, W. Pi, X. Zhu et al., "Long non-coding RNAs transcribed by ERV-9 LTR retrotransposon act in cis to modulate long-range LTR enhancer function," *Nucleic Acids Research*, vol. 45, no. 8, pp. 4479–4492, 2017.

[15] A. Fort, K. Hashimoto, D. Yamada et al., "Deep transcriptome profiling of mammalian stem cells supports a regulatory role for retrotransposons in pluripotency maintenance," *Nature Genetics*, vol. 46, no. 6, pp. 558–566, 2014.

[16] J. R. Prensner, M. K. Iyer, O. A. Balbin et al., "Transcriptome sequencing across a prostate cancer cohort identifies PCAT-1, an unannotated lincRNA implicated in disease progression," *Nature Biotechnology*, vol. 29, no. 8, pp. 742–749, 2011.

[17] J. M. Engreitz, J. E. Haines, E. M. Perez et al., "Local regulation of gene expression by lncRNA promoters, transcription and splicing," *Nature*, vol. 539, no. 7629, pp. 452–455, 2016.

[18] T. Li, X. Mo, L. Fu, B. Xiao, and J. Guo, "Molecular mechanisms of long noncoding RNAs on gastric cancer," *Oncotarget*, vol. 7, no. 8, pp. 8601–8612, 2016.

[19] E. Lau, "Zooming in on lncRNA functions," *Nature Reviews. Genetics*, vol. 15, no. 9, pp. 574-575, 2014.

[20] I. L. Patop, S. Wust, and S. Kadener, "Past, present, and future of circRNAs," *The EMBO Journal*, vol. 38, no. 16, article e100836, 2019.

[21] L. L. Chen and L. Yang, "Regulation of circRNA biogenesis," *RNA Biology*, vol. 12, no. 4, pp. 381–388, 2015.

[22] J. L. C. Richard and P. J. A. Eichhorn, "Deciphering the roles of lncRNAs in breast development and disease," *Oncotarget*, vol. 9, no. 28, pp. 20179–20212, 2018.

[23] J. Ruiz-Orera, X. Messeguer, J. A. Subirana, and M. M. Alba, "Long non-coding RNAs as a source of new peptides," *eLife*, vol. 3, article e03523, 2014.

[24] A. E. Kornienko, P. M. Guenzl, D. P. Barlow, and F. M. Pauler, "Gene regulation by the act of long non-coding RNA transcription," *BMC Biology*, vol. 11, no. 1, p. 59, 2013.

[25] K. O. Cho and J. Hsieh, "The lncRNA Pnky in the brain," *Cell Stem Cell*, vol. 16, no. 4, pp. 344-345, 2015.

[26] I. Grammatikakis and M. Gorospe, "Identification of neural stem cell differentiation repressor complex Pnky-PTBP1," *Stem Cell Investigation*, vol. 3, p. 10, 2016.

[27] A. D. Ramos, R. E. Andersen, S. J. Liu et al., "The long noncoding RNA Pnky regulates neuronal differentiation of embryonic and postnatal neural stem cells," *Cell Stem Cell*, vol. 16, no. 4, pp. 439–447, 2015.

[28] I. Cajigas, D. E. Leib, J. Cochrane et al., "Evf2 lncRNA/BRG1/DLX1 interactions reveal RNA-dependent inhibition of chromatin remodeling," *Development*, vol. 142, no. 15, pp. 2641–2652, 2015.

[29] B. Chattopadhyaya, G. di Cristo, C. Z. Wu et al., "GAD67-mediated GABA synthesis and signaling regulate inhibitory synaptic innervation in the visual cortex," *Neuron*, vol. 54, no. 6, pp. 889–903, 2007.

[30] A. M. Bond, M. J. W. VanGompel, E. A. Sametsky et al., "Balanced gene regulation by an embryonic brain ncRNA is critical for adult hippocampal GABA circuitry," *Nature Neuroscience*, vol. 12, no. 8, pp. 1020–1027, 2009.

[31] W. Gong, J. Li, G. Zhu, Y. Wang, G. Zheng, and Q. Kan, "Chlorogenic acid relieved oxidative stress injury in retinal ganglion cells through lncRNA-TUG1/Nrf2," *Cell Cycle*, vol. 18, no. 14, pp. 1549–1559, 2019.

[32] T. L. Young, T. Matsuda, and C. L. Cepko, "The noncoding RNA taurine upregulated gene 1 is required for differentiation of the murine retina," *Current Biology*, vol. 15, no. 6, pp. 501–512, 2005.

[33] A. Samuel, A. M. Rubinstein, T. T. Azar, Z. Ben-Moshe Livne, S. H. Kim, and A. Inbal, "Six3 regulates optic nerve development via multiple mechanisms," *Scientific Reports*, vol. 6, no. 1, article 20267, 2016.

[34] N. A. Rapicavoli, E. M. Poth, H. Zhu, and S. Blackshaw, "The long noncoding RNA Six3OS acts in trans to regulate retinal development by modulating Six3 activity," *Neural Development*, vol. 6, no. 1, p. 32, 2011.

[35] I. Pavlaki, F. Alammari, B. Sun et al., "The long non-codingRNAPauparpromotesKAP1-dependent chromatin changes and regulates olfactory bulb neurogenesis," *The EMBO Journal*, vol. 37, no. 10, 2018.

[36] S. Iyengar and P. J. Farnham, "KAP1 protein: an enigmatic master regulator of the genome," *The Journal of Biological Chemistry*, vol. 286, no. 30, pp. 26267–26276, 2011.

[37] S. M. Jang, A. Kauzlaric, J. P. Quivy et al., "KAP1 facilitates reinstatement of heterochromatin after DNA replication," *Nucleic Acids Research*, vol. 46, no. 17, pp. 8788–8802, 2018.

[38] L. A. Remez, A. Onishi, Y. Menuchin-Lasowski et al., "Pax6 is essential for the generation of late-born retinal neurons and for inhibition of photoreceptor-fate during late stages of retinogenesis," *Developmental Biology*, vol. 432, no. 1, pp. 140–150, 2017.

[39] T. Xiong, C. Huang, J. Li et al., "LncRNA NRON promotes the proliferation, metastasis and EMT process in bladder cancer," *Journal of Cancer*, vol. 11, no. 7, pp. 1751–1760, 2020.

[40] H. Imam, A. Shahr Bano, P. Patel, P. Holla, and S. Jameel, "The lncRNA NRON modulates HIV-1 replication in a NFAT-dependent manner and is differentially regulated by early and late viral proteins," *Scientific Reports*, vol. 5, no. 1, article 8639, 2015.

[41] N. M. Moussa-Pacha, S. M. Abdin, H. A. Omar, H. Alniss, and T. H. Al-Tel, "BACE1 inhibitors: current status and future directions in treating Alzheimer's disease," *Medicinal Research Reviews*, vol. 40, no. 1, pp. 339–384, 2020.

[42] L. Feng, Y. T. Liao, J. C. He et al., "Plasma long non-coding RNA BACE1 as a novel biomarker for diagnosis of Alzheimer disease," *BMC Neurology*, vol. 18, no. 1, p. 4, 2018.

[43] Y. Liu, X. Chang, C. G. Hahn, R. E. Gur, P. A. M. Sleiman, and H. Hakonarson, "Non-coding RNA dysregulation in the amygdala region of schizophrenia patients contributes to the pathogenesis of the disease," *Translational Psychiatry*, vol. 8, no. 1, p. 44, 2018.

[44] Q. Meng, K. Wang, T. Brunetti et al., "TheDGCR5long noncoding RNA may regulate expression of several schizophrenia-related genes," *Science Translational Medicine*, vol. 10, no. 472, article eaat6912, 2018.

[45] Y. Lang, Y. Li, H. Yu et al., "HOTAIR drives autophagy in midbrain dopaminergic neurons in the substantia nigra compacta in a mouse model of Parkinson's disease by elevating NPTX2viamiR-221-3p binding," *Aging*, vol. 12, no. 9, pp. 7660–7678, 2020.

[46] Y. J. Sun, J. Li, and C. H. Chen, "Effects of miR-221 on the apoptosis of non-small cell lung cancer cells by lncRNA HOTAIR," *European Review for Medical and Pharmacological Sciences*, vol. 23, no. 10, pp. 4226–4233, 2019.

[47] L. X. Yang, L. K. Yang, J. Zhu, J. H. Chen, Y. H. Wang, and K. Xiong, "Expression signatures of long non-coding RNA and mRNA in human traumatic brain injury," *Neural Regeneration Research*, vol. 14, no. 4, pp. 632–641, 2019.

[48] Z. Li, K. Han, D. Zhang, J. Chen, Z. Xu, and L. Hou, "The role of long noncoding RNA in traumatic brain injury," *Neuropsychiatric Disease and Treatment*, vol. 15, pp. 1671–1677, 2019.

[49] J. Shi, B. Dong, J. Cao et al., "Long non-coding RNA in glioma: signaling pathways," *Oncotarget*, vol. 8, no. 16, pp. 27582–27592, 2017.

[50] Z. Xiong, L. Wang, Q. Wang, and Y. Yuan, "LncRNA MALAT1/miR-129 axis promotes glioma tumorigenesis by targeting SOX2," *Journal of Cellular and Molecular Medicine*, vol. 22, no. 8, pp. 3929–3940, 2018.

[51] S.-Y. Jing, Y.-Y. Lu, J.-K. Yang, W.-Y. Deng, Q. Zhou, and B.-H. Jiao, "Expression of long non-coding RNA CRNDE in glioma and its correlation with tumor progression and patient survival," *European Review for Medical and Pharmacological Sciences*, vol. 20, no. 19, pp. 3992–3996, 2016.

[52] H. L. Lang, G. W. Hu, B. Zhang et al., "Glioma cells enhance angiogenesis and inhibit endothelial cell apoptosis through the release of exosomes that contain long non-coding RNA CCAT2," *Oncology Reports*, vol. 38, no. 2, pp. 785–798, 2017.

[53] W. Shang, Y. Yang, J. Zhang, and Q. Wu, "Long noncoding RNA BDNF-AS is a potential biomarker and regulates cancer development in human retinoblastoma," *Biochemical and Biophysical Research Communications*, vol. 497, no. 4, pp. 1142–1148, 2018.

[54] H. Yin, Y. Jiang, Y. Zhang, H. Ge, and Z. Yang, "The inhibition of BDNF/TrkB/PI3K/Akt signal mediated by AG1601 promotes apoptosis in malignant glioma," *Journal of Cellular Biochemistry*, vol. 120, no. 11, pp. 18771–18781, 2019.

[55] R. Su, J. Ma, J. Zheng et al., "PABPC1-induced stabilization of BDNF-AS inhibits malignant progression of glioblastoma cells through STAU1-mediated decay," *Cell Death & Disease*, vol. 11, no. 2, p. 81, 2020.

[56] Q. Wang, Z. Wang, Z. Bao, C. Zhang, Z. Wang, and T. Jiang, "PABPC1relevant bioinformatic profiling and prognostic value in gliomas," *Future Oncology*, vol. 16, no. 1, pp. 4279–4288, 2020.

[57] S. Ghafouri-Fard, M. Esmaeili, and M. Taheri, "H19 lncRNA: roles in tumorigenesis," *Biomedicine & Pharmacotherapy*, vol. 123, article 109774, 2020.

[58] Z. Z. Liu, Y. F. Tian, H. Wu, S. Y. Ouyang, and W. L. Kuang, "LncRNA H19 promotes glioma angiogenesis through miR-138/HIF-1$\alpha$/VEGF axis," *Neoplasma*, vol. 67, no. 1, pp. 111–118, 2020.

[59] H. D. Zhang, L. H. Jiang, D. W. Sun, J. Li, and Z. L. Ji, "The role of miR-130a in cancer," *Breast Cancer*, vol. 24, no. 4, pp. 521–527, 2017.

[60] H. Hanieh, E. A. Ahmed, R. Vishnubalaji, and N. M. Alajez, "SOX4: epigenetic regulation and role in tumorigenesis," *Seminars in Cancer Biology*, vol. 67, pp. 91–104, 2019.

[61] Q. Hu, J. Yin, A. Zeng et al., "H19 functions as a competing endogenous RNA to regulate EMT by sponging miR-130a-3p in glioma," *Cellular Physiology and Biochemistry*, vol. 50, no. 1, pp. 233–245, 2018.

[62] Z. Shi, B. Pan, and S. Feng, "The emerging role of long non-coding RNA in spinal cord injury," *Journal of Cellular and Molecular Medicine*, vol. 22, no. 4, pp. 2055–2061, 2018.

[63] X. D. Ren, C. X. Wan, and Y. L. Niu, "Overexpression of lncRNA TCTN2 protects neurons from apoptosis by enhancing cell autophagy in spinal cord injury," *FEBS Open Bio*, vol. 9, no. 7, pp. 1223–1231, 2019.

[64] L. Chen, X. Han, Z. Hu, and L. Chen, "The PVT1/miR-216b/Beclin-1 regulates cisplatin sensitivity of NSCLC cells via modulating autophagy and apoptosis," *Cancer Chemotherapy and Pharmacology*, vol. 83, no. 5, pp. 921–931, 2019.

[65] H. R. Lv, "lncRNA-Map2k4 sequesters miR-199a to promote FGF1 expression and spinal cord neuron growth," *Biochemical and Biophysical Research Communications*, vol. 490, no. 3, pp. 948–954, 2017.

[66] X. Zhang, K. Chen, C. Song, and C. Song, "Inhibition of long non-coding RNA IGF2AS has profound effect on inducing neuronal growth and protecting local-anesthetic induced neurotoxicity in dorsal root ganglion neurons," *Biomedicine & Pharmacotherapy*, vol. 82, pp. 298–303, 2016.

[67] S. Saraswat Ohri, A. N. Bankston, S. A. Mullins et al., "Blocking autophagy in oligodendrocytes limits functional recovery after spinal cord injury," *The Journal of Neuroscience*, vol. 38, no. 26, pp. 5900–5912, 2018.

[68] B. Elbaz and B. Popko, "Molecular control of oligodendrocyte development," *Trends in Neurosciences*, vol. 42, no. 4, pp. 263–277, 2019.

[69] D. He, J. Wang, Y. Lu et al., "lncRNA functional networks in oligodendrocytes reveal stage-specific myelination control by an lncOL1/Suz12 complex in the CNS," *Neuron*, vol. 93, no. 2, pp. 362–378, 2017.

[70] M. A. Anderson, J. E. Burda, Y. Ren et al., "Astrocyte scar formation aids central nervous system axon regeneration," *Nature*, vol. 532, no. 7598, pp. 195–200, 2016.

[71] J. Wang, B. Hu, F. Cao, S. Sun, Y. Zhang, and Q. Zhu, "Down regulation of lncSCIR1 after spinal cord contusion injury in rat," *Brain Research*, vol. 1624, pp. 314–320, 2015.

[72] Y. Song, S. Lv, F. Wang et al., "Overexpression of BMP-7 reverses TGF-$\beta$1-induced epithelial-mesenchymal transition by attenuating the Wnt3/$\beta$-catenin and TGF-$\beta$1/Smad2/3 signaling pathways in HK-2 cells," *Molecular Medicine Reports*, vol. 21, no. 2, pp. 833–841, 2020.

[73] Y. Yu, F. Cao, Q. Ran, and F. Wang, "Long non-coding RNA Gm4419 promotes trauma-induced astrocyte apoptosis by targeting tumor necrosis factor $\alpha$," *Biochemical and Biophysical Research Communications*, vol. 491, no. 2, pp. 478–485, 2017.

[74] I. C. Hoogland, C. Houbolt, D. J. van Westerloo, W. A. van Gool, and D. van de Beek, "Systemic inflammation and microglial activation: systematic review of animal experiments," *Journal of Neuroinflammation*, vol. 12, no. 1, p. 114, 2015.

[75] A. M. Ghaleb and V. W. Yang, "Krüppel-like factor 4 (KLF4): what we currently know," *Gene*, vol. 611, pp. 27–37, 2017.

[76] Z. S. Jiang and J. R. Zhang, "LncRNA SNHG5 enhances astrocytes and microglia viability via upregulating KLF4 in spinal cord injury," *International Journal of Biological Macromolecules*, vol. 120, Part A, pp. 66–72, 2018.

[77] Y. Yu, M. Zhu, Y. Zhao, M. Xu, and M. Qiu, "Overexpression of TUSC7 inhibits the inflammation caused by microglia activation via regulating miR-449a/PPAR-$\gamma$," *Biochemical and Biophysical Research Communications*, vol. 503, no. 2, pp. 1020–1026, 2018.

[78] D. Sun, Z. Yu, X. Fang et al., "LncRNA GAS5 inhibits microglial M2 polarization and exacerbates demyelination," *EMBO Reports*, vol. 18, no. 10, pp. 1801–1816, 2017.

[79] C. M. Noller, S. L. Groah, and M. S. Nash, "Inflammatory stress effects on health and function after spinal cord injury," *Topics in Spinal Cord Injury Rehabilitation*, vol. 23, no. 3, pp. 207–217, 2017.

[80] S. Carpenter, T. Carlson, J. Dellacasagrande et al., "TRIL, a functional component of the TLR4 signaling complex, highly expressed in brain," *Journal of Immunology*, vol. 183, no. 6, pp. 3989–3995, 2009.

[81] H. Jia, H. Ma, Z. Li et al., "Downregulation of LncRNA TUG1 inhibited TLR4 signaling pathway-mediated inflammatory damage after spinal cord ischemia reperfusion in rats via suppressing TRIL expression," *Journal of Neuropathology and Experimental Neurology*, vol. 78, no. 3, pp. 268–282, 2019.

[82] T. S. Huang, K. C. Wang, S. Quon et al., "LINC00341 exerts an anti-inflammatory effect on endothelial cells by repressing VCAM1," *Physiological Genomics*, vol. 49, no. 7, pp. 339–345, 2017.

[83] R. E. Zigmond and F. D. Echevarria, "Macrophage biology in the peripheral nervous system after injury," *Progress in Neurobiology*, vol. 173, pp. 102–121, 2019.

[84] H. Wang, J. Wu, X. Zhang, L. Ding, and Q. Zeng, "Microarray analysis of the expression profile of lncRNAs reveals the key role of lncRNA BC088327 as an agonist to heregulin-1$\beta$-induced cell proliferation in peripheral nerve injury," *International Journal of Molecular Medicine*, vol. 41, no. 6, pp. 3477–3484, 2018.

[85] W. Wu, X. Ji, and Y. Zhao, "Emerging roles of long noncoding RNAs in chronic neuropathic pain," *Frontiers in Neuroscience*, vol. 13, article 1097, 2019.

[86] G. Baskozos, J. M. Dawes, J. S. Austin et al., "Comprehensive analysis of long noncoding RNA expression in dorsal root ganglion reveals cell-type specificity and dysregulation after nerve injury," *Pain*, vol. 160, no. 2, pp. 463–485, 2019.

[87] B. Yu, S. Zhou, W. Hu et al., "Altered long noncoding RNA expressions in dorsal root ganglion after rat sciatic nerve injury," *Neuroscience Letters*, vol. 534, pp. 117–122, 2013.

[88] B. Chen, Q. Chen, D. B. Parkinson, and X. P. Dun, "Analysis of Schwann cell migration and axon regeneration following nerve injury in the sciatic nerve bridge," *Frontiers in Molecular Neuroscience*, vol. 12, p. 308, 2019.

[89] J. A. Gomez-Sanchez, K. S. Pilch, M. van der Lans et al., "After nerve injury, lineage tracing shows that myelin and Remak Schwann cells elongate extensively and branch to form repair Schwann cells, which shorten radically on remyelination," *The Journal of Neuroscience*, vol. 37, no. 37, pp. 9086–9099, 2017.

[90] C. Yao, Y. Wang, H. Zhang et al., "lncRNA TNXA-PS1 modulates Schwann cells by functioning as a competing endogenous RNA following nerve injury," *The Journal of Neuroscience*, vol. 38, no. 29, pp. 6574–6585, 2018.

[91] W. Lv, B. Deng, W. Duan et al., "Schwann cell plasticity is regulated by a weakened intrinsic antioxidant defense system in acute peripheral nerve injury," *Neuroscience*, vol. 382, pp. 1–13, 2018.

[92] Y. Ma, D. Zhai, W. Zhang et al., "Down-regulation of long non-coding RNA MEG3 promotes Schwann cell proliferation and migration and repairs sciatic nerve injury in rats," *Journal of Cellular and Molecular Medicine*, vol. 24, no. 13, pp. 7460–7469, 2020.

[93] C. Yao, Y. Chen, J. Wang et al., "LncRNA BC088259 promotes Schwann cell migration through Vimentin following peripheral nerve injury," *Glia*, vol. 68, no. 3, pp. 670–679, 2020.

[94] B. Pan, Z. J. Shi, J. Y. Yan, J. H. Li, and S. Q. Feng, "Long noncoding RNA NONMMUG014387 promotes Schwann cell proliferation after peripheral nerve injury," *Neural Regeneration Research*, vol. 12, no. 12, pp. 2084–2091, 2017.

[95] Y. Wang, C. Jiaqi, C. Zhaoying, and C. Huimin, "MicroRNA-506-3p regulates neural stem cell proliferation and differentiation through targeting TCF3," *Gene*, vol. 593, no. 1, pp. 193–200, 2016.

[96] M. Li, X. Sun, H. Cai et al., "Long non-coding RNA ADNCR suppresses adipogenic differentiation by targeting miR-204," *Biochimica et Biophysica Acta (BBA)-Gene Regulatory Mechanisms*, vol. 1859, no. 7, pp. 871–882, 2016.

[97] T. Lepko, M. Pusch, T. Müller et al., "Choroid plexus-derived miR-204 regulates the number of quiescent neural stem cells in the adult brain," *The EMBO Journal*, vol. 38, no. 17, article e100481, 2019.

[98] L. Long, C. Zeng, H. Chen, T. Zhou, L. Wu, and X. Cai, "ADNCR modulates neural stem cell differentiation and

proliferation through the regulation of TCF3 expression," *Annals of Translational Medicine*, vol. 8, no. 15, p. 927, 2020.

[99] M. Winzi, N. Casas Vila, M. Paszkowski-Rogacz et al., "The long noncoding RNA lncR492 inhibits neural differentiation of murine embryonic stem cells," *PLoS One*, vol. 13, no. 1, article e0191682, 2018.

[100] T. Ohnishi, M. Shirane, and K. I. Nakayama, "SRRM4-dependent neuron-specific alternative splicing of protrudin transcripts regulates neurite outgrowth," *Scientific Reports*, vol. 7, no. 1, article 41130, 2017.

[101] N. Doumpas, F. Lampart, M. D. Robinson et al., "TCF/LEF-dependent and independent transcriptional regulation of Wnt/$\beta$-catenin target genes," *The EMBO Journal*, vol. 38, no. 2, 2019.

[102] M. G. Garstang, P. W. Osborne, and D. E. Ferrier, "TCF/Lef regulates the Gsx ParaHox gene in central nervous system development in chordates," *BMC Evolutionary Biology*, vol. 16, no. 1, p. 57, 2016.

[103] R. C. Gimple, S. Bhargava, D. Dixit, and J. N. Rich, "Glioblastoma stem cells: lessons from the tumor hierarchy in a lethal cancer," *Genes & Development*, vol. 33, no. 11-12, pp. 591–609, 2019.

[104] S. S. Tang, B. Y. Zheng, and X. D. Xiong, "LincRNA-p21: implications in human diseases," *International Journal of Molecular Sciences*, vol. 16, no. 8, pp. 18732–18740, 2015.

[105] W. Yang, H. Yu, Y. Shen, Y. Liu, Z. Yang, and T. Sun, "MiR-146b-5p overexpression attenuates stemness and radioresistance of glioma stem cells by targeting HuR/lincRNA-p21/beta-catenin pathway," *Oncotarget*, vol. 7, no. 27, pp. 41505–41526, 2016.

[106] H. Wang, L. Tan, X. Dong et al., "MiR-146b-5p suppresses the malignancy of GSC/MSC fusion cells by targeting SMARCA5," *Aging*, vol. 12, no. 13, pp. 13647–13667, 2020.

Hindawi
Oxidative Medicine and Cellular Longevity
Volume 2021, Article ID 6660193, 12 pages
https://doi.org/10.1155/2021/6660193

*Research Article*

# Palmatine Protects against Cerebral Ischemia/Reperfusion Injury by Activation of the AMPK/Nrf2 Pathway

**Chaoliang Tang,[1] Junmou Hong,[2] Chengyun Hu,[1] Chunxia Huang,[3] Jie Gao,[4] Jun Huang,[5] Di Wang,[3] Qingtian Geng,[1] and Yongfei Dong[6]**

[1]*Department of Anesthesiology, The First Affiliated Hospital of USTC, Division of Life Sciences and Medicine, University of Science and Technology of China, Hefei, Anhui 230001, China*
[2]*Department of Vascular Surgery, Zhongshan Hospital, Xiamen University, Xiamen, Fujian 361004, China*
[3]*Department of Anesthesiology, The Second Affiliated Hospital of Anhui Medical University, Hefei, Anhui 230601, China*
[4]*Department of Anesthesiology, The First Affiliated Hospital of Anhui Medical University, Hefei, Anhui 230022, China*
[5]*Department of Anesthesiology, The People's Hospital of Chizhou, Chizhou, Anhui 247000, China*
[6]*Department of Neurosurgery, The First Affiliated Hospital of USTC, Division of Life Sciences and Medicine, University of Science and Technology of China, Hefei, Anhui 230001, China*

Correspondence should be addressed to Qingtian Geng; gengqingtian@sina.com and Yongfei Dong; dyf.w@163.com

Received 13 November 2020; Revised 5 February 2021; Accepted 21 February 2021; Published 13 March 2021

Academic Editor: Shi Yuan Xu



Palmatine (PAL), a natural isoquinoline alkaloid, possesses extensive biological and pharmaceutical activities, including antioxidative stress, anti-inflammatory, antitumor, neuroprotective, and gastroprotective activities. However, it is unknown whether PAL has a protective effect against ischemic stroke and cerebral ischemia/reperfusion (I/R) injury. In the present study, a transient middle cerebral artery occlusion (MCAO) mouse model was used to mimic ischemic stroke and cerebral I/R injury in mice. Our study demonstrated that PAL treatment ameliorated cerebral I/R injury by decreasing infarct volume, neurological scores, and brain water content. PAL administration attenuated oxidative stress, the inflammatory response, and neuronal apoptosis in mice after cerebral I/R injury. In addition, PAL treatment also decreases hypoxia and reperfusion- (H/R-) induced neuronal injury by reducing oxidative stress, the inflammatory response, and neuronal apoptosis. Moreover, the neuroprotective effects of PAL were associated with the activation of the AMP-activated protein kinase (AMPK)/nuclear factor E2-related factor 2 (Nrf2) pathway, and Nrf2 knockdown offsets PAL-mediated antioxidative stress and anti-inflammatory effects. Therefore, our results suggest that PAL may be a novel treatment strategy for ischemic stroke and cerebral I/R injury.

## 1. Introduction

Stroke, an acute cerebrovascular disease, is an important contributor to mortality and permanent disability worldwide [1, 2]. Epidemiological data showed that ischemic strokes account for approximately 87% of these incidences [3, 4]. Currently, early restoration of the blood supply is considered the main treatment strategy for acute ischemic stroke. However, reperfusion processes after ischemic attack may further exacerbate brain damage, which is named cerebral ischemia/reperfusion (I/R) injury [5, 6]. It is increasingly understood that multiple pathophysiological processes, including oxidative stress, the inflammatory response, neuronal death, and apoptosis, play a pivotal role in the development of cerebral I/R injury [7–10]. Thus, treatments based on the above mechanisms are proposed as a promising strategy to attenuate the outcomes of stroke and cerebral I/R injury.

Palmatine (PAL) is a natural isoquinoline alkaloid extracted from *Coptidis rhizome* [11, 12]. A growing body of evidence indicates that PAL possesses extensive biological and pharmaceutical activities, including antioxidative stress, anti-inflammatory, antitumor, neuroprotective, and gastroprotective activities [11, 13, 14]. Lee et al. reported that PAL treatment inhibited the inflammation and apoptosis of

hepatocytes during acute liver injury [15]. In addition, PAL alleviated ulcerative colitis-induced injury by preserving the integrity of intestinal barrier and mitigating colonic inflammation [16]. Kim et al. also reported that PAL attenuated myocardial I/R injury via suppressing oxidative stress and the inflammatory response [17]. However, it is unknown whether PAL has protective effect against ischemic stroke and cerebral I/R injury.

In the present study, we found that PAL exerts its neuroprotective effect by attenuating cerebral I/R-induced oxidative stress, neuroinflammation, and neuronal apoptosis. In addition, the protective function of PAL in cerebral I/R injury is involved in the activation of the AMP-activated protein kinase (AMPK)/nuclear factor E2-related factor 2 (Nrf2) signaling pathway. Therefore, our results indicate that PAL may be a novel treatment strategy for ischemic stroke and cerebral I/R injury.

## 2. Materials and Methods

*2.1. Animal and Animal Experiments.* Nine- to ten-week-old C57BL/6J mice ($n = 120$) housed in a barrier system with free access to food and water. All procedures were approved by the Animal Experimentation Ethics Committee of Anhui Medical University. The transient middle cerebral artery occlusion (MCAO) model in mice was performed by occluding the middle cerebral artery (MCA) according to our previous research [18]. The sham-operated mice underwent the same protocol, but without MCA ligation. One hour before cerebral ischemia, PAL (MedChemExpress LLC., USA) was dissolved in physiological saline solution (PBS) and was administered orally (50 or 100 mg/kg) to the animals. The 120 mice were randomly allocated into the following four groups ($n = 30$/group): sham group, MCAO group, PAL (50 mg/kg) group, and PAL (100 mg/kg) group.

*2.2. Neurological Deficits Evaluation.* After reperfusion for 24 h, neurological deficits were assessed according to the following scoring criteria [19]: 0, no neurological deficits; 1, unable to extend the contralateral forelimb; 2, circling to paretic side; 3, falling to the contralateral side; and 4, unable to engage in spontaneous activity.

*2.3. Infarct Volume Measurement.* Mice were euthanized using 2% pentobarbital sodium, and intact brains were rapidly collected after neurological deficit evaluation. The brains were cut into four coronal sections and incubated with 2% TTC solution. All images were collected and analyzed using ImageJ (NIH, USA), as described previously [20].

*2.4. Brain Water Content.* Brain water content was assessed using the wet/dry method according to our previous research [18]. Briefly, the brains were carefully removed and promptly weighed to measure the wet weight. Dry weight was evaluated after the brains were dried at 105°C for 24 h.

*2.5. Cell Culture and Treatment.* The PC12 cells were purchased from the China Centre for Type Culture Collection and cultured according to our previous research [18]. First, the PC12 cells were transferred to a hypoxic incubator with 95% $N_2$/5% $CO_2$ and placed in a CB-210 hypoxia workstation (BINDER, Germany) for 6 h. Next, the medium was replaced with fresh maintenance medium and recovered under normoxic conditions for 18 h. In addition, the cells were treated with PAL for 6 h before hypoxic treatment. To knockdown Nrf2, PC12 cells were transfected with si-Nrf2 (Invitrogen, USA) using Lipofectamine 2000 (Thermo Fisher Scientific, USA) according to the manufacturer's recommendation.

*2.6. Oxidative Stress Measurement.* 8-Hydroxydeoxyguanosine (8-OHdG) staining was performed as previously described [21]. Briefly, the brain tissues were quickly isolated and sectioned at a thickness of 4 $\mu$m. Then, the sections were incubated with 8-OHdG monoclonal antibody (Sigma, USA) and placed under a fluorescence microscope (Olympus, Japan). In addition, superoxide dismutase (SOD) and catalase (CAT) activities, and malondialdehyde (MDA) contents in the brain tissues and PC12 cells were measured according to the protocol recommended (Beyotime Biotechnology, China).

*2.7. ELISA Analysis.* The brain tissues were quickly isolated and prepared as homogenates in a homogenizer. The concentrations of interleukin- (IL-) 1$\beta$, IL-6, and tumor necrosis factor- (TNF-) $\alpha$ were detected using ELISA kits (R&D Systems, USA).

*2.8. TUNEL Staining.* TUNEL staining was performed to detect the extent of cell apoptosis as previously described [22]. The images were collected using an automatic fluorescence microscope and analyzed using ImageJ (NIH, USA).

*2.9. Western Blot.* Total proteins extracted from ischemic side cerebral cortex and PC12 cells were collected and fractionated on SDS-PAGE gels [23]. Then, the protein was incubated with primary antibodies against Bax (1 : 1000, Abcam, USA), Bcl-2 (1 : 1000, Abcam, USA), p-AMPK (1 : 1000, Abcam, USA), AMPK (1 : 1000, Abcam, USA), Nrf2 (1 : 1000, Cell Signaling Technology, USA), lamin B (1 : 1000, Abcam, USA), and $\beta$-actin (1 : 1000, Abcam, USA). After that, the membranes were incubated with the corresponding secondary antibodies (1 : 5000, Abcam, USA) and scanned using Odyssey imaging system (LI-COR, USA). The relative band intensity was normalized to that of $\beta$-actin or lamin B.

*2.10. qRT-PCR.* Total RNA was extracted from ischemic side cerebral cortex and PC12 cells according to the manufacturer's instructions [24]. Then, total RNA was reverse-transcribed, and amplification was quantified using SYBR Premix Ex Taq2. The mRNA expression level was normalized to the $\beta$-actin level. Primer sequences of qRT-PCR analysis are presented in Table 1.

*2.11. Statistical Analysis.* The population data are expressed as the means ± SD. One-way analysis of variance (ANOVA) tests were used to examine the statistical difference. $P$ values below 0.05 were considered to be significant.

## 3. Results

*3.1. PAL Protected Mice against Cerebral I/R Injury.* As shown in Figure 1, the MCAO model resulted in an increase

Table 1: Primer sequences for RT-PCR assays.

| Gene | Species | | Sequence (5′-3′) |
|---|---|---|---|
| IL-1$\beta$ | Mouse | Forward | GGGCCTCAAAGGAAAGAATC |
| | | Reverse | TACCAGTTGGGGAACTCTGC |
| IL-1$\beta$ | Rat | Forward | GTGCTGTCTGACCCATGTGA |
| | | Reverse | CACAGGGATTTTGTCGTTGCT |
| IL-6 | Mouse | Forward | AGTTGCCTTCTTGGGACTGA |
| | | Reverse | TCCACGATTTCCCAGAGAAC |
| IL-6 | Rat | Forward | GTTGCCTTCTTGGGACTGATG |
| | | Reverse | ATACTGGTCTGTTGTGGGTGGT |
| TNF-$\alpha$ | Mouse | Forward | CCCAGGGACCTCTCTCTAATC |
| | | Reverse | ATGGGCTACAGGCTTGTCACT |
| TNF-$\alpha$ | Rat | Forward | CTACTCCCAGGTTCTCTTCAA |
| | | Reverse | GCTGACTTTCTCCTGGTATGA |
| $\beta$-Actin | Mouse | Forward | TATTGGCAACGAGCGGTTCC |
| | | Reverse | GGCATAGAGGTCTTTACGGATGT |
| $\beta$-Actin | Rat | Forward | CAAGAAGGTGGTGAAGCAG |
| | | Reverse | AAAGGTGGAAGAATGGGAG |

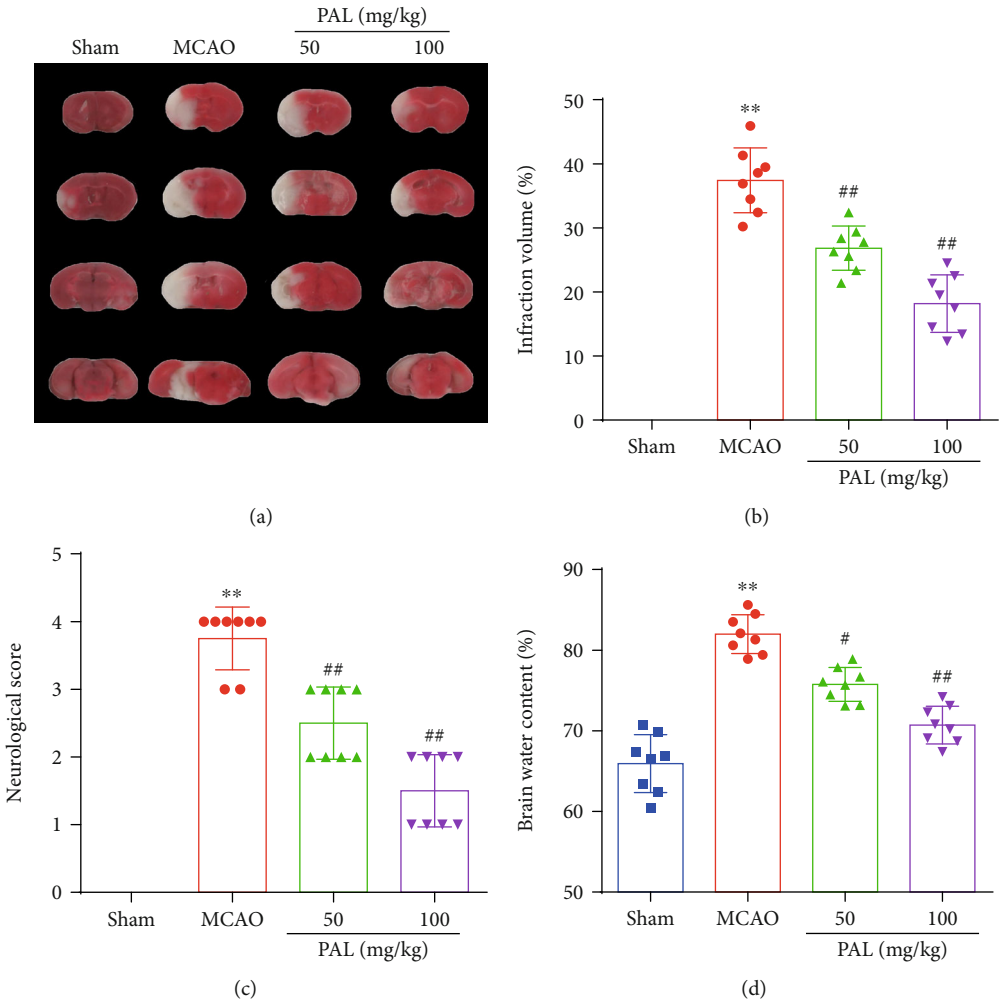


Figure 1: PAL protected mice against cerebral I/R injury. (a, b) Effects of PAL on infarct volume ($n = 8$). (c) Effects of PAL on neurological scores ($n = 8$). (d) Effects of PAL on brain water content ($n = 8$). $^{**}P < 0.01$ vs. sham group; $^{\#}P < 0.05$ and $^{\#\#}P < 0.01$ vs. MCAO group. PAL: palmatine.

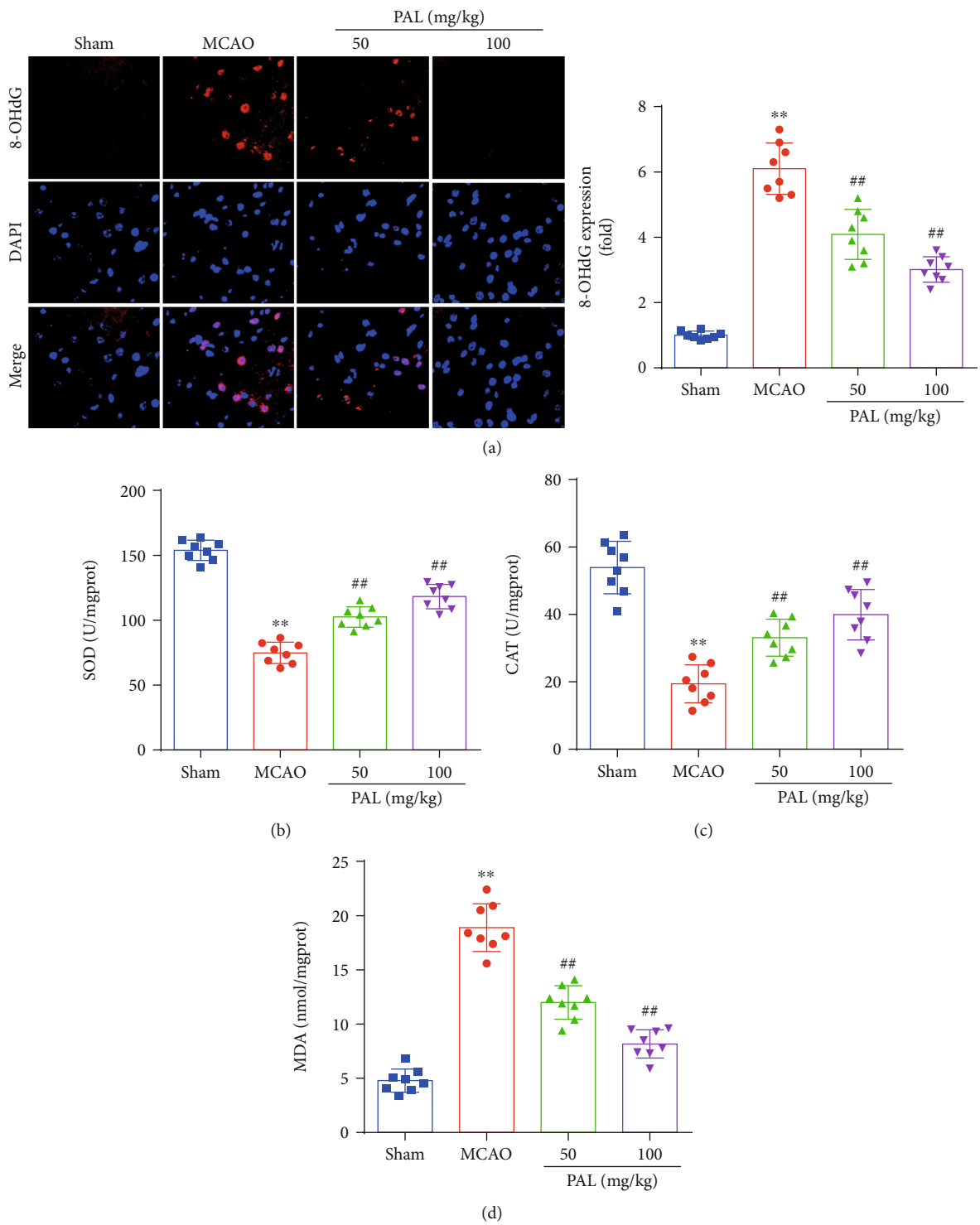


Figure 2: PAL suppresses oxidative stress after cerebral I/R injury. (a) 8-OHdG staining and quantitative analysis ($n = 8$; scale bar, 25 $\mu$m). (b–d) Effects of PAL on SOD and CAT activities, and MDA contents ($n = 8$). $^{**}P < 0.01$ vs. sham group; $^{\#\#}P < 0.01$ vs. MCAO group. PAL: palmatine.

in the infarct volume and neurological scores compared with those of the sham group. In addition, PAL treatment significantly decreased the infarct volume and neurological scores at 24 h after MCAO (Figures 1(a)–1(c)). As anticipated, PAL treatment also reduced brain water content in a dose-dependent manner (Figure 1(d)). Together, these findings strongly support that PAL plays a protective role in mouse cerebral I/R injury.

*3.2. PAL Suppresses Oxidative Stress after Cerebral I/R Injury.* Oxidative stress has been proven to be a critical pathological process responsible for ischemic stroke and cerebral I/R

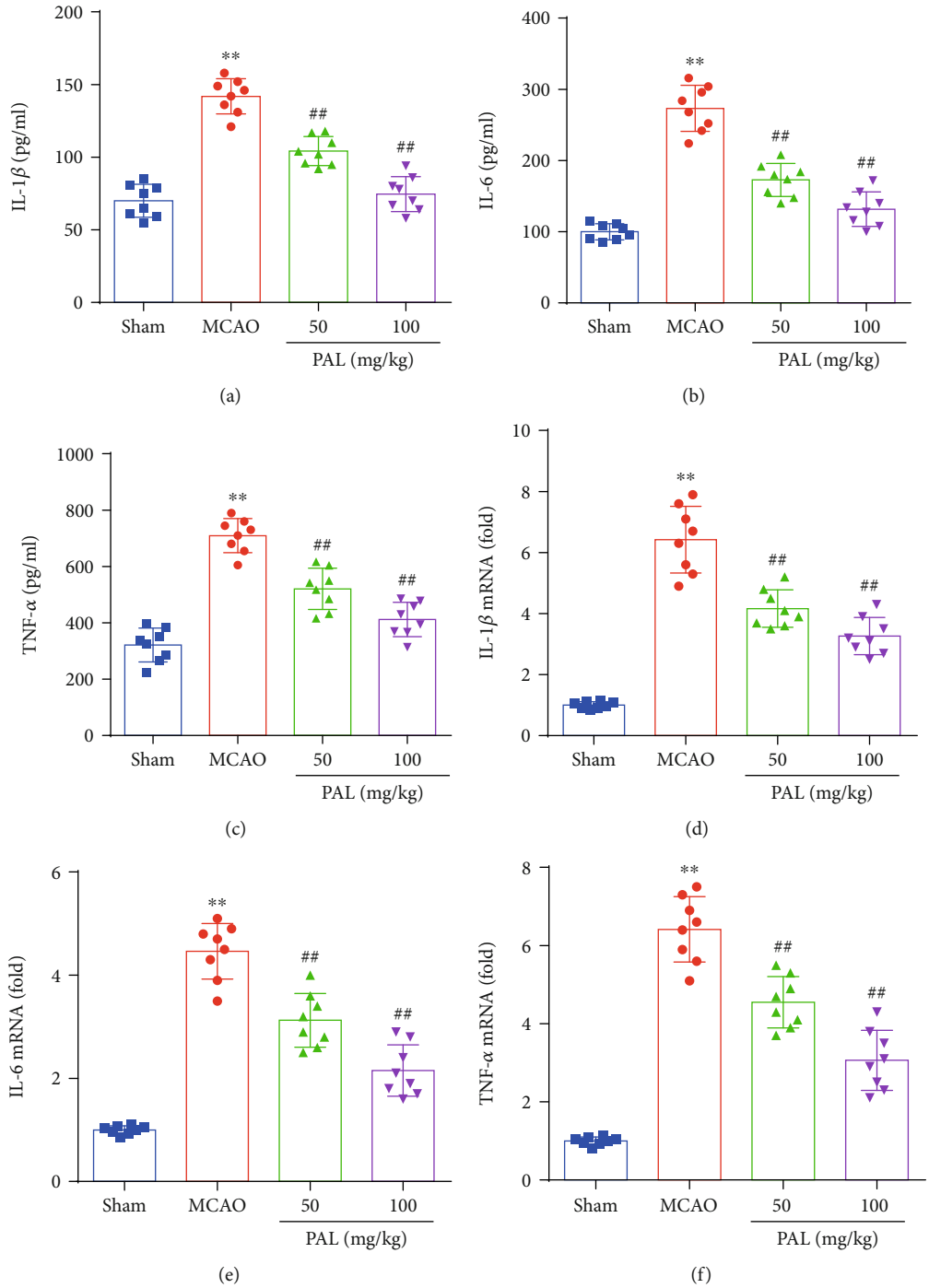


Figure 3: PAL reduces the inflammatory response after cerebral I/R injury. (a–c) The expression of IL-1$\beta$, IL-6, and TNF-$\alpha$ protein in the ischemic cerebral cortex ($n = 8$). (d–f) The relative mRNA levels of IL-1$\beta$, IL-6, and TNF-$\alpha$ in the ischemic cerebral cortex ($n = 8$). $^{**}P < 0.01$ vs. sham group; $^{\#\#}P < 0.01$ vs. MCAO group. PAL: palmatine.

injury [25]. We therefore investigated the effect of PAL on oxidative stress. Consistent with previous studies, 8-OHdG expression in the MCAO group was higher than that in the sham group, which was mitigated by PAL (Figure 2(a)). Moreover, a significant reduction in SOD and CAT activities and an increase in MDA contents were also observed in the MCAO group compared with the sham group (Figures 2(b)–2(d)). Interestingly, PAL administration significantly restored SOD and CAT activity, and reduced the MDA content, in the brain after MCAO (Figures 2(b)–2(d)).

*3.3. PAL Reduces the Inflammatory Response after Cerebral I/R Injury.* Previous studies have found that the inflammatory response is an important mediator of ischemic stroke and cerebral I/R injury [26]. Thus, we evaluated the potential role of PAL in the inflammatory response after cerebral

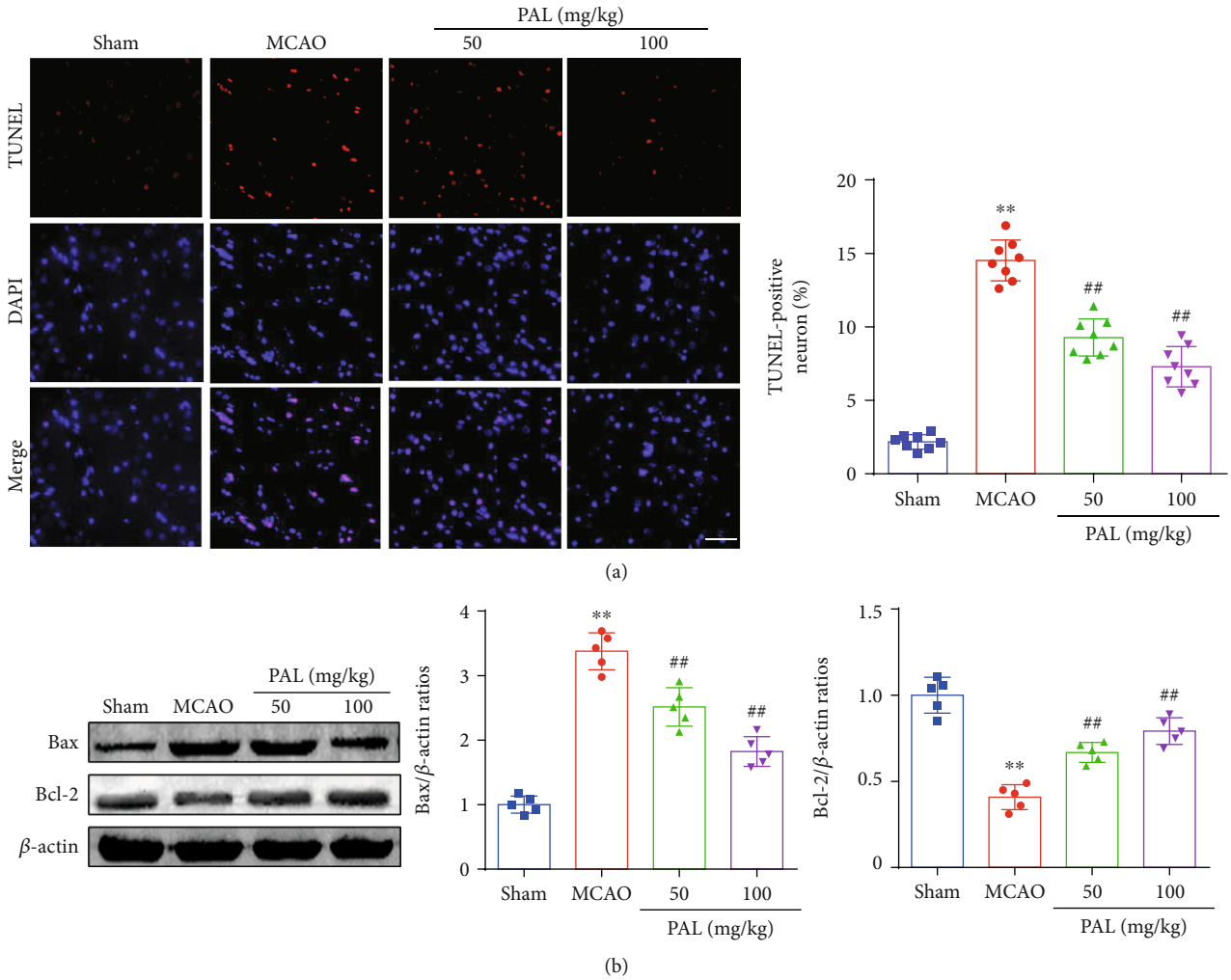


Figure 4: PAL attenuates neuronal apoptosis after cerebral I/R injury. (a) TUNEL staining and quantitative analysis ($n = 8$; scale bar, 50 $\mu$m). (b) Effects of PAL on Bax and Bcl-2 expression ($n = 5$). $^{**}P < 0.01$ vs. sham group; $^{\#\#}P < 0.01$ vs. MCAO group. PAL: palmatine.

I/R injury. As shown in Figures 3(a)–3(c), the levels of inflammatory cytokines, including IL-1$\beta$, IL-6, and TNF-$\alpha$, were significantly increased in the MCAO group compared with the sham group. In addition, PAL treatment prevented the increase in IL-1$\beta$, IL-6, and TNF-$\alpha$ in the brain after MCAO (Figures 3(a)–3(c)). RT-PCR results also showed that PAL treatment reduces the mRNA expression of these inflammatory cytokines (Figures 3(d)–3(f)), indicating that PAL treatment reduces the inflammatory response after cerebral I/R injury.

*3.4. PAL Attenuates Neuronal Apoptosis after Cerebral I/R Injury.* TUNEL staining results showed that neuronal apoptosis was increased in the MCAO group compared with the sham group but reduced in PAL-treated mice (Figure 4(a)). In addition, the expression of Bax in the MACO group was higher and the expression of Bcl-2 in the MACO group was lower than that in the sham group (Figure 4(b)). However, PAL administration significantly decreased Bax expression and upregulated Bcl-2 expression at 24 h after MCAO (Figure 4(b)).

*3.5. PAL Reduces Oxidative Stress, the Inflammatory Response, and Neuronal Apoptosis In Vitro.* As shown in Figures 5(a)–5(c), a significant reduction in SOD and CAT activities and an increase in MDA contents were observed in the H/R group compared with the control group (Figures 5(a)–5(c)). In addition, PAL administration significantly restored SOD and CAT activity, and reduced the MDA content in PC12 cells following H/R (Figures 5(a)–5(c)). Consistent with the results of animal experiments, PAL administration also significantly decreased the mRNA expression of IL-1$\beta$, IL-6, and TNF-$\alpha$ in PC12 cells following H/R (Figures 5(d)–5(f)). In addition, the expression of Bax in the H/R group was higher, and the expression of Bcl-2 in the H/R group was lower than that in the PBS group (Figure 5(g)). However, PAL administration significantly decreased Bax expression and upregulated Bcl-2 expression in PC12 cells following H/R (Figure 5(g)).

*3.6. PAL Activates the AMPK/Nrf2 Signaling Pathway.* Previous research has strongly suggested that the AMPK/Nrf2 signaling pathway plays an important role in cerebral I/R injury

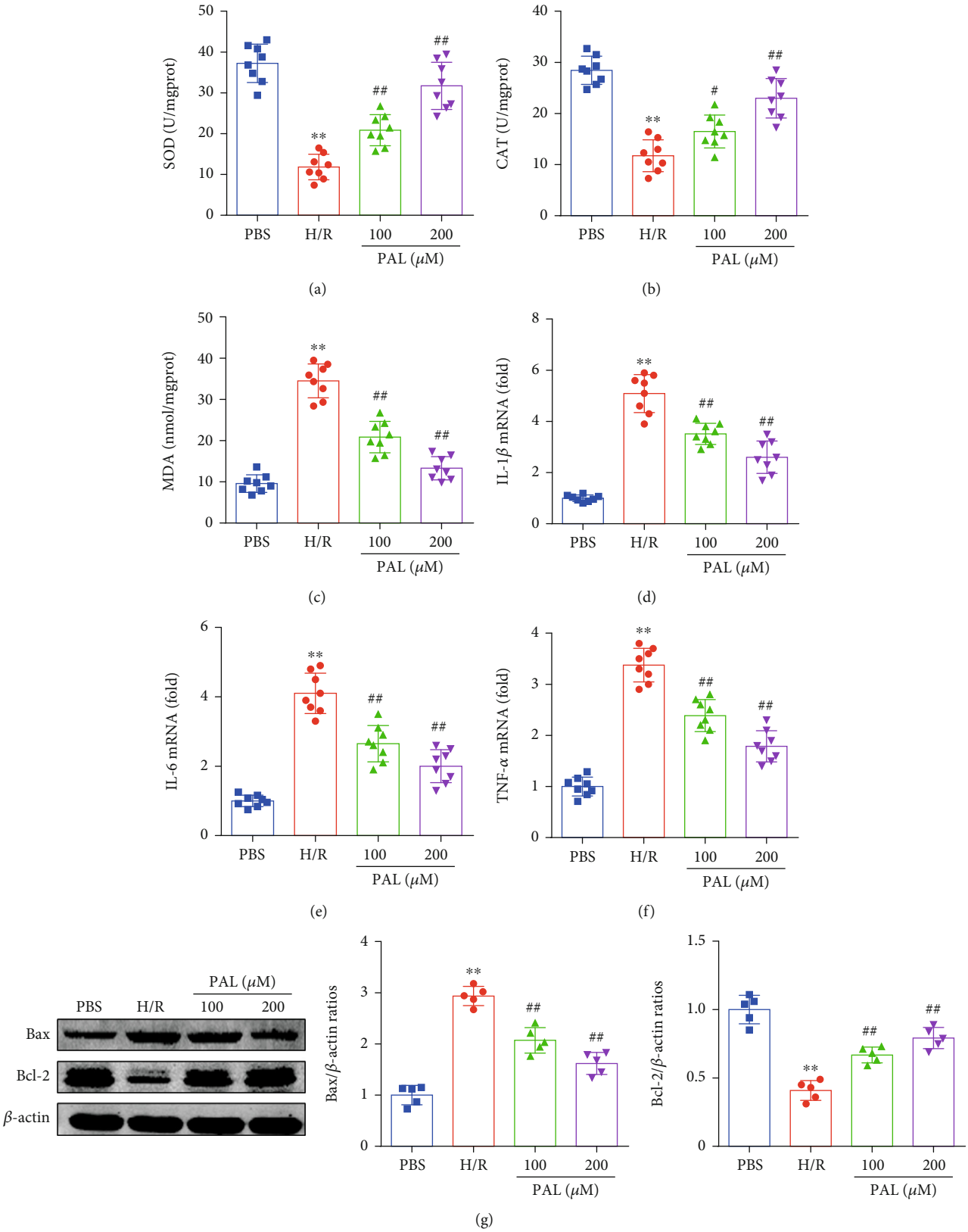


Figure 5: PAL reduces oxidative stress, the inflammatory response, and neuronal apoptosis in vitro. (a–c) Effects of PAL on SOD and CAT activities, and MDA contents ($n = 8$). (d–f) The relative mRNA levels of IL-1$\beta$, IL-6, and TNF-$\alpha$ ($n = 8$). (g) Effects of PAL on Bax and Bcl-2 expression ($n = 5$). $^{**}P < 0.01$ vs. PBS group; $^{\#\#}P < 0.01$ vs. H/R group. PAL: palmatine.

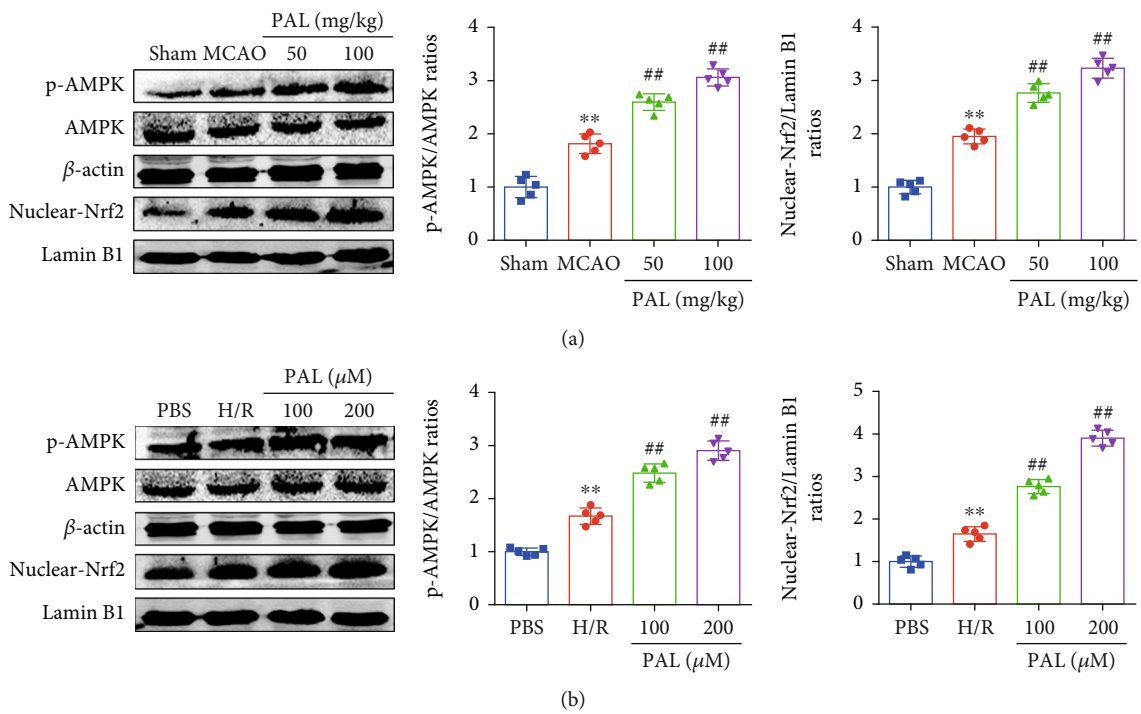


Figure 6: PAL activates the AMPK/Nrf2 signaling pathway. (a) Effects of PAL on p-AMPK, AMPK, and nuclear Nrf2 expression in the ischemic cerebral cortex ($n = 5$). (b) Effects of PAL on p-AMPK, AMPK, and nuclear Nrf2 expression in PC12 cells ($n = 5$). $^{**}P < 0.01$ vs. sham or PBS group; $^{\#\#}P < 0.01$ vs. MCAO or H/R group. PAL: palmatine.

[27, 28]. Hence, we detected whether the neuroprotective function of PAL is associated with the AMPK/Nrf2 signaling pathway. The results revealed that the phosphorylation level of AMPK and the expression of nuclear Nrf2 were upregulated in the MCAO group compared with the sham group (Figure 6(a)). In addition, PAL administration further increased the phosphorylation level of AMPK and the expression of nuclear Nrf2 after cerebral I/R injury (Figure 6(a)). Consistent with the results of animal experiments, PAL administration also significantly increased the phosphorylation level of AMPK and the expression of nuclear Nrf2 in PC12 cells following H/R (Figure 6(b)).

*3.7. Nrf2 Knockdown Abolishes the Neuroprotective Effects of PAL In Vitro.* To further confirm the effect of the AMPK/Nrf2 signaling pathway in PAL-mediated neuroprotection, si-Nrf2 transfection was performed to knockdown Nrf2 in vitro. The results showed that Nrf2 knockdown abolished the PAL-mediated antioxidative stress effects, as evidenced by reduced SOD and CAT activities and increased MDA contents (Figures 7(a)–7(c)). In addition, Nrf2 knockdown offsets PAL-mediated anti-inflammatory and anti-neuronal apoptosis (Figures 7(d)–7(g)). The above results revealed that the AMPK/Nrf2 pathway plays a central role in PAL-mediated neuroprotective effects.

## 4. Discussion

In this study, our research revealed a neuroprotective function of PAL in mediating cerebral I/R injury. Our study demonstrated that PAL treatment ameliorated cerebral I/R injury by decreasing infarct volume, neurological scores, and brain water content. PAL administration attenuated oxidative stress, the inflammatory response, and neuronal apoptosis in mice after cerebral I/R injury. In addition, PAL treatment also decreased H/R-induced oxidative stress, the inflammatory response, and neuronal apoptosis in PC12 cells. Moreover, the neuroprotective function of PAL was associated with the activation of the AMPK/Nrf2 pathway, and Nrf2 knockdown offset PAL-mediated antioxidative stress and anti-inflammatory effects.

As a natural isoquinoline alkaloid, the neuroprotective effect of PAL has attracted the attention of many researchers [29, 30]. PAL was proven to treat Alzheimer's disease by reducing β-amyloid plaques and tau protein aggregation [29]. In addition, PAL exhibited antidepressant activity by decreasing nitrite and corticosterone levels and inhibiting monoamine oxidase-A activity [30]. However, the protective effect and the molecular mechanism of PAL in ischemic stroke and cerebral I/R injury are not well studied. In the present study, the MCAO mouse model was used to mimic ischemic stroke and cerebral I/R injury in vivo. The results showed that PAL treatment significantly decreased the infarct volume, neurological scores, and brain water content in mice at 24 h after MCAO, suggesting that PAL plays a protective role in ischemic stroke and cerebral I/R injury.

Reactive oxygen species (ROS) are crucial protagonists of oxidative stress, and causing neuronal injury and death [31, 32]. Multiple antioxidants and/or ROS scavengers have been shown to improve cerebral I/R injury and strongly support that suppressing oxidative stress is an attractive potential therapeutic target to counteract ischemic stroke and cerebral

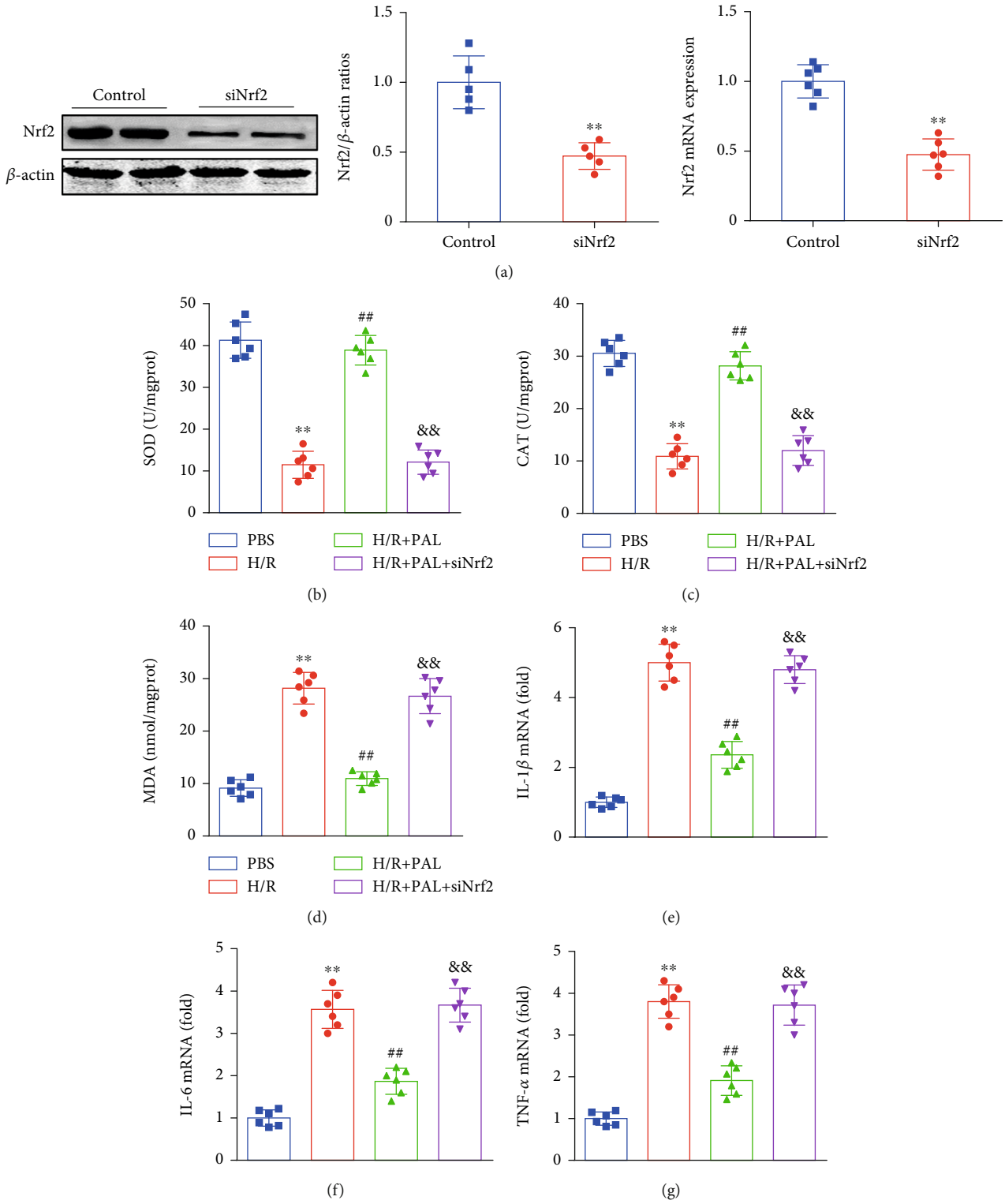


Figure 7: Continued.

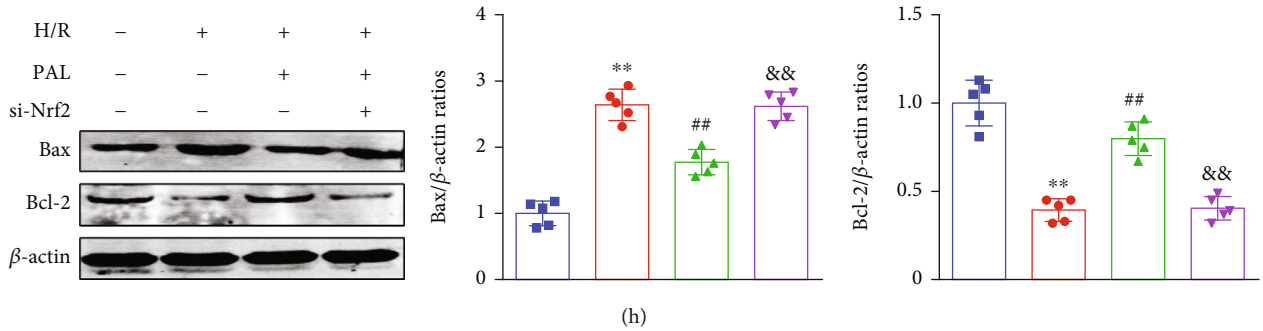


Figure 7: Nrf2 knockdown abolishes the neuroprotective effects of PAL in vitro. (a) Effects of Nrf2 expression after siRNA treatment ($n = 5$). (b–d) Effects of Nrf2 knockdown on SOD and CAT activities, and MDA contents ($n = 6$). (e–g) The relative mRNA levels of IL-1$\beta$, IL-6, and TNF-$\alpha$ ($n = 6$). (h) Effects of PAL on Bax and Bcl-2 expression ($n = 5$). $^{**}P < 0.01$ vs. PBS group; $^{\#\#}P < 0.01$ vs. H/R group; $^{\&\&}P < 0.01$ vs. H/R+PAL group. PAL: palmatine.

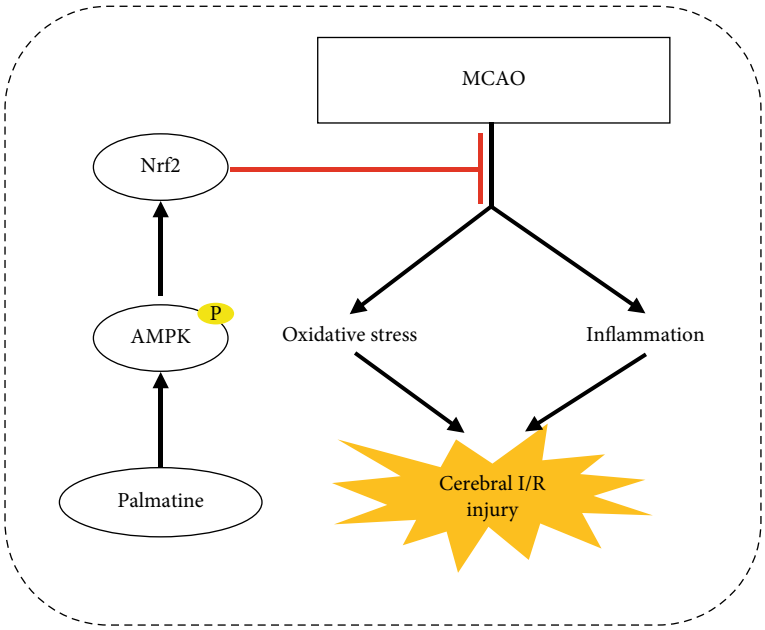


Figure 8: Palmatine protects against cerebral ischemia/reperfusion injury by activation of the AMPK/Nrf2 pathway.

I/R injury [33, 34]. Previous research has shown that PAL possesses extensive biological and pharmaceutical activities [11, 29]. Thus, we investigated whether PAL affects oxidative stress after cerebral I/R injury.

In our study, 8-OHdG staining was performed to assess oxidative DNA damage and the results showed that 8-OHdG expression in the MCAO group was higher than that in the sham group, which was mitigated by PAL. Thus, it can be speculated that PAL could decrease oxidative DNA damage during cerebral I/R injury. SOD catalyzes the conversion of superoxide anion radicals to hydrogen peroxide, and the latter is further reduced into molecular oxygen and water by CAT [35, 36]. As a product of lipid peroxidation, MDA has been used to assess free radical levels in cerebral I/R injury [37]. Consistent with previous studies, significant reductions in SOD and CAT activities and increases in MDA contents were also observed after cerebral I/R injury. We further found that PAL significantly increased SOD and CAT activities, and reduced the MDA content in I/R mouse brain tissues and PC12 cells following H/R. These results directly reflect that PAL attenuates cerebral I/R injury by suppressing oxidative stress.

Intensive research has revealed that the inflammatory response is closely related to oxidative stress, and aggravating neuronal damage [38, 39]. In addition, proinflammatory cytokines, including IL-1, IL-6, IL-17, and TNF-$\alpha$, have been detected in the brain of ischemic stroke patients and the infarction area of animal models [40, 41]. Previous studies have suggested that PAL has an anti-inflammatory effect in multiple diseases [11]. Thus, we evaluated the potential role of PAL in the inflammatory response after cerebral I/R injury. The results showed that PAL administration suppressed cerebral I/R-induced neuroinflammation by decreasing the expression of inflammatory cytokines, including IL-1$\beta$, IL-6, and TNF-$\alpha$. Consistent with the results of animal experiments, PAL administration also significantly decreased the mRNA expression of IL-1$\beta$, IL-6, and TNF-$\alpha$ in PC12 cells following H/R. In addition, we further

demonstrated the potential molecular mechanisms by which PAL exerts neuroprotective effects in cerebral I/R injury.

As a serine/threonine protein kinase, AMPK was proven to participate in the regulation of cellular stress and energy homeostasis and is considered as an important regulatory factor of oxidative stress and inflammation [27, 42]. Many results indicate that AMPK is activated after cerebral I/R injury and protects neurons from oxidative damage and inflammation [27, 43]. In addition, the neuroprotective potential of AMPK is closely related to the activation of Nrf2 signaling [28, 44]. In the current experimental protocol, we investigated whether the protective function of PAL is associated with the AMPK/Nrf2 signaling pathway. We found that PAL treatment significantly upregulated the phosphorylation of AMPK and nuclear Nrf2 expression after cerebral I/R injury. In addition, Nrf2 knockdown abolished the PAL-mediated antioxidative stress anti-inflammatory effects, indicating that the AMPK/Nrf2 pathway plays a central role in PAL-mediated neuroprotective effects.

In conclusion, PAL decreases oxidative stress, the inflammatory response, and neuronal apoptosis after cerebral I/R injury via activation of the AMPK/Nrf2 pathway (Figure 8). Our data indicate that PAL may be a novel therapeutic approach for ischemic stroke and cerebral I/R injury.

## Data Availability

The datasets generated and/or analyzed during the current study are available from the corresponding author on reasonable request in compliance with ethical standards.

## Conflicts of Interest

No conflicts of interests are declared by the authors.

## Authors' Contributions

Chaoliang Tang and Junmou Hong were involved in the design and execution of experiments, data analysis, and manuscript writing. Qingtian Geng and Yongfei Dong were involved in the design of the study, data analysis, and manuscript writing. Chengyun Hu, Chunxia Huang, Jie Gao, Jun Huang, and Di Wang were all involved in the execution of experiments and data analysis. All authors provided final approval of the version to be submitted. Chaoliang Tang, Junmou Hong, and Chengyun Hu contributed equally to this work.

## Acknowledgments

This study was supported by grants from the National Natural Science Foundation of China (Grant No. 81801175 to Chaoliang Tang), the China Postdoctoral Science Foundation (Grant No. 2019M662179 to Chaoliang Tang), the Anhui Province Postdoctoral Science Foundation (Grant No. 2019B324 to Chaoliang Tang), and the Fundamental Research Funds for the Central Universities (Grant No. WK9110000044 to Chaoliang Tang).

## References

[1] C. Chen, H. Qin, J. Tan, Z. Hu, and L. Zeng, "The role of ubiquitin-proteasome pathway and autophagy-lysosome pathway in cerebral ischemia," *Oxidative Medicine and Cellular Longevity*, vol. 2020, Article ID 5457049, 12 pages, 2020.

[2] J. Wajda, M. Swiat, A. J. Owczarek, A. Brzozowska, M. Olszanecka-Glinianowicz, and J. Chudek, "Severity of vitamin D deficiency predicts mortality in ischemic stroke patients," *Disease Markers*, vol. 2019, Article ID 3652894, 10 pages, 2019.

[3] M. Bladowski, J. Gawrys, D. Gajecki, E. Szahidewicz-Krupska, A. Sawicz-Bladowska, and A. Doroszko, "Role of the platelets and nitric oxide biotransformation in ischemic stroke: a translative review from bench to bedside," *Oxidative Medicine and Cellular Longevity*, vol. 2020, Article ID 2979260, 18 pages, 2020.

[4] P. B. Gorelick, "The global burden of stroke: persistent and disabling," *Lancet Neurology*, vol. 18, no. 5, pp. 417-418, 2019.

[5] M. Pérez-Mato, R. Iglesias-Rey, A. Vieites-Prado et al., "Blood glutamate $EAAT_2$-cell grabbing therapy in cerebral ischemia," *EBioMedicine*, vol. 39, pp. 118–131, 2019.

[6] M. Dai, L. Wu, K. Yu et al., "D-Carvone inhibit cerebral ischemia/reperfusion induced inflammatory response TLR4/NLRP3 signaling pathway," *Biomed Pharmacother*, vol. 132, article 110870, 2020.

[7] J. D. Bernstock, L. Peruzzotti-Jametti, T. Leonardi et al., "SUMOylation promotes survival and integration of neural stem cell grafts in ischemic stroke," *EBioMedicine*, vol. 42, pp. 214–224, 2019.

[8] Y. Jiao, J. Wang, H. Zhang et al., "Inhibition of microglial receptor-interacting protein kinase 1 ameliorates neuroinflammation following cerebral ischaemic stroke," *Journal of Cellular and Molecular Medicine*, vol. 24, no. 21, pp. 12585–12598, 2020.

[9] W. Hu, H. Wang, Q. Shu, M. Chen, and L. Xie, "Green tea polyphenols modulated cerebral SOD expression and endoplasmic reticulum stress in cardiac arrest/cardiopulmonary resuscitation rats," *BioMed Research International*, vol. 2020, Article ID 5080832, 9 pages, 2020.

[10] D. Zhang, L. Mei, R. Long et al., "RiPerC attenuates cerebral ischemia injury through regulation of miR-98/PIK3IP1/PI3-K/AKT signaling pathway," *Oxidative Medicine and Cellular Longevity*, vol. 2020, Article ID 6454281, 12 pages, 2020.

[11] J. Long, J. Song, L. Zhong, Y. Liao, L. Liu, and X. Li, "Palmatine: a review of its pharmacology, toxicity and pharmacokinetics," *Biochimie*, vol. 162, pp. 176–184, 2019.

[12] Z. Xu, W. Feng, Q. Shen et al., "Rhizoma coptidis and berberine as a natural drug to combat aging and aging-related diseases via anti-oxidation and AMPK activation," *Aging and Disease*, vol. 8, no. 6, pp. 760–777, 2017.

[13] L. Zhang, J. Li, F. Ma et al., "Synthesis and cytotoxicity evaluation of 13-n-alkyl berberine and palmatine analogues as anticancer agents," *Molecules*, vol. 17, no. 10, pp. 11294–11302, 2012.

[14] W. Hui, Y. Feng, X. Ruihua et al., "Comparative proteomics analysis indicates that palmatine contributes to transepithelial migration by regulating cellular adhesion," *Pharmaceutical Biology*, vol. 58, no. 1, pp. 646–654, 2020.

[15] W. C. Lee, J. K. Kim, J. W. Kang et al., "Palmatine attenuates D-galactosamine/lipopolysaccharide-induced fulminant hepatic

failure in mice," *Food and Chemical Toxicology*, vol. 48, no. 1, pp. 222–228, 2010.

[16] X. J. Zhang, Z. W. Yuan, C. Qu et al., "Palmatine ameliorated murine colitis by suppressing tryptophan metabolism and regulating gut microbiota," *Pharmacological Research*, vol. 137, pp. 34–46, 2018.

[17] Y. M. Kim, Y. M. Ha, Y. C. Jin et al., "Palmatine from _Coptidis rhizoma_ reduces ischemia -reperfusion-mediated acute myocardial injury in the rat," *Food and Chemical Toxicology*, vol. 47, no. 8, pp. 2097–2102, 2009.

[18] C. Tang, Y. Hu, H. Lyu et al., "Neuroprotective effects of 1-O-hexyl-2,3,5-trimethylhydroquinone on ischaemia/reperfusion-induced neuronal injury by activating the Nrf2/HO-1 pathway.," *Journal of Cellular and Molecular Medicine*, vol. 24, no. 18, pp. 10468–10477, 2020.

[19] E. Z. Longa, P. R. Weinstein, S. Carlson, and R. Cummins, "Reversible middle cerebral artery occlusion without craniectomy in rats," *Stroke*, vol. 20, no. 1, pp. 84–91, 1989.

[20] J. Li, K. Zhang, Q. Zhang et al., "PPAR-$\gamma$ Mediates Ta-VNS-Induced Angiogenesis and Subsequent Functional Recovery after Experimental Stroke in Rats," *BioMed Research International*, vol. 2020, Article ID 8163789, 12 pages, 2020.

[21] Y. Katayama, T. Inaba, C. Nito, S. Suda, and M. Ueda, "Neuroprotective effects of clarithromycin against neuronal damage in cerebral ischemia and in cultured neuronal cells after oxygen-glucose deprivation," *Life Sciences*, vol. 168, pp. 7–15, 2017.

[22] H. Wu, C. Tang, L. W. Tai et al., "Flurbiprofen axetil attenuates cerebral ischemia/reperfusion injury by reducing inflammation in a rat model of transient global cerebral ischemia/reperfusion," *Bioscience Reports*, vol. 38, no. 4, 2018.

[23] C. Tang, Y. Hu, J. Gao et al., "Dexmedetomidine pretreatment attenuates myocardial ischemia reperfusion induced acute kidney injury and endoplasmic reticulum stress in human and rat," *Life Sciences*, vol. 257, article 118004, 2020.

[24] C. Tang, G. Yin, C. Huang et al., "Peroxiredoxin-1 ameliorates pressure overload-induced cardiac hypertrophy and fibrosis," *Biomed Pharmacother*, vol. 129, article 110357, 2020.

[25] H. Chen, H. Yoshioka, G. S. Kim et al., "Oxidative stress in ischemic brain damage: mechanisms of cell death and potential molecular targets for neuroprotection," *Antioxidants & Redox Signaling*, vol. 14, no. 8, pp. 1505–1517, 2011.

[26] J. Anrather and C. Iadecola, "Inflammation and stroke: an overview," *Neurotherapeutics*, vol. 13, no. 4, pp. 661–670, 2016.

[27] W. Zhao, X. Zhang, Y. Chen, Y. Shao, and Y. Feng, "Downregulation of TRIM8 protects neurons from oxygen-glucose deprivation/re- oxygenation-induced injury through reinforcement of the AMPK/Nrf2/ARE antioxidant signaling pathway," *Brain Research*, vol. 1728, article 146590, 2020.

[28] J. Yu, W. N. Wang, N. Matei et al., "Ezetimibe attenuates oxidative stress and neuroinflammation via the AMPK/Nrf2/TXNIP pathway after MCAO in rats," *Oxidative Medicine and Cellular Longevity*, vol. 2020, Article ID 4717258, 14 pages, 2020.

[29] D. Tarabasz and W. Kukula-Koch, "Palmatine: a review of pharmacological properties and pharmacokinetics," *Phytotherapy Research*, vol. 34, no. 1, pp. 33–50, 2019.

[30] D. Dhingra and A. Bhankher, "Behavioral and biochemical evidences for antidepressant-like activity of palmatine in mice subjected to chronic unpredictable mild stress," *Pharmacological Reports*, vol. 66, no. 1, pp. 1–9, 2014.

[31] A. Neves Carvalho, O. Firuzi, M. Joao Gama, J. van Horssen, and L. Saso, "Oxidative stress and antioxidants in neurological diseases: is there still hope?," *Current Drug Targets*, vol. 18, no. 6, pp. 705–718, 2017.

[32] M. L. Zuo, A. P. Wang, G. L. Song, and Z. B. Yang, "miR-652 protects rats from cerebral ischemia/reperfusion oxidative stress injury by directly targeting NOX2," *Biomedicine & Pharmacotherapy*, vol. 124, article 109860, 2020.

[33] X. Hu, S. Li, D. M. Doycheva et al., "Rh-CSF1 attenuates oxidative stress and neuronal apoptosis via the CSF1R/PLCG2/PKA/UCP2 signaling pathway in a rat model of neonatal HIE," *Oxidative Medicine and Cellular Longevity*, vol. 2020, Article ID 6801587, 20 pages, 2020.

[34] M. S. Khan, A. Khan, S. Ahmad et al., "Inhibition of JNK Alleviates Chronic Hypoperfusion-Related Ischemia Induces Oxidative Stress and Brain Degeneration via Nrf2/HO-1 and NF-$\kappa$B Signaling," *Oxidative Medicine and Cellular Longevity*, vol. 2020, Article ID 5291852, 18 pages, 2020.

[35] S. Antonucci, M. Di Sante, F. Tonolo et al., "The determining role of mitochondrial reactive oxygen species generation and monoamine oxidase activity in doxorubicin-induced cardiotoxicity," *Antioxidants & Redox Signaling*, vol. 34, no. 7, pp. 531–550, 2021.

[36] L. Jiang, Y. Gong, Y. Hu et al., "Peroxiredoxin-1 overexpression attenuates doxorubicin-induced cardiotoxicity by inhibiting oxidative stress and cardiomyocyte apoptosis," *Oxidative Medicine and Cellular Longevity*, vol. 2020, Article ID 2405135, 11 pages, 2020.

[37] Z. Yang, C. Weian, H. Susu, and W. Hanmin, "Protective effects of mangiferin on cerebral ischemia-reperfusion injury and its mechanisms," *European Journal of Pharmacology*, vol. 771, pp. 145–151, 2016.

[38] J. Zhao, X. Piao, Y. Wu et al., "Cepharanthine attenuates cerebral ischemia/reperfusion injury by reducing NLRP3 inflammasome-induced inflammation and oxidative stress via inhibiting 12/15-LOX signaling," *Biomedicine & Pharmacotherapy*, vol. 127, article 110151, 2020.

[39] L. Zhang, C. Liu, C. Huang, X. Xu, and J. Teng, "miR-155 knockdown protects against cerebral ischemia and reperfusion injury by targeting MafB," *BioMed Research International*, vol. 2020, Article ID 6458204, 11 pages, 2020.

[40] B. Zhang, H. X. Zhang, S. T. Shi et al., "Interleukin-11 treatment protected against cerebral ischemia/reperfusion injury," *Biomed Pharmacothery*, vol. 115, article 108816, 2019.

[41] K. L. Lambertsen, K. Biber, and B. Finsen, "Inflammatory cytokines in experimental and human stroke," *Journal of Cerebral Blood Flow & Metabolism*, vol. 32, no. 9, pp. 1677–1698, 2012.

[42] Y. Wang, Y. Huang, Y. Xu et al., "A dual AMPK/Nrf2 activator reduces brain inflammation after stroke by enhancing microglia M2 polarization," *Antioxidants & Redox Signaling*, vol. 28, no. 2, pp. 141–163, 2018.

[43] F. Zhou, M. Wang, J. Ju et al., "Schizandrin A protects against cerebral ischemia-reperfusion injury by suppressing inflammation and oxidative stress and regulating the AMPK/Nrf2 pathway regulation," *American Journal of Translational Research*, vol. 11, no. 1, pp. 199–209, 2019.

[44] M. Wang, C. Li, and W. Shi, "Stomatin-like protein-2 confers neuroprotection effect in oxygen-glucose deprivation/reoxygenation-injured neurons by regulating AMPK/Nrf2 signalling," *Journal of Drug Targeting*, vol. 28, no. 6, pp. 600–608, 2020.

Hindawi
Oxidative Medicine and Cellular Longevity
Volume 2021, Article ID 8253742, 10 pages
https://doi.org/10.1155/2021/8253742

*Research Article*

# RXRα Blocks Nerve Regeneration after Spinal Cord Injury by Targeting p66shc

**Pei Yu**,[1] **Kai Yang**,[2] **and Min Jiang**[2]

[1]*Department of Orthopedics, Ruijin Hospital Affiliated to Shanghai Jiao Tong University School of Medicine, 97 Ruijin 2nd Road, Shanghai 200025, China*
[2]*Shanghai Key Laboratory for Prevention and Treatment of Bone and Joint Diseases, Shanghai Institute of Traumatology and Orthopaedics, Ruijin Hospital, Shanghai Jiao Tong University School of Medicine, 197 Ruijin 2nd Road, Shanghai 200025, China*

Correspondence should be addressed to Pei Yu; yupei_ortho@163.com and Min Jiang; jiangm263@163.com

Received 26 May 2020; Revised 28 December 2020; Accepted 17 January 2021; Published 10 February 2021

Academic Editor: Zhengyuan Xia



Nerve regeneration after spinal cord injury is regulated by many factors. Studies have found that the expression of retinoid X receptor α (RXRα) does not change significantly after spinal cord injury but that the distribution of RXRα in cells changes significantly. In undamaged tissues, RXRα is distributed in motor neurons and the cytoplasm of glial cells. RXRα migrates to the nucleus of surviving neurons after injury, indicating that RXRα is involved in the regulation of gene expression after spinal cord injury. p66shc is an important protein that regulates cell senescence and oxidative stress. It can induce the apoptosis and necrosis of many cell types, promoting body aging. The absence of p66shc enhances the resistance of cells to reactive oxygen species (ROS) and thus prolongs life. It has been found that p66shc deletion can promote hippocampal neurogenesis and play a neuroprotective role in mice with multiple sclerosis. To verify the function of RXRα after spinal cord injury, we established a rat T9 spinal cord transection model. After RXRα agonist or antagonist administration, we found that RXRα agonists inhibited nerve regeneration after spinal cord injury, while RXRα antagonists promoted the regeneration of injured neurites and the recovery of motor function in rats. The results showed that RXRα played an impeding role in repair after spinal cord injury. Immunofluorescence staining showed that p66shc expression was upregulated in neurons after spinal cord injury (*in vivo* and *in vitro*) and colocalized with RXRα. RXRα overexpression in cultured neurons promoted the expression of p66shc, while RXRα interference inhibited the expression of p66shc. Using a luciferase assay, we found that RXRα could bind to the promoter region of p66shc and regulate the expression of p66shc, thereby regulating nerve regeneration after spinal cord injury. The above results showed that RXRα inhibited nerve regeneration after spinal cord injury by promoting p66shc expression, and interference with RXRα or p66shc promoted functional recovery after spinal cord injury.

## 1. Introduction

Nerve regeneration after spinal cord injury is a key determinant that hinders functional recovery in injured bodies. Repair after spinal cord injury is affected by many factors, including the ability of neurons to repair themselves, the proliferation of astrocytes, the inflammatory response induced by microglia and the ability to remove apoptotic necrotic tissues, and the remyelination of oligodendrocytes. Of these, the repair ability of neurons themselves after injury is a key determinant of neurite regeneration [1]. Cholesterol is an important component in the formation of nerve cell membranes and myelin sheaths. The free cholesterol content in the brain accounts for 1/4 of the total cholesterol content in the whole body. Cholesterol in the brain is typically synthesized by the brain itself because cholesterol cannot pass through the blood-brain barrier. The synthesis, storage, transport, and exclusion of cholesterol maintain a dynamic balance, playing a crucial role in the formation and maintenance of neuroplasticity and the execution of various functions [2]. Studies have found that retinoic acid receptors (RARs) and retinoic X receptors (RXRs) form heterodimers

as ligand-activated transcription factors to promote axon regeneration and affect glial differentiation and the regulation of inflammation [3, 4]. The RXR$\alpha$-mediated transmembrane cholesterol transport system plays an important role in maintaining the balance of intracellular and extracellular cholesterol. As a ligand transcription factor, RXR$\alpha$ plays an important role in regulating cell growth, differentiation, death, and metabolism. Studies have found that the downregulation of RXR$\alpha$ expression can promote the regeneration of the caudal spinal cord of adult salamanders [5]. RXR$\alpha$ is expressed in the cytoplasm of neurons, astrocytes, and some oligodendrocytes before spinal cord injury; after spinal cord injury, RXR$\alpha$ is expressed in the nucleus of neurons, astrocytes, and activated microglia [3]. After entering the nucleus, RXR$\alpha$ can interact with RAR$\beta$ and other molecules to bind to the promoter region of downstream regulatory genes and participate in promoting or inhibiting the expression of downstream signaling proteins [6]. p66shc protein, which is encoded by the protooncogene shcA, is involved in the regulation of reactive oxygen species (ROS) levels and age-related organ dysfunction. Knockout of the p66shc gene can prolong the lifespan of mice. p66Shc is highly expressed in neural stem cells and neural precursor cells, but its expression is significantly reduced in adult individuals [7]. Studies have shown that the expression level of brain-derived neurotrophic factor (BDNF) at the base of the hippocampus in p66shc$^{-/-}$ mice is significantly increased, thereby improving the cognitive ability and anti-inflammatory ability of mice [8]. Studies have found that p66shc plays a role in the regulation of redox and energy metabolism in neurons [9]. p66shc can also be used as a regulator of neuronal differentiation and proliferation during neuron development [10]. Therefore, we speculate that p66shc plays an important role in repair after spinal cord injury. Our study found that RXR$\alpha$ inhibited neurite regeneration and functional recovery after spinal cord injury in rats. The expression of p66shc was upregulated after spinal cord injury, and p66shc colocalized with RXR$\alpha$. We also demonstrated that RXR$\alpha$ inhibited neurite regeneration after spinal cord injury by downregulating p66shc expression. Currently, there are few studies on the function of RXR$\alpha$ and p66shc after spinal cord injury. Therefore, in this study, we focused on the role of RXR$\alpha$ in the regeneration of neurites after spinal cord injury via regulating the expression of p66shc.

## 2. Material and Methods

*2.1. Rat Spinal Cord Injury Model.* Animal experiments were approved by the ethics review committee of Ruijin Hospital affiliated with Shanghai Jiao Tong University, China. A total of 360 Sprague-Dawley (SD) rats (8-week-old, male) were purchased from Shanghai Laboratory Animal Center (SLAC), China. Animals were housed in a ventilated room at constant temperature (24°C), in 50-60% humidity, and under a 12-hour light/dark cycle, with standard rat diet and free access to water. After 1 week of feeding, a dorsal hemisection was performed at the T9 segment of the spinal cord. Rats that only underwent laminectomy and hemisection were used as the sham control group. The bladder was manually emptied every 8 hours after injury. Three hundred sixty rats were randomly divided into 4 groups: sham control group ($n = 90$), injury group ($n = 90$), RXR$\alpha$ agonist group ($n = 90$), and RXR$\alpha$ antagonist group ($n = 90$). Five rats in each group were used for tissue sectioning, 5 rats were used for RNA extraction, and 5 rats were used for protein extraction. Each group of rats was evaluated for motor function at 3 days, 1 week, 2 weeks, 3 weeks, 4 weeks, and 5 weeks after spinal cord injury, and tissues were collected to be used in the above experiments after motor function evaluation. The RXR$\alpha$ agonist CD3254 (MCE, USA) was administered at 100 mg/kg/day by gavage, and the RXR$\alpha$ antagonist PA452 (MCE, USA) was administered at 1 mg/kg/day by gavage. Drugs were given starting the first day after injury until tissue collection.

*2.2. Primary Neuron Culture and In Vitro Injury Model.* Rat spinal cord tissue from 18-day-old embryos was collected for primary spinal cord neuron culture. Tissues were removed and digested with 0.05% trypsin-ethylene diamine tetraacetic acid (EDTA) (Thermo Scientific, USA) at 37°C for 15 min. After the cells were pipetted into a single cell suspension, Dulbecco's modified Eagle's medium (DMEM)+10% fetal bovine serum (FBS) (Thermo Scientific, USA) was added and mixed, and then, the cells were seeded in 6-well plates. After 4 hours, the culture medium was replaced with Neurobasal+1% $N_2$+2% B27 (Thermo Scientific, USA) culture medium for 3-10 days. Primary spinal neurons cultured *in vitro* were used for the scratch assay after 3 days. A cell scraper or 20 $\mu$l pipette tip was used to scratch the cell monolayer. *In vitro* culture was continued for 7-10 days to observe the regeneration of neurites after *in vitro* neuronal injury. The final concentrations of the RXR$\alpha$ agonist CD3254 and RXR$\alpha$ antagonist PA452 in the *in vitro* culture system were 50 $\mu$g/l and 0.1 $\mu$M, respectively.

*2.2.1. Primary Spinal Cord Slice Culture.* SD rat embryonic (E) 18-day-old rat spinal cord tissue (thoracolumbar spinal cord segment) was collected for spinal cord slice culture. After cutting the spinal cord tissue into thin slices with microscissors, tissues were placed on a coverslip precoated with Matrigel (R&D, USA). The coverslips were placed into a 24-well plate, 200 $\mu$l of culture medium (DF12+10% FBS) was then added, and the plate was placed in an incubator to culture for 4 hours; subsequently, 300 $\mu$l of medium (DF12 +10% FBS) was added, and the cells were cultured for another 7 days, with the medium being changed every other day. After 7 days of culture, the growth of neurites was observed. If the growth of the neurites was good, the neurites were removed along the spinal cord slices with a blade under a microscope, and the *in vitro* culture was continued for 7-10 days to observe the regeneration of neurites after *in vitro* neuronal injury. The measurement of neurites was performed using 3 slices per group, and 10 fields of view (200x magnification) were observed under a microscope (Olympus, Japan) for each slice. The lengths of neurites in all images were measured and averaged. Comparisons between groups were performed. In the spinal cord slices, the lengths of all neurites were measured and compared between groups.

*2.3. Immunohistochemical Staining and Immunofluorescence Staining.* Rats were anesthetized with 2% sodium pentobarbital (Sinopharm Group Co., Ltd., China), perfused with 100 ml of normal saline (Sinopharm Group Co., Ltd., China), and fixed with 200 ml of 4% paraformaldehyde (Beyotime, China). Spinal cord tissue was removed and placed in paraformaldehyde at 4°C overnight and then sequentially replaced with 20% sucrose (Sinopharm Group Co., Ltd., China) and 30% sucrose for dehydration; the samples were then used for frozen tissue sectioning. The thickness of each frozen section was 15-20 $\mu$m. The tissue sections were placed on a metal sectioning rack in a beaker containing sodium citrate, an antigen retrieval solution (Beyotime, China). The antigen retrieval solution in the beaker covered the tissue sections. The solution was heated to 95°C for 15 min, followed by natural cooling to room temperature; then, the sections were washed with 0.01 M PBS (Beyotime, China) for 5 min, 3 times, and incubated with 3% $H_2O_2$ (Beyotime, China) at room temperature for 10 min to inactivate endogenous peroxidases. The samples were then washed with 0.01 M PBS for 5 min, 3 times, and incubated with blocking solution containing 5% normal goat serum (Beyotime, China) at room temperature for 30 min. Rat $\beta$-III-tubulin antibody (Abcam, USA) was diluted 1 : 1000 in primary antibody dilution solution (Beyotime, China), mixed well, added dropwise onto the surface of the tissue, and incubated at 37°C for 2 hours, followed by the dropwise addition of polymerized HRP-labeled anti-rabbit/rat IgG (Beyotime, China). The samples were incubated at 37°C for 30 min and washed with PBS for 2 min, 3 times; DAB was used for color development. Immunofluorescence staining was performed as follows. Tissue sections or coverslips were incubated with blocking solution containing 5% normal goat serum for 30 min at room temperature. Rat $\beta$-III-tubulin antibody was diluted 1 : 500, rat RXR$\alpha$ antibody was diluted 1 : 500 (Abcam, USA), and rabbit p66shc antibody was diluted 1 : 200 in primary antibody dilution solution, mixed well, and added dropwise to the surface of the tissue; the samples were incubated at 4°C overnight and then washed with 0.01 M PBS for 10 min, 3 times. Goat anti-mouse 488 secondary antibody and goat anti-rabbit 555 secondary antibody (Thermo Scientific, USA) were diluted 1 : 500 in secondary antibody dilution solution, mixed well, and added dropwise to the surface of tissues or cells; the samples were incubated at 37°C for 1 hour and then washed with 0.01 M PBS for 10 min, 3 times. DAPI (Thermo Scientific, USA) staining solution was added dropwise to the tissue sections. The slices were covered with coverslips, and the staining results were observed under an upright fluorescence microscope (Olympus, Japan).

*2.4. Lentivirus Transfection and Luciferase Assay.* Lentiviruses for the interference and overexpression of RXR$\alpha$ and p66shc were purchased from Shanghai Genechem Co., Ltd., China, with a titer of $1 \times 10^8$ TU/ml. Neurobasal medium was used to prepare a suspension of primary neuronal cells at a density of $5 \times 10^6$ cells/ml, and the cells were seeded in 6 cm Petri dishes. When the inoculation density reached more than 90%, 400 $\mu$l of virus infection enhancement solution HitransG A and 100 $\mu$l of lentivirus or negative control (neg-control), each with a titer of $1 \times 10^8$ TU/ml, were added, and the cells were incubated at 37°C for 24 hours. The medium was changed every other day for continued culture. Approximately 72 hours after infection, the infection efficiency (number of GFP-positive cells) was observed. When the efficiency reached or exceeded 90%, infection was considered successful, and subsequent experiments were performed.

*2.5. Evaluation of Motor Function after Spinal Cord Injury.* The assessment of motor function after spinal cord injury was performed using the Basso Mouse Scale (BMS) motor score, the rotarod test, and footprint length. BMS motor scoring involved placing the rats in an open field (diameter: 100-200 cm), after which the rats were observed by 2 trained observers for 4 min; the score ranged from 0 to 9 points (0 points: complete hindlimb paralysis; 9 points: normal motor function). The results of this study were based on the results of hindlimb motor performance in an open field, including hindlimb joint movement, weight support, plantar stepping, coordination, paw position, and trunk and tail control. For the rotarod test, pretrained animals were placed on a carousel with an accelerating rotation speed of 3 to 15 rpm (revolutions per minute) for more than 2 min. Five tests were conducted each time. The latent period of the rats on the rotating rod was recorded according to the time when the rats fell in each experiment, and then, the times were averaged to obtain the final result for each experiment. Footprint length was measured using an unbiased step-scanning device. All rats walked on the electronic treadmill belt at a speed of 11 cm/s for 20 seconds. The digital data (footprint and body movement) were analyzed using TreadScan software (CleverSys Inc., Reston, VA). Each parameter was compared between the ipsilateral and contralateral sides and between the treatment group and the control group.

*2.6. Western Blot.* Tissue or cellular protein was extracted and subjected to BCA protein quantification to determine protein concentration. Sodium dodecyl sulfate-polyacrylamide gel electrophoresis (SDS-PAGE) was performed. Twenty micrograms of total protein was loaded onto each well for gel electrophoresis. The proteins were transferred to a PVDF membrane (Millipore, USA) and blocked at room temperature for 30 min. Primary antibodies, i.e., mouse polyclonal RXR$\alpha$ antibody (Abcam, USA), rabbit polyclonal shc antibody (Abcam, USA), and the corresponding secondary antibodies, i.e., goat anti-mouse HRP (CST, USA) and goat anti-rabbit HRP (CST, USA), were used to protein bands. Protein quantification was performed using IPP software. The differences between groups were compared.

*2.7. Real-Time PCR.* Samples were collected according to the conventional RNA extraction method. One milliliter of TRIzol (Invitrogen, USA) was added to cells and vascular tissues, and then, 200 $\mu$l of chloroform (Sinopharm Group Co., Ltd., China) was added; the samples were mixed, allowed to stand for 10 min, and centrifuged at 12000 rpm for 15 min at 4°C. The upper aqueous phase was transferred to a new RNase-free EP tube. Five hundred microliters of isopropanol was

added, and the samples were mixed well. After standing for 10 min, the samples were centrifuged at 12000 g for 10 min. The supernatant was discarded, and the RNA pellet was washed with 75% ethanol and dried. When the RNA pellet became colorless and transparent, 30 $\mu$l of diethyl pyrocarbonate (DEPC) water was added to dissolve the RNA, which was then stored at -80°C. Quantitative PCR detection of genes was performed using a TB Green® Premix Ex Taq™ kit (Takara, Japan). A 20 $\mu$l reaction system was used, with the following reaction conditions: predenaturation at 95°C for 30 seconds, followed by 40 cycles of 95°C for 5 seconds and 60°C for 30 seconds. The amplification curve and melting curve were confirmed after the reaction. The relative amount of the detected gene was calculated according to the formula $2^{-\Delta\Delta CT}$. Comparisons between groups were performed. The following were the primer sequences: p66shc: forward: 5′-GATTCAATTCCGGAGTTCTTA-3′, reverse: 5′-TTAGATCCATTCCCGAATTG-3′ and GADPH: forward: 5′-CTTGCTCAAGCTTAGTTCTAGG-3′, reverse: 5′-GAGTGCTCAGTGGTATTGC -3′.

*2.8. Luciferase Assay.* Primary cultured neurons were seeded in 6-well plates at a density of $2 \times 10^5$ per well. Lentivirus containing either PDS131_psiCHECK-2 blank vector (6273 bp), PDS131_psiCHECK-2-p66shc wild-type, or PDS131_psiCHECK-2-p66shc mutant (mut, deletion mutation of "GGCTATTCGTA" in the promoter region of the wild-type p66shc gene) (Shanghai Genechem Co. Ltd., Shanghai, China) was added to neurons, with an inoculation density above 90%. After 72 hours of transfection, the luciferase activity in each group was detected using a dual-luciferase reporter gene detection system (Beyotime, China). First, the corresponding value of the fluorescence emitted by firefly luciferase- (FL-) induced substrate was detected using a microplate reader, and then, the fluorescence released by Renilla luciferase- (RL-) induced substrate was detected using a microplate reader. The measured FL to RL ratio for each sample was used as the relative luciferase activity of the reporter gene.

*2.9. Statistical Analysis.* All statistical results were analyzed using SPSS 17.0 (SPSS Inc., Chicago, USA). All quantitative indicators are expressed as the mean ± SD. The experimental data were analyzed using one-way analysis of variance and Tukey's post hoc test. $P < 0.05$ indicated significant differences between groups.

## 3. Results

*3.1. RXRα Inhibited Neurite Regeneration after Spinal Cord Injury in Rats.* First, we clarified the role of RXRα in neurite regeneration after spinal cord injury. The results showed that an RXRα agonist inhibited neuronal repair after spinal cord injury, while an RXRα antagonist promoted neuronal repair after spinal cord injury. Furthermore, the RXRα agonist caused a large number of neurons around the injury site to lose their normal morphological characteristics; that is, they were in an apoptotic state, making it difficult for neurite regeneration. The RXRα antagonist protected neurons after spinal cord injury and maintained their morphological characteristics; neurite regeneration was superior to that in the spinal cord injury group (Figure 1(a)). *In vitro* cultured neuronal injury experiments also showed that after neuronal injury, the administration of the RXRα agonist led to neurite growth suppression, while the administration of the RXRα antagonist promoted neurite growth, results that were significantly different from those in the control group (Figure 1(b)). We also used spinal cord slice culture to further clarify the role of RXRα in the regeneration of spinal cord neurites. When the neurites were cut along the periphery of the spinal cord slices and the RXRα agonist or RXRα antagonist was administered, it was found that in the RXRα agonist group, spinal cord slices only grew a small number of neurites, and their lengths were short; in the RXRα antagonist group, neurite regeneration was significantly promoted after injury. We also observed that the addition of the RXRα agonist to the spinal cord slices before injury also inhibited neurite growth (Figure 1(c)). The above results indicate that RXRα can inhibit the growth and regeneration of spinal cord neurites.

*3.2. RXRα Inhibited Functional Recovery after Spinal Cord Injury in Rats.* Because RXRα inhibited the regeneration of spinal cord neurites, does RXRα affect the recovery of motor function in rats after spinal cord injury? We used the BMS motor score, rotarod test, and footprint length to observe the motor function of rats at 3 days, 1 week, 2 weeks, 3 weeks, 4 weeks, and 5 weeks after spinal cord injury. The results showed that the BMS motor scores of rats in all groups were close to 0 at 3 days after injury. The motor scores gradually increased with the injury time. At 4 weeks after injury, the motor scores of rats treated with the RXRα antagonist were significantly higher than those of rats in the spinal cord injury group. At 5 weeks after injury, the motor scores of the rats treated with RXRα agonist were significantly lower than those of rats in the spinal cord injury group (Figures 2(a) and 2(b)), indicating that inhibition of RXRα can promote functional recovery after spinal cord loss in rats. The results of the rotarod test showed that neither the RXRα agonist nor antagonist affected the rotarod test time for rats at 3 weeks after injury. Five weeks after spinal cord injury, the rotarod test time of rats treated with the RXRα agonist was significantly shorter than that of rats in the spinal cord injury group, while the rotarod test time of rats treated with the RXRα antagonist was significantly longer than that of rats in the spinal cord injury group, which also showed that RXRα blocked the recovery of motor function after spinal cord injury in rats (Figure 2(c)). Footprint length measurement experiments also showed that RXRα blocked the recovery of motor function after spinal cord injury in rats (Figure 2(d)). Based on the above research results, RXRα inhibits functional recovery after spinal cord injury in rats.

*3.3. The Expression of p66shc Was Upregulated after Spinal Cord Injury and Colocalized with RXRα.* As a ligand-activated transcription factor, RXRα regulates downstream signaling molecules and is involved in the inhibition of neurite regeneration after spinal cord injury. We used

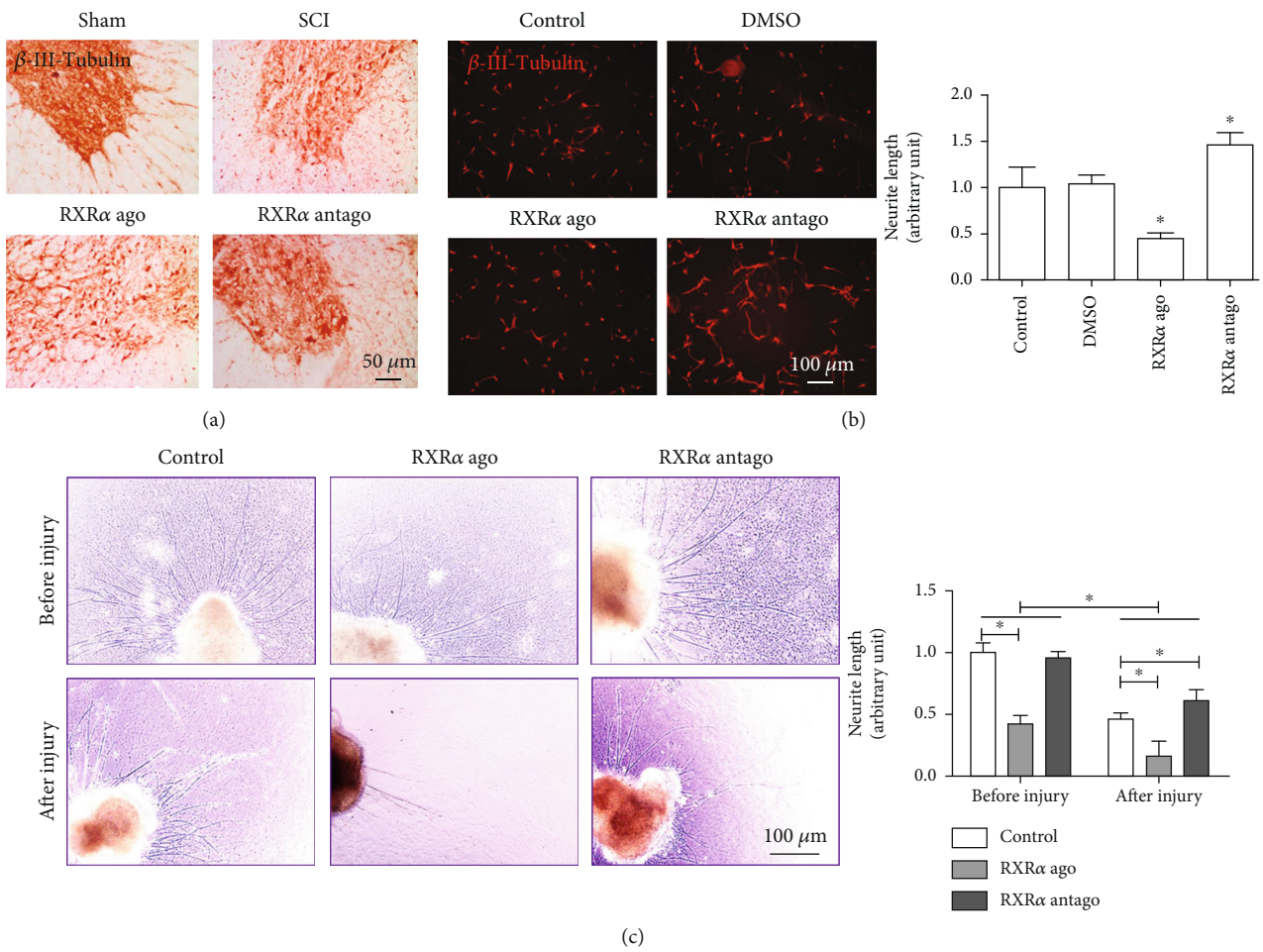


Figure 1: RXRα inhibited nerve regeneration after spinal cord injury. (a) β-III-Tubulin immunohistochemical staining showed that after spinal cord injury, the number of neuronal cells in the injured area was reduced, and the neurite continuity was interrupted. After RXRα agonist administration, the morphology of the tissue lacked integrity, and the neurons were in an apoptotic state; there were no continuous neurites. After RXRα antagonist administration, the number of neuronal cells increased, the cell morphology was good, and there was some neurite regeneration. (b) β-III-Tubulin immunofluorescence staining of primary spinal cord neuronal cells cultured *in vitro* showed that after scratch damage, the length of neurites in the RXRα agonist group was significantly shorter than that of neurites in the control group, while the length of neurites in the RXRα antagonist group was significantly longer than that of neurites in the control group. The results suggest that RXRα inhibits neurite regeneration after spinal cord injury. (c) Compared with that of neurites in the postinjury control group, the length of the regenerated neurites in the spinal cord slices cultured *in vitro* in the RXRα agonist group was significantly shortened after injury, while the length of the regenerated neurites in the RXRα antagonist group significantly increased. The length of postinjury neurites in each group was significantly shorter than that before injury. $N = 5$/group; *vs. control, $P < 0.05$, scale bar: 50 or 100 μm.

immunofluorescence staining to find that p66shc, a protein associated with cell senescence and oxidative stress, was expressed at low levels before spinal cord injury; p66shc expression significantly increased after spinal cord injury, and p66shc colocalized with RXRα (Figure 3(a)). We also found the same phenomenon in primary spinal neurons cultured *in vitro*; that is, the expression of p66shc in spinal cord neurons before injury was significantly lower than that after injury, and p66shc colocalized with RXRα in neuronal cells (Figure 3(b)). Based on the above research results, we speculate that RXRα may participate in the regulation of neurite regeneration after spinal cord injury by regulating p66shc expression.

*3.4. RXRα Regulated p66shc Expression after Spinal Cord Injury.* To further verify the regulatory relationship between RXRα and p66shc, we constructed RXRα overexpression and interference lentiviral plasmids to observe whether RXRα regulated p66shc expression in neuronal cells. The results showed that RXRα overexpression promoted p66shc expression in neurons, while RXRα interference also inhibited p66shc expression in neurons (Figure 4(a)). Therefore, RXRα regulates p66shc expression. Does RXRα play a direct or indirect role in the regulation of p66shc expression? We first examined the effect of RXRα overexpression or interference on the mRNA level of p66shc. We found that after RXRα overexpression, the expression of p66shc increased at

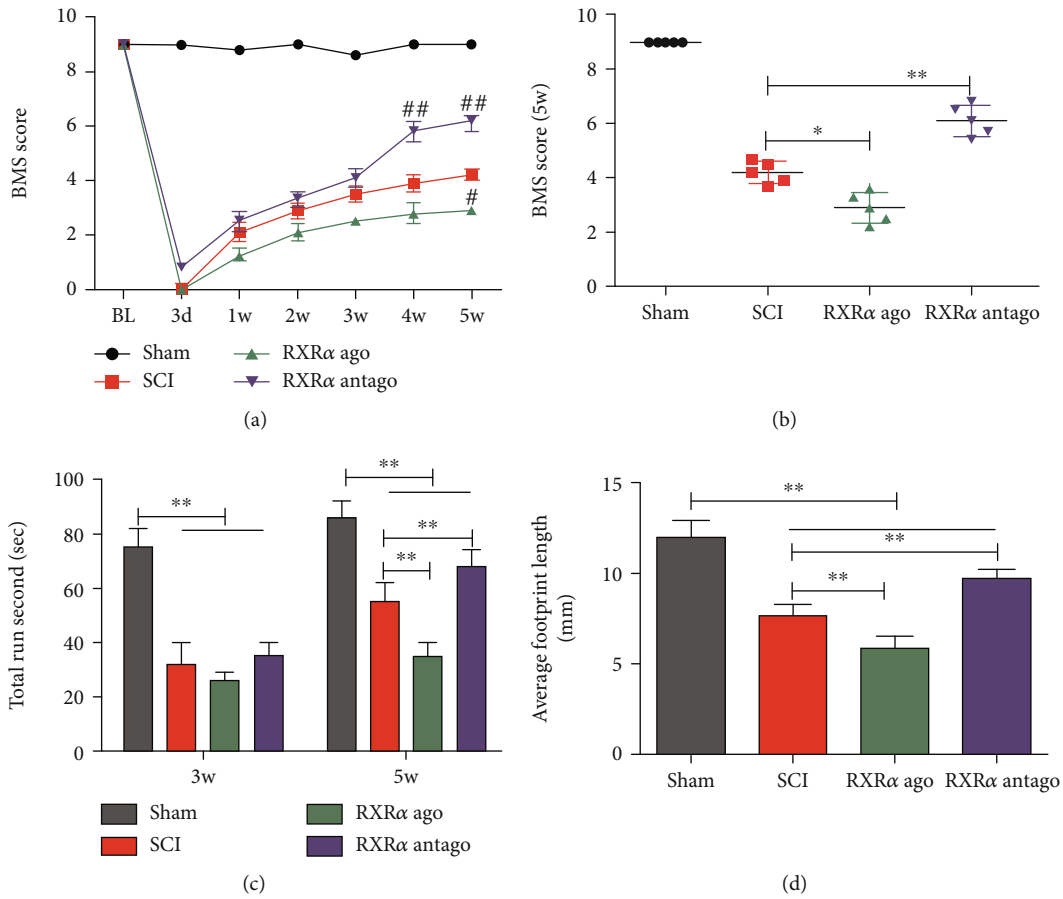


Figure 2: RXRα inhibited functional recovery after spinal cord injury in rats. (a) The BMS motor scores of rats in all groups were close to 0 at 3 days after injury. The motor scores gradually increased with the injury time. At 4 weeks after injury, rats that received RXRα antagonist had significantly higher motor scores than did rats in the spinal cord injury group, whereas the rats that received RXRα agonist had significantly lower motor scores than did rats in the spinal cord injury group 5 weeks after injury. (b) Five weeks after injury, the BMS motor scores of rats that received RXRα agonist were significantly lower than those of rats in the spinal cord injury group, and the BMS motor scores of rats that received RXRα antagonist were significantly higher than those of rats in the spinal cord injury group. (c) Rotarod test results showed that neither the RXRα agonist nor antagonist affected the rotarod test time for rats at 3 weeks after injury. The rotarod test time for rats given the RXRα agonist was significantly shorter than that for rats in the spinal cord injury group at 5 weeks after spinal cord injury. The rotarod test time for rats given RXRα antagonist was significantly longer than that for rats in the spinal cord injury group, indicating that RXRα hindered the recovery of motor function after spinal cord injury in rats. (d) Footprint length experiments showed that the distance between the 2 footprints for rats in the RXRα agonist group was significantly shorter than that for rats in the control group and the spinal cord injury group, while the distance between 2 footprints was significantly longer for the rats in the RXRα antagonist group than that for rats in the control group; however, recovery to the preinjury level was not attained. $N = 5$/group. $^{*}$vs. control, $P < 0.05$; $^{**}$vs. control, $P < 0.01$; $^{\#}$vs. spinal cord injury (SCI) group, $P < 0.05$; $^{\#\#}$vs. SCI group, $P < 0.01$.

the mRNA level; after RXRα interference, the expression of p66shc decreased at the mRNA level. Therefore, a luciferase assay was performed to further verify whether RXRα can bind to the promoter region of p66shc. The results showed that RXRα could indeed bind to the promoter region of p66shc and participate in the regulation of p66shc expression (Figure 4(b)).

*3.5. RXRα Inhibited Neurite Regeneration after Spinal Cord Injury by Downregulating p66shc Expression.* Based on the above results, we further verified the effect of RXRα targeting of p66shc on neurite regeneration after spinal cord injury. We added an RXRα agonist to spinal cord neurons with p66shc interference and found that the RXRα agonist did not inhibit neurite regeneration after spinal cord injury. Similarly, we added an RXRα antagonist to spinal cord neurons overexpressing p66shc and found that the RXRα antagonist did not promote neurite regeneration after spinal cord injury (Figures 5(a) and 5(b)). The above results demonstrate that RXRα inhibited neurite regeneration after spinal cord injury by downregulating p66shc expression.

## 4. Discussion

The loss of body function caused by spinal cord injury severely affects the quality of life of patients. Promoting neurite regeneration and functional recovery after spinal cord injury is an urgent issue that needs to be addressed [1, 11]. Current treatment methods for spinal cord injury include high-dose hormone use at the early stage and rehabilitation

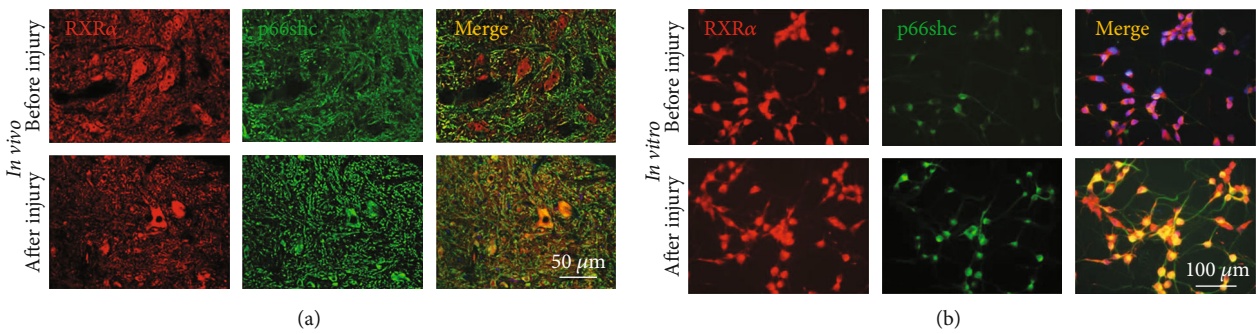


Figure 3: Expression of p66shc before and after spinal cord injury. Immunofluorescence staining showed that there was no significant difference in the expression of RXR$\alpha$ before and after spinal cord injury (rat spinal cord tissue (a) and primary neurons cultured *in vitro* (b)), while p66shc was expressed at low levels before spinal cord injury and the expression significantly increased after spinal cord injury. p66shc was colocalized with RXR$\alpha$. $N = 5$/group, scale bar: 50 or 100 $\mu$m.

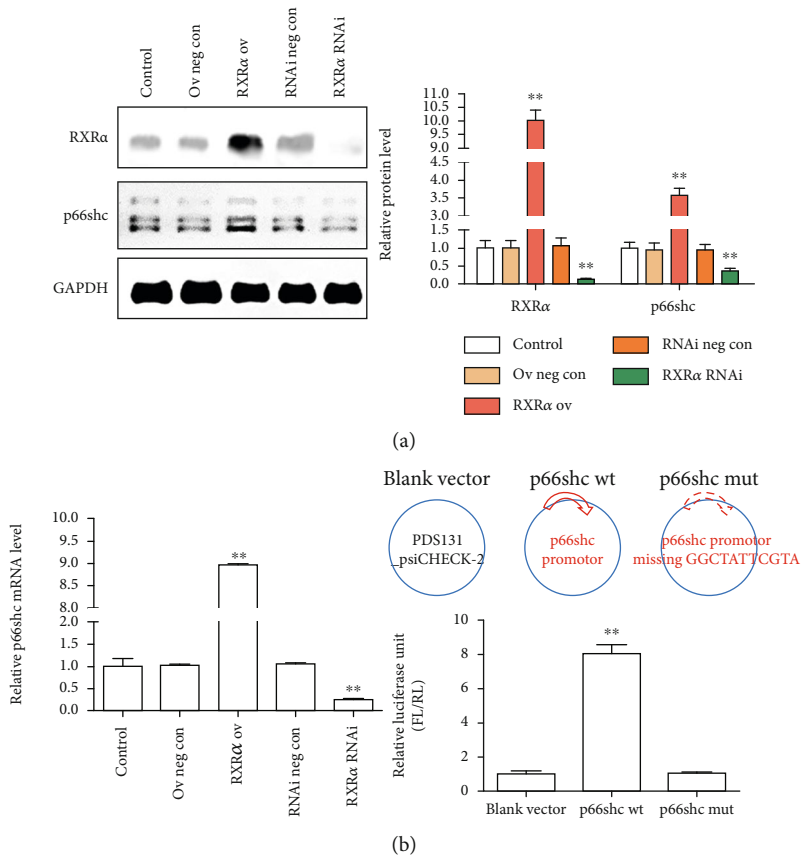


Figure 4: RXR$\alpha$ promoted p66shc expression after spinal cord injury. (a) Western blot analysis showed that RXR$\alpha$ overexpression promoted p66shc expression in primary spinal cord neurons cultured *in vitro*, while RXR$\alpha$ interference inhibited p66shc expression in primary spinal cord neurons cultured *in vitro*. (b) Real-time PCR and luciferase assays showed that RXR$\alpha$ inhibited the expression of p66shc at the mRNA level by binding to the promoter region of p66shc. $N = 5$/group; $^{**}$vs. control, $P < 0.01$.

at the late stage [12–14]. The study of nerve regeneration after spinal cord injury will provide a basis for the treatment of spinal cord injuries. RXR, as a member of the nuclear hormone receptor superfamily, mediates the cellular biological effects of various hormones and drugs [15, 16]. The increase in retinal dehydrogenase activity after spinal cord injury is the first direct evidence that retinoid acid (RA) substances participate in the physiological response to spinal cord injury. Injury leads to a significant increase in retinaldehyde dehydrogenase 2 (RALDH2) activity, reaching a peak 8-14 days after injury [17, 18]. In the uninjured rat spinal cord, RALDH2 is only present in the meninges, oligodendrocytes, pericytes, and NG2-positive glial cell populations around the injury site [18, 19]. After spinal cord injury, the expression of RARs only changes slightly, but the cell distribution changes significantly. In noninjured tissue, RAR$\alpha$, RXR$\alpha$, and RXR$\beta$

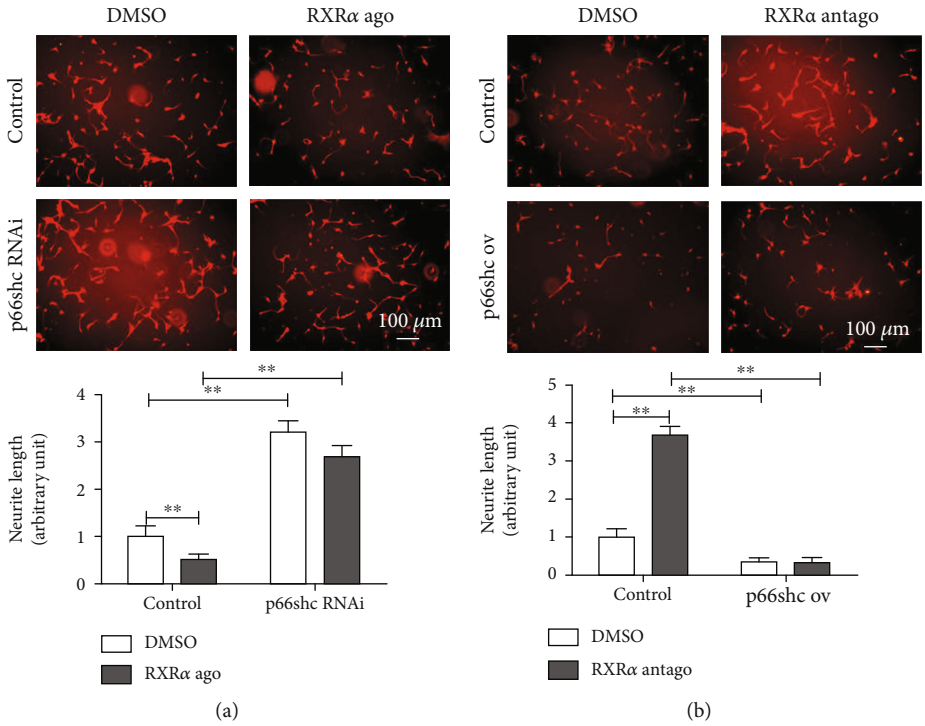


Figure 5: RXR$\alpha$ inhibited neurite regeneration after spinal cord injury by downregulating p66shc expression. (a) RXR$\alpha$ agonist significantly inhibited neurite regeneration of the cultured primary spinal cord neurons; this effect can be blocked by p66shc interference in the *in vitro* cultured primary spinal cord neurons. (b) RXR$\alpha$ antagonist significantly promoted neurite regeneration of the cultured primary spinal cord neurons; this effect was blocked by p66shc overexpression. $N = 5$/group. $^{*}$vs. control, $P < 0.05$; $^{**}$vs. control, $P < 0.01$; scale bar: 100 $\mu$m.

are found in the cytoplasm of motor neurons and glial cells. In the neurons that survive injury, there is nuclear localization of RAR$\alpha$, RXR$\alpha$, and RXR$\beta$ [3]. In the context of increased local RA synthesis, the observation of the translocation of RARs to the nucleus indicates that neurons, glial cells, and macrophages are the targets of RA signaling after spinal cord injury, which is consistent with spinal cord development data [20–23]. Studies have shown that the RA-RAR$\beta$ pathway may have transcriptional inhibitory effects on axon regeneration and myelination signaling pathways [6]. RAR$\beta$ can bind to RXR and then bind to the promoter region of downstream target proteins to participate in signal regulation [24]. However, the role and regulatory mechanism of RXR$\alpha$ in rat spinal cord injury remain unclear. Using a rat spinal cord injury model, we observed that RXR$\alpha$ played a role in inhibiting neuronal regeneration after spinal cord injury. This effect can be achieved by regulating the aging-related and oxidative stress-related protein p66shc.

Studies have shown that the activation of p66shc by redox stress is associated with a shortened life span and mitochondrial dysfunction. However, it is still unclear how p66shc provides neuroprotective effects on secondary stress. After an injury response or an oxidative stress response, p66shc relocates to the nucleus and mitochondria to participate in the regulation of mitochondrial function and oxidative stress [25, 26]. After spinal cord injury, severe oxidative stress responses occur in the injured area, and injured cells simultaneously initiate 2 signaling pathways: apoptosis and repair. In p66shc knockout mice, hippocampal neurons maintain certain nerve regeneration and participate in the regulation of hippocampal neuron aging [27, 28]. Is p66shc associated with nerve regeneration after spinal cord injury? Our study found that the expression of p66shc was upregulated after spinal cord injury. The upregulation of p66shc as an aging gene promoted cell senescence, and the regenerative ability of the injured neurons was reduced. The increased expression of the aging gene p66shc further inhibited neurite regeneration. Is the increase in p66shc expression regulated by RXR$\alpha$? We used *in vivo* and *in vitro* studies to demonstrate that RXR$\alpha$ binds to the promoter region of p66shc and promotes the expression of p66shc, thereby further inhibiting regeneration after spinal cord injury. p66shc is a protein associated with the extensive regulation of cellular oxidative stress and aging. Its physiological and pathological functions are not limited to the inhibition of neurite regeneration after spinal cord injury. We speculate that p66shc is also involved in regulating the survival and aging of spinal cord neurons after injury. Neuronal survival and aging also play important roles in the repair of spinal cord injury, which needs to be further studied.

As a transcription factor, RXR$\alpha$ regulates the expression of a variety of target genes. As a senescence-related and oxidative stress-related protein, p66shc is also widely involved in the regulation of cell functions. This study only focused on RXR$\alpha$ and its downstream target gene p66shc, resulting in certain limitations. However, both RXR$\alpha$ and p66shc have wide ranges of functions in the body, and their roles in spinal cord injury are not clear. Therefore, we first need to clarify

the function of RXR$\alpha$ and p66shc after spinal cord injury and then further study the mechanism of action. The present study demonstrates that RXR$\alpha$ and p66shc play negative regulatory roles in neural regeneration after spinal cord injury. RXR$\alpha$ achieves this negative regulatory function through the targeted promotion of p66shc expression. However, in the inhibition of regeneration after spinal cord injury, in addition to regulating the expression of p66shc, are more downstream target genes involved in the regulation of neuronal function after spinal cord injury? In addition to inhibiting neurite regeneration, does p66shc also inhibit repair after spinal cord injury by exacerbating oxidative stress and promoting neuronal apoptosis and aging? Recent research reported that repressor activator protein 1 (Rap1), an established telomere-associated protein, which is essential for the maintenance of telomere structural integrity, acted as a novel modulator of hypoxia-induced apoptosis in myocardial ischemia/reperfusion injury [29]. Telomere, which defines the ends of chromosome, has close relationship with cell senescence and apoptosis [30]; therefore, Rap1 is an important senescence-associated protein. p66shc is an oxidoreductase that promotes mammalian aging by producing reactive oxygen species in mitochondria, hydrogen peroxide ($H_2O_2$) stress was used as an artificial means of aging in the cells, and this resulted in RAP1 levels decreasing; whether Rap1 is related to neuronal apoptosis, aging, and regeneration after SCI remains to be further studied; we speculate that p66shc promotes the production of reactive oxygen species in mitochondria, decreases the level of telomere binding protein Rap1, and shortens telomere lengths, leading to cell senescence; in-depth research is still needed to address these questions.

## Data Availability

The accessibility data used to support the findings of this study were collected according to scientific research criteria and can be available from the corresponding authors upon request.

## Conflicts of Interest

The authors declare that they have no conflicts of interest.

## Authors' Contributions

Pei Yu collected the experimental data and wrote the manuscript. Pei Yu and Min Jiang supervised the whole project. Experiments were performed by Pei Yu and Kai Yang. Pei Yu and Kai Yang contributed equally to this work and should be considered co-first authors.

## Acknowledgments

This study was funded by the Youth Science and Technology Innovation Studio of Shanghai Jiaotong University School of Medicine (JYKCGZS01).

## References

[1] D. Holmes, "Spinal-cord injury: spurring regrowth," *Nature*, vol. 552, no. 7684, p. S49, 2017.

[2] D. Wang and W. Zheng, "Dietary cholesterol concentration affects synaptic plasticity and dendrite spine morphology of rabbit hippocampal neurons," *Brain Research*, vol. 1622, pp. 350–360, 2015.

[3] K. Schrage, G. Koopmans, E. A. J. Joosten, and J. Mey, "Macrophages and neurons are targets of retinoic acid signaling after spinal cord contusion injury," *The European Journal of Neuroscience*, vol. 23, no. 2, pp. 285–295, 2006.

[4] J. Mey, "New therapeutic target for CNS injury? The role of retinoic acid signaling after nerve lesions," *Journal of Neurobiology*, vol. 66, no. 7, pp. 757–779, 2006.

[5] S. E. Walker, R. Nottrodt, L. Maddalena, C. Carter, G. E. Spencer, and R. L. Carlone, "Retinoid X receptor alpha downregulation is required for tail and caudal spinal cord regeneration in the adult newt," *Neural Regeneration Research*, vol. 13, no. 6, pp. 1036–1045, 2018.

[6] R. Puttagunta and S. Di Giovanni, "Retinoic acid signaling in axonal regeneration," *Frontiers in Molecular Neuroscience*, vol. 4, p. 59, 2012.

[7] T. Nakamura, S. Muraoka, R. Sanokawa, and N. Mori, "N-Shc and Sck, two neuronally expressed Shc adapter homologs: their differential regional expression in the brain and roles in neurotrophin and Src signaling," *The Journal of Biological Chemistry*, vol. 273, no. 12, pp. 6960–6967, 1998.

[8] A. Berry, D. Carnevale, M. Giorgio et al., "Greater resistance to inflammation at adulthood could contribute to extended life span of $p66^{Shc-/-}$ mice," *Experimental Gerontology*, vol. 45, no. 5, pp. 343–350, 2010.

[9] A. M. Kleman, J. E. Brown, S. L. H. Zeiger et al., "p66(shc)'s role as an essential mitophagic molecule in controlling neuronal redox and energetic tone," *Autophagy*, vol. 6, no. 7, pp. 948-949, 2014.

[10] L. Abballe, A. Mastronuzzi, E. Miele et al., "Numb isoforms deregulation in medulloblastoma and role of p66 isoform in cancer and neural stem cells," *Frontiers in Pediatrics*, vol. 6, p. 315, 2018.

[11] D. Holmes, "Repairing the neural highway," *Nature*, vol. 552, no. 7684, pp. S50–S51, 2017.

[12] K. D. Kim and J. D. Ament, "Spinal cord injury Treatment," *Spine*, vol. 42, Supplementary 7, p. S21, 2017.

[13] J. J. Wyndaele, "Developing a spinal cord injury research strategy," *Spinal Cord*, vol. 53, no. 10, p. 713, 2015.

[14] S. K. Frye, A. Ogonowska-Slodownik, and P. R. Geigle, "Aquatic exercise for people with spinal cord injury," *Archives of Physical Medicine and Rehabilitation*, vol. 98, no. 1, pp. 195–197, 2017.

[15] S. Yamada and H. Kakuta, "Retinoid X receptor ligands: a patent review (2007 - 2013)," *Expert Opinion on Therapeutic Patents*, vol. 24, no. 4, pp. 443–452, 2014.

[16] W. Krezel, R. Ruhl, and A. R. de Lera, "Alternative retinoid X receptor (RXR) ligands," *Molecular and Cellular Endocrinology*, vol. 491, p. 110436, 2019.

[17] J. Mey, D. J Morassutti, G. Brook et al., "Retinoic acid synthesis by a population of NG2-positive cells in the injured spinal cord," *The European Journal of Neuroscience*, vol. 21, no. 6, pp. 1555–1568, 2005.

[18] J. Kern, K. Schrage, G. C. Koopmans, E. A. Joosten, P. McCaffery, and J. Mey, "Characterization of retinaldehyde

dehydrogenase-2 induction in NG2-positive glia after spinal cord contusion injury," *International Journal of Developmental Neuroscience*, vol. 25, no. 1, pp. 7–16, 2007.

[19] J. Levine, "The reactions and role of NG2 glia in spinal cord injury," *Brain Research*, vol. 1638, pp. 199–208, 2016.

[20] S. Sockanathan, T. Perlmann, and T. M. Jessell, "Retinoid receptor signaling in postmitotic motor neurons regulates rostrocaudal positional identity and axonal projection pattern," *Neuron*, vol. 40, no. 1, pp. 97–111, 2003.

[21] J. Vermot, B. Schuhbaur, H. le Mouellic et al., "Retinaldehyde dehydrogenase 2 and Hoxc8 are required in the murine brachial spinal cord for the specification of Lim1+ motoneurons and the correct distribution of Islet1+ motoneurons," *Development*, vol. 132, no. 7, pp. 1611–1621, 2005.

[22] L. Wuarin and N. Sidell, "Differential susceptibilities of spinal cord neurons to retinoic acid-induced survival and differentiation," *Developmental Biology*, vol. 144, no. 2, pp. 429–435, 1991.

[23] L. Wuarin, N. Sidell, and J. de Vellis, "Retinoids increase perinatal spinal cord neuronal survival and astroglial differentiation," *International Journal of Developmental Neuroscience*, vol. 8, no. 3, pp. 317–326, 1990.

[24] E. H. Harrison, C. dela Sena, A. Eroglu, and M. K. Fleshman, "The formation, occurrence, and function of $\beta$-apocarotenoids: $\beta$-carotene metabolites that may modulate nuclear receptor signaling," *The American Journal of Clinical Nutrition*, vol. 96, no. 5, pp. 1189S–1192S, 2012.

[25] A. Berry, I. Amrein, S. Nötzli et al., "Sustained hippocampal neurogenesis in females is amplified in P66(Shc-/-) mice: an animal model of healthy aging," *Hippocampus*, vol. 22, no. 12, pp. 2249–2259, 2012.

[26] R. D. Spescha, Y. Shi, S. Wegener et al., "Deletion of the ageing gene p66(Shc) reduces early stroke size following ischaemia/reperfusion brain injury," *European Heart Journal*, vol. 34, no. 2, pp. 96–103, 2013.

[27] A. Berry and F. Cirulli, "The $p66^{Shc}$ gene paves the way for healthspan: evolutionary and mechanistic perspectives," *Neuroscience and Biobehavioral Reviews*, vol. 37, no. 5, pp. 790–802, 2013.

[28] R. D. Spescha, J. Klohs, A. Semerano et al., "Post-ischaemic silencing of p66Shc reduces ischaemia/reperfusion brain injury and its expression correlates to clinical outcome in stroke," *European Heart Journal*, vol. 36, no. 25, pp. 1590–1600, 2015.

[29] Y. Cai, F. Ying, H. Liu et al., "Deletion of Rap1 protects against myocardial ischemia/reperfusion injury through suppressing cell apoptosis via activation of STAT3 signaling," *The FASEB Journal*, vol. 34, no. 3, pp. 4482–4496, 2020.

[30] J. W. Shay, "Role of telomeres and telomerase in aging and cancer," *Cancer Discovery*, vol. 6, no. 6, pp. 584–593, 2016.

Hindawi
Oxidative Medicine and Cellular Longevity
Volume 2021, Article ID 6683270, 15 pages
https://doi.org/10.1155/2021/6683270

*Research Article*

# *Amauroderma rugosum* Protects PC12 Cells against 6-OHDA-Induced Neurotoxicity through Antioxidant and Antiapoptotic Effects

**Jingjing Li,[1] Renkai Li,[1] Xiaoping Wu,[1] Ruby Lai-Chong Hoo,[1] Simon Ming-Yuen Lee,[2] Timothy Man-Yau Cheung,[3] Bryan Siu-Yin Ho,[3] and George Pak-Heng Leung[1]**

[1]*Department of Pharmacology and Pharmacy, The University of Hong Kong, Hong Kong, China*
[2]*State Key Laboratory of Quality Research in Chinese Medicine and Institute of Chinese Medical Sciences, University of Macau, Macao, China*
[3]*Tian Ran Healthcare Limited, Hong Kong, China*

Correspondence should be addressed to George Pak-Heng Leung; gphleung@hku.hk

Received 10 November 2020; Revised 1 January 2021; Accepted 25 January 2021; Published 10 February 2021

Academic Editor: Wei Zhao



*Amauroderma rugosum* (AR) is a dietary mushroom in the *Ganodermataceae* family whose pharmacological activity and medicinal value have rarely been reported. In this study, the antioxidant capacity and neuroprotective effects of AR were investigated. The aqueous extract of AR was confirmed to contain phenolic compounds, polysaccharides, and triterpenes. The results of 2,2-diphenyl-1-picryl-hydrazyl-hydrate (DPPH) and total antioxidant capacity assays revealed that AR extract scavenged reactive oxygen species. Moreover, AR extract decreased the cytotoxicity, oxidative stress, mitochondrial dysfunction, and apoptosis of PC12 cells induced by 6-hydroxydopamine (6-OHDA). In addition, 6-OHDA upregulated the expressions of proapoptotic proteins and downregulated the Akt (protein kinase B)/mTOR- (mammalian target of rapamycin-) and MEK (mitogen-activated protein kinase kinase)/ERK- (extracellular signal-regulated kinases-) dependent signaling pathways. These effects of 6-OHDA were abolished or partially reversed by AR extract. Furthermore, the neuroprotective effects of AR in 6-OHDA-treated PC12 cells were significantly abolished by Akt and MEK inhibitor. Thus, AR extract possesses neuroprotective effects, probably through its antioxidant and antiapoptotic effects. These findings suggest the potential application of AR in the prevention or treatment of oxidative stress-related neurodegenerative diseases such as Parkinson's disease.

## 1. Introduction

To date, Parkinson's disease remains the second most common neurodegenerative disease worldwide, and its incidence is increasing in people over 60 years of age [1]. It is characterized by a selective and progressive loss of dopaminergic neurons in the substantia nigra pars compacta, leading to serious movement disturbances including postural instability, uncontrollable tremors, rigidity, and bradykinesia [2]. Currently, available treatments for Parkinson's disease include dopaminergic replacement therapy and deep brain stimulation therapy [3]. However, neither of these treatments can halt nor slow the progression of Parkinson's disease. Therefore, it is crucial to develop novel drugs that can slow the neurodegenerative process.

Although the pathological mechanisms of Parkinson's disease remain elusive, accumulating scientific evidence suggests that oxidative stress-induced cell injury plays an indispensable role in the degeneration of dopaminergic neurons [4]. Interrupting the physiological maintenance of redox potential severely interferes with many biological processes in neurons, eventually leading to cell apoptosis [5]. Oxidative stress occurs when the rate of reactive oxygen species (ROS) scavenging is overwhelmed by the rate of ROS production [6]. Excessive accumulation of ROS in dopaminergic neurons can damage most biological molecules, including lipids,

proteins, and nucleic acids, thereby activating the intracellular inflammatory response, which induces cellular damage, mitochondrial dysfunction, oxidative DNA injury, and neuroinflammation [7–9]. Therefore, decreasing oxidative injury in dopaminergic neurons has been widely proposed as an effective approach for the treatment of Parkinson's disease.

Various experimental models have been established for investigating the role of oxidative stress in dopaminergic neuronal degeneration. These models involve the use of neurotoxins such as 1-methyl-4-phenyl-1,2,3,6-tetrahydropyridine (MPTP), rotenone, 1,1′-dimethyl-4,4′-bipyridinium dichloride (paraquat) and 6-hydroxydopamine (6-OHDA) [5]. The compound 6-OHDA, the hydroxylated analog of natural neurotransmitter dopamine, is a widely used neurotoxin that can be applied to establish different *in vitro* and *in vivo* Parkinson disease models. It is taken up by dopaminergic neurons via dopamine and norepinephrine transporters and is subsequently oxidized intracellularly, thereby releasing ROS including hydrogen peroxide, superoxide, and hydroxyl radicals [10–12].

*Amauroderma rugosum* (AR) is a basidiomycete in the *Ganodermataceae* family. This mushroom has a black stipe and a white surface covered with numerous pores. A notable characteristic of the mushroom is that its surface becomes red when it is scratched. Hence, it is also known as "blood Linzhi" in Chinese. Although AR is commonly consumed by people in China and South Asia, very few scientific studies have explored its beneficial effects on health or its medicinal value. Nevertheless, a previous study reported that the extract of AR mycelia has antioxidant and anti-inflammatory effects in lipopolysaccharide-stimulated RAW 264.7 cells. Thus, AR might be a potential therapeutic agent or health supplement useful in the management of oxidative stress-related diseases [13]. The aims of this study were to investigate the antioxidant capacity and neuroprotective activity of AR in a 6-OHDA-induced neurodegenerative cell model and to elucidate its underlying mechanisms of action.

## 2. Materials and Methods

*2.1. Chemicals and Reagents.* Dulbecco's modified Eagle's medium (DMEM), fetal bovine serum (FBS), 4′,6-diamidino-2-phenylindole (DAPI), penicillin–streptomycin, and 0.25% (*w*/*v*) trypsin containing 1 mM ethylenediaminetetraacetic acid were purchased from Invitrogen (Carlsbad, CA), and 6-OHDA, 2,2-diphenyl-1-picryl-hydrazyl-hydrate (DPPH), vitamin C, dimethyl sulfoxide (DMSO), Akt inhibitor IV, MEK inhibitor (PD 98059), and 3-(4,5-dimethylthiazol-2-yl)-2,5-diphenyltetrazoliumbromide (MTT) were purchased from Sigma-Aldrich (St. Louis, MO). Nerve growth factor (NGF) was obtained from R&D Systems (Minneapolis, MN, USA). A total antioxidant capacity assay kit was purchased from Abcam (Cambridge, UK). A lactate dehydrogenase (LDH) cytotoxicity assay kit was purchased from Cayman Chemical (Ann Arbor, MI). A Caspase 3/7 activity detection kit was obtained from Promega (Madison, USA). Antibodies for western blotting were purchased from Cell Signaling Technology (Danvers, MA). All chemicals were dissolved in appropriate solvents and stored at −20°C before use to maintain their chemical stability.

*2.2. Reflux Extraction of AR.* Fruiting bodies of AR were provided by Hong Kong Ganoderma Centre Limited (Hong Kong, China), an organic farm that had been granted an organic crop production certificate by the Hong Kong Organic Resource Centre. The samples were dried in an oven and ground into powder. A reflux system for the extraction process was used to prepare the crude extract. Two grams of the powdered sample was extracted with 50 mL of distilled water at 95 ± 2°C for 60 min. The crude extract was centrifuged at 4000 rpm for 20 min. Afterward, the supernatant was collected, and the sample residue was reextracted twice via the steps described above. Subsequently, all extracts were pooled, filtered, and concentrated to 80 mL with a rotary evaporator. The extract was stored at -20°C until further use.

*2.3. Determination of Total Phenolic Compounds, Polysaccharides, and Triterpenes.* To measure the total phenolic content of AR extract, 50 $\mu$L of 10% Folin-Ciocalteu phenol reagent was added to 50 $\mu$L AR extract and incubated in dark at room temperature for 3 min. Afterwards, 100 $\mu$L of 10% $Na_2CO_3$ was added to the mixture for 1 h. The absorbance at 750 nm was measured with a microplate absorbance reader. Gallic acid was used as a standard phenolic compound. All determinations were expressed as mg gallic acid equivalent per g (mg GAE/g).

Before the measurement of the total polysaccharides, 0.1 mL AR extract was precipitated with 1 mL of 95% ethanol overnight at 4°C. The precipitate was collected by centrifugation at 10,000 rpm for 10 min at 4°C. Then, the precipitate was dissolved in 50 $\mu$L water. Total polysaccharide content was measured by adding 2.5 $\mu$L phenol (80%) and then 125 $\mu$L concentrated sulfuric acid. After incubation for 10 min, the mixture was shaken and then incubated at 30°C for 20 min. The absorbance at 490 nm was measured with a microplate absorbance reader using glucose as standard. The results were expressed as mg glucose equivalent per g (mg GE/g).

To measure the total triterpenes, 100 $\mu$L AR extract was transferred to 15 mL tube and evaporated to dryness using nitrogen flow. Then, 0.4 mL 5% vanillin–acetic acid solution and 1 mL perchloric acid were added into the tube, mixed and incubated at 60°C for 15 min. Afterwards, 5 mL acetic acid was added and incubated at room temperature for 15 min. The absorbance at 549 nm was measured with a microplate absorbance reader. A solution of oleanolic acid was used as the standard. The results were expressed as mg oleanolic acid equivalent per g (mg OA/g).

*2.4. DPPH Assay.* The free radical scavenging capacity (SC) of AR extract was measured with DPPH assays. Briefly, 5 $\mu$L of AR extract was mixed with 195 $\mu$L of DPPH solution (24 mg/L) in a 96-well plate. The reaction proceeded in the dark for 60 min. Afterward, the absorbance of the reaction mixture at 515 nm was measured with a microplate absorbance reader. Vitamin C dissolved in distilled water served

as the positive control. The $SC_{50}$ was estimated as the concentration of extract that scavenged 50% of the free radicals.

*2.5. Total Antioxidant Capacity Assay.* The total antioxidant capacity (TAC) of AR extract was evaluated with a TAC Assay Kit, which measured the ability of antioxidants to reduce $Cu^{2+}$ to $Cu^{+}$. The resulting $Cu^{+}$ formed a colored complex with a specific dye reagent in the assay kit. In brief, 5 $\mu$L of AR extract was diluted into 100 $\mu$L with deionized water and then mixed with 100 $\mu$L of Trolox standard in a 96-well plate. The reaction was performed by the addition of 100 $\mu$L of $Cu^{2+}$ working solution, and the plate was shaken for 90 min in dark at room temperature. The absorbance at 570 nm was measured with a microplate absorbance reader.

*2.6. Cell Culture and Treatment.* PC12 rat pheochromocytoma cells were obtained from the American Type Culture Collection (Manassas, VA). The cells were cultured in DMEM supplemented with 10% heat-inactivated FBS and 1% penicillin-streptomycin and then incubated at 37°C in a humidified atmosphere with 5% $CO_2$. For the experiments with 6-OHDA, PC12 cells in DMEM with low serum (0.5% FBS) were seeded in 12- or 96-well plates. The cells were incubated with different concentrations of AR extract (0-2 mg/mL) for 2 h and then treated with 500 $\mu$M 6-OHDA for 24 h. The differentiation of PC12 cells was described previously [14]. Neuronal differentiation was induced in the culture medium by treating the PC12 cells with 100 ng/mL NGF and 1% FBS for 5 days. Differentiated PC12 cells were then collected for further analysis and compared with nondifferentiated treated PC12 cells.

*2.7. Cell Viability Assay.* The cell viability was measured with MTT assays according to the manufacturer's protocol. In brief, the cultured medium was discarded, and the cells were incubated with MTT solution (at a final concentration of 0.5 mg/mL) for 4 h at 37°C. Dimethyl sulfoxide was then added to lyse the cells and dissolve the violet formazan crystals that had formed inside the cells. The absorbance at 570 nm was measured with a microplate absorbance reader.

*2.8. LDH Assay.* Cellular injury was determined by measurement of the LDH released into the culture medium. LDH activity was measured with a detection kit according to the manufacturer's instructions. The absorbance at 490 nm was measured with a microplate absorbance reader.

*2.9. DAPI and Annexin V-Fluorescein Isothiocyanate (FITC)/Propidium Iodide (PI) Staining.* After drug treatment, the PC12 cells were washed twice with cold PB and stained with DAPI (2.0 $\mu$g/mL) for 20 min. The images were then captured by fluorescence microscopy (IN CELL Analyzer, GE Healthcare Life Sciences, USA). The PC12 cells were also resuspended in binding buffer and then stained with annexin V-FITC and PI (1.0 mg/mL) for 20 min. The stained cells were analyzed immediately with a flow cytometer (BD Biosciences, USA). Ten thousand events were counted for each sample. The data were analyzed in the FlowJo software (BD Biosciences, USA).

*2.10. Mitochondrial Membrane Potential.* The PC12 cells were incubated with JC-1 dye (3 $\mu$g/mL) for 20 min. A portion of the cells was photographed by a fluorescence microscopy, and the remaining cells were washed twice with warm PBS and examined by flow cytometry. The intensity of red fluorescence (excitation 560 nm, emission 595 nm) and green fluorescence (excitation 485 nm, emission 535 nm) was determined in ImageJ (National Institutes of Health, USA). The ratio of red/green fluorescence was calculated for semi-quantitative assessment of mitochondrial polarization states.

*2.11. Analysis of Mitochondrial Respiration.* Mitochondrial oxygen consumption rate (OCR) was measured using Seahorse XFe24 Analyzer (Seahorse Biosciences, MA, USA). PC12 cells ($8 \times 10^3$ cells/well) were seeded into a Seahorse XF 24 well culture microplates and incubated overnight at 37°C in a humidified atmosphere with 5% $CO_2$. After drug treatment, the cultural medium was replaced with Seahorse base medium and incubated in a non-$CO_2$ incubator for 1 h. PC12 cells were sequentially treated with 1 $\mu$M oligomycin (Oligo), 1 $\mu$M carbonyl cyanide-4-(trifluoromethoxy) phenylhydrazone (FCCP), and 1 $\mu$M rotenone plus 1 $\mu$M antimycin A (R + A). OCR was calculated using the Seahorse software. After finishing the assay, the cells were lysed with RIPA buffer (200 $\mu$L/well), and the protein concentration was measured by bicinchoninic acid assay. OCR was normalized to the protein content and presented as pmol/min/$\mu$g protein.

*2.12. Detection of ROS.* ROS was detected with CM-$H_2$DCFDA staining. A portion of the cells was photographed under fluorescence microscopy, and the remaining cells were examined by flow cytometry. The intensity of green fluorescence (excitation 485 nm, emission 535 nm) was determined in the ImageJ software.

*2.13. Caspase 3/7 Activity Assay.* Caspase 3/7 activity in PC12 cells was evaluated with a caspase 3/7 activity detection kit according to the manufacturer's protocol. Luminescence signals were recorded with a microplate absorbance reader.

*2.14. Western Blot Analysis.* Protein was extracted from PC12 cells with lysis buffer containing 1% phenylmethylsulfonyl fluoride and 1% protease inhibitor. Lysates were centrifuged at 12,500 × g for 20 min at 4°C, and the supernatant was collected. The total protein concentration was determined with bicinchoninic acid assays. Equal amounts of protein were subjected to sodium dodecyl sulfate-polyacrylamide gel electrophoresis and then electrically transferred onto a polyvinylidene difluoride membrane, which was subsequently blocked with 5% nonfat milk in Tris-buffered saline containing 0.1% Tween-20 for 1 h. The membrane was subsequently incubated with primary antibodies against mTOR, phospho-mTOR (Ser2448), Akt, phospho-Akt (Ser473), ERK1/2, phospho-ERK1/2 (Thr202/Tyr204), MEK, phospho-MEK (Ser217/221), cleaved-PARP (Asp214), cleaved-caspase 3 (Asp175), cleaved-caspase 9 (Asp315), or GAPDH overnight at 4°C. After being washed with PBS, the membrane was incubated with horseradish peroxidase-conjugated secondary antibodies for 1 h at room temperature. After repeated

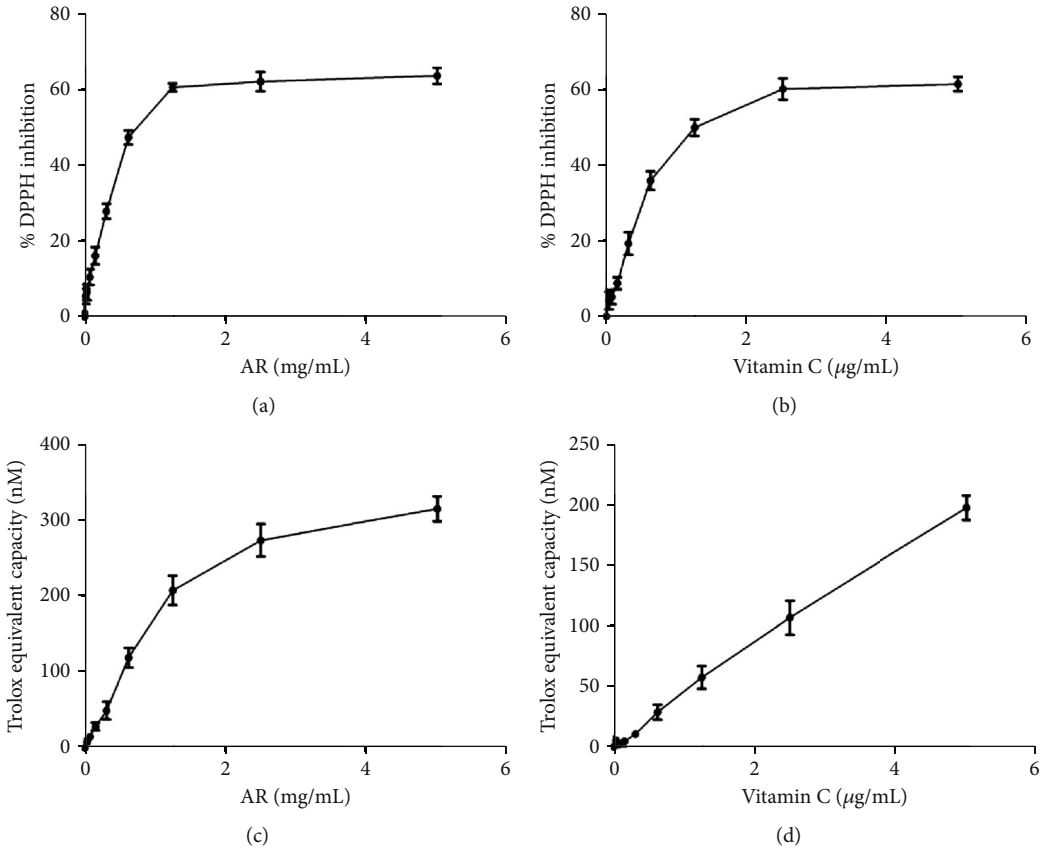


Figure 1: Antioxidant capacity of AR extract and vitamin C. The effects of different concentrations of (a) AR extract and (b) vitamin C on scavenging DPPH were studied. The antioxidant capacity is expressed as percentage DPPH inhibition. The effects of different concentrations of (c) AR extract or (d) vitamin C on total antioxidant capacity were also studied by measuring their ability to reduce $Cu^{2+}$ to $Cu^{+}$. The antioxidant effect is expressed as Trolox equivalent antioxidant capacity. Values are means ± SD of three independent experiments.

washes with PBS, proteins were visualized by enhanced chemiluminescence. Images of protein bands were captured, and densitometric measurements of band intensity were performed with a ChemiDoc XRS Molecular Imager (Bio-Rad Laboratories, Hercules, CA, USA).

*2.15. Data and Statistical Analysis.* Data are expressed as the mean ± standard deviation (SD) of at least three independent experiments. Statistical analyses were performed with one-way ANOVA followed by Tukey's multiple comparison test (two or more groups) in the GraphPad Prism 6.0 software (GraphPad Software Inc., San Diego, CA, USA). $p < 0.05$ was considered statistically significant.

## 3. Results

*3.1. Chemical Contents of AR Extract.* Major contents of AR extract including total phenolic compounds, polysaccharides, and triterpenes were measured by chemical assays. The content of total phenolic compounds of AR extract was 5.53 ± 0.11 mg GAE/g of dry weight. The content of total polysaccharides in AR extract was 1.12 ± 0.23 mg GE/g of dry weight. The content of total triterpenes was 3.20 ± 0.14 mg OA/g of dry weight.

*3.2. Antioxidant Capacity of AR Extract in DPPH and TAC Assays.* The antioxidant capacity of AR extract was studied with DPPH and TAC assays. The ability of AR extract and vitamin C (which served as a positive control) to scavenge DPPH• free radicals increased with the tested concentration (Figures 1(a) and 1(b)). The $SC_{50}$ of AR extract and vitamin C in DPPH assays was 0.58 mg/mL and 1.34 μg/mL, respectively. Similarly, AR extract and vitamin C reduced $Cu^{2+}$ radicals in TAC assays in a concentration-dependent manner (Figures 1(c) and 1(d)).

*3.3. Neuroprotective Effect of AR Extract in PC12 Cells.* PC12 cells were used as the cell model to study the neuroprotective effect of AR extract. First, the cytotoxic effect of AR extract itself was evaluated by incubation of PC12 cells with various concentrations of AR extract (0.06–2 mg/mL) for 24 h. The MTT assays showed that AR extract did not affect the viability of PC12 cells in the concentration range of 0.06 to 2 mg/mL (Figure 2(a)). In addition, LDH release by PC12 cells was not affected by AR extract in the same concentration range (Figure 2(b)). Therefore, this concentration range of AR extract was applied in subsequent experiments. Under 6-OHDA (500 μM) treatment, the viability of PC12 cells decreased by 45%, and LDH release increased by 110% (Figures 2(c) and 2(d)). AR extract protected PC12 cells

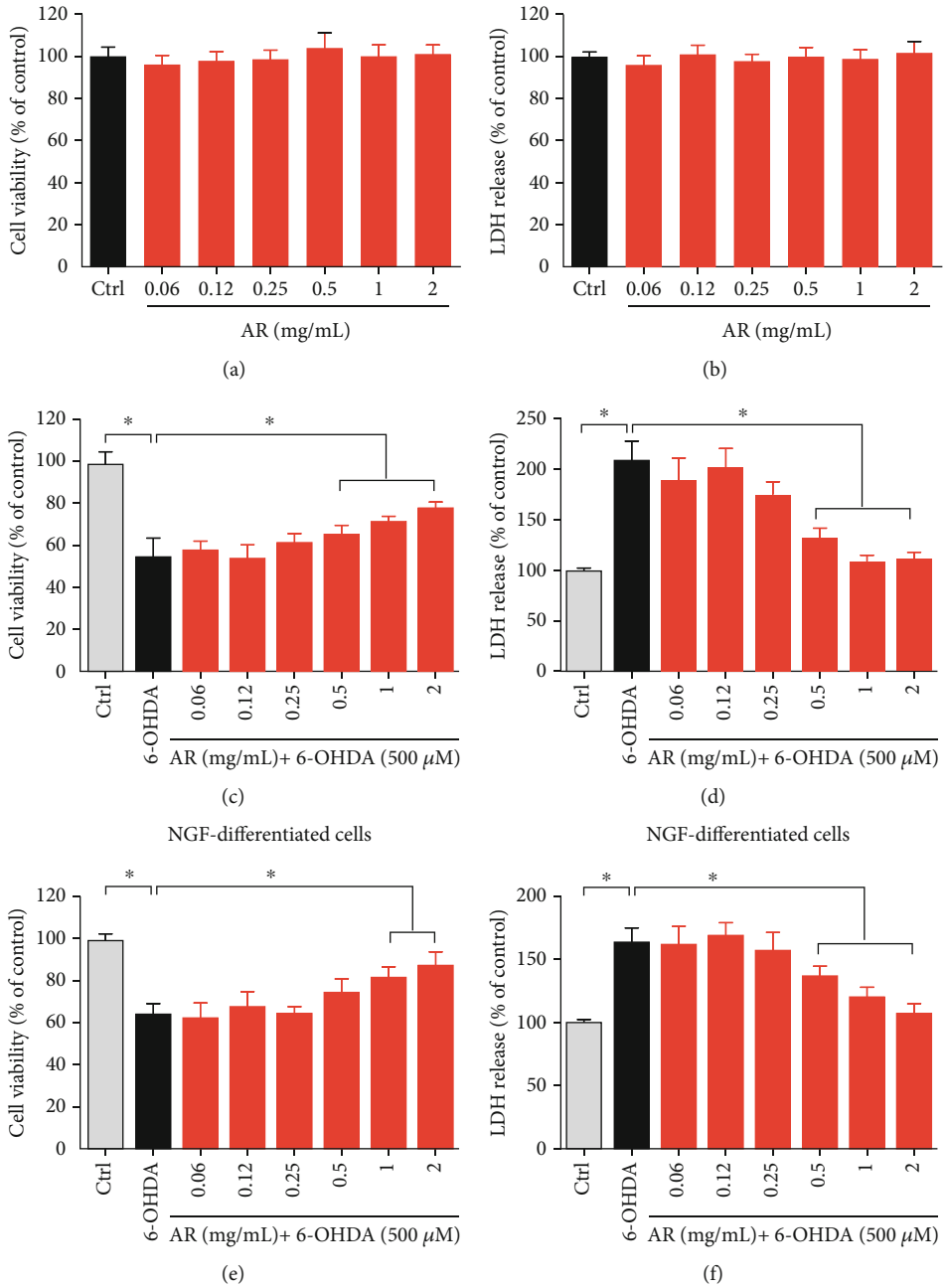


Figure 2: AR extract protects PC12 cells against 6-OHDA-induced cell cytotoxicity. PC12 cells were treated with various concentrations of AR extract (0.06–2 mg/mL) or vehicle (control) for 24 h. Then, (a) cell viability and (b) LDH release were examined with MTT and LDH assays, respectively. PC12 cells were then incubated with different concentrations of AR extract (0–2 mg/mL) for 2 h and subsequently treated with 500 $\mu$M 6-OHDA for 24 h. Cells without the treatment with AR extract and 6-OHDA served as controls. (c) Cell viability and (d) LDH release were again studied. (e, f) NGF-differentiated PC12 cells were treated with AR extract (0–2 mg/mL) for 2 h prior to treatment with 500 $\mu$M 6-OHDA for 24 h. Then, (e) cell viability and (f) LDH release were examined with MTT and LDH assays, respectively. Data are presented as a percentage of control group values (mean ± SD of three independent experiments). $^{*}p < 0.05$ indicates a statistically significant difference.

against 6-OHDA-induced cell death and LDH release, in a concentration-dependent manner. We further investigated the protective effects of AR in NGF-differentiated PC12 cells. Consistent with data of nondifferentiated PC12 cells, AR significantly increased the cell viability and reduced LDH release in NGF-differentiated PC12 cells (Figures 2(e) and 2(f)).

*3.4. Antioxidant Activity of AR Extract in PC12 Cells.* The *in vitro* antioxidant activity of AR extract was studied in PC12 cells treated with 6-OHDA. The intracellular ROS generation was reflected by the green florescent signal produced by the probe CM-H2DCFDA. AR extract itself had no effect on ROS generation in PC12 cells (Figures 3(a) and 3(c)). The ROS level in PC12 cells was elevated significantly, by 9.6-fold,

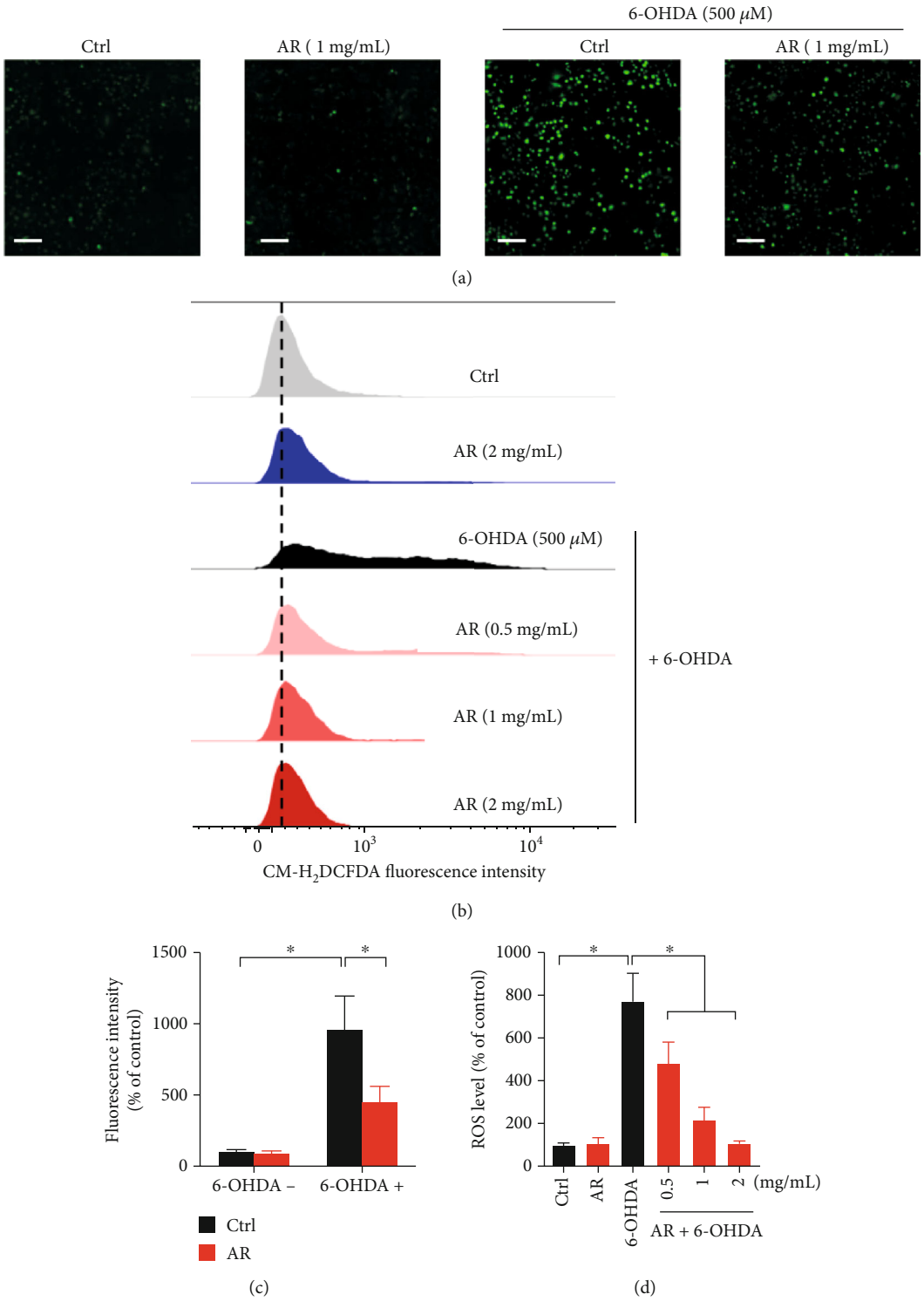


Figure 3: AR extract decreases 6-OHDA-induced ROS generation in PC12 cells. PC12 cells were pretreated with different concentrations of AR extract (0.5–2 mg/mL) or vehicle for 2 h and then treated with or without 500 $\mu$M 6-OHDA for 4 h. Cells without treatment with AR extract and 6-OHDA served as the control. (a) ROS generation in PC12 cells was detected by CM-H2DCFDA staining. ROS in the cells was indicated by the green signals. Scale bar: 200 $\mu$m. (b) Flow cytometry analysis of ROS levels in PC12 cells after CM-H2DCFDA staining. ROS levels in (c) microscopy images and (d) flow cytometry were quantified. Data are presented as a percentage of control group values (mean ± SD of three independent experiments). $^*p < 0.05$ indicates a statistically significant difference.

after treatment with 6-OHDA, but the increase was only 4.6-fold when the cells were pretreated with 1 mg/mL AR extract. Similar results were observed in flow cytometry analysis. The 6-OHDA-induced ROS production in PC12 cells was inhibited by AR extract in a concentration-dependent manner (Figures 3(b) and 3(d)).

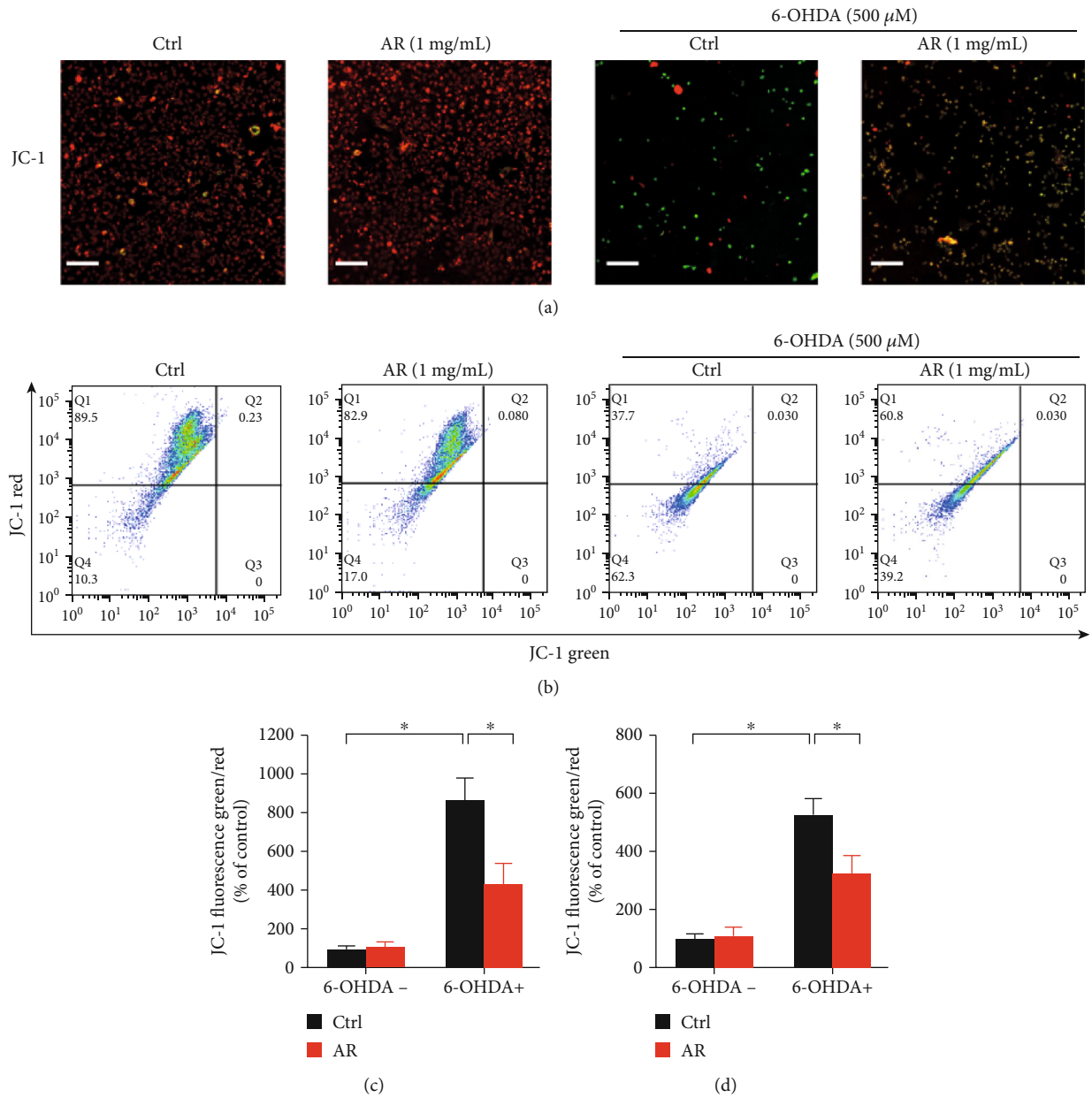


Figure 4: AR extract ameliorates 6-OHDA-induced loss of mitochondrial membrane potential in PC12 cells. PC12 cells were pretreated with 1 mg/mL AR extract or vehicle for 2 h and then treated with or without 500 $\mu$M 6-OHDA for 24 h. (a) Mitochondrial membrane potential in PC12 cells was detected with JC-1 staining. Red and green fluorescence signals indicated JC-1 aggregates and monomers, respectively. Scale bar: 200 $\mu$m. (b) Flow cytometry analysis of mitochondrial membrane potential in PC12 cells after JC-1 staining. The mitochondrial membrane potential in (c) microscopy image and (d) flow cytometry was quantified. Data are presented as a percentage of control group values (mean ± SD of three independent experiments). $^*p < 0.05$ indicates a statistically significant difference.

*3.5. Mitochondrial Protective Effect of AR Extract on PC12 Cells.* Mitochondrial membrane potential is an important indicator of mitochondrial function, and the loss of mitochondrial membrane potential is typically regarded as a hallmark of apoptosis [15]. The membrane-permeant JC-1 dye was used for evaluating the mitochondrial membrane potential. The color of JC-1 dye changes from red to green when the mitochondrial membrane potential decreases. Green fluorescence signals were scarcely observed in both the control and AR extract-treated PC12 cells. However, the ratio of the green fluorescence to red fluorescence signal significantly increased, by 8.7-fold, under 500 $\mu$M 6-OHDA treatment (Figures 4(a) and 4(c)), revealing disruption of the mitochondrial membrane potential. However, the 6-OHDA-induced increase in the ratio of the green fluorescence to red fluorescence signal was only 4.3-fold when the PC12 cells were pretreated with 1 mg/mL AR extract. Similar results were observed with flow cytometry. The ratio of the green fluorescence to red fluorescence signal increased by 5.3-fold under 500 $\mu$M 6-OHDA treatment but by only 3.2-fold when the PC12 cells were first preincubated with 1 mg/mL AR extract (Figures 4(b) and 4(d)).

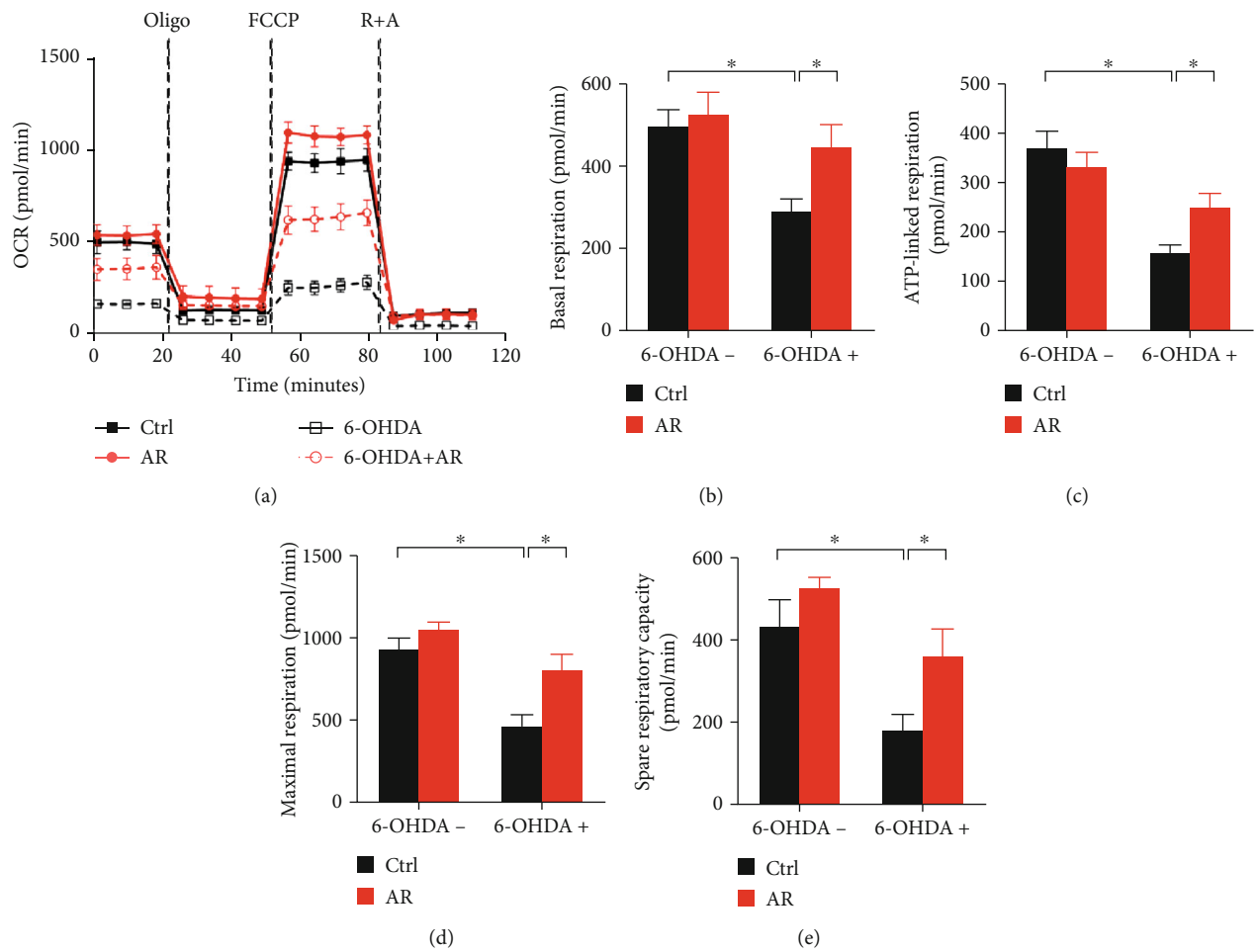


Figure 5: AR extract reduces 6-OHDA-induced mitochondrial respiratory dysfunction in PC12 cells. PC12 cells were pretreated with 1 mg/mL AR extract or vehicle for 2 h and then treated with or without 500 $\mu$M 6-OHDA for 24 h. (a) Mitochondrial oxygen consumption rate (OCR) in PC12 cells was monitored using a Seahorse metabolic analyzer. The response of PC12 cells after addition of 1 $\mu$M oligomycin (Oligo), 1 $\mu$M FCCP, and 1 $\mu$M rotenone plus 1 $\mu$M antimycin (R + A) was recorded. (b–e) Quantitative analysis of (b) basal respiration, (c) ATP-linked respiration, (d) maximal respiration, and (e) spare respiratory capacity in PC12 cells, respectively. The values represent the mean ± SD ($n = 3$). $^*p < 0.05$ indicates a statistically significant difference.

*3.6. Protective Effect of AR Extract against 6-OHDA-Induced Mitochondrial Respiratory Dysfunction PC12 Cells.* Mitochondrial respiratory function of PC12 cells was further evaluated using a Seahorse Bioscience extracellular flux analyzer. The drop of basal OCR by oligomycin could be used to deduce ATP-linked respiration. Stimulation by FCCP could result in a maximal respiration. The gap between maximal and basal OCR was the spare respiratory capacity. Addition of rotenone (mitochondrial complex I inhibitor) and antimycin (mitochondrial complex III inhibitor) into the cells could shut down the electron transfer, allowing the calculation of nonmitochondrial respiration. In comparison with control group, treatment with AR caused a mild increase in basal respiration, maximal respiration, spare respiratory capacity, and a mild decrease in ATP-linked respiration (Figure 5(a)). In contrast, 6-OHDA decreased basal respiration, ATP-linked respiration, maximal respiration, and spare respiratory capacity by 41%, 57%, 50%, and 59%, respectively (Figures 5(b)–5(e)). The 6-OHDA-induced mitochondrial respiratory dysfunction was significantly reversed by AR extract (Figure 5(a)). In comparison with 6-OHDA treatment, AR remarkably restored mitochondrial basal respiration, ATP-linked respiration, maximal respiration, and spare respiratory capacity by 31%, 25%, 37%, and 42%, respectively (Figures 5(b)–5(e)).

*3.7. Protective Effect of AR Extract against Apoptosis in PC12 Cells.* Decreased mitochondrial membrane potential often leads to cell apoptosis. DAPI staining was applied to evaluate apoptosis in PC12 cells. No nuclear condensation or fragmentation was observed in the control and AR extract-treated cells. In contrast, many bright condensed dots representing apoptotic bodies were clearly identified in 6-OHDA-treated cells (Figure 6(a)). The number of apoptotic cells increased by 10.3-fold after treatment with 6-OHDA but by only 4.3-fold when the PC12 cells were first pretreated with AR extract (Figure 6(c)). Next, we further studied the antiapoptotic effect of AR extract on PC12 cells by using annexin V-FITC/PI double staining and flow cytometry (Figure 6(b)). 500 $\mu$M of 6-OHDA increased the number of

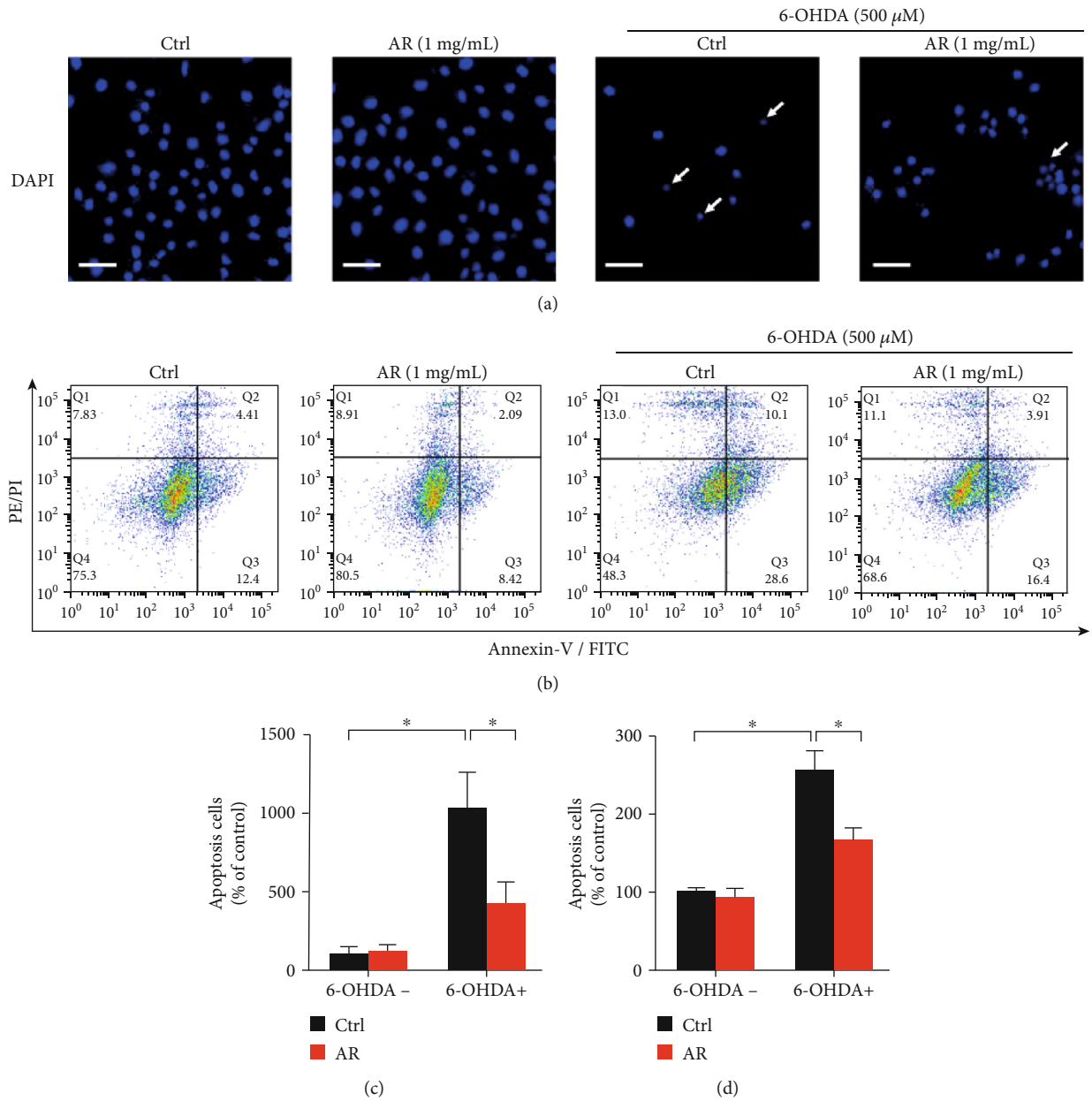


Figure 6: AR extract protects PC12 cells against 6-OHDA-induced apoptosis. PC12 cells were pretreated with 1 mg/mL AR extract or vehicle for 2 h and then treated with or without 500 $\mu$M 6-OHDA for 24 h. (a) Apoptotic cells were identified by DAPI staining. Blue signals indicate the nuclei of PC12 cells. White arrows indicate apoptotic cells. Scale bar: 50 $\mu$m. (b) Cells were double stained by annexin V and PI for 20 min and then analyzed by flow cytometry. The number of apoptotic cells in microscopy images (c) and flow cytometry (d) was quantified. Data are presented as a percentage of control group values (mean ± SD of three independent experiments). $^*p < 0.05$ indicates a statistically significant difference.

apoptotic cells by 2.6-fold but by only 1.7-fold when the cells were preincubated with AR extract (Figure 6(d)).

*3.8. Inhibitory Effect of AR Extract on 6-OHDA-Induced Proapoptotic Protein Expression in PC12 Cells.* Expression levels of proteins involved in apoptotic pathways were studied with Western blot analysis (Figure 7(a)). The expression levels of cleaved-caspase 9, cleaved-caspase 3, and cleaved-PARP were significantly elevated by treatment with 500 $\mu$M 6-OHDA, by 137%, 255%, and 441%, respectively. The 6-OHDA-induced expression of cleaved-caspase 9 and cleaved-caspase 3 was abolished by treatment with 1 mg/mL of AR extract, whereas the 6-OHDA-induced expression of cleaved-PARP was partially inhibited by AR extract (Figures 7(b)–7(d)). Moreover, biochemical assays showed that the caspase 3/7 activity under 6-OHDA treatment increased by 3.8-fold but by only 2.6-fold when the PC12 cells were pretreated with AR extract (Figure 7(e)).

*3.9. Restorative Effects of AR Extract on Akt/mTOR and MEK/ERK Signaling Pathways in PC12 Cells.* Akt/mTOR and MEK/ERK signaling pathways play key roles not only

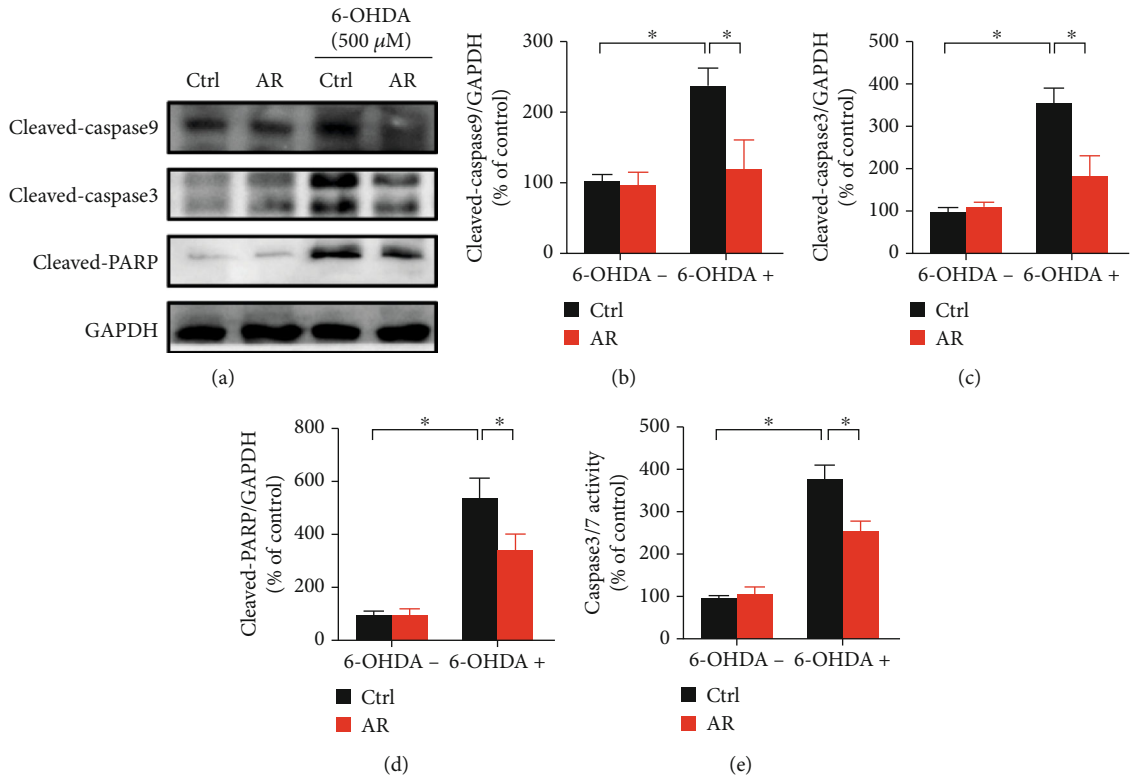


Figure 7: AR extract inhibits 6-OHDA-induced proapoptotic protein expression in PC12 cells. (a) PC12 cells were pretreated with 1 mg/mL AR extract or vehicle for 2 h and then treated with or without 500 $\mu$M 6-OHDA for 24 h. Protein expression levels of cleaved-caspase 9, cleaved-caspase 3, and cleaved-PARP in PC12 cells were examined by Western blot analysis. (b–d) Quantitative analysis of protein expression levels. (e) Caspase 3/7 activity in PC12 cells was measured with a biochemical assay kit. Data are presented as a percentage of control group values (mean ± SD of three independent experiments). $^*p < 0.05$ indicates a statistically significant difference.

in the stimulation of neuron proliferation but also in the regulation of neuron apoptosis. Therefore, we studied the effects of AR extract on the changes in Akt/mTOR and MEK/ERK signaling pathways in PC12 cells. 500 $\mu$M 6-OHDA decreased the expression of phospho-Akt, phospho-mTOR, phospho-MEK1/2, and phospho-ERK1/2 in PC12 cells by 92%, 88%, 45%, and 60%, respectively, whereas the total amounts of Akt, mTOR, MEK1/2, and ERK1/2 were not affected (Figure 8). With the pretreatment of PC12 cells with AR extract, the 6-OHDA-induced decrease in expression of phospho-MEK1/2 was completely restored, whereas the expression of phospho-Akt, phospho-mTOR, and phospho-ERK1/2 was partly restored.

*3.10. Involvement of the Akt/mTOR and MEK/ERK Signaling Pathway in Protective Effect of AR against 6-OHDA-Induced Cell Injury in PC12 Cells.* To further investigate the role of Akt/mTOR and MEK/ERK signals in protective effect of AR against 6-OHDA-induced cell injury in PC12 cells, Akt inhibitor IV and MEK inhibitor (PD98059) were applied to observe the neuroprotective effect of AR. As shown in Figure 9, 1 $\mu$M Akt inhibitor had no effect on the cell viability of PC12 cells whereas 10 $\mu$M MEK inhibitor (PD98059) slightly decreased the cell viability. Notably, both Akt inhibitor (Figure 9(a)) and MEK inhibitor (Figure 9(b)) abolished the protective effect of AR in PC12 cells. In 6-OHDA-induced cell injury model, the increase of cell viability induced by AR was significantly decreased from 75% to 58% and 52% in the presence of Akt inhibitor IV and PD98059, respectively.

## 4. Discussion

Oxidative stress is widely believed to be involved in the pathogenesis of many age-related diseases, such as neurodegenerative diseases, cardiovascular diseases, and cancer. Some antioxidants have been demonstrated to be effective in the prevention or treatment of oxidative stress-related diseases [16]. For instance, N-acetylcysteine can be used for the treatment of chronic obstructive pulmonary disease, in which oxidative stress is closely associated with its pathology and complications [17]. Vitamins are a class of essential micronutrients showing abundant antioxidant effects in humans. Their health-protective and therapeutic potential has been extensively studied. For instance, several large observational studies involving more than 100,000 participants have suggested that higher intake of vitamins significantly decreases the risk of coronary artery disease [18, 19]. Moreover, a community-based study in Rotterdam indicated that a high intake of dietary vitamin E may decrease the occurrence of Parkinson's disease in the population between 55 and 95 years of age [20].

*Ganoderma lucidum*, also known as "Lingzhi" in Chinese, is a well-known and popular edible and medicinal mushroom in Asia. In traditional Chinese medicine, it is used

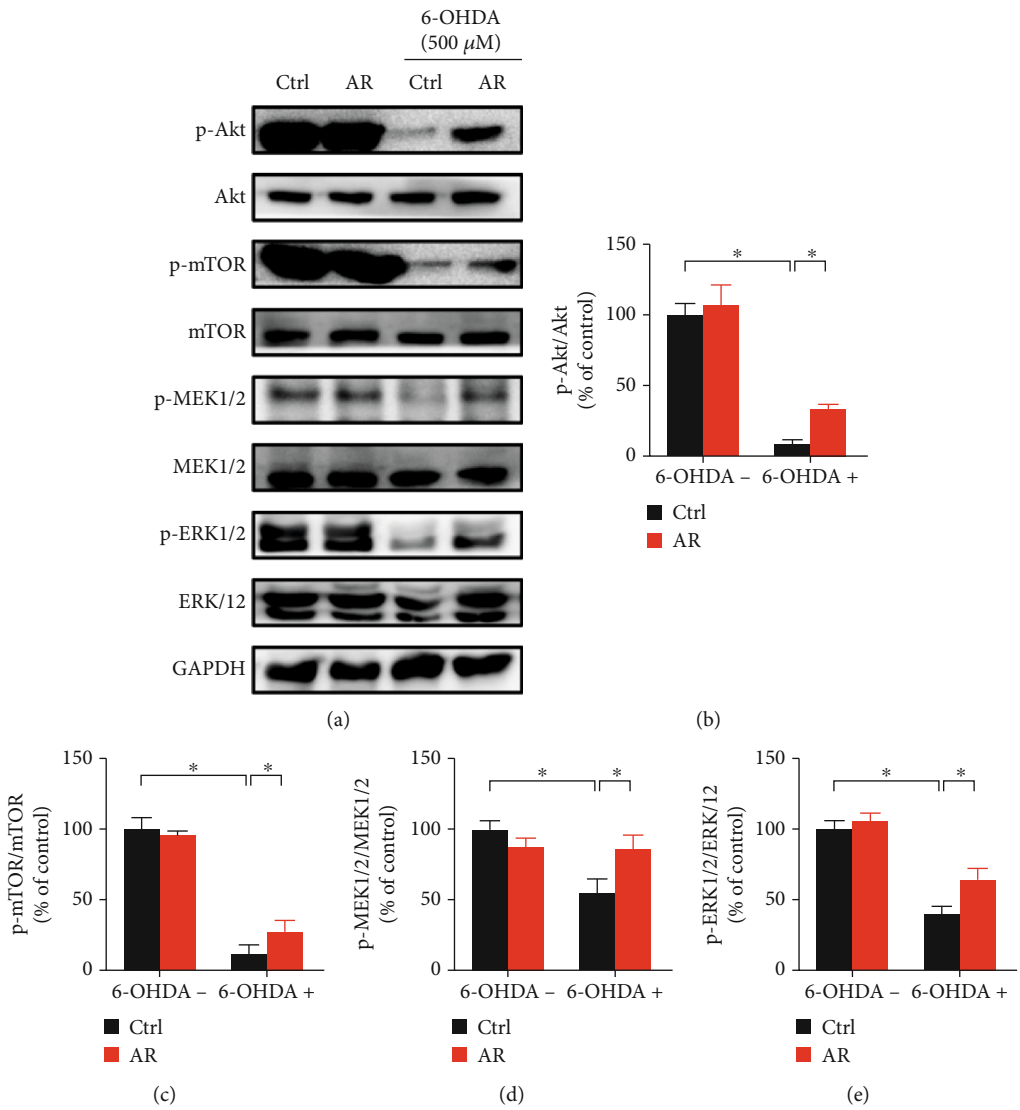


Figure 8: AR extract restores 6-OHDA-induced downregulation of the Akt/mTOR and MEK/ERK signaling pathway in PC12 cells. (a) PC12 cells were pretreated with 1 mg/mL AR extract or vehicle for 2 h and then treated with or without 500 $\mu$M 6-OHDA for 24 h. Protein expression levels of p-Akt, Akt, p-mTOR, mTOR, p-MEK1/2, MEK1/2, p-ERK1/2, and ERK1/2 in PC12 cells were examined by Western blot analysis. (b–e) Quantitative analysis of protein expression levels. Data are presented as a percentage of control group values (mean ± SD of three independent experiments). $^*p < 0.05$ indicates a statistically significant difference.

to promote health and longevity [21]. Numerous studies have demonstrated that *Ganoderma lucidum* exerts significant beneficial effects in neurodegeneration, diabetes mellitus, cardiovascular diseases, and tumor development [22]. These promising pharmacological activities of *Ganoderma lucidum* are at least partly attributed to its remarkable antioxidant and free radical scavenging activity. For instance, *Ganoderma lucidum* extract ameliorates MPTP-induced parkinsonism and protects dopaminergic neurons from oxidative stress via regulating mitochondrial function, autophagy, and apoptosis [23]. In a rat model, preadministration of *Ganoderma lucidum* was found to prevent hippocampus neurons from mitochondrial dysfunction and apoptosis by alleviating oxidative stress [24]. These findings suggest that other dietary mushrooms in the *Ganodermataceae* family may also exhibit potential effects in the prevention or treatment of oxidative stress-related diseases. AR is a species in the *Ganodermataceae* family whose pharmacological effects have rarely been explored. There were only two studies related to the chemical constituents of AR. These studies reported that ethanolic extract of AR contained phenolic compounds [13, 25], but there was no information about polysaccharides and triterpenes, which are well-known active ingredients in *Ganoderma lucidum*. Moreover, the major chemical contents of aqueous extract of AR have never been explored. This missing information is important because water decoction is the traditional method of extraction.

In the present study, the results of chemical assays demonstrated that the aqueous extract of AR contained phenolic compounds, polysaccharides, and triterpenes. The contents of total polysaccharides and triterpenes of AR extract were lower than that of aqueous extract of *Ganoderma lucidum*

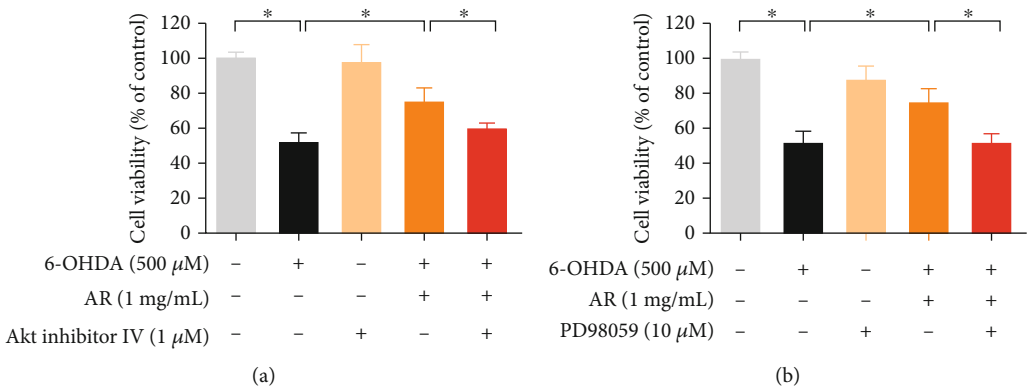


Figure 9: Akt inhibitor and MEK inhibitor abolish the neuroprotective effects of AR in 6-OHDA-treated PC12 cells. PC12 cells were pretreated with (a) 1 $\mu$M AKT inhibitor IV or (b) 10 $\mu$M MEK inhibitor (PD98059) for 30 min prior to incubation with 1 mg/mL AR for another 2 h, and then, the cells were exposed to 500 $\mu$M 6-OHDA for 24 h to induce cell damage. Then, cell viability was examined with MTT assays. Data are presented as a percentage of control group values (mean ± SD of three independent experiments). $^*p < 0.05$ indicates a statistically significant difference.

[26, 27]. Interestingly, the contents of total phenolic compounds of AR extract could reach the level of 5.52 mg GAE/g, which is unexpectedly much higher than that of aqueous extract of *Ganoderma lucidum* reported in other studies [28]. Indeed, numerous studies have shown that phenolic contents are highly correlated to antioxidant activities [29]. Therefore, we sought to investigate whether AR possess potential antioxidant activity, which may be useful in neuroprotection. At the beginning of the present study, we clearly demonstrated that the aqueous extract of AR had significant antioxidative activity in DPPH and TAC assays. In good agreement with the higher phenolic content of AR, the antioxidant capacity of AR extract was also stronger than that reported for aqueous extract of *Ganoderma lucidum* [26]. The antioxidant effect of AR extract was further examined in an *in vitro* model of Parkinson's disease, with PC12 cells. These cells are derived from the pheochromocytoma of the rat adrenal medulla, and they exhibit similar characteristics to those of neurons, owing to their common embryonic origin from the neural crest [12, 30]. PC12 cells have been widely adopted as an *in vitro* model to study neuronal development and neurological disease.

In the present study, 6-OHDA was used to induce neurotoxicity in PC12 cells. In line with findings from other studies [11, 30], our results indicated that 6-OHDA significantly induced ROS generation, loss of mitochondrial membrane potential, and apoptosis in PC12 cells (Figure 10). Although PC12 cells share many similarities with neurons, they still cannot be regarded as true neurons [31]. Therefore, we used NGF-differentiated PC12 cells to compare the neuroprotective effects of AR with nondifferentiated PC12 cells. The results showed that AR could protect against 6-OHDA-induced neurotoxicity in both NGF-differentiated and nondifferentiated PC12 cells, which suggests the potential activity of AR in protecting neurons. Therefore, PC12 cells are a feasible and reliable *in vitro* model for studying the antioxidant and neuroprotective effects of AR extract.

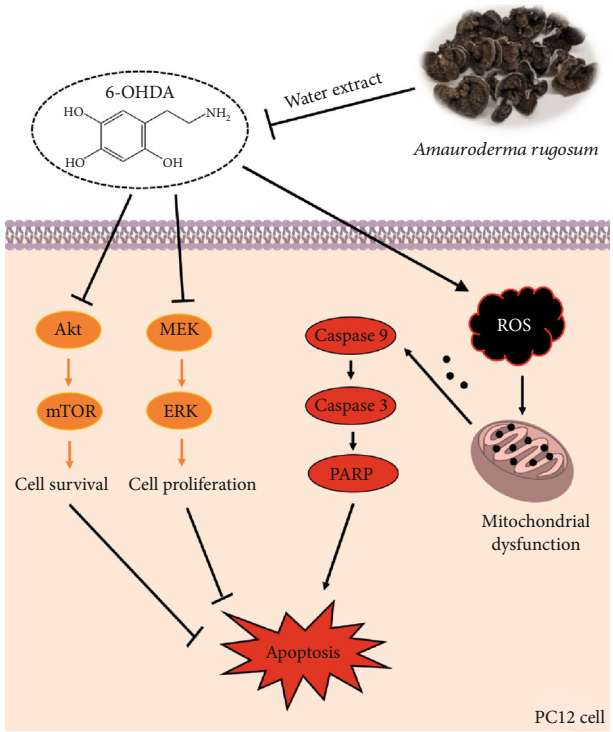


Figure 10: A schematic diagram illustrated the neuroprotective mechanisms of AR in PC12 cells.

Oxidative stress is considered as one of the major mechanisms contributing to dopaminergic neuron death in Parkinson's disease. Apart from being an important source of ROS production, mitochondria are also susceptible to oxidative stress. Increased oxidative stress can lead to mitochondrial dysfunction, which in turn triggers the further generation of ROS. Therefore, a vicious circle may form, in which oxidative stress and mitochondrial dysfunction feed each other forward [32]. The increased ROS production is involved in the reduction of mitochondrial ATP production, resulting in oxidative phosphorylation deficiency and then mitochondrial respiratory dysfunction [33]. 6-OHDA

impairs oxidative phosphorylation and mitochondrial respiration through the direct suppression of mitochondrial complexes I and IV activity [1, 34]. Consistent with previous reports, we found that 6-OHDA were able to induce massive ROS generation and impair mitochondrial respiration severely in PC12 cells. AR extract could exert protective effects on PC12 cells by removing 6-OHDA-induced ROS generation and attenuating 6-OHDA-induced mitochondrial respiratory dysfunction, which revealed its promising neuroprotective activity.

In addition, emerging evidence has indicated that the accumulation of ROS causes mitochondrial damage and induces apoptosis via the upregulation of proapoptotic protein expression (e.g., caspase 3/7/9 and PARP), resulting in the loss of dopaminergic neurons in Parkinson's disease. The expression of cleaved-caspase 3/8/9 in dopaminergic neurons is significantly higher in people with Parkinson's disease than in healthy individuals [35, 36]. Similar results have also been observed in preclinical studies using *in vitro* and *in vivo* models [37, 38]. These findings have revealed the important role of apoptosis in the pathogenesis of Parkinson's disease. Drugs with antioxidant and antiapoptotic effects may provide an attractive way to protect neurons from cell death and slow the progression of neurodegeneration [39]. In this study, we found that 6-OHDA upregulated the expressions of proapoptotic proteins, such as cleaved-caspase 9, caspase 3, and PARP, in PC12 cells, but this effect was significantly decreased by AR extract. This experimental result suggests that the neuroprotective action of AR extract may be attributed to its inhibitory effects on proapoptotic protein expression.

Beyond apoptotic proteins, previous studies have reported that Akt/mTOR- and MEK/ERK-dependent signaling pathways regulate cell survival and proliferation in different types of cells, including endothelial cells, cancer cells, and neuronal cells [40–44]. Disruption of the molecular signals in Akt/mTOR- and MEK/ERK-dependent pathways may severely affect the development of Parkinson's disease. For instance, the activity of Akt and mTOR is significantly lower in the neurons of patients with Parkinson's disease compared with unaffected individuals. In postmortem dopaminergic neurons, the protein levels of phosphorylated Akt and mTOR are severely depleted, leading to neuron degeneration [45]. In addition, data from *in vivo* animal studies and *in vitro* neuronal and neuroepithelial cell studies have demonstrated that MEK and ERK promote neuron cell survival and proliferation by antagonizing cell death and apoptosis [46, 47]. Hence, Akt/mTOR- and MEK/ERK-dependent signaling pathways may be potential therapeutic targets for treating neurodegenerative diseases. In the present study, 6-OHDA strongly abolished the protein expressions of phospho-Akt, mTOR, MEK, and ERK in PC12 cells, suggesting that the activities of those signaling pathways might be greatly reduced. Interestingly, the effects of 6-OHDA on the expressions of these signaling molecules were completely or partly restored by AR extract, revealing that the underlying neuroprotective mechanisms of AR extract may involve the regulation of Akt/mTOR and MEK/ERK signaling transduction. Next, we used Akt inhibitor IV and MEK inhibitor (PD98059) to further investigate the role of Akt/mTOR and MEK/ERK signals in protective effect of AR against 6-OHDA-induced cell injury in PC12 cells. Notably, both Akt inhibitor IV and PD98059 abolished the protective effect of AR in PC12 cells, which suggests that the neuroprotective effects of AR in PC12 cells are possibly through the upregulation of Akt/mTOR and MEK/ERK signaling pathways.

In conclusion, this study has demonstrated that AR can protect PC12 cells from 6-OHDA-induced oxidative stress, mitochondrial dysfunction, and apoptosis. In addition to the direct ROS scavenging effect, AR extract may downregulate proapoptotic proteins and upregulate the Akt/mTOR- and MEK/ERK-dependent signaling pathways. This is the first study reporting the neuroprotective effect of AR. Our findings provide useful information for future investigation of the potential application of AR or its active ingredients in the prevention and treatment of oxidative stress-related neurodegenerative diseases such as Parkinson's disease.

## Data Availability

The data used to support the findings of this study are available from the corresponding author upon request.

## Conflicts of Interest

The authors declare no conflict of interest.

## Authors' Contributions

G.L. and T.C. contributed to the conceptualization. X.W., R.H., and S.L. contributed to the methodology. J.L. and R.L. contributed to the formal analysis. J.L. and R.L contributed to the investigation. T.C. and B.H. contributed to the resources. J.L. and R.L. contributed to the data curation. J.L. contributed to the writing—original draft preparation. G.L. contributed to the writing—review and editing. G.L. contributed to the supervision. G.L. contributed to the project administration. G.L. contributed to the funding acquisition. Jingjing Li and Renkai Li contributed equally to the article.

## References

[1] H. Zhou, M. Shao, X. Yang et al., "Tetramethylpyrazine analogue T-006 exerts neuroprotective effects against 6-hydroxydopamine-induced Parkinson's disease in vitro and in vivo," *Oxidative Medicine and Cellular Longevity*, vol. 2019, Article ID 8169125, 14 pages, 2019.

[2] W. Poewe, C. M. Tanner, G. M. Halliday et al., "Parkinson disease," *Nature Reviews. Disease Primers*, vol. 3, no. 1, article 17013, 2017.

[3] N. J. Ray, N. Jenkinson, S. Wang et al., "Local field potential beta activity in the subthalamic nucleus of patients with Parkinson's disease is associated with improvements in bradykinesia after dopamine and deep brain stimulation," *Experimental Neurology*, vol. 213, no. 1, pp. 108–113, 2008.

[4] O. Hwang, "Role of oxidative stress in Parkinson's disease," *Experimental neurobiology*, vol. 22, no. 1, pp. 11–17, 2013.

[5] V. Dias, E. Junn, and M. M. Mouradian, "The role of oxidative stress in Parkinson's disease," *Journal of Parkinson's Disease*, vol. 3, no. 4, pp. 461–491, 2013.

[6] B. Bhandary, A. Marahatta, H.-R. Kim, and H.-J. Chae, "An involvement of oxidative stress in endoplasmic reticulum stress and its associated diseases," *International Journal of Molecular Sciences*, vol. 14, no. 1, pp. 434–456, 2012.

[7] J. Blesa, I. Trigo-Damas, A. Quiroga-Varela, and V. R. Jackson-Lewis, "Oxidative stress and Parkinson's disease," *Frontiers in Neuroanatomy*, vol. 9, p. 91, 2015.

[8] A. Federico, E. Cardaioli, P. da Pozzo, P. Formichi, G. N. Gallus, and E. Radi, "Mitochondria, oxidative stress and neurodegeneration," *Journal of the Neurological Sciences*, vol. 322, no. 1-2, pp. 254–262, 2012.

[9] J.-D. Guo, X. Zhao, Y. Li, G.-R. Li, and X.-L. Liu, "Damage to dopaminergic neurons by oxidative stress in Parkinson's disease (review)," *International Journal of Molecular Medicine*, vol. 41, no. 4, pp. 1817–1825, 2018.

[10] D. Xu, H. Duan, Z. Zhang et al., "The novel tetramethylpyrazine bis-nitrone (TN-2) protects against MPTP/$MPP^+$-induced neurotoxicity via inhibition of mitochondrial-dependent apoptosis," *Journal of Neuroimmune Pharmacology*, vol. 9, no. 2, pp. 245–258, 2014.

[11] Z. Zhang, W. Cui, G. Li et al., "Baicalein protects against 6-OHDA-induced neurotoxicity through activation of Keap1/Nrf2/HO-1 and involving PKC$\alpha$ and PI3K/AKT signaling pathways," *Journal of Agricultural and Food Chemistry*, vol. 60, no. 33, pp. 8171–8182, 2012.

[12] W. Dauer and S. Przedborski, "Parkinson's disease: mechanisms and models," *Neuron*, vol. 39, no. 6, pp. 889–909, 2003.

[13] P.-M. Chan, G. Kanagasabapathy, Y.-S. Tan, V. Sabaratnam, and U. R. Kuppusamy, "Amauroderma rugosum (Blume & T. Nees) Torrend: nutritional composition and antioxidant and potential anti-inflammatory properties," *Evidence-based Complementary and Alternative Medicine*, vol. 2013, Article ID 304713, 10 pages, 2013.

[14] C. M. Lin, Y. T. Lin, R. D. Lin, W. J. Huang, and M. H. Lee, "Neurocytoprotective effects of aliphatic hydroxamates from lovastatin, a secondary metabolite from *monascus*-fermented red mold rice, in 6-hydroxydopamine (6-OHDA)-treated nerve growth factor (NGF)-differentiated PC12 cells," *ACS Chemical Neuroscience*, vol. 6, no. 5, pp. 716–724, 2015.

[15] J. Li, Y. Wu, D. Wang et al., "Oridonin synergistically enhances the anti-tumor efficacy of doxorubicin against aggressive breast cancer via pro-apoptotic and anti-angiogenic effects," *Pharmacological Research*, vol. 146, article 104313, 2019.

[16] O. Firuzi, R. Miri, M. Tavakkoli, and L. Saso, "Antioxidant therapy: current status and future prospects," *Current Medicinal Chemistry*, vol. 18, no. 25, pp. 3871–3888, 2011.

[17] S. Dodd, O. Dean, D. L. Copolov, G. S. Malhi, and M. Berk, "*N*-acetylcysteine for antioxidant therapy: pharmacology and clinical utility," *Expert Opinion on Biological Therapy*, vol. 8, no. 12, pp. 1955–1962, 2008.

[18] E. B. Rimm, M. J. Stampfer, A. Ascherio, E. Giovannucci, G. A. Colditz, and W. C. Willett, "Vitamin E consumption and the risk of coronary heart disease in men," *The New England Journal of Medicine*, vol. 328, no. 20, pp. 1450–1456, 1993.

[19] S. Todd, M. Woodward, H. Tunstall-Pedoe, and C. Bolton-Smith, "Dietary antioxidant vitamins and fiber in the etiology of cardiovascular disease and all-causes mortality: results from the Scottish Heart Health Study," *American Journal of Epidemiology*, vol. 150, no. 10, pp. 1073–1080, 1999.

[20] M. C. de Rijk, M. M. Breteler, J. den Breeijen et al., "Dietary antioxidants and Parkinson disease: the Rotterdam Study," *Archives of neurology*, vol. 54, no. 6, pp. 762–765, 1997.

[21] D. Sliva, "*Ganoderma lucidum* (Reishi) in cancer treatment," *Integrative Cancer Therapies*, vol. 2, no. 4, pp. 358–364, 2003.

[22] Z. Lin and A. Deng, "Antioxidative and free radical scavenging activity of *Ganoderma* (Lingzhi)," *Advances in Experimental Medicine and Biology*, vol. 1182, pp. 271–297, 2019.

[23] Z. L. Ren, C. D. Wang, T. Wang et al., "*Ganoderma lucidum* extract ameliorates MPTP-induced parkinsonism and protects dopaminergic neurons from oxidative stress via regulating mitochondrial function, autophagy, and apoptosis," *Acta Pharmacologica Sinica*, vol. 40, no. 4, pp. 441–450, 2019.

[24] Y. Zhou, Z. Q. Qu, Y. S. Zeng et al., "Neuroprotective effect of preadministration with *Ganoderma lucidum spore* on rat hippocampus," *Experimental and Toxicologic Pathology*, vol. 64, no. 7-8, pp. 673–680, 2012.

[25] P.-M. Chan, Y.-S. Tan, K.-H. Chua, V. Sabaratnam, and U. R. Kuppusamy, "Attenuation of inflammatory mediators (TNF-alpha and nitric oxide) and up-regulation of IL-10 by wild and domesticated basidiocarps of *Amauroderma rugosum* (Blume & T. Nees) Torrend in LPS-stimulated RAW264.7 cells," *PLoS One*, vol. 10, no. 10, article e0139593, 2015.

[26] B. Poniedziałek, M. Siwulski, A. Wiater et al., "The effect of mushroom extracts on human platelet and blood coagulation: in vitro screening of eight edible species," *Nutrients*, vol. 11, no. 12, 2019.

[27] M. Zhu, Q. Chang, L. K. Wong, F. S. Chong, and R. C. Li, "Triterpene antioxidants from *Ganoderma lucidum*," *Phytotherapy Research*, vol. 13, no. 6, pp. 529–531, 1999.

[28] J. Mishra, A. Joshi, R. Rajput, K. Singh, A. Bansal, and K. Misra, "Phenolic rich fractions from mycelium and fruiting body of *Ganoderma lucidum* inhibit bacterial pathogens mediated by generation of reactive oxygen species and protein leakage and modulate hypoxic stress in HEK 293 cell line," *Advances in Pharmacological Sciences*, vol. 2018, Article ID 6285615, 10 pages, 2018.

[29] Z. Kalaycioglu and F. B. Erim, "Total phenolic contents, antioxidant activities, and bioactive ingredients of juices from pomegranate cultivars worldwide," *Food Chemistry*, vol. 221, pp. 496–507, 2017.

[30] C. Zhang, C. Li, S. Chen et al., "Berberine protects against 6-OHDA-induced neurotoxicity in PC12 cells and zebrafish through hormetic mechanisms involving PI3K/AKT/Bcl-2 and Nrf2/HO-1 pathways," *Redox Biology*, vol. 11, pp. 1–11, 2017.

[31] E. T. Kavanagh, J. P. Loughlin, K. R. Herbert et al., "Functionality of NGF-protected PC12 cells following exposure to 6-hydroxydopamine," *Biochemical and Biophysical Research Communications*, vol. 351, no. 4, pp. 890–895, 2006.

[32] S. R. Subramaniam and M. F. Chesselet, "Mitochondrial dysfunction and oxidative stress in Parkinson's disease," *Progress in Neurobiology*, vol. 106-107, pp. 17–32, 2013.

[33] I. G. Kirkinezos and C. T. Moraes, "Reactive oxygen species and mitochondrial diseases," *Seminars in Cell & Developmental Biology*, vol. 12, no. 6, pp. 449–457, 2001.

[34] B. P. Dranka, J. Zielonka, A. G. Kanthasamy, and B. Kalyanaraman, "Alterations in bioenergetic function induced by Parkinson's disease mimetic compounds: lack of

correlation with superoxide generation," *Journal of Neurochemistry*, vol. 122, no. 5, pp. 941–951, 2012.

[35] A. Hartmann, S. Hunot, P. P. Michel et al., "Caspase-3: a vulnerability factor and final effector in apoptotic death of dopaminergic neurons in Parkinson's disease," *Proceedings of the National Academy of Sciences of the United States of America*, vol. 97, no. 6, pp. 2875–2880, 2000.

[36] A. Hartmann, J. D. Troadec, S. Hunot et al., "Caspase-8 is an effector in apoptotic death of dopaminergic neurons in Parkinson's disease, but pathway inhibition results in neuronal necrosis," *The Journal of Neuroscience*, vol. 21, no. 7, pp. 2247–2255, 2001.

[37] R. von Coelln, S. Kügler, M. Bähr, M. Weller, J. Dichgans, and J. B. Schulz, "Rescue from death but not from functional impairment: caspase inhibition protects dopaminergic cells against 6-hydroxydopamine-induced apoptosis but not against the loss of their terminals," *Journal of Neurochemistry*, vol. 77, no. 1, pp. 263–273, 2001.

[38] S. F. Xu, Y. H. Zhang, S. Wang et al., "Lactoferrin ameliorates dopaminergic neurodegeneration and motor deficits in MPTP-treated mice," *Redox Biology*, vol. 21, article 101090, 2019.

[39] N. Lev, E. Melamed, and D. Offen, "Apoptosis and Parkinson's disease," *Progress in Neuro-Psychopharmacology & Biological Psychiatry*, vol. 27, no. 2, pp. 245–250, 2003.

[40] J. Li, F. Li, F. Tang et al., "AGS-30, an andrographolide derivative, suppresses tumor angiogenesis and growth *in vitro* and *in vivo*," *Biochemical Pharmacology*, vol. 171, article 113694, 2020.

[41] J. Li, F. Tang, R. Li et al., "Dietary compound glycyrrhetinic acid suppresses tumor angiogenesis and growth by modulating antiangiogenic and proapoptotic pathways *in vitro* and *in vivo*," *The Journal of Nutritional Biochemistry*, vol. 77, article 108268, 2020.

[42] J. Polivka Jr. and F. Janku, "Molecular targets for cancer therapy in the PI3K/AKT/mTOR pathway," *Pharmacology & Therapeutics*, vol. 142, no. 2, pp. 164–175, 2014.

[43] D. Morgensztern and H. L. McLeod, "PI3K/Akt/mTOR pathway as a target for cancer therapy," *Anti-Cancer Drugs*, vol. 16, no. 8, pp. 797–803, 2005.

[44] J. Zhang, J. Li, Z. Shi et al., "pH-sensitive polymeric nanoparticles for co-delivery of doxorubicin and curcumin to treat cancer via enhanced pro-apoptotic and anti-angiogenic activities," *Acta Biomaterialia*, vol. 58, pp. 349–364, 2017.

[45] C. Malagelada, Z. H. Jin, and L. A. Greene, "RTP801 is induced in Parkinson's disease and mediates neuron death by inhibiting Akt phosphorylation/activation," *The Journal of Neuroscience*, vol. 28, no. 53, pp. 14363–14371, 2008.

[46] Z. Xia, M. Dickens, J. . Raingeaud, R. J. Davis, and M. E. Greenberg, "Opposing effects of ERK and JNK-p38 MAP kinases on apoptosis," *Science*, vol. 270, no. 5240, pp. 1326–1331, 1995.

[47] L. Colucci-D'Amato, C. Perrone-Capano, and U. di Porzio, "Chronic activation of ERK and neurodegenerative diseases," *BioEssays*, vol. 25, no. 11, pp. 1085–1095, 2003.

Hindawi
Oxidative Medicine and Cellular Longevity
Volume 2021, Article ID 8831535, 8 pages
https://doi.org/10.1155/2021/8831535

*Research Article*

# Effects of Occupational Exposure to Waste Anesthetic Gas on Oxidative Stress and DNA Damage

**Hai-Xin Hua**,[1] **Hai-Bo Deng**,[2] **Xiu-Ling Huang**,[1] **Chang-Qing Ma**,[1] **Ping Xu**,[1] **Ye-Hua Cai**,[1] **and Hai-Tang Wang**[3]

[1]*Department of Anesthesiology, Zhujiang Hospital of Southern Medical University, 253 Gongye Ave., Guangzhou, China 510282*
[2]*Department of Anesthesiology, Huizhou Third People's Hospital, Guangzhou Medical University, No. 1, Xuebei Street, Huicheng District, Huizhou City, Guangdong Province, China*
[3]*Department of Anesthesiology, Nanfang Hospital of Southern Medical University, 1838 Guangzhoudadaobei, Guangzhou, China 510515*

Correspondence should be addressed to Ye-Hua Cai; caiyh2007@163.com and Hai-Tang Wang; wanghaitang8888@163.com

Received 6 August 2020; Revised 27 October 2020; Accepted 8 January 2021; Published 20 January 2021

Academic Editor: Mithun Sinha



*Objective*. The aim of the study was to investigate the potential effects of waste anesthetic gas (WAG) on oxidative stress, DNA damage, and vital organs. *Methods*. A total of 150 members of the staff at a hospital were assigned to an exposure group or control group. The 68 operating room (OR) staff in the exposure group were exposed to WAG, and the 82 non-OR staff in the control group were not exposed to WAG. Air samples were collected in the OR, and the sevoflurane concentrations in the samples were determined. Superoxide dismutase (SOD), glutathione peroxidase (GSH-px), and malondialdehyde (MDA) in plasma from the participants were determined to assess oxidative stress. Western blot analysis was used to detect $\gamma H_2AX$ in peripheral blood to assess DNA damage. Hematopoietic parameters, liver function, kidney function, and changes in electrophysiology were assessed to identify the effects on the vital organs. *Results*. The mean (±standard deviation) sevoflurane concentration in 172 air samples from 22 operating rooms was $1.11 \pm 0.65$ ppm. The superoxide dismutase activity and vital organ parameters (lymphocyte, hemoglobin, and total protein concentrations and heart rate) were significantly lower ($P < 0.05$) in the exposed group than the control group. The malondialdehyde, total bilirubin, and creatinine concentrations and QT and QTc intervals were significantly higher ($P < 0.05$) in the exposed group than the control group. There were no significant differences between the glutathione peroxidase activities and $\gamma$H2AX concentrations for the exposed and control groups. *Conclusions*. Long-term occupational exposure to waste anesthetic gas may affect the antioxidant defense system and probably affects vital organ functions to some extent. No correlation between DNA damage and chronic exposure to WAG was observed.

## 1. Introduction

Inhaled anesthetics are widely used because the dose can be readily controlled. However, waste anesthetic gas (WAG) can leak into an operating room (OR). Medical personnel in ORs suffer long-term exposure to WAG [1]. There is concern about the risks posed to the health of people suffering long-term exposure to WAG. It has been found that occupational exposure to WAG can cause an imbalance between oxidation and antioxidation, changes in antioxidant enzymes, increases in oxygen free radical concentrations, DNA damage, and even genotoxicity [2–5]. Large epidemiological investigations have indicated that exposure to WAG can increase the risks of chronic diseases (e.g., liver dysfunction and renal insufficiency), spontaneous abortion, and congenital malformation occurring and can decrease the birth rate and increase the stillbirth rate [6–8]. However, most of these studies were performed decades ago, and few relevant studies have been published in recent years. There have recently been great changes in anesthesiological methods, drugs, and equipment. Sevoflurane and desflurane have gradually replaced nitrous oxide, enflurane, and isoflurane and are now widely used in clinical anesthesiological practice. New ventilation strategies, such as low tidal volume

ventilation, that are increasingly used by clinical anesthesiologists may decrease WAG emissions. Laminar flow systems and scavenging systems, which are now widely used in ORs, may decrease WAG emissions. These changes may have decreased WAG concentrations in ORs and the effects of WAG exposure on OR staff [9]. The effects of WAGs on medical staff in ORs need to be reassessed. In this study, WAG concentrations in ORs were investigated, and potential effects of occupational exposure to low concentrations of sevoflurane in OR staff were assessed by investigating oxidative stress, DNA damage, changes in hematopoietic parameters, liver function, kidney function, and electrophysiological changes.

## 2. Materials and Methods

*2.1. Study Design and Participants.* The study was approved (approval no. 2017-MZK-001) by the Medical Ethics Committee of Zhujiang Hospital, part of the Southern Medical University, and was registered in the Chinese Clinical Trial Registry (registration no. ChiCTR-IOR-17013915). The cross-sectional study was performed at Zhujiang Hospital, part of the Southern Medical University, Guangzhou, China. Written informed consent was obtained from each participant. The participants, full-time Zhujiang Hospital staff aged 22–50 y with 2–25 y service, were assigned to two groups. The exposure group contained OR staff who were exposed to anesthetic gases but not to any other hazardous agents. The control group contained non-OR staff matched to the exposure group in terms of age, sex, length of service, smoking habits, and drinking habits and with no occupational exposure to hazardous agents such as radiation and anesthetic gases. The exclusion criteria were (1) history of anesthesia, surgery, radiological diagnosis, or treatment in the previous three months; (2) current pregnancy or lactation; (3) autoimmune disease, malignancy, infectious disease, or other acute or chronic disease that could affect oxidative stress and DNA levels; (4) long-term use of vitamin supplements or antioxidants; and (5) refusal to participate in the study.

*2.2. Sevoflurane Concentration in the OR.* The Zhujiang Hospital ORs used for the study were equipped with air conditioning systems and scavenging devices. Sevoflurane has been the only available inhaled anesthetic for several decades and is used frequently to induce and maintain anesthesia. Air samples were collected from different sites within the ORs between 8:00 and 8:30 a.m. on weekdays. Anesthetists and anesthetic nurses each wore a sampler close to (~10 cm from) the respiratory area during personal exposure (P1). Each sampler was turned on as soon as sevoflurane started to be administered. Each sampler had a flow rate of 100 mL/min, and the sampling tube was replaced every 2 h. Sampling continued for 8 h. Samplers were also placed on the nurses' tables in the ORs (P2). Each sampling tube was sealed immediately after the sample collection period had ended and then sent to the laboratory, where the sevoflurane concentration was determined using an HP6890N gas chromatograph (Agilent Technologies, Santa Clara, CA, USA).

*2.3. Demographic Data.* Demographic data for each participant (including age, sex, body mass index, length of service, occupation, smoking habits, and drinking habits) and clinical characteristics (including medical history and current medication) were recorded. Blood samples were collected from all of the participants and were preserved.

*2.4. Oxidative Stress.* Peripheral venous blood (2 mL) was obtained from each participant into a sterile tube containing heparin (an anticoagulant). The blood was centrifuged at 3500 revolutions/min for 10 min; then, the supernatant was transferred to a fresh tube and stored at −20°C until analysis. Each sampling tube was given a unique label, stored in a portable refrigerator, and transferred to the laboratory for processing within 3 h of collection. The investigators did not know which participant was allocated to which group. The superoxide dismutase (SOD) activity, glutathione peroxidase (GSH-px) activity, and malondialdehyde (MDA) concentration in each plasma sample were determined to allow oxidative stress to be assessed. The SOD activity, GSH-px activity, and MDA concentration were prepared using a superoxide dismutase assay kit (Beyotime Biotechnology, Shanghai, China), a lipid oxidation assay kit (Beyotime Biotechnology), and a glutathione peroxidase assay kit (Nanjing Jiancheng Bioengineering Institute, Nanjing, China), respectively, and the prepared samples were analyzed using a DR5000 ultraviolet/visible spectrophotometer.

*2.5. DNA Damage and Vital Organ Functions.* Peripheral venous blood (2 mL) was obtained from each participant into a sterile tube containing heparin and then diluted to 4 mL. The sample was then slowly added to a lymphocyte separation solution in a 20 mL centrifuge tube. The mixture was then centrifuged at 1500 revolutions/min for 20 min. The liquid separated into three layers. The upper layer was light yellow plasma, the middle layer was milky white and contained the white blood cells, and the bottom layer contained the blood cells. The white blood cell layer was collected using a pipette and placed in a sterile 1.5 mL centrifuge tube. The liquid was then centrifuged at 10000 revolutions/min for 5 min, and the white precipitate was transferred to another tube and stored at −80°C for Western blot analysis. Additional DNA damage was avoided by performing every step under indirect light. $\gamma$-H2AX protein in each sample was measured using a Western blot analysis kit (Promega, Madison, WI, USA) to assess DNA damage.

Peripheral venous blood (2 mL) was obtained from each participant into a tube containing EDTA (an anticoagulant) to allow a complete blood count to be performed, and 4 mL of venous blood was obtained into a dry tube without additives for use in biochemical tests to assess blood lipid concentrations, liver function, and renal function. Each tube was labeled and then analyzed. Complete blood counts were performed using an SE5000 automatic blood cell analyzer. Blood biochemical analyses were performed on the day the blood samples were collected using a Mindray BS2001 automatic biochemical analyzer. A 12-lead electrocardiogram (ECG) of each subject in a resting state was acquired in the morning using an ECG-9620P2 ECG machine (Shanghai). The same

technician acquired the ECGs of all the participants. The ECG results were analyzed by another technician who did not know to which group each participant had been allocated.

*2.6. Sample Size Calculation.* The sample size was calculated using Formula 1, which was published previously [10]. The difference ($D$), standard deviation ($S$), and test efficiency were 3.3, 5.4, and 8, respectively. The ratio between the participants in the exposure and control groups was 1. We estimated that 172 participants (86 in each group) were required.

$$N = \frac{2MS^2}{D^2}, \quad (1)$$

Formula 1 is used to determine the sample size ($N$). $M$ is the test efficiency, $S$ is the standard deviation, and $D$ is difference.

*2.7. Statistical Methods.* Data analysis was performed using the SPSS 20.0 software (IBM, Armonk, NY, USA). If a dataset had a normal distribution, the data were represented as $\bar{x} \pm s$. Independent sample $t$-tests were used to identify differences between two independent samples. The median (lower quartile, upper quartile) were used to describe data that did not follow the normal distribution. Nonparametric rank-sum tests were used to compare groups of data. Chi-square tests or Fisher's exact probability tests were used to analyze enumeration data. The alpha level was 0.05 (bilateral). $P < 0.05$ was considered to indicate a statistically significant result.

## 3. Results

*3.1. Sevoflurane Concentrations in the ORs.* A total of 172 air samples from 22 ORs were collected. The sevoflurane concentration in each sample was determined. A total of 88 of the samples were collected in areas in which anesthesiologists or anesthesia nurses worked (P1), and 84 samples were collected from areas in which OR nurses worked (P2). The sevoflurane concentrations were 0.07–3.84 ppm (mean 1.11 ± 0.65 ppm). The sevoflurane concentrations in the P1 samples were 0.26–3.84 ppm (mean 1.44 ± 0.65 ppm). The sevoflurane concentrations in 28% of the P1 air samples exceeded the Chinese standard for occupational exposure. The sevoflurane concentrations in the P2 samples were 0.07–1.78 ppm (mean 0.70 ± 0.36 ppm). The sevoflurane concentrations in >8% of the P2 air samples exceeded the Chinese standard for occupational exposure. The sevoflurane concentrations were significantly higher in the P1 samples than the P2 samples. The results are shown in Figure 1.

*3.2. Demographic Characteristics.* A total of 180 members of staff were screened for eligibility, and 153 met the inclusion criteria. A total of 150 members of staff were included in the study (one was excluded because of pregnancy, one because of a chronic infectious disease, and one because the serum creatinine concentration was above the upper limit of the normal range). Of the 150 participants, 68 were OR personnel (anesthesiologists, anesthesia nurses, itinerant nurses, and instrument nurses) and were assigned to the exposure group. The control group contained 82 non-OR staff from the departments of digestive medicine, hematology, rehabilitation, rheumatic immunology, ultrasound, respiratory medicine, pediatrics, and geriatrics. There were no significant differences between the demographic characteristics of the two groups. The demographic characteristics of the groups are shown in Table 1.

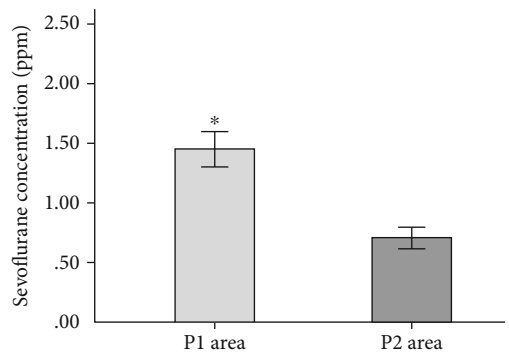


Figure 1: Sevoflurane concentrations in the different working areas. Notes. P1: anesthesiologist and anesthesia nurse working areas; P2: operating room nurse working areas.

Table 1: Demographic characteristics of the exposure and control groups ($\bar{x} \pm s$).

| Group | Exposure group ($n = 68$) | Control group ($n = 82$) | $P$ value |
|---|---|---|---|
| Sex | | | |
| Man | 19 | 26 | 0.72 |
| Woman | 49 | 56 | |
| Age | 31.56 ± 5.64 | 29.54 ± 5.86 | 0.06 |
| LOS | 8.29 ± 5.15 | 7.37 ± 6.24 | 0.39 |
| Smoking | | | |
| Yes | 4 | 6 | 0.72 |
| No | 64 | 76 | |
| Drinking | | | |
| Yes | 6 | 9 | 0.78 |
| No | 62 | 73 | |
| BMI | 21.28 ± 2.37 | 21.17 ± 2.74 | 0.88 |

Notes. (1) Smoking was defined as smoking at least one cigarette per day for more than a year or having quit smoking for <1 y. (2) Drinking was defined as consuming alcohol at least once per week for more than half a year. (3) LOS: length of service. (4) BMI: body mass index.

*3.3. Oxidative Stress.* Normal distribution tests were performed on the SOD activity, GSH-px activity, and MDA concentration data. The SOD activity data did not follow a normal distribution, so the median and quartiles were used in comparative analyses. The median (lower quartile, upper quartile) SOD activities were 51.42 (49.80, 52.27) U/mL for the exposure group and 52.11 (51.19, 52.80) U/mL for the control group. A nonparametric rank-sum test indicated that the SOD activities for the exposure and control groups were significantly different ($Z = -2.84$). The MDA concentration

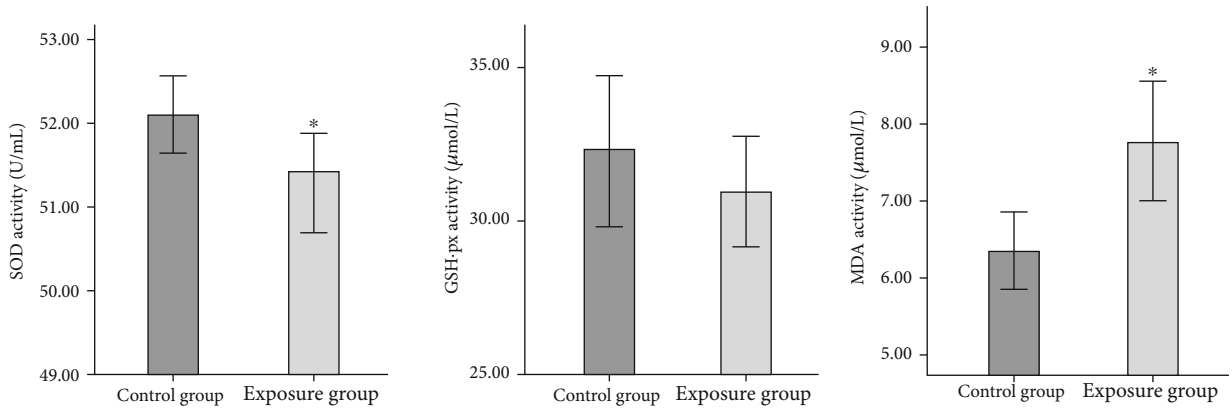


Figure 2: Superoxide dismutase (SOD) activities, glutathione peroxidase (GSH-px) activities, and malondialdehyde (MDA) concentrations for the exposure and control groups. Note. (1) Compared with the control group; (2) $^{*}P < 0.05$.

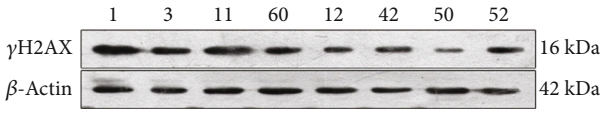


Figure 3: γH2AX and β-actin bands for the exposure and control groups. Notes. The exposure group samples contained the 1, 3, 60, and 42 bands, and the control group contained the 11, 12, 50, and 52 bands

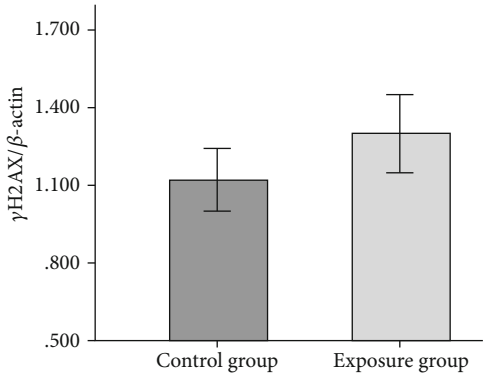


Figure 4: γH2AX/β-actin ratios for the control and exposure groups. No difference was found between the γH2AX expression in the control and exposure groups.

was higher for the exposure group (7.77 ± 2.99 μmol/L) than the control group (6.35 ± 1.81 μmol/L). The GSH-px activities for the exposure group (30.93 ± 6.19 μmol/L) and control group (32.33 ± 7.54 μmol/L) were not significantly different (Figure 2).

*3.4. DNA Damage.* Western blot analysis was performed to detect the γH2AX expression in the exposure and control group samples. The γH2AX and β-actin bands for the two groups are shown in Figure 3. The γH2AX/β-actin ratios for the exposure and control groups were 1.29 ± 0.51 and 1.12 ± 0.42, respectively. The γH2AX expression results for the exposure and control groups were not significantly different. The results are shown in Figure 4.

Table 2: Complete blood count results for the exposure and control groups ($(\bar{x} \pm s)$ or median (lower quartile, upper quartile)).

| Indexes | Exposure group ($n = 68$) | Control group ($n = 82$) | $P$ value |
|---|---|---|---|
| HGB (g/L) | 121.75 ± 12.89 | 133.62 ± 16.56 | 0.02 |
| WBC ($10^9$/L) | 6.53 ± 1.60 | 7.04 ± 1.80 | 0.21 |
| PLT ($10^9$/L) | 232.62 ± 53.15 | 228.55 ± 43.13 | 0.76 |
| RBC ($10^{12}$/L) | 4.52 ± 0.51 | 4.70 ± 0.87 | 0.16 |
| NEUT ($10^9$/L) | 3.77 ± 1.36 | 3.78 ± 1.58 | 0.99 |
| LYM ($10^9$/L) | 2.31 ± 0.51 | 2.63 ± 0.82 | 0.04 |
| EON ($10^9$/L) | 0.10 (0.06, 0.19) | 0.11 (0.07, 0.25) | 0.54 |
| BASON ($10^9$/L) | 0.016 ± 0.009 | 0.018 ± 0.006 | 0.50 |

Notes. HGB: hemoglobin; RBC: red blood cell count; WBC: white blood cell count; PLT: blood platelet count; LYM: lymphocyte count; NEUT: neutrophil count; EON: eosinophil count; BASON: basophil cell count.

*3.5. Complete Blood Count.* The hemoglobin concentrations in the exposure and control group samples were 121.75 ± 12.89 and 133.62 ± 16.56 g/L, respectively. The hemoglobin concentrations were much lower in the exposure group samples than the control group samples. The lymphocyte concentrations were lower in the exposure group samples ($2.31 \pm 0.51 \times 10^9$/L) than the control group samples ($2.63 \pm 0.82 \times 10^9$/L). The white blood cell, blood platelet, red blood cell, neutrophil, eosinophil, and basophil cell counts for the control and exposure groups were not significantly different. The results are shown in Table 2.

*3.6. Liver Function and Renal Function.* The total protein concentrations were much lower in the serum samples from the exposure group than in the serum samples from the control group ($P < 0.05$). The creatinine concentrations were much higher for the exposure group (85.73 ± 14.16 μmol/L) than the control group (79.55 ± 16.91 μmol/L). The total bilirubin concentrations were also higher for the exposure group (14.11 ± 3.91 μmol/L) than the control group (11.23 ± 5.08 μmol/L). The concentrations of the other

Table 3: Blood biochemical test results for the exposure and control groups ($(\bar{x} \pm s)$ or median (lower quartile, upper quartile)).

| Indexes | Exposure group ($n = 68$) | Control group ($n = 82$) | $P$ value |
|---|---|---|---|
| CHO (mmol/L) | 4.70 ± 0.9 | 4.77 ± 0.95 | 0.77 |
| TG (mmol/L) | 0.83 (0.58, 1.23) | 0.89 (0.65, 1.47) | 0.39 |
| TP (g/L) | 70.65 ± 4.43 | 76.24 ± 5.61 | 0.03 |
| T-BIL ($\mu$mol/L) | 14.11 ± 3.91 | 11.23 ± 5.08 | 0.03 |
| D-BIL ($\mu$mol/L) | 4.53 ± 1.99 | 4.34 ± 2.05 | 0.73 |
| ALT (u/L) | 15.00 (12.00, 19.00) | 14.50 (10.75, 27.25) | 0.76 |
| AST (u/L) | 18.38 ± 5.42 | 20.91 ± 8.12 | 0.16 |
| CRE ($\mu$mol/L) | 85.73 ± 14.16 | 79.55 ± 16.91 | 0.02 |
| BUN (mmol/L) | 5.25 ± 1.52 | 4.67 ± 1.29 | 0.32 |
| UA ($\mu$mol/L) | 283.67 ± 74.26 | 296.74 ± 69.16 | 0.25 |

Notes. CHO: total cholesterol; TG: triglycerides; TP: total protein; T-BIL: total bilirubin; D-BIL: direct bilirubin; ALT: alanine aminotransferase; AST: aspartate aminotransferase; BUN: blood urea nitrogen; CRE: creatinine; UA: uric acid.

biochemical markers (total cholesterol, triglycerides, direct bilirubin, alanine aminotransferase, aspartate aminotransferase, blood urea nitrogen, and uric acid) for the exposure and control groups were not significantly different. The results are shown in Table 3.

*3.7. ECG.* The ECGs indicated that one person in the exposure group had coronary sinus rhythm, four had sinus arrhythmia, three had sinus arrhythmia, three had sinus bradycardia accompanied by arrhythmia, one had sinus arrhythmia and occasional atrial premature contraction, two had sinus arrhythmia with ST segment changes, four had sinus rhythm with ST segment changes, one had sinus rhythm with occasional ventricular premature contraction, two had sinus rhythm with left ventricular high voltage, two had sinus rhythm with clockwise transposition, two had sinus rhythm with incomplete right bundle branch block, and 46 had normal ECG. The ECGs indicated that three people in the control group had sinus arrhythmia, two had sinus bradycardia accompanied by arrhythmia, one had sinus arrhythmia with occasional premature atrial contraction, one had sinus tachycardia with T-wave changes, two had sinus arrhythmia with ST segment changes, four had sinus rhythm with ST segment changes, one had sinus rhythm with occasional premature ventricular contraction, one had sinus rhythm with preexcitation syndrome, two had sinus rhythm with a prolonged P–R interval, one had sinus rhythm with incomplete right bundle branch block, one had sinus rhythm with complete right bundle branch block, and 63 had normal ECG. The normal ECGs only included sinus rhythm and sinus rhythm with limb lead low voltage. Abnormal ECGs were found for 22 of the 68 people in the exposure group and 19 of the 82 people in the control group. The numbers of abnormal ECGs for the exposure and control groups were not significantly different (Table 4). The HR, PR interval, QRS interval, QT interval, QTc interval, RV5 amplitude, SV1 amplitude, and RV5+SV1 amplitude data for the exposure and control groups were compared. The HR was significantly lower for the exposure group (69.59 ± 9.63) than the control group (74.96 ± 7.87). The QT interval was significantly longer for the exposure group (median 387.00 ms (lower quartile 372.00 ms, upper quartile 394.50 ms)) than the control group (372.00 ms (lower quartile 360.00 ms, upper quartile 388.00 ms)). The QTc interval was also significantly longer for the exposure group (402.79 ± 15.30 ms) than the control group (393.60 ± 11.42 ms). The RV5, SV1, and RV5+SV1 amplitudes for the exposure and control groups were not significantly different (Table 5).

Table 4: Electrocardiogram results for the exposure and control groups.

| ECG results | Exposure group ($n = 68$) | Control group ($n = 82$) | $\chi^2$ | $P$ value |
|---|---|---|---|---|
| Normal | 22 | 19 | 1.578 | 0.27 |
| Abnormal | 46 | 63 | | |

## 4. Discussion

Even though the ORs had laminar flow and scavenging systems, the antioxidant defense systems and vital organ functions of staff exposed to WAG in the long term could have been affected. However, no difference in DNA damage markers was found between the exposure and control groups. The time-weighted average sevoflurane concentrations in the ORs were lower than the Chinese limit of 2 ppm, but 28% of the air samples from the anesthesiologist work areas and 8% of the air samples from the OR nurse work areas had sevoflurane concentrations > 2 ppm. This indicated that OR staff may be exposed to high WAG concentrations at work.

Volatile inhaled anesthetics are widely used in ORs. However, anesthetic gas may escape into the OR while the anesthetic is being administered [11, 12]. Staff in the OR may therefore be exposed to WAG while working. There is much evidence suggesting that chronic exposure to WAG can increase oxidative stress [3, 5, 13] and cause genotoxicity [14] and carcinogenicity [15, 16]. In some large epidemiological investigations, medical staff exposed to WAG have been found to have increased risks of chronic diseases (e.g., cancer, liver dysfunction, and renal insufficiency), spontaneous abortion, and congenital malformation and to have low birth rates and high stillbirth rates [6–8]. However, most of these studies were performed decades ago. Recent changes in conditions, such as different anesthetic agents being used and OR ventilation equipment being installed, mean that exposure of OR staff to WAGs needs to be reassessed. We found relatively high levels of oxidative stress in OR staff exposed to WAG over a long period, similar to the results of previous studies [13]. Long-term exposure to WAGs can cause radical damage and the antioxidant defense system to become less

Table 5: Electrocardiogram characteristics for the exposure and control groups ($(\bar{x} \pm s)$ or median (lower quartile, upper quartile)).

| Indexes | Exposure group ($n = 68$) | Control group ($n = 82$) | $P$ value |
|---|---|---|---|
| HR (bpm) | 69.59 ± 9.63 | 74.96 ± 7.87 | 0.00 |
| PR (ms) | 149.9 ± 16.77 | 147.72 ± 17.91 | 0.38 |
| QRS (ms) | 89.45 ± 9.03 | 86.94 ± 8.19 | 0.13 |
| QT (ms) | 387.00 (372.00, 394.50) | 372.00 (360.00, 388.00) | 0.01 |
| QTc(ms) | 402.79 ± 15.30 | 393.60 ± 11.42 | 0.00 |
| $RV_5$(mV) | 1.38 ± 0.45 | 1.35 ± 0.42 | 0.75 |
| $SV_1$(mV) | 0.91 ± 0.42 | 0.89 ± 0.33 | 0.69 |
| $RV_5$+$SV_1$(mV) | 2.29 ± 0.70 | 2.25 ± 0.58 | 0.74 |

effective. Long-term exposure to WAGs can decrease the SOD activity, GSH-px activity, trace element concentrations, and red blood cell count [2].

A series of stress responses can occur once DNA damage has occurred in a cell. These stress responses induce a signal cascade and even stop the cell cycle until the damage has been repaired. One of the main components of the signal cascade is H2AX, which can be phosphorylated when DNA double-strand breaks (DSBs) occur and then initiate the damage repair mechanism. H2AX plays an extremely important role in the DSB identification and repair process [17]. H2AX is a member of the histone H2A family. Phosphorylated H2AX recognizes DSBs, forms a focal point for DSBs, and participates in the recruitment of proteins to repair DSBs [18]. DSBs are closely related to $\gamma$H2AX production, possibly at a rate of one $\gamma$H2AX molecule per DSB [19]. $\gamma$H2AX is therefore considered to be a specific index for detecting DSBs in cells. The DNA damage marker concentrations in the exposure and control groups were not significantly different in our results. Similar results have been found in previous studies in which no significant changes were found in genotoxicity biomarkers in physicians using modern anesthesia workstations in ORs during medical residency programs [20, 21]. However, DNA damage caused by occupational exposure to WAGs remains controversial [22–24]. Costa et al. found increased risks of DNA damage and oxidative stress in young professionals and that more DNA damage and oxidative stress occurred after exposure to WAG for 22 months than after exposure to WAG for eight or 16 months [22]. El-Ebiary et al. and Chandrasekhar et al. found that exposure to WAG for >10 y caused DNA damage [25, 26]. Most published studies of the relationship between DNA damage and exposure to WAG were performed many years ago or in developing countries in which ORs did not contain laminar flow systems. The results could have been different in different previous studies because different sample sizes, anesthetic agents, air conditions, and WAG concentrations were used.

The blood lipid concentrations and liver and renal functions of the people exposed to WAG for a long time were compared. The total protein concentration in the peripheral blood and the total bilirubin and creatinine concentrations were significantly lower in the exposed group than the control group. The other biochemical indicators (total cholesterol, triglycerides, direct bilirubin, alanine aminotransferase, aspartate aminotransferase, blood urea nitrogen, and uric acid concentrations) in the exposed group and control group samples were not significantly different. In medical workers, exposure to low concentrations of anesthetic exhaust gas has been found to increase alanine aminotransferase, glutamyltransferase, and total bilirubin concentrations and lymphocyte and neutrophil counts [27]. Prokes [28] found mild changes in liver function in workers exposed to anesthetic exhaust. Caciari et al. [29] found that WAGs can affect liver and kidney functions. However, many factors (e.g., disease, fatigue, sleep, stress, alcohol, and medication) affect liver and kidney functions. More sensitive indicators and broader studies are required to determine whether WAGs affect blood lipid concentrations and liver and kidney functions.

The sevoflurane concentrations were, overall, lower than the Chinese workplace limit, but some OR staff (particularly anesthesiologists and anesthesia nurses, who work near their patients) could be exposed to sevoflurane concentrations higher than the Chinese workplace limit. Better laminar flow and ventilation systems therefore need to be installed in ORs, anesthesia delivery equipment needs to be inspected regularly for leaks, medical supervision needs to be maintained, and hazard awareness training is required. Actions to control WAG emissions (particularly installing and maintaining scavenging systems, using double masks, adequately managing airflow, and using closed or semiclosed low-flow anesthesia procedures) are required to decrease the exposure of OR staff to WAG as much as possible [30].

No significant difference was found between the rates of abnormal ECGs for the exposure and control groups. The HR was significantly lower for the exposed group than the control group, and the QT interval and QTc interval were significantly longer for the exposed group than the control group, although both were within the normal ranges. The PR intervals and RV5, SV1, and RV5+SV1 amplitudes for the exposure and control groups were not significantly different. Many factors (e.g., antiarrhythmic drugs, antibiotics, electrolyte disturbances, antipsychotic drugs, and sympathetic nerve excitement) affect the HR, QT interval, and QTc interval. Further studies are required to determine whether long-term exposure to sevoflurane at low concentrations changes the ECG parameters of anesthesiology staff.

The study had some limitations. First, the study was performed at a single site. Second, some biometric indicators (e.g., the concentrations of sevoflurane and its metabolite hexafluoroisopropanol in urine and blood) were not used to measure exposure to WAG. Third, only γH2AX was used to measure DNA damage. γH2AX reflects only DNA damage caused by recent exposure but not cumulative effects. More indicators of DNA damage should be assessed in future studies. Lastly, there could be many causes of changes in oxidative stress in the participants. Exposure to WAG may only be one of the causes of changes in oxidative stress. The contribution of exposure to WAG to changes in oxidative stress needs to be assessed in future studies.

## Data Availability

All data used to support the findings of this study are available from the corresponding author upon request.

## Conflicts of Interest

The authors declare no competing financial interests.

## Authors' Contributions

Hai-Xin Hua and Hai-Bo Deng contributed equally to this work.

## Acknowledgments

The work was supported by a Guangdong Science and Technology Project (grant no. 2014A020213018) awarded to Ye-Hua Cai.

## References

[1] H. B. Deng, F. X. Li, Y. H. Cai, and S. Y. Xu, "Waste anesthetic gas exposure and strategies for solution," *Journal of Anesthesia*, vol. 32, no. 2, pp. 269–282, 2018.

[2] H. Turkan, A. Aydin, and A. Sayal, "Effect of volatile anesthetics on oxidative stress due to occupational exposure," *World Journal of Surgery*, vol. 29, no. 4, pp. 540–542, 2005.

[3] Z. Baysal, M. Cengiz, A. Ozgonul, M. Cakir, H. Celik, and A. Kocyigit, "Oxidative status and DNA damage in operating room personnel," *Clinical Biochemistry*, vol. 42, no. 3, pp. 189–193, 2009.

[4] T. Wronska-Nofer, J. Palus, W. Krajewski et al., "DNA damage induced by nitrous oxide: study in medical personnel of operating rooms," *Mutation Research*, vol. 666, no. 1-2, pp. 39–43, 2009.

[5] S. Sardas, S. Izdes, E. Ozcagli, O. Kanbak, and E. Kadioglu, "The role of antioxidant supplementation in occupational exposure to waste anaesthetic gases," *International Archives of Occupational and Environmental Health*, vol. 80, no. 2, pp. 154–159, 2006.

[6] N. Cohen, J. W. Bellville, and B. W. Brown, "Anesthesia, pregnancy, and miscarriage: a study of operating room nurses and anesthetists," *Anesthesiology*, vol. 35, no. 4, pp. 343–347, 1971.

[7] E. N. Cohen, B. W. Brown, D. L. Bruce et al., "Occupational disease among operating room personnel: a national study. Report of an Ad Hoc Committee on the Effect of Trace Anesthetics on the Health of Operating Room Personnel, American Society of Anesthesiologists," *Anesthesiology*, vol. 41, no. 4, pp. 321–340, 1974.

[8] P. O. Pharoah, E. Alberman, P. Doyle, and G. Chamberlain, "Outcome of pregnancy among women in anaesthetic practice," *Lancet*, vol. 1, no. 8001, pp. 34–36, 1977.

[9] J. Herzog-Niescery, H. Vogelsang, P. Gude et al., "The impact of the anesthetic conserving device on occupational exposure to isoflurane among intensive care healthcare professionals," *Minerva Anestesiologica*, vol. 84, no. 1, pp. 25–32, 2018.

[10] R. Schmatz, M. R. Bitencourt, L. D. Patias et al., "Evaluation of the biochemical, inflammatory and oxidative profile of obese patients given clinical treatment and bariatric surgery," *Clinica Chimica Acta*, vol. 465, pp. 72–79, 2017.

[11] J. van der Kooy, J. P. De Graaf, Z. M. Kolder et al., "A newly developed scavenging system for administration of nitrous oxide during labour: safe occupational use," *Acta Anaesthesiologica Scandinavica*, vol. 56, no. 7, pp. 920–925, 2012.

[12] E. Chessor, M. Verhoeven, C. Y. Hon, and K. Teschke, "Evaluation of a modified scavenging system to reduce occupational exposure to nitrous oxide in labor and delivery rooms," *Journal of Occupational and Environmental Hygiene*, vol. 2, no. 6, pp. 314–322, 2005.

[13] T. Wronska-Nofer, J. R. Nofer, J. Jajte et al., "Oxidative DNA damage and oxidative stress in subjects occupationally exposed to nitrous oxide ($N_2O$)," *Mutation Research*, vol. 731, no. 1-2, pp. 58–63, 2012.

[14] L. M. C. Lucio, M. G. Braz, P. do Nascimento Junior, J. R. C. Braz, and L. G. Braz, "Occupational hazards, DNA damage, and oxidative stress on exposure to waste anesthetic gases," *Revista Brasileira de Anestesiologia*, vol. 68, 2017.

[15] M. Fenech, "Cytokinesis-block micronucleus cytome assay," *Nature Protocols*, vol. 2, no. 5, pp. 1084–1104, 2007.

[16] R. Sivaci, A. Kahraman, M. Serteser, D. A. Sahin, and O. N. Dilek, "Cytotoxic effects of volatile anesthetics with free radicals undergoing laparoscopic surgery," *Clinical Biochemistry*, vol. 39, no. 3, pp. 293–298, 2006.

[17] H. Wang, M. Wang, H. Wang, W. Bocker, and G. Iliakis, "Complex H2AX phosphorylation patterns by multiple kinases including ATM and DNA-PK in human cells exposed to ionizing radiation and treated with kinase inhibitors," *Journal of Cellular Physiology*, vol. 202, no. 2, pp. 492–502, 2005.

[18] U. Weyemi, C. E. Redon, and W. M. Bonner, "H2AX and EMT: deciphering beyond DNA repair," *Cell Cycle*, vol. 15, no. 10, pp. 1305-1306, 2016.

[19] K. Rothkamm and M. Lobrich, "Evidence for a lack of DNA double-strand break repair in human cells exposed to very low x-ray doses," *Proceedings of the National Academy of Sciences of the United States of America*, vol. 100, no. 9, pp. 5057–5062, 2003.

[20] A. G. Aun, M. A. Golim, F. R. Nogueira et al., "Monitoring early cell damage in physicians who are occupationally exposed to inhalational anesthetics," *Mutation Research*, vol. 812, pp. 5–9, 2018.

[21] K. Szyfter, I. Stachecki, M. Kostrzewska-Poczekaj, M. Szaumkessel, J. Szyfter-Harris, and P. Sobczynski, "Exposure to volatile anaesthetics is not followed by a massive induction of single-strand DNA breaks in operation theatre personnel," *Journal of Applied Genetics*, vol. 57, no. 3, pp. 343–348, 2016.

[22] E. R. da Costa Paes, M. G. Braz, J. T. de Lima et al., "DNA damage and antioxidant status in medical residents occupationally exposed to waste anesthetic gases," *Acta Cirúrgica Brasileira*, vol. 29, no. 4, pp. 280–286, 2014.

[23] G. Cakmak, D. Eraydin, A. Berkkan, S. Yagar, and S. Burgaz, "Genetic damage of operating and recovery room personnel occupationally exposed to waste anaesthetic gases," *Human & Experimental Toxicology*, vol. 38, no. 1, pp. 3–10, 2019.

[24] M. G. Braz, L. I. M. Carvalho, C.-. Y. O. Chen et al., "High concentrations of waste anesthetic gases induce genetic damage and inflammation in physicians exposed for three years: a cross-sectional study," *Indoor Air*, vol. 30, no. 3, pp. 512–520, 2020.

[25] A. A. El-Ebiary, A. A. Abuelfadl, N. I. Sarhan, and M. M. Othman, "Assessment of genotoxicity risk in operation room personnel by the alkaline comet assay," *Human & Experimental Toxicology*, vol. 32, no. 6, pp. 563–570, 2012.

[26] M. Chandrasekhar, P. V. Rekhadevi, N. Sailaja et al., "Evaluation of genetic damage in operating room personnel exposed to anaesthetic gases," *Mutagenesis*, vol. 21, no. 4, pp. 249–254, 2006.

[27] T. Casale, T. Caciari, M. V. Rosati et al., "Anesthetic gases and occupationally exposed workers," *Environmental Toxicology and Pharmacology*, vol. 37, no. 1, pp. 267–274, 2014.

[28] B. Prokes, "Hepatologic parameters in health personnel after several years of occupational exposure to anesthetic gases," *Medicinski Pregled*, vol. 50, no. 3-4, pp. 103–107, 1997.

[29] T. Caciari, A. Capozzella, F. Tomei et al., "Professional exposure to anaesthetic gases in health workers: estimate of some hepatic and renal tests," *La Clinica Terapeutica*, vol. 164, no. 1, pp. e5–e9, 2013.

[30] J. M. Boiano and A. L. Steege, "Precautionary practices for administering anesthetic gases: a survey of physician anesthesiologists, nurse anesthetists and anesthesiologist assistants," *Journal of Occupational and Environmental Hygiene*, vol. 13, no. 10, pp. 782–793, 2016.

Hindawi
Oxidative Medicine and Cellular Longevity
Volume 2020, Article ID 7301615, 10 pages
https://doi.org/10.1155/2020/7301615

*Review Article*

# Biologic Effect of Hydrogen Sulfide and Its Role in Traumatic Brain Injury

**Jiaxin Zhang**,[1] **Shaoyi Zhang**,[1] **Haiyan Shan**,[2] **and Mingyang Zhang**[1]

[1]*Institute of Forensic Sciences, School of Biology & Basic Medical Sciences, Soochow University, Suzhou, China*
[2]*Department of Obstetrics and Gynecology, The Affiliated Suzhou Hospital of Nanjing Medical University, Suzhou, China*

Correspondence should be addressed to Haiyan Shan; ghostqth@163.com and Mingyang Zhang; mingyangzhang@suda.edu.cn

Received 20 July 2020; Revised 27 November 2020; Accepted 5 December 2020; Published 23 December 2020

Academic Editor: Shi Yuan Xu



Ever since endogenous hydrogen sulfide ($H_2S$) was found in mammals in 1989, accumulated evidence has demonstrated that $H_2S$ functions as a novel neurological gasotransmitter in brain tissues and may play a key role in traumatic brain injury. It has been proved that $H_2S$ has an antioxidant, anti-inflammatory, and antiapoptosis function in the neuron system and functions as a neuroprotective factor against secondary brain injury. In addition, $H_2S$ has other biologic effects such as regulating the intracellular concentration of $Ca^{2+}$, facilitating hippocampal long-term potentiation (LTP), and activating ATP-sensitive K channels. Due to the toxic nature of $H_2S$ when exceeding the physiological dose in the human body, only a small amount of $H_2S$-related therapies was applied to clinical treatment. Therefore, it has huge therapeutic potential and has great hope for recovering patients with traumatic brain injury.

## 1. Introduction

Traumatic brain injury (TBI) is the leading cause of high mortality and high morbidity in young adults and a major cause of death and disability across all ages in all countries, with a huge burden on individuals and society in economic and healthy development. Significant progress has been made in providing treatment for TBI and achieving more equitable and sustained improvements across health services. Our group demonstrated for the first time that decreased endogenous hydrogen sulfide ($H_2S$) levels and $H_2S$ synthesis enzyme cystathionine beta-synthase (CBS) expression in the brain were associated with increased lesion volume and mortality after TBI and the protective effect of exogenous $H_2S$ on TBI [1–3]. Accumulating evidence has demonstrated the protective effect of $H_2S$ on TBI [1, 2, 4–8].

$H_2S$ that smells disgusting odor is classified as the third gaseous transmitter following carbon monoxide and nitric oxide. Nowadays, evidence has demonstrated that $H_2S$ was found to be produced endogenously in various parts of the body such as the heart, blood, and central nervous system (CNS) [9, 10]. Moreover, it also refers to the actions of $H_2S$ which is involved in the regulation of intracellular signaling molecules, ion channel function, and the release and function of amino acid neurotransmitters [11]. However, it was recently proposed that the neurological actions of $H_2S$ were continuously modulated primarily by circulating sulfide rather than by endogenous production [12]. This was disproved based on recent studies showing that $H_2S$ found in the CNS is more likely to be derived directly from the brain than from the blood [13, 14]. Moreover, investigations over the past two decades have shown that the concentration of $H_2S$ has a detectable change going up or down which is related to brain injury. These results have shown that brain-derived $H_2S$ seems to serve as an important regulatory mechanism in the growth and development of neurons and the protection of neurons against brain injury.

In TBI, primary damage occurs at the time of impact and the damage is preventable but not treatable. The process will continue to cause following mitochondrial dysfunction, immune responses, the release of excitatory neurotransmitters, cerebrovascular dysfunction, and others that constitute the secondary injury [15]. In order to verify whether $H_2S$ has the neuroprotective effect after injury, exogenous $H_2S$

as an endogenous donor has been added into preclinical trials. Most of the neuroprotective drugs tested in mice have failed in human clinical trials because they target a single factor, which mediates secondary injury in TBI. Whether exogenous $H_2S$ can affect brain-derived $H_2S$ and has multiple neuroprotective effects on the secondary injury after TBI, it needs more evidence to verify. Therefore, this article focuses on the effective molecular mechanism of $H_2S$ in TBI and puts forward some views on future research.

## 2. The Severity of TBI

In the clinical setting, the Glasgow Coma Scale (GCS) is a 15-point behavioral observation scale that defines severity based on eye, verbal, and motor response. On the basis of direct observation of a limited number of objective variables, the GCS sums three scores to produce total scores of 3–8 (severe TBI), 9–12 (moderate TBI), and 13–15 (mild TBI). This scoring standard is also not absolute for dividing the severity of TBI. Moreover, there are still some limitations in judging some situations such as patients who are intubated and sedated or paralyzed and a wide range of injury magnitude represented by GCS scores of 3–8 [16]. Patients with GCS scores of 13 were considered moderate TBI for purposes in some studies. Moreover, computed tomography (CT) was used to assess the severity of TBI and a combination of clinical and imaging variables demonstrated a strong correlation with outcome when evaluated using the databases for several clinical trials. Subsequently, Magnetic Resonance Imaging (MRI) was also used as imaging evidence to participate in the assessment of damage. The Centers for Disease Control and Prevention provides one or more of the conditions about changes in consciousness and memory to define the severity of TBI. Therefore, other aforementioned clinical practice guidelines also incorporate structural imaging, duration of loss of consciousness and posttraumatic amnesia, and the GCS in their criteria for classifying injury severity (Table 1).

The establishment of the animal model is an excellent platform to delineate key injury mechanisms that associate with types of injury (concussion, contusion, and penetration injuries) that occur clinically for the investigation of mild, moderate, and severe forms of TBI [17], considering that the evaluation criteria for clinical use cannot be applied to the preclinical models. Therefore, well-defined grading guidelines for defining mild, moderate, and severe TBI in the rodent model are needed. Tissue loss about lesion size analysis is also recognized as a parameter to grade TBI severity. A number of studies utilized loss of cortical and hippocampal tissue to define TBI severity. Mild TBI has been defined as lesions confined to the cortical layer, a moderate injury was associated with considerable cortical tissue loss with little to no overt hippocampal loss, and severe TBI was often defined as extensive overt hippocampal lesions along with cortical tissue loss [18, 19]. There are several common methods for establishing rodent TBI models, including the fluid percussion injury, controlled cortical impact (CCI), and weight-drop model [15]. CCI is well regarded because it allows researchers to quantify the relationship between measurable engineered parameters (e.g., force, velocity, and depth of tissue deformation) and the extent of (either functional and/or tissue) impairment [20]. The CCI model was originally developed to investigate moderate to severe TBI and is infrequently used to mimic mild TBI because of the necessity of a craniectomy. However, modified versions of CCI have now been developed which means that CCI can induce the TBI model with different degrees of injury. According to previous articles, for mild TBI, the depth of impact in the cortex ranged from 0.1 to 1.0 mm and velocity ranged from 3.0 to 6.0 m/s; for moderate TBI, the depth of impact in the cortex ranged from 0.5 to 3.0 mm and velocities of 1.5–6.0 m/s, and severe injury used impact depths of 0.5–2.0 mm and velocities of 3.0–6.0 m/s [15, 20–23]. Many studies use a composite neurological evaluation to assess the severity of motor deficits following TBI, but the

Table 1: Characteristics of different degrees of TBI in different species.

| Species | |
|---|---|
| Human | *Mild TBI*<br>(1) Any period of loss of consciousness up to 30 min<br>(2) Posttraumatic amnesia not exceeding 24 h<br>(3) Any period of confusion or disorientation<br>(4) Transient neurological abnormalities<br>(5) A GCS score of 13–15<br>(6) Normal structural imaging<br>(7) Postconcussion symptoms may resolve during 12 weeks<br>*Moderate TBI*<br>(1) A possible loss of consciousness lasting up to a few hours<br>(2) Confusion lasting from days to weeks<br>(3) Physical, cognitive, and/or behavioral impairments lasting for months<br>(1) Abnormal structural imaging<br>(2) A GCS score of 9–12<br>*Severe TBI*<br>(1) Sustained loss of consciousness (>24 h)<br>(2) Surviving patients exhibiting chronic physical and emotional disabilities<br>(3) Abnormal structural imaging<br>(4) A GCS score of less than 9 |
| Mouse | *Mild TBI*<br>(1) CCI: depth: 0.1–1.0 mm; velocity: 3.0–6.0 m/s<br>(2) Tissue loss: lesions confined to the cortical layer<br>(3) Cortical depression <0.5 mm, velocities <4.0 m/s<br>*Moderate TBI*<br>(1) CCI: depth: 0.5–3.0 mm; velocity: 1.5–6.0 m/s<br>(2) Tissue loss: considerable cortical tissue loss with little to no overt hippocampal loss<br>(3) Cortical depression 1.0–1.5 mm, velocities 4.0–5.0 m/s<br>*Severe TBI*<br>(1) CCI: depth: 0.5–2.0 mm; velocity: 3.0–6.0 m/s<br>(2) Tissue loss: extensive overt hippocampal lesions along with cortical tissue loss<br>(3) Cortical depression >2.0 mm, velocities >5.0 m/s |

Note: TBI: traumatic brain injury; CCI: controlled cortical impact; GCS: the Glasgow Coma Scale.

problem is still that the assessment criteria cannot be unified. Thus, CCI affords pristine ability to analyze the biomechanical parameters of injury of interest in TBI research.

Although each case of TBI is unique and affected individuals display different degrees of injury (Table 1), we will discuss some of the common underlying neurochemical and molecular mechanisms and common secondary events following different severity of TBI.

## 3. Production and Storage of Endogenous $H_2S$

Under physiological conditions, endogenous $H_2S$ in human bodies is generated via enzymatic and nonenzymatic pathways [24]. $H_2S$ via nonenzymatic pathways is mainly produced by the decomposition of an inorganic substance, which accounts for a little percentage of $H_2S$ production. The main generation of $H_2S$ in the human body mainly depends on the enzymatic pathways using L-cysteine as the substrate. Three types of enzymes play a key role in these pathways, including cystathionine-$\beta$-synthase (CBS), cystathionine-$\gamma$-lyase (CSE), and 3-mercaptopyruvate transferase (3-MST) [25]. CBS hydrolyzes cysteine to produce $H_2S$, with L-serine as the by-product. Furthermore, CBS could catalyze the condensation of cysteine and homocysteine to form cystathionine and $H_2S$. The release of $H_2S$ could also depend on the reaction on the thiol of cysteine by CBS catalyzing to form s-thiolate. In addition, cysteine also may be hydrolyzed by CSE to produce $H_2S$ with the concomitant production of pyruvate and ammonia. In addition to CBS and CSE, 3-MST as a pyridoxal-5'-phosphate-independent enzyme is also involved in the production of $H_2S$ and is identified in the neurons. 3-MST acts together with cysteine aminotransferase (CAT) to generate $H_2S$ from cysteine (Cys) in the presence of $\alpha$-ketoglutarate. The additional pathway for $H_2S$ biosynthesis has been reported that 3-MST along with D-amino acid oxidase (DAO) produces $H_2S$ from D-cysteine by the interaction of mitochondria and peroxisomes which occurs mainly in the cerebellum and the kidney. Both CBS and CSE are pyridoxal-5′-phosphate-dependent enzymes, but they mediate, respectively, the production of $H_2S$ in different tissues and organs. CBS is expressed mainly in the central nervous system, liver, and kidney while CSE is expressed mainly in the vascular smooth muscle, nonvascular smooth muscle, and a little in the liver, kidney, uterus, placenta, pancreas, and other organs [26]. The location of these enzymes in different tissues is very important because the regulation of endogenous $H_2S$ production can be achieved by targeting each enzyme separately or simultaneously.

Under physiological conditions (pH = 7.4), $H_2S$ largely exists in two forms: the neutral molecular form ($H_2S$) and an ionic form ($HS^-$). The two forms are able to transform into each other and maintain the dynamic equilibrium at a ratio of one to two [27]. Although endogenous $H_2S$ can be synthesized and released immediately, the storage forms of $H_2S$ are also known. The acid-labile pool and the sulfane sulfur pool, which include hydrodisulfides/persulfides, are accepted storage forms of $H_2S$ ([28]), of which the acid-labile pool consists of iron-sulfur-containing proteins located in mitochondrial enzymes and can only release $H_2S$ at an acid pH of 5.4. The sulfane sulfur pool is localized in the cytoplasm and releases $H_2S$ under reducing conditions of pH 8.4 [29]. Because mitochondria are not in the acidic condition, acid-labile sulfur may not be a physiologic source of $H_2S$. Free $H_2S$ is immediately absorbed and stored as bound sulfur. 3-MST and CAT are located in the mitochondria and can produce $H_2S$ from cysteine in the brain [30]. It is speculated that $H_2S$ produced by the 3-MST/CAT enzymatic pathway is stored in the bound sulfane sulfur pool [9, 31].

## 4. The Change of Endogenous Hydrogen Sulfide in TBI

Up to now, multiple experiments have been designed to examine and describe the change of $H_2S$ concentration after TBI both in animal models and in human patients. Our group demonstrated for the first time that the concentration of $H_2S$ presented a dynamic change in the TBI model. The level of endogenous $H_2S$ and CBS expression in the blood and brain exhibits a downtrend after TBI [2, 3]. Recently, our group also reported that pretreated with NaHS, a $H_2S$ donor, a limited lesion volume in the ipsilateral cortex has been observed in the TBI model of mice [1]. Jiang et al. reported NaHS treatment increased the $H_2S$ level of brain tissue and endogenous antioxidant enzymatic activities and decreased oxidative product levels in the brain tissue of TBI-challenged rats [5]. Campolo et al. reported that ATB-346, a hydrogen sulfide-releasing derivative of naproxen, significantly reduced the severity of inflammation and restored neurotrophic factors that characterized the secondary events of TBI [4]. Karimi et al. reported that NaHS has a neuroprotective effect on TBI-induced memory impairment in rats [6]. Xu et al. reported that NaHS restores mitochondrial function and inhibits autophagy by activating the PI3K/Akt/mTOR signaling pathway to improve functional recovery after TBI [7]. The experimental evidence indicates that $H_2S$ functions as an important neuroprotective mediator in TBI models and may offer clinical therapy for TBI treatment.

## 5. Biologic Effect of Exogenous Hydrogen Sulfide in TBI

Ever since $H_2S$ was described for the first time in 1713, the toxicity of $H_2S$ to the human has become the focus of everyone's attention. $H_2S$ is often considered as one of the most unusual and reliable toxic gas [32]. $H_2S$ exerts its toxic effects characterized by acute central neurotoxicity, pulmonary edema, conjunctivitis, and odor perception followed by respiratory paralysis which is mainly due to the binding of sulfide to cytochrome c oxidase in mitochondria. Clinical symptoms of acute sulfide poisoning are featured by memory loss and brain dysfunction, which can be explained by the process that excess $H_2S$ in brain tissue lowers the level of neurotransmitters by inhibiting monoamine oxidase [10]. However, in recent years with the increasing study on $H_2S$, its biological effect is gradually being recognized, especially its neuroprotective ability after TBI (Figure 1).

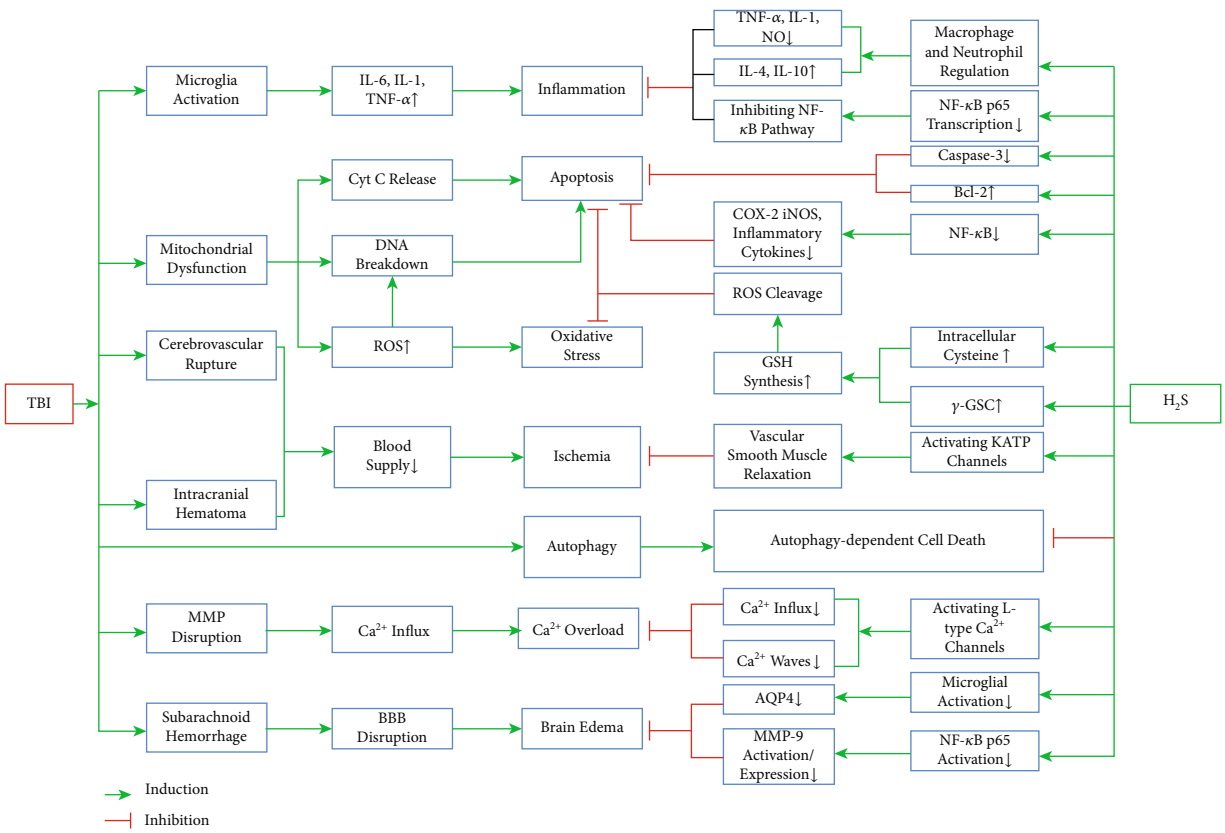


Figure 1: The potential therapeutic effects of $H_2S$ on TBI. The diagram shows the mechanisms of TBI-induced pathological change in the brain tissues and the nervous system, along with part of the neuroprotective pathways of $H_2S$. Note: ↑: upregulated; ↓: downregulated.

*5.1. Anti-Inflammatory Role of $H_2S$.* Neuroinflammation, which is characterized by the activation of glial cells, recruitment of neutrophils and macrophages, and upregulation of cytokines, adhesion factors, and chemokines, can be triggered from the surrounding to the site of injury and cause secondary neuronal injury after TBI [33, 34]. The pioneering work revealed the anti-inflammatory properties of $H_2S$ in different disease models. In the TBI model, the neuroprotective effect of $H_2S$ in inflammatory is generally achieved by the regulation of macrophages and neutrophils. $H_2S$ inhibits the release of proinflammatory factors such as tumor necrosis factor-$\alpha$ (TNF-$\alpha$), interleukin-1$\beta$ (IL-1$\beta$), and NO from astrocytes and microglial cells [10] and increases anti-inflammatory cytokines like interleukin-4 (IL-4) or interleukin-10 (IL-10) [35]. One of the possible anti-inflammatory mechanisms is that $H_2S$ inhibits the iNOS, NF-$\kappa$B, ERK, and p38 MAPK signaling pathways [36]. NF-$\kappa$B transcription factors are ubiquitously expressed in mammalian cells and are known to upregulate the expressions of cytokines and chemokines. The NF-$\kappa$B family (also known as the Rel family) consists of five members: p50, p52, p65 (also known as Rel A), c-Rel, and Rel B. Inflammation begins to be mediated when activated NF-$\kappa$B enters the nucleus to induce transcription of a myriad of genes. It has been reported that ATB-346, a hydrogen sulfide-releasing cyclooxygenase inhibitor, significantly reduced the translocation of the p65 submit following TBI in rats [4]. Xiang et al. showed that $H_2S$ alleviates lipopolysaccharide- (LPS-) induced inflammatory via inhibition of NF-$\kappa$B p65 translocation [37]. In addition, $H_2S$ can also polarize microglia to an anti-inflammatory phenotype (M2) by activating calmodulin-dependent protein kinase $\beta$- (CaMKK$\beta$-) dependent AMP-activated protein kinase (AMPK) [38]. However, the role of $H_2S$ in the inflammatory reaction still remains controversial. Some groups have observed that $H_2S$ plays a proinflammatory role in severe burn injury and LPS-induced inflammation [39, 40]. Consequently, $H_2S$ is currently accepted to be one of the pivotal factors that regulate the inflammatory reaction following TBI, but the precise mechanism that $H_2S$ modulates inflammation remains to be elucidated.

*5.2. Antioxidant Role of $H_2S$.* During the process of TBI, the physical and secondary damage at the trauma site result in mitochondrial dysfunction and changes in membrane permeability, causing the breakdown of the balance between the generation and elimination of intracellular reactive oxygen species (ROS) (Campolo et al.). Then, tremendous intracellular accumulation of ROS induces cytotoxicity, causing a large amount of cell death.

Oxygen consumption of brain tissue accounts for nearly 20% of the entire body, making brain tissue more sensitive to oxidative stress-related disorders such as TBI, stroke, and Alzheimer's disease [40, 41]. Glutathione (GSH), a tripeptide consisting of cysteine, glutamate, and glycine, is a major antioxidant in the cellular defense against oxidative stress, and $H_2S$ can promote the production of GSH ([42]; Kimura and

[43]). The intracellular concentration of cysteine is much lower than the other two substrates of GSH [44], and cysteine exists in the extracellular space in an oxidized form, cystine [45], so the availability of intracellular cysteine significantly determined the rate of GSH synthesis. Evidence has shown that $H_2S$ reduces cysteine into cystine and activates the cysteine/glutamate antiporter (xc-) which couples the import of cysteine and export of glutamate [46], consequently increasing the intracellular concentration of cysteine. On the other hand, $H_2S$ is able to potentiate the activity of $\gamma$-glutamylcysteine synthase ($\gamma$-GSC), which functions as a rate-limiting enzyme in the production of GSH (Kimura and [43]). In addition, $H_2S$ may have a synergistic effect with other antioxidative systems including haem oxygenase (HO), superoxide dismutase (SOD), and especially nuclear factor erythroid-2-related factor2 (Nrf2) [47]. More evidence shows $H_2S$ can induce the upregulation of Nrf2 and drive it into the nucleus, and it can regulate the level of antioxidant enzymes and enhance the antioxidant reaction which is certified in the diverse damage models [48]. Meanwhile, it is reported that $H_2S$ can reduce the production of prooxidase, which still represents the inhibition of the occurrence of oxidative stress [49]. It is worth pointing out that $H_2S$ produced by 3-MST, which is localized in the mitochondria, can directly reduce the generation of ROS and protects cells [50]. Our group reported that $H_2S$ protects against cell damage induced by scratch injury through modulation of the PI3K/Akt/Nrf2 pathway, suggesting $H_2S$ may have therapeutic efficacy in TBI [51].

*5.3. Regulation of Cell Death Signaling Mediated by $H_2S$.* Neuronal cell death following TBI is an important factor in neurological deficits. TBI can trigger localized neuronal apoptosis within a few hours after the trauma. Increased cytosolic free $Ca^{2+}$ can induce the collapse of the mitochondrial membrane potential and the production of free radicals and lipid peroxidation. This leads to further attack on the mitochondrial membranes, which leads to the release of cytochrome C through the outer mitochondrial membrane. Then, cytochrome C enters the cytoplasm, inducing caspase-dependent apoptosis [52]. Meanwhile, ROS produced from dysfunctional mitochondria can also induce neuronal apoptosis by directly causing the breakdown of DNA. As is discussed above, part of the antiapoptotic effect of $H_2S$ is achieved through the inhibition of the ROS injury. It has been observed that $H_2S$ is able to inhibit the $H_2O_2$-activated calcium signaling pathways in mouse hippocampal neurons [53]. In the model of oxygen-glucose deprivation/reoxygenation- (OGD/R-) induced neuronal apoptosis, $H_2S$ is observed to inhibit a ROS-mediated caspase-3 pathway [54]. Ji et al. found that $H_2S$ preconditioning considerably reduced TUNEL-positive cells and cleaved caspase-3 in the cerebral ischemia/reperfusion injury model, and the protective effects of $H_2S$ are possibly achieved by the induction of HSP70 through the PI3K/Akt/Nrf2 pathway [55]. Caspase-3, Bcl-2, and Bax protein function as important mediators in the TBI-induced apoptosis [56]. We found that NaHS pretreatment can reverse the effects on the cleaved caspase-3 increase and Bcl-2 decrease in the injured cortex and hippocampus after TBI [1]. In addition, $H_2S$ plays another antiapoptotic role via the regulation of the NF-$\kappa$B signaling pathway, which plays a complex role in integrating signaling between and within neurons and glial. $H_2S$ reduces the expression of NF-$\kappa$B followed by the decrease of the expression of iNOS, COX-2, and proinflammatory cytokines. Sen et al. showed that $H_2S$ sulfhydrate, the p65 subunit of NF-$\kappa$B at cysteine-38 which augments its ability to bind its coactivator RPS3 and the activator/coactivator complex, then stimulates the transcription of antiapoptotic genes [57].

Autophagy is a physiological process that helps maintain a balance between the manufacture of cellular components and breakdown of damaged organelles and other toxic cellular constituents [58]. Sarkar et al. have shown that autophagic clearance is impaired early after TBI and correlates with neuronal cell death [59]. The Nomenclature Committee of Cell Death defines autophagy-dependent cell death as "a form of regulated cell death that mechanistically depends on the autophagic machinery" and "a distinct mechanism of cell death that occurs independently of apoptosis or necrosis" [60, 61]. Autophagy as an attractive therapeutic target can be developed new therapeutic strategies to achieve better outcomes for patients suffering from TBI [62]. Our group has shown that $H_2S$ regulated autophagy-dependent cell death after TBI [1, 51, 63]. We also showed that 3-MST was mainly located in living neurons and may be implicated in the autophagy of neurons and involved in the pathophysiology of the brain after TBI [8].

*5.4. Cerebral Vasodilation Mediated by $H_2S$.* Research conducted in laboratory animals and humans has investigated the effects of TBI on cerebral blood flow (CBF). Many investigations have revealed that focal or global cerebral ischemia occurs frequently by detection within a temporal range from ultraearly to late stages after TBI. The mechanism may be that the rupture of cerebral vessels, nerve parenchyma, and edema formed by intracranial hematoma may block blood flows, resulting in insufficient blood supply. After TBI, CBF autoregulation, which refers to cerebrovascular constriction or dilation in response to increases or decreases in cerebral perfusion pressure (CPP), is impaired or abolished in most patients. The defect of automatic adjustment of cerebral blood flow occurs in an uncertain time after injury, which can occur immediately after the trauma or may develop at other times after injury. Furthermore, about more than one-third of TBI patients show cerebral vasospasm, and in all patients with vasospasm, 50% have hypoperfusion. In this process, the destruction of neuronal membrane and dysfunction of various ion channels located on the membrane can cause disrupted ion homeostasis, during which $Na^+$ and $Ca^{2+}$ accumulate in the cytoplasm and a large amount of $K^+$ is pumped out. As a result, the brain cells become sensitive to ischemia [64]. Multiple studies have proved that $H_2S$ dilates cerebral vessels following TBI via activation of the ATP-sensitive K channels ($K_{ATP}$ channels) [5]. According to reports, specific molecular targets of $H_2S$ appear to be cysteine 6 and 26 in the extracellular portion of the rvSUR1 subunit of the $K_{ATP}$ channel complex. The opening of the $K_{ATP}$ channels inactivates cell membrane polarization and voltage-

Table 2: Summary of the biologic effects of hydrogen sulfide after TBI.

| Effects | Mechanisms | References |
|---|---|---|
| Anti-inflammation | Inhibiting the TNF-$\alpha$, IL-1$\beta$, and NO | [10] |
| | Increasing the IL-6 and IL-10 | [35] |
| | Inhibiting the iNOS, NF-$\kappa$B, ERK, and p38 MAPK pathways | [36] |
| Antioxidation | Activation of cysteine/glutamate antiporter | [46] |
| | Activation of $\gamma$-GCS | (Kimura and [43]) |
| | Cooperating with HO, SOD, and Nrf2 antioxidative system | (Kimura and [43]) |
| | Decreasing the production of the prooxidase | (Kimura and [43]) |
| Antiapoptosis | Inhibiting the $H_2O_2$-activated calcium pathways | [53] |
| | Reducing caspase-3 and increasing Bcl-2 | [54] |
| | Regulating the NF-$\kappa$B signaling pathway | [57] |
| Regulating autophagy-dependent cell death | Reducing Beclin-1 and LC-3 | [1] [8] |
| | LC3-positive cells were partly colocalized with PI | [63] [51] |
| Vasodilation | Activating the $K_{ATP}$ channels (CSE-generated $H_2S$) | [65] |
| | Liberating NO from S-nitrosothiols | [78] |
| $Ca^{2+}$ modulation | Activating the L-type $Ca^{2+}$ channels | [68] |
| | Inducing $Ca^{2+}$ waves | [70] |
| Attenuating edema | Alleviating BBB disruption and reducing AQP4 expression | [72] |
| Facilitating LTP | Potentiating the NMDA receptor | [77] |
| Antiexcitotoxicity | Reducing glutamate release after TBI | [64] |

gated calcium channels, which in turn lead to a reduction in $Ca^{2+}$, which ultimately leads to the relaxation and expansion of blood vessels. In a vitro model of rat aortic tissues, $H_2S$ activates $K_{ATP}$ channels by inducing the efflux of intracellular potassium and the hyperpolarization of the membrane of vascular smooth muscle cells [65]. Later, another group reported that $H_2S$ has a similar mechanism of vasodilation in the cerebral cortical pial arteriole of newborn pigs [66]. However, conflicting reports have emerged showing that the contribution of the $K_{ATP}$ channels to $H_2S$-induced vasodilation is minimal and that vasodilation is due to metabolic inhibition such as the decrease in ATP, intracellular pH changes, and modulation of $Cl^-/HCO_3^-$ channels. There are also indications that $H_2S$ may stimulate vasodilation by liberating $^{\cdot}NO$ from S-nitrosothiols. Although the mechanism of cerebral vasodilation is still unclear, it is certain that hydrogen sulfide has the effect of dilating cerebral blood vessels after TBI.

*5.5. $H_2S$ Mediates Intracellular Calcium Concentration.* After the primary injury of TBI, the disruption of mitochondrial membrane potential (MMP) and intracellular excessive ROS lead to intracellular calcium accumulation, causing calcium overload-induced neurotoxicity [67]. $Ca^{2+}$ activates lipid peroxidases, proteases, and phospholipases which in turn increase the intracellular concentration of free fatty acids and free radicals. Calcium overload, which is at the core of the cellular and molecular network of secondary neuronal injury, is involved in three neurotoxic cascade reactions leading to neuronal apoptosis or necrosis [64]. It has been noted that $H_2S$ is capable of regulating $Ca^{2+}$ in all important brain cell types, namely, neurons, microglia, and astrocytes. The physiological concentrations of $H_2S$ selectively were initially found to be a neuromodulator and facilitate the induction of hippocampal long-term potentiation (LTP) by enhancing the activity of N-methyl-D-aspartate (NMDA) receptors in neurons and increase the influx of $Ca^{2+}$ into astrocytes. $H_2S$ could raise cytosolic calcium in neurons through the activation of L-type $Ca^{2+}$ channels. Some groups have observed a concentration-dependent $H_2S$-induced $Ca^{2+}$ elevation in neurons, and such effects of $H_2S$ on cytosolic $Ca^{2+}$ concentration can be attenuated by the antagonist of L-type calcium channel and N-methyl-D-aspartate receptor [68, 69]. In TBI, $H_2S$ released from neurons or glia in response to neuronal excitation activates $Ca^{2+}$ channels of astrocytes, inducing $Ca^{2+}$ waves that propagate to the neighboring astrocytes [70], and $H_2S$ may mediate signals between neurons and glia. However, there are still some reports suggesting that $H_2S$ elevates neuronal $Ca^{2+}$ concentration and may exacerbate the formation of calcium overload in secondary neuronal injury [64].

*5.6. $H_2S$ Attenuates the TBI-Induced Brain Edema.* Brain edema, which is usually formed in the early brain injury following subarachnoid hemorrhage, can result in brain swelling and increased intracranial pressure followed with neuronal cell death, herniation, and death [71]. Our group

reported that TBI significantly increases the percentage of water content in the injured ipsilateral cortex, leading to the formation of TBI-induced brain edema [1]. It is also reported that exogenous $H_2S$ treatment can effectively ameliorate the development of TBI-induced brain edema [1]. Another group demonstrated that the effect of $H_2S$ on the inhibition of brain edema formation might be involved with alleviating blood-brain barrier (BBB) disruption and reducing aquaporin-4 (AQP4) expression, both of which are induced by matrix metalloprotease- (MMP-) mediated tight junction proteins (TJPs) [72]. Classically, brain edema was thought to be triggered by the disruption of BBB integrity in the acute stage of subarachnoid hemorrhage [73]. Then, the degeneration of the basal lamina and the increased permeability of BBB result in the extracellular accumulation of water in the cortex [74]. In recent years, however, multiple investigations demonstrated that the dysfunction of ion and water channels plays a vital role in glial and neuron swelling [75]. Evidence showed that the deletion of AQP4, a main water channel protein concentrated on the astrocyte endfeet, protects BBB integrity by reducing inflammatory responses due to the upregulation of PPAR-$\gamma$ expression and attenuation of proinflammatory cytokine release [76]. In addition, studies also proved that $H_2S$ attenuates brain edema by inhibiting the expression/activation of MMP-9, which is possibly associated with the regulation of NF-$\kappa$B p65 activation [72]. It is now demonstrated that $H_2S$ may attenuate the AQP4-induced cellular edema via inhibition of microglial activation and suppression of proinflammatory cytokine release in the cortex, but the underlying mechanisms of $H_2S$ alleviating brain edema through cellular pathways still demand further investigation.

*5.7. Other Mechanisms of $H_2S$ following TBI.* Apart from the biologic effects of $H_2S$ following TBI mentioned above, the underlying mechanisms of $H_2S$ are reflected in many other aspects. It was found that $H_2S$ facilitates hippocampus long-term potentiation via mediation of the N-methyl-D-aspartate receptor in the $H_2S$-activated cAMP/PKA pathway [11, 77]. Moreover, $H_2S$ also counteracts glutamate-mediated excitotoxicity in the secondary injury following TBI via activation of $K_{ATP}$ channels, which may directly result in neuronal glutamate release in response to calcium influx after TBI [64].

According to all that have been mentioned above, the mechanisms of $H_2S$ following TBI can be summarized in Table 2.

## 6. Conclusion

Although $H_2S$ has multiple biologic effects as a neuroprotective gasotransmitter and considerable part of them has already been confirmed through experiments in laboratory, applying $H_2S$-related therapy to clinical treatment still has a long way to go. $H_2S$ can function as a neuroprotective mediator when it is controlled within physiological dose, while excess $H_2S$ has chemotoxic and cytotoxic effects on human bodies [79]. $H_2S$ still remains many potential mechanisms which have not been totally figured out, but it is beyond doubt that $H_2S$ therapy, especially on TBI patients, will become an available treatment option in the near future.

## Abbreviations

3-MST: 3-Mercaptopyruvate transferase
$\gamma$-GCS: $\gamma$-Glutamylcysteine synthase
AMPK: AMP-activated protein kinase
AQP4: Aquaporin-4
ATB-346: 2-(6-Methoxynapthalen-2-yl)-propionic acid 4-thiocarbamoyl-phenyl ester
ATP: Adenosine triphosphate
BBB: Blood-brain barrier
Bcl-2: B-cell lymphoma-2
CaMKK$\beta$: Calmodulin-dependent protein kinase $\beta$
cAMP: Cyclic adenosine monophosphate
CAT: Cysteine aminotransferase
CBF: Cerebral blood flow
CBS: Cystathionine-$\beta$-synthase
CCI: Controlled cortical impact
CNS: Central nervous system
CPP: Cerebral perfusion pressure
CSE: Cystathionine-$\gamma$-lyase
CT: Computed tomography
Cys: Cysteine
DAO: D-Amino acid oxidase
ERK: Extracellular signal-regulated kinase
GCS: Glasgow Coma Scale
GSH: Glutathione
$H_2O_2$: Hydrogen peroxide
$H_2S$: Hydrogen sulfide
HO: Haem oxygenase
HSP70: Heat shock protein 70
IL-1$\beta$: Interleukin-1$\beta$
IL-4: Interleukin-4
IL-10: Interleukin-10
INOS: Inducible nitric oxide synthase
LPS: Lipopolysaccharide
LTP: Long-term potentiation
MAPK: Mitogen-activated protein kinase
MMP: Mitochondrial membrane potential
MMPs: Matrix metalloproteases
MRI: Magnetic Resonance Imaging
mTOR: Mammalian/mechanistic target of rapamycin
NaHS: Sodium hydrosulfide hydrate
NF-$\kappa$B: Nuclear factor-kappa B
NMDA: N-Methyl-D-aspartate
NO: Nitric oxide
Nrf2: Nuclear factor erythroid-2 related factor2
OGD/R: Oxygen-glucose deprivation/reoxygenation
PI: Propidium iodide
PI3K: Phosphoinositide 3-kinase
PKA: Protein kinase A
PPAR-$\gamma$: Peroxisome proliferator-activated receptors $\gamma$
ROS: Reactive oxygen species
SOD: Superoxide dismutase
TBI: Traumatic brain injury

TJPs: Tight junction proteins
TNF-$\alpha$: Tumor necrosis factor-$\alpha$
TUNEL: Terminal deoxynucleotidyl transferase-mediated dUTP-biotin in situ nick-end labeling.

## Conflicts of Interest

The authors declare that they have no conflict of interest.

## Authors' Contributions

Jiaxin Zhang and Shaoyi Zhang contributed equally to this study.

## Acknowledgments

This study was funded by the National Natural Science Foundation of China (No. 82071382 and No. 81601306), the Priority Academic Program Development of Jiangsu Higher Education Institutions (PAPD), the Jiangsu Talent Youth Medical Program (QNRC2016245), the Jiangsu Maternal and Child Health Research Key Project (F202013) and the Suzhou Science and Technology Development Project (SYS2020089 and SYS2018082).

## References

[1] M. Zhang, H. Shan, P. Chang et al., "Hydrogen Sulfide Offers Neuroprotection on Traumatic Brain Injury in Parallel with Reduced Apoptosis and Autophagy in Mice," *PLoS ONE*, vol. 9, no. 1, p. e87241, 2014.

[2] M. Zhang, H. Shan, T. Wang et al., "Dynamic Change of Hydrogen Sulfide After Traumatic Brain Injury and its Effect in Mice," *Neurochemical Research*, vol. 38, no. 4, pp. 714–725, 2013.

[3] M. Zhang, H. Shan, Y. Wang et al., "The expression changes of cystathionine-$\beta$-synthase in brain cortex after traumatic brain injury," *Journal of Molecular Neuroscience*, vol. 51, no. 1, pp. 57–67, 2013.

[4] M. Campolo, E. Esposito, A. Ahmad et al., "Hydrogen sulfide-releasing cyclooxygenase inhibitor ATB-346 enhances motor function and reduces cortical lesion volume following traumatic brain injury in mice," *J Neuroinflammation*, vol. 11, no. 1, p. 196, 2014.

[5] X. Jiang, Y. Huang, W. Lin, D. Gao, and Z. Fei, "Protective effects of hydrogen sulfide in a rat model of traumatic brain injury via activation of mitochondrial adenosine triphosphate-sensitive potassium channels and reduction of oxidative stress," *The Journal of Surgical Research*, vol. 184, no. 2, pp. e27–e35, 2013.

[6] S. A. Karimi, N. Hosseinmardi, M. Janahmadi, M. Sayyah, and R. Hajisoltani, "The protective effect of hydrogen sulfide ($H_2S$) on traumatic brain injury (TBI) induced memory deficits in rats," *Brain Research Bulletin*, vol. 134, pp. 177–182, 2017.

[7] K. Xu, F. Wu, K. Xu et al., "NaHS restores mitochondrial function and inhibits autophagy by activating the PI3K/Akt/mTOR signalling pathway to improve functional recovery after traumatic brain injury," *Chemico-Biological Interactions*, vol. 286, pp. 96–105, 2018.

[8] M. Zhang, H. Shan, P. Chang et al., "Upregulation of 3-MST Relates to Neuronal Autophagy After Traumatic Brain Injury in Mice," *Cellular and Molecular Neurobiology*, vol. 37, no. 2, pp. 291–302, 2017.

[9] B. Geng, J. Yang, Y. Qi et al., "$H_2S$ generated by heart in rat and its effects on cardiac function," *Biochemical and Biophysical Research Communications*, vol. 313, no. 2, pp. 362–368, 2004.

[10] M. W. Warenycia, L. R. Goodwin, C. G. Benishin et al., "Acute hydrogen sulfide poisoning: Demonstration of selective uptake of sulfide by the brainstem by measurement of brain sulfide levels," *Biochemical Pharmacology*, vol. 38, no. 6, pp. 973–981, 1989.

[11] P. K. Kamat, A. Kalani, and N. Tyagi, "Role of hydrogen sulfide in brain synaptic remodeling," *Methods in Enzymology*, vol. 555, pp. 207–229, 2015.

[12] K. R. Olson, M. J. Healy, Z. Qin et al., "Hydrogen sulfide as an oxygen sensor in trout gill chemoreceptors," *American Journal of Physiology-Regulatory, Integrative and Comparative Physiology*, vol. 295, no. 2, pp. R669–R680, 2008.

[13] B. Kim, J. Lee, J. Jang, D. Han, and K.-H. Kim, "Prediction on the Seasonal Behavior of Hydrogen Sulfide Using a Neural Network Model," *The Scientific World JOURNAL*, vol. 11, 1004 pages, 2011.

[14] M. Whiteman, J. S. Armstrong, S. H. Chu et al., "The novel neuromodulator hydrogen sulfide: an endogenous peroxynitrite 'scavenger'?," *Journal of Neurochemistry*, vol. 90, no. 3, pp. 765–768, 2004.

[15] L. Siebold, A. Obenaus, and R. Goyal, "Criteria to define mild, moderate, and severe traumatic brain injury in the mouse controlled cortical impact model," *Experimental Neurology*, vol. 310, pp. 48–57, 2018.

[16] S. Yamamoto, H. S. Levin, and D. S. Prough, "Mild, moderate and severe," *Current Opinion in Neurology*, vol. 31, no. 6, pp. 672–680, 2018.

[17] C.-C. Chiu, Y.-E. Liao, L.-Y. Yang et al., "Neuroinflammation in animal models of traumatic brain injury," *Journal of Neuroscience Methods*, vol. 272, pp. 38–49, 2016.

[18] A. Hånell, J. Hedin, F. Clausen, and N. Marklund, "Facilitated Assessment of Tissue Loss Following Traumatic Brain Injury," *Frontiers in Neurology*, vol. 3, 2012.

[19] P. R. Lees-Haley, P. Green, M. L. Rohling, D. D. Fox, and L. M. Allen 3rd, "The lesion(s) in traumatic brain injury: implications for clinical neuropsychology," *Archives of Clinical Neuropsychology*, vol. 18, no. 6, pp. 585–594, 2003.

[20] N. D. Osier, J. R. Korpon, and C. E. Dixon, *Controlled Cortical Impact Model*, F. H. Kobeissy, Ed., Brain Neurotrauma, Boca Raton (FL), 2015.

[21] E. W. Baker, H. A. Kinder, J. M. Hutcheson et al., "Controlled cortical impact severity results in graded cellular, tissue, and functional responses in a piglet traumatic brain injury model," *Journal of Neurotrauma*, vol. 36, no. 1, pp. 61–73, 2019.

[22] N. Osier and C. E. Dixon, "The Controlled Cortical Impact Model of Experimental Brain Trauma: Overview, Research Applications, and Protocol," *Methods in Molecular Biology*, vol. 1462, pp. 177–192, 2016.

[23] P. Sellappan, J. Cote, P. A. Kreth et al., "Variability and uncertainty in the rodent controlled cortical impact model of traumatic brain injury," *Journal of Neuroscience Methods*, vol. 312, pp. 37–42, 2019.

[24] X. Cao, L. Ding, Z. Z. Xie et al., "A review of hydrogen sulfide synthesis, metabolism, and measurement: is modulation of hydrogen sulfide a novel therapeutic for cancer?," *Antioxidants & Redox Signaling*, vol. 31, no. 1, pp. 1–38, 2019.

[25] J. Zhang, H. Shan, L. Tao, and M. Zhang, "Biological Effects of Hydrogen Sulfide and Its Protective Role in Intracerebral Hemorrhage," *Journal of Molecular Neuroscience*, vol. 70, no. 12, pp. 2020–2030, 2020.

[26] E. Łowicka and J. Bełtowski, "Hydrogen sulfide (H2S) - the third gas of interest for pharmacologists," *Pharmacological Reports*, vol. 59, no. 1, pp. 4–24, 2007.

[27] N. Shibuya, M. Tanaka, M. Yoshida et al., "3-Mercaptopyruvate Sulfurtransferase Produces Hydrogen Sulfide and Bound Sulfane Sulfur in the Brain," *Antioxidants & Redox Signaling*, vol. 11, no. 4, pp. 703–714, 2009.

[28] T. S. Bailey, L. N. Zakharov, and M. D. Pluth, "Understanding hydrogen sulfide storage: probing conditions for sulfide release from hydrodisulfides," *Journal of the American Chemical Society*, vol. 136, no. 30, pp. 10573–10576, 2014.

[29] M. Ishigami, K. Hiraki, K. Umemura, Y. Ogasawara, K. Ishii, and H. Kimura, "A source of hydrogen sulfide and a mechanism of its release in the brain," *Antioxidants & Redox Signaling*, vol. 11, no. 2, pp. 205–214, 2009.

[30] W. Guo, J.-t. Kan, Z.-y. Cheng et al., "Hydrogen sulfide as an endogenous modulator in mitochondria and mitochondria dysfunction," *Oxidative Medicine and Cellular Longevity*, vol. 2012, Article ID 878052, 9 pages, 2012.

[31] B. V. Nagpure and J. S. Bian, "Interaction of Hydrogen Sulfide with Nitric Oxide in the Cardiovascular System," *Oxidative Medicine and Cellular Longevity.*, vol. 2016, article 6904327, pp. 1–16, 2016.

[32] T. L. Guidotti, "Hydrogen sulfide: advances in understanding human toxicity," *International Journal of Toxicology*, vol. 29, no. 6, pp. 569–581, 2010.

[33] D. Lozano, G. S. Gonzales-Portillo, S. Acosta et al., "Neuroinflammatory responses to traumatic brain injury: etiology, clinical consequences, and therapeutic opportunities," *Neuropsychiatric Disease and Treatment*, vol. 11, pp. 97–106, 2015.

[34] S. J. Schimmel, S. Acosta, and D. Lozano, "Neuroinflammation in traumatic brain injury: A chronic response to an acute injury," *Brain Circulation*, vol. 3, no. 3, pp. 135–142, 2017.

[35] H. A. Seifert and K. R. Pennypacker, "Molecular and Cellular Immune Responses to Ischemic Brain Injury," *Translational Stroke Research*, vol. 5, no. 5, pp. 543–553, 2014.

[36] Q. Zhang, L. Yuan, D. Liu et al., "Hydrogen sulfide attenuates hypoxia-induced neurotoxicity through inhibiting microglial activation," *Pharmacological Research*, vol. 84, pp. 32–44, 2014.

[37] N.-l. Xiang, J. Liu, Y.-j. Liao et al., "Abrogating ClC-3 Inhibits LPS-induced Inflammation via Blocking the TLR4/NF- $\kappa$B Pathway," *Scientific Reports*, vol. 6, 2016.

[38] X. Zhou, Y. Cao, G. Ao et al., "CaMKK$\beta$-Dependent Activation of AMP-Activated Protein Kinase Is Critical to Suppressive Effects of Hydrogen Sulfide on Neuroinflammation," *Antioxidants & Redox Signaling*, vol. 21, no. 12, pp. 1741–1758, 2014.

[39] L. Li, M. Bhatia, Y. Z. Zhu et al., "Hydrogen sulfide is a novel mediator of lipopolysaccharide-induced inflammation in the mouse," *The FASEB Journal*, vol. 19, no. 9, pp. 1196–1198, 2005.

[40] J. Zhang, S. W. S. Sio, S. Moochhala, and M. Bhatia, "Role of Hydrogen Sulfide in Severe Burn Injury-Induced Inflammation in Mice," *Molecular Medicine*, vol. 16, pp. 417–424, 2010.

[41] E. Tönnies and E. Trushina, "Oxidative Stress, Synaptic Dysfunction, and Alzheimer's Disease," *Journal of Alzheimer's Disease*, vol. 57, no. 4, pp. 1105–1121, 2017.

[42] Y. Kimura, Y.-I. Goto, and H. Kimura, "Hydrogen Sulfide Increases Glutathione Production and Suppresses Oxidative Stress in Mitochondria," *Antioxidants & Redox Signaling*, vol. 12, no. 1, pp. 1–13, 2010.

[43] Y. Kimura and H. Kimura, "Hydrogen sulfide protects neurons from oxidative stress," *The FASEB Journal*, vol. 18, no. 10, pp. 1165–1167, 2004.

[44] O. W. Griffith, "Biologic and pharmacologic regulation of mammalian glutathione synthesis," *Free Radical Biology & Medicine*, vol. 27, no. 9-10, pp. 922–935, 1999.

[45] J.-i. Sagara, K. Miura, and S. Bannai, "Cystine Uptake and Glutathione Level in Fetal Brain Cells in Primary Culture and in Suspension," *Journal of Neurochemistry*, vol. 61, no. 5, pp. 1667–1671, 1993.

[46] T. H. Murphy, M. Miyamoto, A. Sastre, R. L. Schnaar, and J. T. Coyle, "Glutamate toxicity in a neuronal cell line involves inhibition of cystine transport leading to oxidative stress," *Neuron*, vol. 2, no. 6, pp. 1547–1558, 1989.

[47] T. Corsello, N. Komaravelli, and A. Casola, "Role of hydrogen sulfide in NRF2- assssssnd sirtuin-dependent maintenance of cellular redox balance," *Antioxidants*, vol. 7, no. 10, p. 129, 2018.

[48] S. Zhao, T. Song, Y. Gu et al., "Hydrogen sulfide alleviates liver injury via S-sulfhydrated-Keap1/Nrf2/LRP1 pathway," *Hepatology*, 2020.

[49] C. Szabó, "Hydrogen sulphide and its therapeutic potential," *Nature Reviews Drug Discovery*, vol. 6, no. 11, pp. 917–935, 2007.

[50] Q. Xiao, J. Ying, L. Xiang, and C. Zhang, "The biologic effect of hydrogen sulfide and its function in various diseases," *Medicine*, vol. 97, no. 44, p. e13065, 2018.

[51] J. Zhang, C. Shi, H. Wang et al., "Hydrogen sulfide protects against cell damage through modulation of PI3K/Akt/Nrf2 signaling," *The International Journal of Biochemistry & Cell Biology*, vol. 117, p. 105636, 2019.

[52] B. M. Polster, K. W. Kinnally, and G. Fiskum, "BH3 death domain peptide induces cell type-selective mitochondrial outer membrane permeability," *Journal of Biological Chemistry*, vol. 276, pp. 37887–37894, 2001.

[53] Y. Luo, X. Liu, Q. Zheng et al., "Hydrogen sulfide prevents hypoxia-induced apoptosis via inhibition of an $H_2O_2$-activated calcium signaling pathway in mouse hippocampal neurons," *Biochemical and Biophysical Research Communications*, vol. 425, no. 2, pp. 473–477, 2012.

[54] Y. Luo, X. Yang, S. Zhao et al., "Hydrogen sulfide prevents OGD/R-induced apoptosis via improving mitochondrial dysfunction and suppressing an ROS-mediated caspase-3 pathway in cortical neurons," *Neurochemistry International*, vol. 63, no. 8, pp. 826–831, 2013.

[55] K. Ji, L. Xue, J. Cheng, and Y. Bai, "Preconditioning of $H_2S$ inhalation protects against cerebral ischemia/reperfusion injury by induction of HSP70 through PI3K/Akt/Nrf2 pathway," *Brain Research Bulletin*, vol. 121, pp. 68–74, 2016.

[56] M.-y. Hong, J.-z. Cui, R. Li et al., "Effect of expression of c-jun N-terminal kinase on neuron autophagy following diffuse

brain injury in rats," *Zhonghua Wai Ke Za Zhi*, vol. 50, no. 2, pp. 166–170, 2012.

[57] N. Sen, B. D. Paul, M. M. Gadalla et al., "Hydrogen Sulfide-Linked Sulfhydration of NF-κB Mediates Its Antiapoptotic Actions," *Molecular Cell*, vol. 45, no. 1, pp. 13–24, 2012.

[58] J. Wu and M. M. Lipinski, "Autophagy in Neurotrauma: Good, Bad, or Dysregulated," *Cells*, vol. 8, no. 7, p. 693, 2019.

[59] C. Sarkar, Z. Zhao, S. Aungst, B. Sabirzhanov, A. I. Faden, and M. M. Lipinski, "Impaired autophagy flux is associated with neuronal cell death after traumatic brain injury," *Autophagy*, vol. 10, no. 12, pp. 2208–2222, 2015.

[60] S. Bialik, S. K. Dasari, and A. Kimchi, "Autophagy-dependent cell death - where, how and why a cell eats itself to death," *Journal of Cell Science*, vol. 131, no. 18, p. jcs215152, 2018.

[61] D. Denton and S. Kumar, "Autophagy-dependent cell death," *Cell Death & Differentiation*, vol. 26, no. 4, pp. 605–616, 2019.

[62] L. Zhang and H. Wang, "Autophagy in Traumatic Brain Injury: A New Target for Therapeutic Intervention," *Frontiers in Molecular Neuroscience*, vol. 11, 2018.

[63] C. Gao, P. Chang, L. Yang et al., "Neuroprotective effects of hydrogen sulfide on sodium azide-induced oxidative stress in PC12 cells," *International Journal of Molecular Medicine*, vol. 41, pp. 242–250, 2017.

[64] J.-F. Wang, Y. Li, J.-N. Song, and H.-G. Pang, "Role of hydrogen sulfide in secondary neuronal injury," *Neurochemistry International*, vol. 64, pp. 37–47, 2014.

[65] W. Zhao, "The vasorelaxant effect of H2S as a novel endogenous gaseous KATP channel opener," *The EMBO Journal*, vol. 20, no. 21, pp. 6008–6016, 2001.

[66] C. W. Leffler, H. Parfenova, S. Basuroy, J. H. Jaggar, E. S. Umstot, and A. L. Fedinec, "Hydrogen sulfide and cerebral microvascular tone in newborn pigs," *American Journal of Physiology-Heart and Circulatory Physiology*, vol. 300, no. 2, pp. H440–H447, 2011.

[67] C.-X. Liu, Y.-R. Tan, Y. Xiang, C. Liu, X.-A. Liu, and X.-Q. Qin, "Hydrogen Sulfide Protects against Chemical Hypoxia-Induced Injury via Attenuation of ROS-Mediated Ca2+ Overload and Mitochondrial Dysfunction in Human Bronchial Epithelial Cells," *BioMed Research International*, vol. 2018, 9 pages, 2018.

[68] M. A. García-Bereguiaín, A. K. Samhan-Arias, F. J. Martín-Romero, and C. Gutiérrez-Merino, "Hydrogen sulfide raises cytosolic calcium in neurons through activation of L-type Ca2+ channels," *Antioxid Redox Signal*, vol. 10, no. 1, pp. 31–42, 2008.

[69] Q. C. Yong, C. H. Choo, B. H. Tan, C.-M. Low, and J.-S. Bian, "Effect of hydrogen sulfide on intracellular calcium homeostasis in neuronal cells," *Neurochemistry International*, vol. 56, no. 3, pp. 508–515, 2010.

[70] Y. Nagai, M. Tsugane, J.-I. Oka, and H. Kimura, "Hydrogen sulfide induces calcium waves in astrocytes," *The FASEB Journal*, vol. 18, no. 3, pp. 557–559, 2004.

[71] W. J. Cahill, J. H. Calvert, and J. H. Zhang, "Mechanisms of early brain injury after subarachnoid hemorrhage," *Journal of Cerebral Blood Flow & Metabolism*, vol. 26, no. 11, pp. 1341–1353, 2006.

[72] S. Cao, P. Zhu, X. Yu et al., "Hydrogen sulfide attenuates brain edema in early brain injury after subarachnoid hemorrhage in rats: Possible involvement of MMP-9 induced blood- brain barrier disruption and AQP4 expression," *Neuroscience Letters*, vol. 621, pp. 88–97, 2016.

[73] T. Dóczi, "The pathogenetic and prognostic significance of blood-brain barrier damage at the acute stage of aneurysmal subarachnoid haemorrhage. Clinical and experimental studies," *Acta Neurochirurgica*, vol. 77, pp. 110–132, 1985.

[74] K. Schöller, A. Trinkl, M. Klopotowski et al., "Characterization of microvascular basal lamina damage and blood-brain barrier dysfunction following subarachnoid hemorrhage in rats," *Brain Research*, vol. 1142, pp. 237–246, 2007.

[75] G. T. Manley, M. Fujimura, T. Ma et al., "Aquaporin-4 deletion in mice reduces brain edema after acute water intoxication and ischemic stroke," *Nature Medicine*, vol. 6, no. 2, pp. 159–163, 2000.

[76] F. Zhao, J. Deng, X. Xu et al., "Aquaporin-4 deletion ameliorates hypoglycemia-induced BBB permeability by inhibiting inflammatory responses," *Journal of Neuroinflammation*, vol. 15, no. 1, p. 157, 2018.

[77] H. Kimura, "Hydrogen Sulfide Induces Cyclic AMP and Modulates the NMDA Receptor," *Biochemical and Biophysical Research Communications*, vol. 267, no. 1, pp. 129–133, 2000.

[78] A. Stein and S. M. Bailey, "Redox biology of hydrogen sulfide: Implications for physiology, pathophysiology, and pharmacology," *Redox Biology*, vol. 1, no. 1, pp. 32–39, 2013.

[79] J.-y. Zhang, Y.-p. Ding, Z. Wang, Y. Kong, R. Gao, and G. Chen, "Hydrogen sulfide therapy in brain diseases: from bench to bedside," *Medical Gas Research*, vol. 7, no. 2, pp. 113–119, 2017.

Hindawi
Oxidative Medicine and Cellular Longevity
Volume 2020, Article ID 4635163, 14 pages
https://doi.org/10.1155/2020/4635163

*Research Article*

# Resveratrol Mitigates Hippocampal Tau Acetylation and Cognitive Deficit by Activation SIRT1 in Aged Rats following Anesthesia and Surgery

**Jing Yan, Ailin Luo, Rao Sun, Xiaole Tang, Yilin Zhao, Jie Zhang, Biyun Zhou, Hua Zheng, Honghui Yu, and Shiyong Li**

*Department of Anesthesiology, Tongji Hospital, Tongji Medical College, Huazhong University of Science and Technology, 1095 Jiefang Avenue, Wuhan, 430030 Hubei, China*

Correspondence should be addressed to Shiyong Li; shiyongli@hust.edu.cn

Received 11 July 2020; Revised 9 November 2020; Accepted 28 November 2020; Published 16 December 2020

Academic Editor: Wei Zhao



Postoperative cognitive dysfunction (POCD) is a sever postsurgical neurological complication in the elderly population. As the global acceleration of population ageing, POCD is proved to be a great challenge to the present labor market and healthcare system. In the present study, our findings showed that tau acetylation mediated by SIRT1 deficiency resulted in tau hyperphosphorylation in the hippocampus of the aged POCD model and consequently contributed to cognitive impairment. Interestingly, pretreatment with resveratrol almost restored the expression of SIRT1, reduced the levels of acetylated tau and hyperphosphorylated tau in the hippocampus, and improved the cognitive performance in the behavioral tests. What is more, we observed that microglia-derived neuroinflammation resulting from SIRT1 inhibition in microglia probably aggravated the tau acetylation in cultured neurons in vitro. Our findings supported the notion that activation SIRT1 provided dually beneficial effect in the aged POCD model. Taken together, our findings provided the initial evidence that tau acetylation was associated with cognitive impairment in the aged POCD model and paved a promising avenue to prevent POCD by inhibiting tau acetylation in a SIRT1-dependent manner.

## 1. Introduction

Postoperative cognitive dysfunction (POCD) is a postsurgical neurological sequela characterized by a reduction in memory, learning, attention, and executive function in the short- and long-term following anesthesia and surgical procedure [1–3]. It is an age-related complication and occurs highly in the geriatric surgical individuals [4]. Clinical findings suggested that this cognitive impairment was associated with prolonged hospitalization, increased mortality, and growing burden of the medical care system [5]. Although a plethora of studies major in elucidating pathophysiologic processes of POCD and exploring feasible targets for therapeutic or preventive intervention, up to date, the neuropathogenesis of POCD remains largely ambiguous.

A growing body of studies showed that Alzheimer's disease- (AD-) like neuropathogenesis was involved in POCD, particularly in the elderly population [6–9]. Tau hyperphosphorylation was extensively investigated and proposed to participate in cognitive decline after anesthesia and surgery [6, 7]. This hypothesis was supported by clinical findings that the classical markers of AD in cerebrospinal fluid(CSF) were associated with postoperative cognitive changes in the elderly surgical population [10–15]. Correspondingly, the abnormal level of specific hyperphosphorylated sites of tau was found in the experimental POCD models [6–8, 15–17]. Concerning the role of tauopathies in neurodegenerative diseases, hyperphosphorylation is one type of neurotoxic modification. Other pathological modifications of tau include acetylation, glycosylation, glycation, acetylation, truncation, and nitration [18, 19]. Among these, tau acetylation was found in the physiological aging and preceded tau hyperphosphorylation in pathological settings [20–24]. A line of studies established that neuronal tau acetylation was directly mediated by

SIRT1 and further promoted accumulation of tau hyperphosphorylation by impeding its degradation [21]. Interestingly, our previous and other studies found that the expression of SIRT1 declined in hippocampal microglia with aging and contributed to age-related neuroinflammation and cognitive impairment in rodent [25]. Taken together, these findings raised the possibility that the hippocampal SIRT1 reduction induced tau acetylation and consequently contributed to cognitive decline following anesthesia and surgery.

Resveratrol (3,4,5-trihydroxystilbene) is a natural polyphenol present in various berries, nuts, grapes, and other plants sources [26]. To date, resveratrol has gained growing interest in the neuroscience community due to its pleiotropic neuroprotective effect, such as antioxidative, anti-inflammatory, and antiaging [27]. Furthermore, resveratrol afforded neuroprotection in multiple pathways dependent on activating SIRT1 in neurodegenerative diseases [28–31]. As mentioned before, resveratrol pretreatment activated SIRT1 and mitigated neuroinflammation and cognitive impairment in POCD models in our previous study [25], but it remains unclear whether resveratrol would mitigate surgery and anesthesia-induced SIRT1 reduction and tau acetylation in aged POCD models.

In the present study, we sought to investigate the role of tau acetylation in cognitive decline following surgery and anesthesia in aged rats. Furthermore, we examined the idea that resveratrol would improve the cognitive ability by activating hippocampal SIRT1 and sequentially reducing tau acetylation in aged POCD models.

## 2. Materials and Methods

*2.1. Animals.* All experimental protocols and animal handling procedures were performed in accordance with the National Institute of Health guidelines and regulations. The experimental protocols were approved by the Committee of Experimental Animals of Tongji Medical College. 21-month-old male Sprague-Dawley rats (weighing 620–670 g at the start of the experiment) were provided by the Center of Experimental Animal of Tongji Medical College. Three to four animals were housed per cage under standard laboratory conditions. As shown in Figure 1, the 21-month-old male rats were randomly assigned to four groups: (1) control+DMSO, rats in the control group were injected with the DMSO-saline solution and treated with a 1 : 1 mix of air and 100% oxygen; (2) sevoflurane+surgery, rats in this group received the DMSO-saline solution followed by splenectomy under sevoflurane anesthesia; (3) resveratrol + DMSO, rats in this group were injected with resveratrol and treated with a 1 : 1 mix of air and 100% oxygen; and (4) sevoflurane+surgery+resveratrol, rats in this group were injected with resveratrol followed by splenectomy under sevoflurane anesthesia.

*2.2. Anesthesia, Surgery, and Treatment.* The anesthesia, surgery, and treatment of each group were shown in Figure 1. The procedure of splenectomy was performed as previously described [25]. Briefly, a small incision approximately 2–3 cm was made in the upper left quadrant, and then the spleen was visualized, isolated, and removed. The surgical procedure was performed under 3% sevoflurane in a 1 : 1 mix of air and 100% oxygen. The wound was infiltrated with 0.25% bupivacaine after the surgery. Rats in the control group were exposed to a 1 : 1 mix of air and 100% oxygen for 2 hours. Resveratrol (Selleck Chemicals, Houston, TX, USA) was prepared by dissolving the powder in a dimethyl sulfoxide- (DMSO-) (Sigma-Aldrich, St. Louis, USA) saline solution and was injected intraperitoneally at 10 mg/kg/day for 7 consecutive days, with the last dose administered 12 hours before surgery. The resveratrol dose was chosen based on a previous study [32].

*2.3. Cell Lines.* The mouse BV2 cell lines were used as an alternative to investigate microglia in vitro. The cell populations were allocated into four groups: (1) control+DMSO, cells in the control group were treated with DMSO-saline solution; (2) LPS+sevoflurane, cells in this group were treated with DMSO+LPS (100 ng/ml, Sigma-Aldrich, St. Louis, USA)+sevoflurane (4% for 6 hours); (3) resveratrol +DMSO, cells in the resveratrol group were treated with resveratrol (20 $\mu$mol, Selleck Chemicals); and (4) LPS+sevoflurane+resveratrol, cells in this group were treated with resveratrol (20 $\mu$mol)+LPS (100 ng/ml)+sevoflurane (4% for 6 hours). Then, another BV2 cell populations were allocated into four groups (Supplementary Figure S1): (1) control +resveratrol, cells in the control group were treated with resveratrol (20 $\mu$mol, Selleck Chemicals); (2) LPS +sevoflurane+resveratrol, cells in this group were treated with DMSO+LPS (100 ng/ml, Sigma-Aldrich, St. Louis, USA)+sevoflurane (4% for 6 hours)+resveratrol (20 $\mu$mol); (3) resveratrol+EX527, cells in this group were treated with resveratrol (20 $\mu$mol) + EX527 (100 nM, Selleck Chemicals); and (4) LPS+sevoflurane+resveratrol+EX527, cells in this group were treated with resveratrol (20 $\mu$mol)+EX527 (100 nM)+LPS (100 ng/ml)+sevoflurane (4% for 6 hours).

*2.4. Conditioned Medium (CM).* CMs were prepared as described [33]. Briefly, BV2 cells were cultured with DMED-F12 FBS medium overnight and then treated with or without LPS and sevoflurane stimulation in the absence or presence of resveratrol. CM was harvested, centrifuged, filtered, and stored at -80°C until use.

*2.5. Primary Hippocampal Neurons.* Primary hippocampal neurons were prepared from both of the hemispheres hippocampus of postnatal day 1 rat as described [34]. Briefly, rats were anesthetized by $CO_2$ and sacrificed, and the hippocampus was isolated and digested in 0.125% trypsin at 37°C for 15-20 min. After centrifuge, cells were cultured with neurobasal medium supplemented with 2% B27, 1% glutamine, and 1% penicillin-streptomycin at 37°C in humidified atmosphere with 5% $CO_2$. The medium was changed every 3 days. Neurons cultured for 7 days were used in the study. Neurons were assigned into four groups: (1) control CM, (2) LPS +sevoflurane CM, (3) resveratrol+DMSO CM, and (4) LPS + sevoflurane+resveratrol CM and treated with corresponding CM for 24 hours. Then, another primary neurons were assigned into four groups: (1) control+resveratrol CM, (2) LPS+sevoflurane+resveratrol CM, (3) resveratrol+EX527

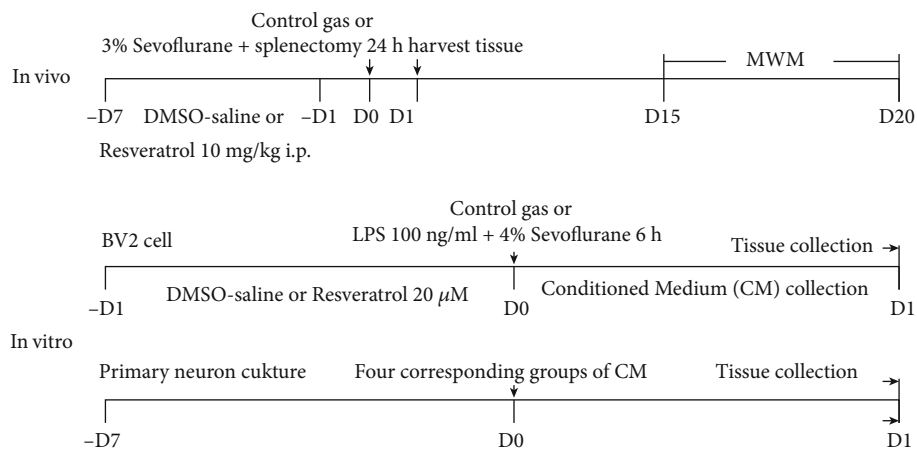


Figure 1: Experimental protocol in vivo and in vitro. In vivo 21-month-old rats were pretreated with DMSO-saline solution or resveratrol via intraperitoneal injection for 7 consecutive days and received control gas or splenectomy under 3% sevoflurane for 2 h. After exposure, part of the rats was decapitated, and tissue samples were collected for biochemistry study, and part of the rats received the MWM test. In vitro BV2 cell was cultured and treated with DMSO-saline solution or resveratrol for 24 h, followed by treatment of control gas or LPS and 4% sevoflurane for 6 h. After exposure, conditioned medium were collected for primary neuron study, and tissue was collected for biochemistry study. After 7-day culture, primary neuron was incubated with four corresponding groups of conditioned medium for 24 h. Tissue was collected for biochemistry study after exposure.

CM, and (4) LPS+sevoflurane+resveratrol+EX527 CM and treated with corresponding CM for 24 hours.

*2.6. Western Blot Analysis.* Western blot was performed as previously reported [35]. The hippocampal tissue was harvested 24 hours after anesthesia and surgery and homogenized at 4°C for 30 min in RIPA lysis buffer. Cells were washed with PBS buffer three times 24 hours after treatment and collected into clean centrifuge tubes. The protein levels in the hippocampal tissues and cells were determined by a BCA assay kit (Boster, Wuhan, China). An equal amount of protein was loaded and separated by SDS-PAGE and transferred to a polyvinylidene difluoride (PVDF) membrane (Millipore, Bedford, MA, USA) by electrophoresis. The membranes were blocked with 5% nonfat skim milk in TBST (0.1% Tween 20 in TBS) for 45 min at room temperature and then incubated overnight at 4°C with an anti-SIRT1 (1 : 1000; Abcam, Cambridge, UK), anti-ac-tau (k280) (1 : 1000, Anaspec, CA, USA), anti-ac-tau (k686) (1 : 1000, EnoGene, Nanjing, China), anti-p-tau (AT8) (1 : 1000, Thermo Fisher Scientific, MA, USA), anti-Acetyl-NF-kappaB (1 : 1000, Affinity, OH, USA), anti-total tau (1 : 1000, Affinity), or anti-$\beta$-actin (1 : 1000, Affinity) antibody. On the second day, the membranes were washed three times with PBST and then incubated with a horseradish peroxidase- (HRP-) conjugated goat anti-mouse or goat anti-rabbit IgG antibody (1 : 2000; Abbkine, Wuhan, China) for 2 hours at room temperature. Bands were quantified using laboratory imaging software, and the experiments were repeated in triplicate.

*2.7. Immunofluorescence.* Immunofluorescence staining was performed as described [25, 36]. Briefly, rats were sacrificed with sodium pentobarbital (85 mg/kg) 24 hours after anesthesia and surgery. Brains were harvested, fixed, and dehydrated. Ten-micron-thick frozen hippocampal sections were cut and incubated with 5% normal donkey serum in PBS for 1 hour, followed by incubation with an anti-SIRT1 (1 : 1000; Abcam) and anti-NeuN (1 : 1000; Millipore, USA) antibody at 4°C overnight. Sections were incubated with donkey anti-Goat IgG conjugated to Alexa Fluor®594 (1 : 500, Abbkine) and donkey anti-Mouse IgG conjugated to Alexa Fluor®488 (1 : 500, Abbkine) in the dark for 1.5 hour at room temperature. Images were acquired with a fluorescence microscope.

*2.8. Morris Water Maze Test.* The Morris water maze test was performed on days 15-20 after anesthesia and surgery as previously described [37]. Briefly, the training protocol for the task of the MWM test consisted of 3 trials (120 s maximum; interval 20 min) each day for five consecutive days. The probe trial (120 s), in which the platform was removed, was performed 24 hours after the end of the fifth day training.

*2.9. Statistical Analysis.* The data obtained from biochemistry studies and escape latency of MWM were represented as the mean ± SD. The data of platform crossing time of MWM were presented as medians with interquartile range. The data were analysed with GraphPad Prism 7.0 (GraphPad Software, CA, USA). Statistical evaluation between 2 groups was performed using two-sided Student's $t$ test. Statistical evaluation between 4 groups in biochemistry studies was performed using two-way analysis of variance (ANOVA) without repeated measurement to evaluate the interaction of group and treatment. Data of escape latency in the MWM test were measured by two-way ANOVA with repeated measurement, followed by the Bonferroni posthoc. The Mann–Whitney $U$ test was used to compare the difference in the platform-crossing times in the MWM test. $P < 0.05$ was considered statistically significant.

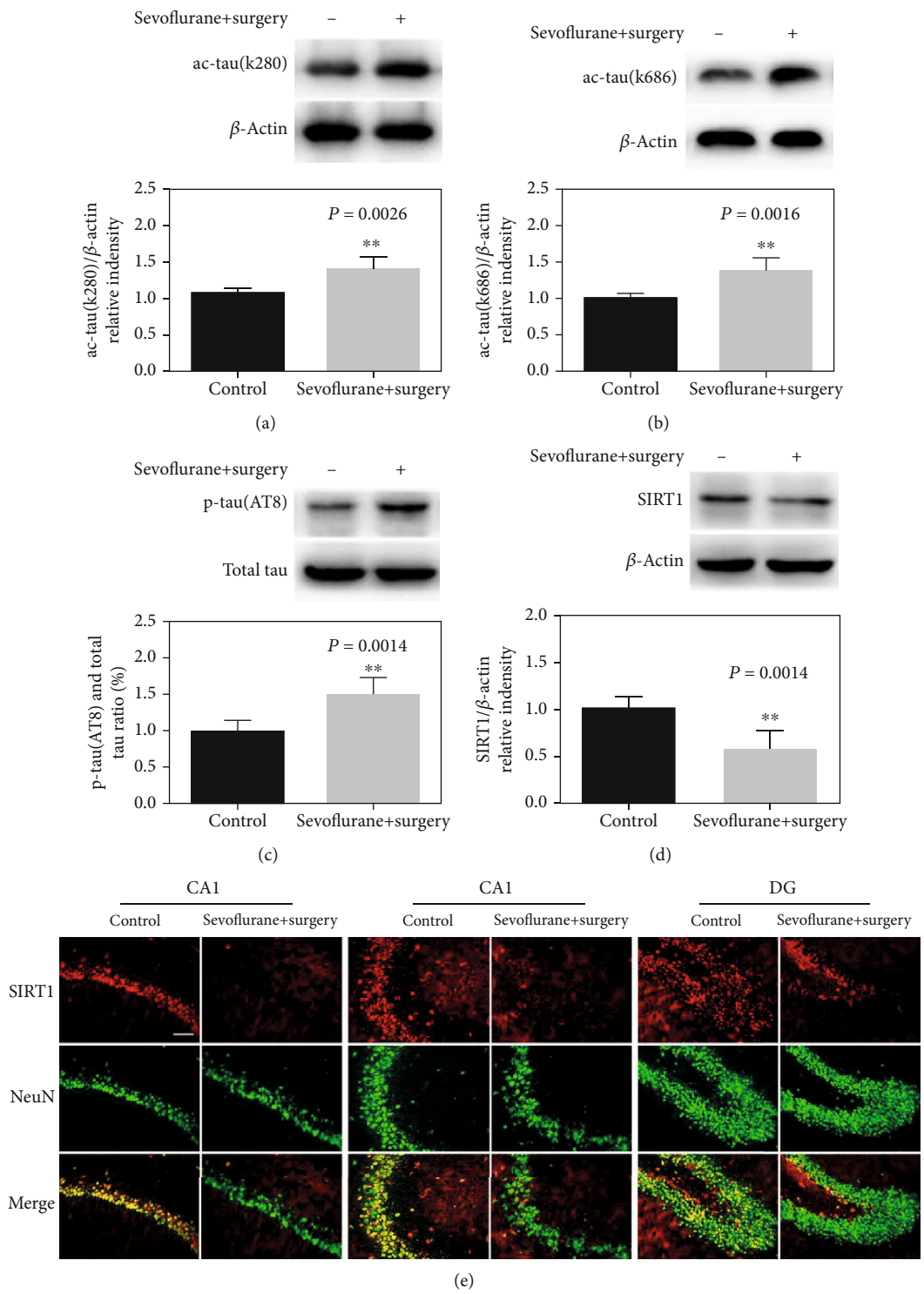


Figure 2: Anesthesia and surgery elevate tau acetylation and decrease the neuronal SIRT1 expression in the hippocampus of aged rats. (a)–(d) Representative immunoblot bands and the corresponding densitometry analysis of ac-tau (k280), ac-tau (k686), SIRT1 expression normalized to $\beta$-actin, and p-tau (AT8) normalized to total tau. (e) Immunostaining of SIRT1 (red) and NeuN (green) in the control and sevoflurane +surgery groups. Data are presented as the mean ± SD. $n = 6$ per group. Scale bar = 50 $\mu$m.

## 3. Results

*3.1. Anesthesia and Surgery Elevates Tau Acetylation and Decreases the Neuronal SIRT1 Expression in the Hippocampus of Aged Rats.* First, we investigated tau acetylation levels after anesthesia and surgery of aged rats. The data showed that the expression of ac-tau (k280) and ac-tau (k686) was significantly

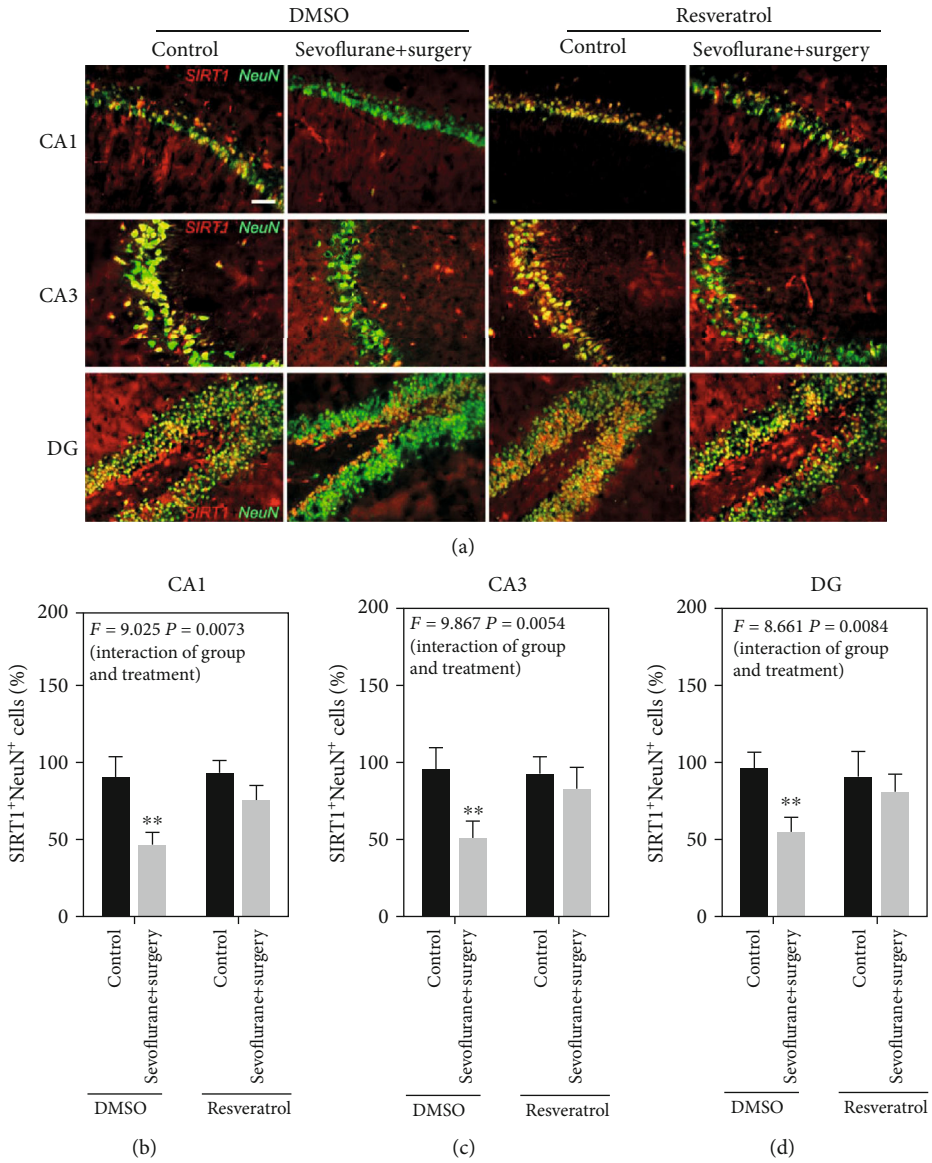


Figure 3: Continued.

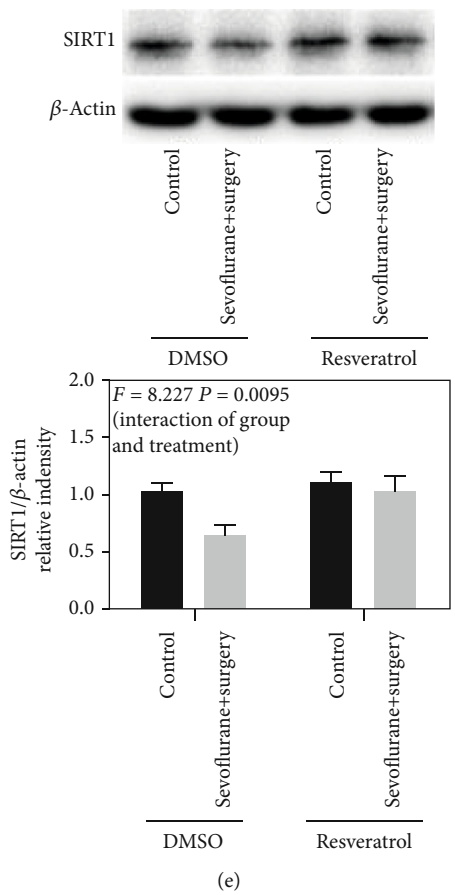


Figure 3: Resveratrol pretreatment increases the neuronal SIRT1 expression in the hippocampus of aged rats exposed to anesthesia and surgery. (a) Immunostaining of SIRT1 (red) and NeuN (green). (b)–(d) Quantification of SIRT1-positive and NeuN-positive cells. (e) Representative immunoblot band and the corresponding densitometry analysis of the SIRT1 expression normalized to $\beta$-actin. Data are presented as the mean ± SD. $n = 6$ per group. Scale bar = 50 $\mu$m.

increased in the hippocampus after anesthesia and surgery ($P = 0.0026$; $P = 0.0016$, Figures 2(a) and 2(b)). Tau acetylation can precede tau hyperphosphorylation in the pathological context, and we further elevated the expression of tau phosphorylation levels. As shown in Figure 1(c), anesthesia and surgery led to a significant increase in the p-tau (AT8) expression in the hippocampus ($P = 0.0014$). Similar to the result with our previous study, anesthesia and surgery significantly decreased the expression of SIRT1 in the hippocampus ($P = 0.0014$, Figure 2(d)). Interestingly, the immunofluorescence results revealed that neuronal SIRT1 was notably decreased in CA1, CA3, and DG regions of the hippocampus after anesthesia and surgery (Figure 2(e)).

*3.2. Resveratrol Pretreatment Increases the Neuronal SIRT1 Expression in the Hippocampus of Aged Rats Exposed to Anesthesia and Surgery.* To verify the function of resveratrol on the SIRT1 expression, we used both immunostaining and western blot to detect SIRT1 in the hippocampus. As shown in Figure 3(a), there is a clear trend of decreasing neuronal SIRT1 levels in CA1, CA3, and DG regions of the hippocampus in the sevoflurane+surgery group compared with the control group, and resveratrol pretreatment blocked the sevoflurane and surgery-induced changes in neuronal SIRT1 levels ($F = 9.025$, $P = 0.0073$; $F = 9.867$, $P = 0.0054$; $F = 8.661$, $P = 0.0084$, Figures 3(b)–3(d)). The western blot data also declared that resveratrol pretreatment remarkably blocked sevoflurane and surgery-induced reduction in SIRT1 levels in the hippocampus ($F = 8.227$, $P = 0.0095$, Figure 3(e)).

*3.3. Activation of SIRT1 Decreases Tau Acetylation and Tau Phosphorylation in the Hippocampus of Aged Rats Exposed to Anesthesia and Surgery.* To verify the function of SIRT1 in the mediation of tau acetylation and tau phosphorylation in the aged POCD model, resveratrol was used to activate the expression of SIRT1. The data showed that activation of SIRT1 reduced anesthesia and surgery-induced tau acetylation and tau phosphorylation, as showed by the increased levels of ac-tau (k280), ac-tau (k686), and p-tau (AT8) in the sevolurane+surgery group compared with the control group, and decreased levels of ac-tau (k280), ac-tau (k686), and p-tau (AT8) in the sevoflurane+surgery+resveratrol group ($F = 9.319$, $P = 0.0063$; $F = 12.25$, $P = 0.0023$; $F = 11.01$, $P = 0.0034$, Figures 4(a)–4(c)).

*3.4. Activation of SIRT1 Ameliorates Cognitive Impairment in Aged Rats of the POCD Model.* To explore the relationship between the SIRT1 level in the hippocampus and cognitive

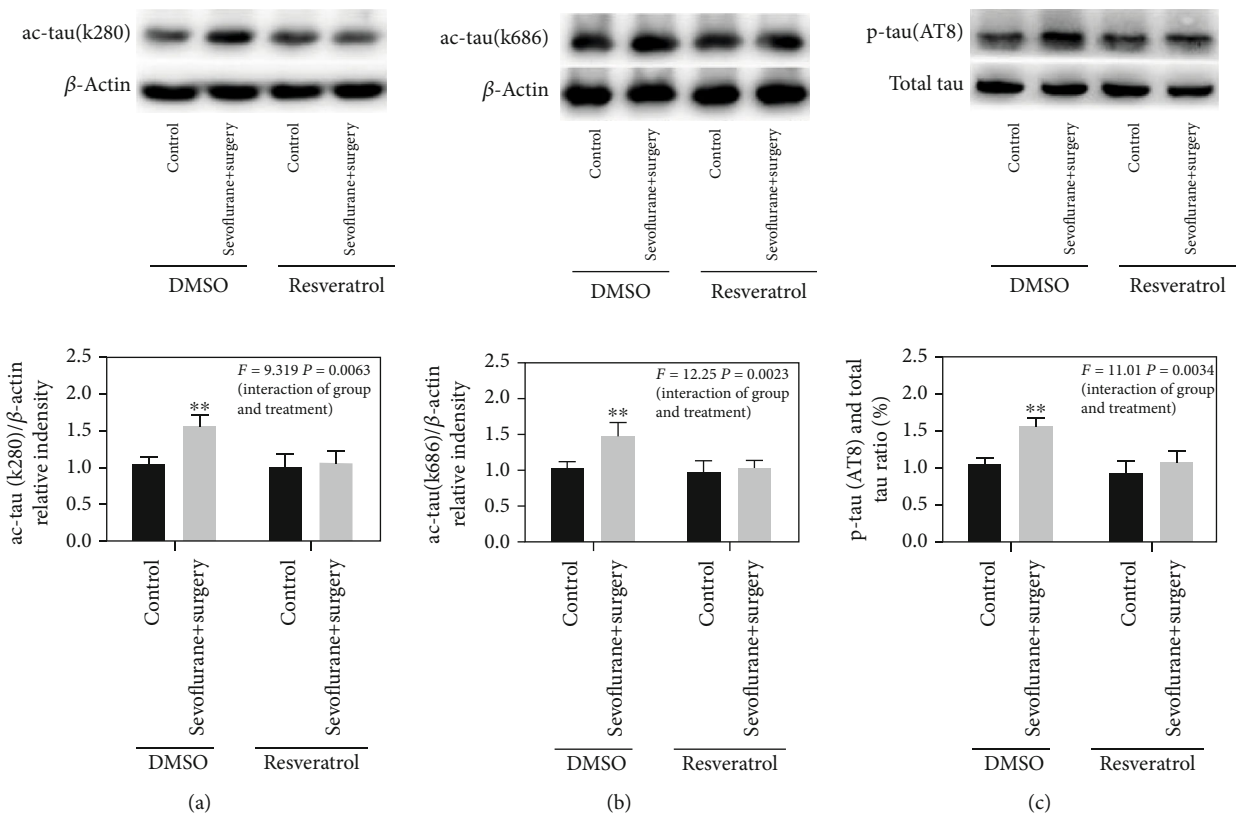


Figure 4: Activation of SIRT1 decreases tau acetylation and tau phosphorylation in the hippocampus of aged rats exposed to anesthesia and surgery. (a)–(c) Representative immunoblot bands and the corresponding densitometry analysis of ac-tau (k280), ac-tau (k686) expression normalized to $\beta$-actin, and p-tau (AT8) expression normalized to total tau. Data are presented as the mean ± SD. $n = 6$ per group.

decline in aged rats of the POCD model, resveratrol was used to activate the expression of SIRT1 in the hippocampus, and Morris water maze was used to evaluate the spatial learning and memory performance of aged rats. During the training phase of MWM, anesthesia and surgery induced cognitive impairment as evidenced by the significant interaction between treatment (control+DMSO condition and sevoflurane+surgery) and time on escape latency ($F = 2.526$, $P = 0.0468$, Figure 5(a)). A Bonferroni posthoc test showed that rats in the sevoflurane+surgery group spent more time locating the hidden platform on the fourth and fifth training day compared with rats in the control group ($P < 0.01$, Figure 5(a)). In the probe trial, the rats in the sevoflurane +surgery group showed a remarkable reduction in the platform crossing times ($P = 0.0269$, Figure 5(b)). Importantly, the cognitive impairment was prevented by resveratrol pretreatment, as shown by no significant interaction between treatment (control+resveratrol condition and sevoflurane +surgery+resveratrol) and time on escape latency ($F = 0.8223$, $P = 0.5143$, Figure 5(c)), and no significant difference in platform crossing times between the control +resveratrol group and sevoflurane+surgery+resveratrol group ($P = 0.8174$, Figure 5(d)).

*3.5. Activation of SIRT1 Reduces LPS+Sevoflurane-Induced Ac-NF-κB and Proinflammatory Cytokine Expression in the BV2 Cell Line.* Our previous study had found that SIRT1 mediated neuroinflammation via regulation of ac-NF-κB in the hippocampus of an aged POCD model. To confirm the relationship of SIRT1 and neuroinflammation, LPS and sevoflurane were used as stimulus to induce the proinflammatory cytokine expression in BV2 cell lines. As showed in Figures 6(a)–6(d), LPS and sevoflurane led to a notable decrease in the SIRT1 expression and increase in the levels of ac-NF-κB and IL-6 in BV2 cell lines. However, resveratrol treatment resulted in a remarkable increase in the SIRT1 expression and decrease in the levels of ac-NF-κB and IL-6 compared with that in BV2 cell lines in the LPS+ sevoflurane group ($F = 10.37$, $P = 0.0043$; $F = 8.480$, $P = 0.0086$; $F = 14.44$, $P = 0.0011$, Figures 6(b)–6(d)). As resveratrol is a polyphenol with pleiotropic neuroprotective properties, we explored EX527, a SIRT1 inhibitor, to validate our hypothesis. We found EX527 obviously weakened the effect of resveratrol which decreased the level of SIRT1 and increased the levels of ac-NF-κB and IL-6 in BV2 cell lines (as shown in Figure S2. A-D). These findings suggested that resveratrol reduced LPS+sevoflurane-induced neuroinflammation by, at least partially, acting on SIRT1 in the BV2 cell line.

*3.6. Activation of SIRT1 Decreased the LPS+Sevoflurane-Conditioned Medium-Induced Tau Acetylation and Tau Phosphorylation in Primary Hippocampal Neurons.* To explore the underline mechanism of neuroinflammation-induced tau acetylation in aged POCD models, conditioned

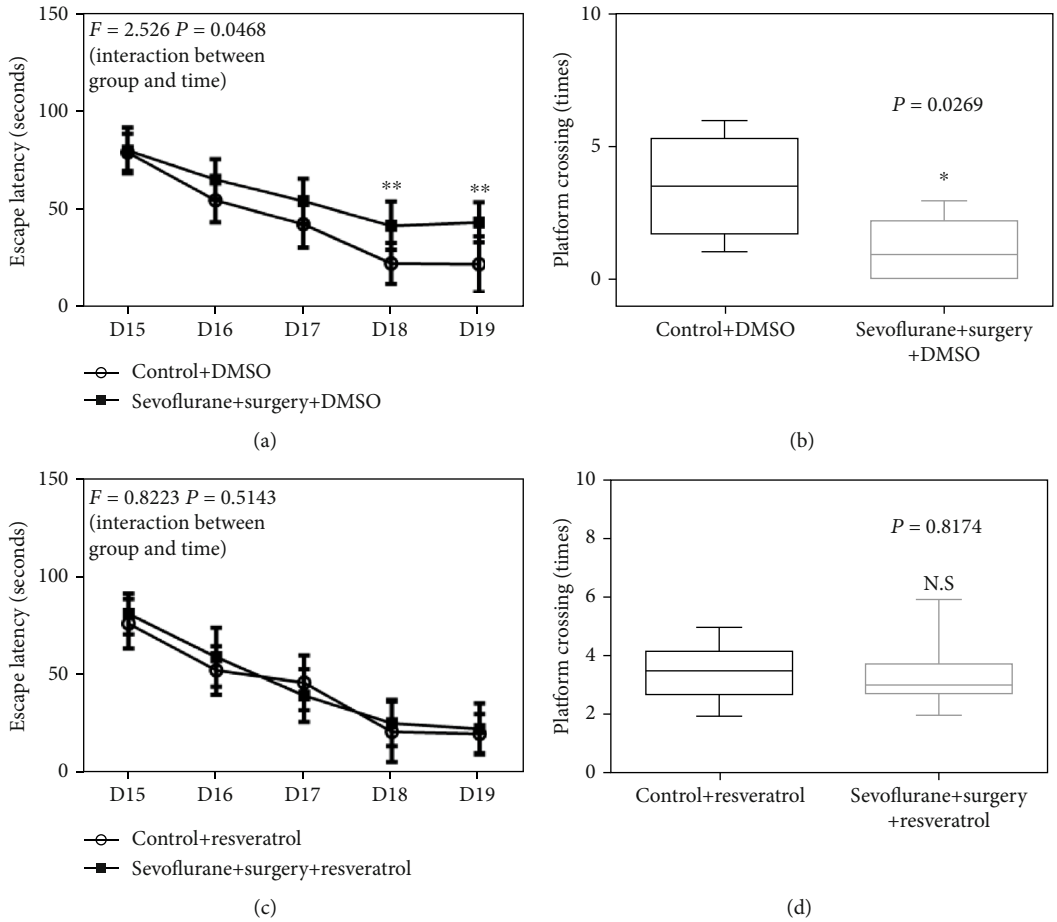


Figure 5: Activation of SIRT1 ameliorates cognitive impairment in aged rats of the POCD model. (a) The difference of escape latency in the MWM in five training days between control and sevoflurane+surgery groups. (b) The difference of platform crossing times in the probe trial of the MWM between control and sevoflurane+surgery groups. (c) The difference of escape latency in the MWM in five training days between resveratrol and sevoflurane+surgery+resveratrol groups. (d) The difference of platform crossing times in the probe trial of the MWM between resveratrol and sevoflurane+surgery+resveratrol groups. Data are presented as the mean ± SD. $n = 10$ per group.

medium of BV2 cells was collected to treat in primary hippocampal neurons. The results indicated that LPS+sevoflurane CM led to a decrease in the SIRT1 expression in primary hippocampal neurons compared with the control CM group, and resveratrol involved conditioned medium induced a remarkable increase in the SIRT1 level ($F = 8.960$, $P = 0.0072$, Figure 7(a)). Besides, LPS+sevoflurane CM induced tau acetylation and tau phosphorylation in primary hippocampal neurons, as shown by increased levels of ac-tau (k280), ac-tau (k686) ,and p-tau (AT8) compared with those in primary hippocampal neurons in the control CM group, whereas resveratrol CM treatment showed remarkable downregulation in ac-tau (k280), ac-tau (k686), and p-tau (AT8) expression ($F = 10.06$, $P = 0.0048$; $F = 9.085$, $P = 0.0069$; $F = 7.564$, $P = 0.0123$, Figures 7(b)–7(d)). However, SIRT1 inhibitor EX527 weakened the effect of resveratrol on tau acetylation and tau phosphorylation by reducing the SIRT1 expression (as shown in Figure S3. A-D). Taken together, SIRT1 activation was associated with resveratrol's effect on LPS+sevoflurane-conditioned medium-induced tau acetylation and tau phosphorylation.

## 4. Discussion

In the present study, we showed that elevated acetylation of tau was mediated by SIRT1 reduction following surgery and anesthesia in aged rat of the POCD model. Pretreatment with resveratrol, a natural activator of SIRT1, mitigated SIRT1 suppression, further downregulated the level of tau acetylation and hyperphosphorylation in the hippocampus and consequently mitigated the cognitive decline of the aged POCD model. Furthermore, we found that microglial cell line-derived neuroinflammation was associated with neuronal tau acetylation in the conditioned culture system in vitro. These findings suggest that tau acetylation is at the nexus of transient neuroinflammation to the prolonged cognitive decline following surgery and anesthesia in the aged POCD models.

POCD is a severe neurological complication, and the symptoms last for days to months or years [3, 38]. Accumulating of well-documented studies regarded neuroinflammation as the main pathological culprit in the POCD model [39–43]. As neuroinflammation is usually a transient process,

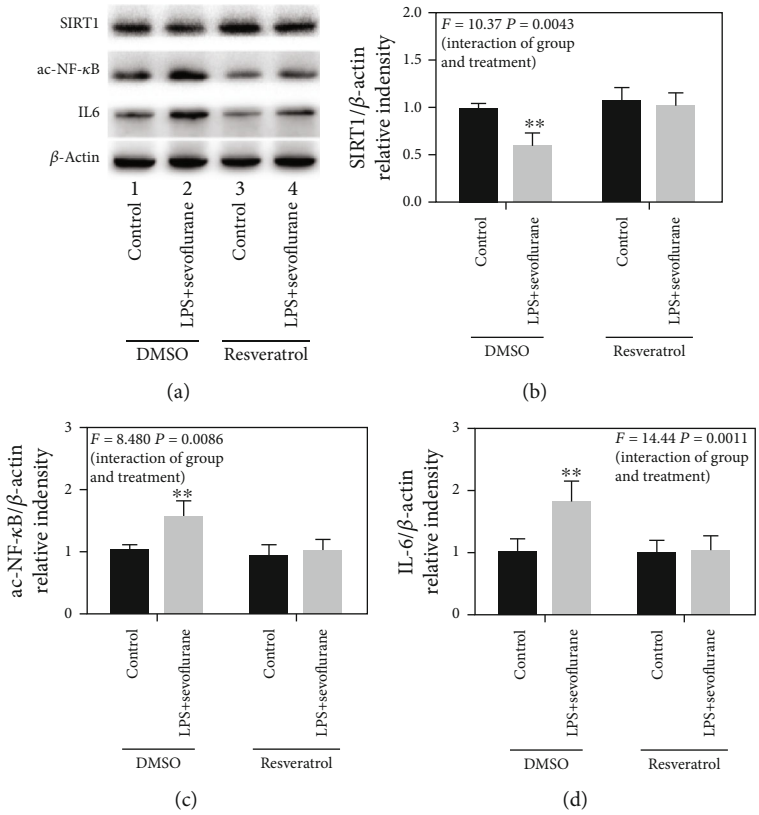


Figure 6: Activation of SIRT1 reduces the LPS + sevoflurane-induced ac-NF-κB and proinflammatory cytokine expression in BV2 cell lines. (a) Representative immunoblot bands of SIRT1, ac-NF-κB, and IL-6 expression in BV2 cell lines. (b)–(d) The corresponding densitometry analysis of SIRT1, ac-NF-κB, and IL-6 expression normalized to β-actin. Data are presented as the mean ± SD. $n = 6$ per group.

tau hyperphosphorylation was once hypothesized as the bridge between neuroinflammation and long-term cognitive impairment in POCD [9]. This idea was supported by previous reports that hyperphosphorylated tau resulted in abnormality of axonal transport, synaptic structure and function, and finally induced cognitive impairment in AD [19, 44, 45]. Several studies found tau hyperphosphorylated in the preexisted AD model following surgery and anesthesia [7, 46–48]. As known, tauopathies include a wide range of abnormal modifications of tau in neurodegenerative diseases [18, 19]. However, it remains poorly understood whether other forms of tauopathies are involved in POCD.

Acetylation is one type of posttranslational modifications of tau [21]. And then a growing number of findings have linked the acetylation of tau to tau neurotoxicity [20–24, 49, 50]. The initial evidence for tau acetylation and its role in AD turned up in 2010 [21]. It showed that tau hyperacetylation was an early event in AD and occurred before the accumulation of tau tangles [20–22, 24]. After this report, tau acetylation was observed in various neurodegenerative diseases. Hyperacetylated tau underlay the neuropathogenesis in a variety of manners, including preventing tau degradation, promoting tau aggregation and propagation, and disrupting synaptic structure and function [20–22, 24, 49, 50]. In the present study, we found that tau acetylation was elevated in the hippocampi of aged rats following anesthesia and surgery. To the best of our knowledge, this is the initial evidence that shows that tau acetylation is associated with cognitive impairment in POCD models. This finding provides insight into exploring the mechanism of POCD and possibly opens a new acetylated tau-targeted therapeutics pipeline for POCD.

Tau acetylation is mediated by acetyltransferases p300 or deacetylases SIRT1 in the pathological condition [21]. SIRT1 is the NAD-dependent class III deacetylase and strongly implicated in various pathophysiological process, including neurodevelopment, aging, stress, inflammation, and cancer [51, 52]. In terms of modulating tau acetylation, SIRT1 could interact with tau directly. SIRT1 reduction led to increased tau acetylation and elevated level of tau phosphorylation, while restoring the SIRT1 expression reduced the level of acetylated and phosphorylated tau [21]. In line with these findings, our present and previous studies observed hippocampal SIRT1 reduction in aged rats of the POCD model [25]. Remarkably, pretreating the model with resveratrol nearly restored the hippocampal expression of SIRT1, suppressed the levels of tau acetylation and phosphorylation, and finally mitigated the cognitive impairment. Base on the present study, we did not rule out the role of p300 that was in tau acetylation in the POCD model and set out to conduct further study to examine this possibility. In summary, our finding suggested that SIRT1 reduction contributed to tau acetylation and cognitive impairment in aged rats following surgery and anesthesia.

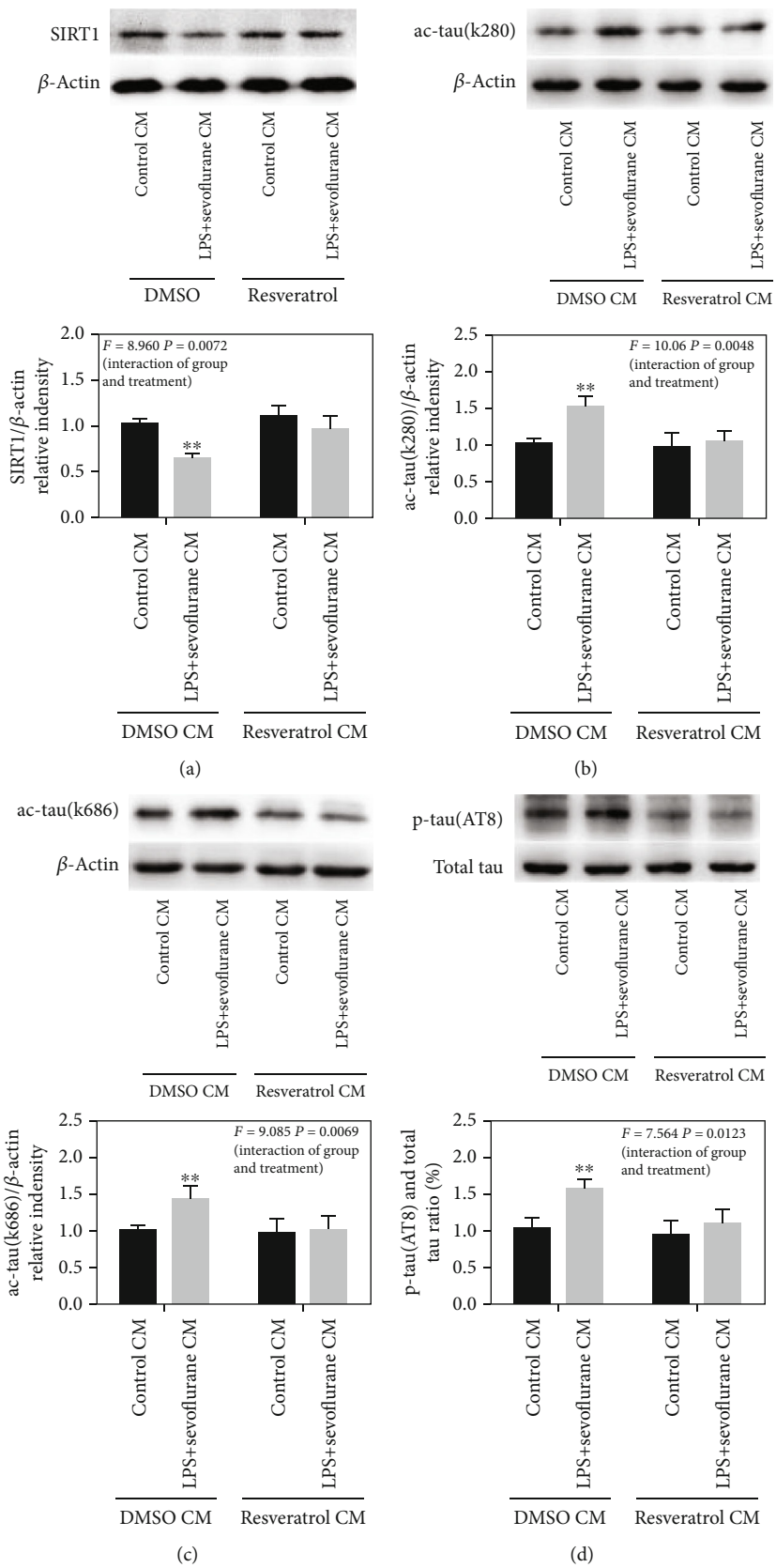


Figure 7: Activation of SIRT1 decreased the LPS+sevoflurane-conditioned medium-induced tau acetylation and tau phosphorylation in primary hippocampal neurons. (a)–(d) Representative immunoblot bands and the corresponding densitometry analysis of SIRT1, ac-tau (k280), ac-tau (k686) expression normalized to β-actin, and p-tau (AT8) expression normalized to total tau. Data are presented as the mean ± SD. $n = 6$ per group.

Neuroinflammation was found to be involved in tau phosphorylation in AD and POCD. In fact, neuroinflammation was considered as the mainstream neuropathogenesis of POCD in preclinical studies [39–43, 53–57]. In the present study, we sought to examine whether it was a link between neuroinflammation and tau acetylation in aged POCD models. It was reported previously that decrease of microglial SIRT1 contributed to aging-related neurodegeneration and cognitive decline [58, 59]. Our previous study found that microglial-derived SIRT1 reduction contributed to neuroinflammation and cognitive impairment in the aged POCD model [25]. However, SIRT1-mediated tau acetylation was found in neurons [21]. As SIRT1 is found both in neurons and microglia, how might neuroinflammation lead to tau acetylation in the aged POCD model? We hypothesized that overactivated neuroinflammation inhibited neuronal SIRT1 and further induced tau hyperacetylation.

To test this hypothesis, we used the conditioned medium cell cultures. In agreement with previous studies [60], we found that SIRT1 was reduced in microglial cell line (BV2), and neuroinflammation was induced by lipopolysaccharide (LPS)+sevoflurane. Incubating neurons with the conditioned medium from LPS+sevoflurane-stimulated BV2 culture medium led to neuronal reduction of SIRT1 and increase of tau acetylation and tau phosphorylation. Conditioned medium pretreated with resveratrol mitigated neuronal SIRT1 reduction and tau acetylation and tau phosphorylation. However, SIRT1 inhibitor EX527 weakened resveratrol's anti-neuroinflammatory and tau-reducing effect. This finding indirectly suggested that the effect of resveratrol on reducing neuroinflammation and tau acetylation and tau phosphorylation was mediated by SIRT1. SIRT1 is also a redox-sensitive sensor. This idea was supported by findings that oxidative stress inhibited the SIRT1 expression and causally led to pathological changes with LPS stimulus [61]. In this regard, we could not rule out the possibility that reactive oxygen species(ROS) released by BV2 activation contributed to neuronal SIRT1 inhibition, because increased ROS was generated in aged rodents of POCD models and associated with cognitive impairment [62–64]. Interestingly, the cerebrospinal fluid level of 15-$F_{2t}$-isoprostane, a specific biomarker of oxidative stress, is increased with aging and exacerbation of cognitive dysfunction [65, 66]. In this regard, these data open a new direction for diagnosis of POCD in the aged population. Taken together, these data suggested that microglia-derived neuroinflammation reduced the level of SIRT1 in hippocampal neurons in vitro.

Resveratrol (3,4′,5-trihydroxystilbene, $C_{14}H_{12}O_3$) is a natural polyphenolic nutraceutical that can be extracted from grapes, the roots of white hellebore, and *Polygonum cuspidatum* [26]. It exhibits pleiotropic activities, including antioxidation, anti-inflammation, antiapoptosis, anticancer, and antiaging under a wide variety of pathological condition [67, 68]. Although the mechanism is not yet clear by which resveratrol confers such a vast range of beneficial effects across various disease models, a wealth of evidence points its neuroprotective property to the sirtuins family, in particular, the SIRT1 [27, 69]. Resveratrol is not a specific activator of SIRT1, but accumulating findings suggest that resveratrol exerts neuroprotection via activation of SIRT1 in neurodegenerative diseases and stroke [21, 29, 31, 58, 70]. In light of the finding that SIRT1 reduction was observed in conditioned medium of the microglial cell line and conditioned medium treated neurons and the fact SIRT1 directly modulated tau acetylation, resveratrol likely afforded the neuroprotective effect by acting on the dual neuropathological changes neuroinflammation and tau acetylation. Indeed, we found that resveratrol pretreatment inhibited neuroinflammation, reduced the levels of acetylated tau and phosphorylated tau, and mitigated the cognitive decline in the aged rat of the POCD model. Considering the efficacy, safety, and pharmacokinetics of resveratrol that have been documented in more than 200 clinical trials [27], but yet absent in the POCD-related trial, we suppose that resveratrol might be a promising measurement to prevent POCD in the elderly surgical population.

There are several limitations to the present study. First, we did not investigate whether tau acetylation and tau phosphorylation worked in parallel or in succession as previously reported in AD. Second, we did not examine whether other enzymes modulated tau acetylation in the present model. Third, our surgery procedure was splenectomy, but not the prevalent laparotomy or tibial fracture, to keep consistency with our previous model. Further, study would be conducted to overcome the flaws of the current study.

## 5. Conclusions

Collectively, this study provides initial evidence that increased hippocampal tau acetylation which was associated with neuroinflammatory stress in aged rat of the POCD model. The hyperacetylated tau, at least partially mediated by SIRT1 inhibition, increased tau phosphorylation and contributed to cognitive impairment in the present experimental model. However, preconditioning with resveratrol mitigated the tau hyperacetylation and hyperphosphorylation and improved the behavioral performance in the learning and memory test. This study proposed a new neuropathological mechanism mediating cognitive impairment in the aged POCD model and paved a promising way to prevent this postoperative neurological complication.

## Data Availability

The data used to support the findings of this study are included within the article.

## Conflicts of Interest

The authors declare that there is no conflict of interests regarding the publication of this paper.

## Authors' Contributions

Jing Yan and Ailin Luo contributing equally to this work.

## Acknowledgments

This work was supported by project grants from the National Natural Science Foundation of China (grant Nos. 81400882,

81771159, 81571047, 81974160, and 81500982) and Science Foundation Projects for Young Scientists of Hubei (grant No. 2017CFB171).

## Supplementary Materials

Figure S1: experimental protocol in vitro. The BV2 cell was cultured and treated with resveratrol or EX527 for 24 h, followed by treatment of control gas or LPS and 4% sevoflurane for 6 h. After exposure, conditioned medium was collected for primary neuron study, and tissue was collected for biochemistry study. After the 7-day culture, primary neuron was incubated with four corresponding groups of conditioned medium for 24 h. Tissue was collected for biochemistry study after exposure. Figure S2: EX527 weakened the effect of resveratrol in reducing LPS+sevoflurane-induced ac-NF-$\kappa$B and proinflammatory cytokine expression in BV2 cell lines. (a) Representative immunoblot bands of SIRT1, ac-NF-$\kappa$B, and IL-6 expression in BV2 cell lines. (b)–(d) The corresponding densitometry analysis of SIRT1, ac-NF-$\kappa$B, and IL-6 expression normalized to $\beta$-actin. Data are presented as the mean ± SD. $n = 6$ per group. Figure S3: EX527 weakened the effect of resveratrol in decreasing the LPS +sevoflurane-conditioned medium-induced tau acetylation and tau phosphorylation in primary hippocampal neurons. (a)–(d) Representative immunoblot bands and the corresponding densitometry analysis of SIRT1, ac-tau (k280), ac-tau (k686) expression normalized to $\beta$-actin, and p-tau (AT8) expression normalized to total tau. Data are presented as the mean ± SD. $n = 6$ per group. *(Supplementary Materials)*

## References

[1] C. D. Hanning, "Postoperative cognitive dysfunction," *British Journal of Anaesthesia*, vol. 95, no. 1, pp. 82–87, 2005.

[2] M. Lewis, P. Maruff, and B. Silbert, "Statistical and conceptual issues in defining post-operative cognitive dysfunction," *Neuroscience & Biobehavioral Reviews*, vol. 28, no. 4, pp. 433–440, 2004.

[3] J. T. Moller, P. Cluitmans, L. S. Rasmussen et al., "Long-term postoperative cognitive dysfunction in the elderly: ISPOCD1 study," *The Lancet*, vol. 351, no. 9106, pp. 857–861, 1998.

[4] T. G. Monk, B. C. Weldon, C. W. Garvan et al., "Predictors of cognitive dysfunction after major noncardiac surgery," *Anesthesiology*, vol. 108, no. 1, pp. 18–30, 2008.

[5] J. Steinmetz, K. B. Christensen, T. Lund, N. Lohse, L. S. Rasmussen, and the ISPOCD Group, "Long-term consequences of postoperative cognitive dysfunction," *Anesthesiology*, vol. 110, no. 3, pp. 548–555, 2009.

[6] C. Li, S. Liu, Y. Xing, and F. Tao, "The role of hippocampal tau protein phosphorylation in isoflurane-induced cognitive dysfunction in transgenic APP695 mice," *Anesthesia & Analgesia*, vol. 119, no. 2, pp. 413–419, 2014.

[7] H. Le Freche, J. Brouillette, F.-J. Fernandez-Gomez et al., "Tau phosphorylation and sevoflurane anesthesia: an association to postoperative cognitive impairment," *Anesthesiology*, vol. 116, no. 4, pp. 779–787, 2012.

[8] Z. Xie and R. E. Tanzi, "Alzheimer's disease and post-operative cognitive dysfunction," *Experimental Gerontology*, vol. 41, no. 4, pp. 346–359, 2006.

[9] X. Luo, L. Yang, X. Chen, and S. Li, "Tau hyperphosphorylation: a downstream effector of isoflurane-induced neuroinflammation in aged rodents," *Medical Hypotheses*, vol. 82, no. 1, pp. 94–96, 2014.

[10] L. Evered, B. Silbert, D. A. Scott, D. Ames, P. Maruff, and K. Blennow, "Cerebrospinal fluid biomarker for Alzheimer disease predicts postoperative cognitive dysfunction," *Anesthesiology*, vol. 124, no. 2, pp. 353–361, 2016.

[11] E. L. Cunningham, B. McGuinness, D. F. McAuley et al., "CSF beta-amyloid 1-42 concentration predicts delirium following elective arthroplasty surgery in an observational cohort study," *Annals of Surgery*, vol. 269, no. 6, pp. 1200–1205, 2019.

[12] Z. Xie, S. McAuliffe, C. A. Swain et al., "Cerebrospinal fluid A$\beta$ to tau ratio and postoperative cognitive change," *Annals of Surgery*, vol. 258, no. 2, pp. 364–369, 2013.

[13] L. Evered, B. Silbert, D. A. Scott, H. Zetterberg, and K. Blennow, "Association of changes in plasma neurofilament light and tau levels with anesthesia and Surgery," *JAMA Neurology*, vol. 75, no. 5, pp. 542–547, 2018.

[14] C. P. Casey, H. Lindroth, R. Mohanty et al., "Postoperative delirium is associated with increased plasma neurofilament light," *Brain*, vol. 143, no. 1, pp. 47–54, 2020.

[15] B. Zhang, M. Tian, H. Zheng et al., "Effects of anesthetic isoflurane and desflurane on human cerebrospinal fluid A$\beta$ and $\tau$ level," *Anesthesiology*, vol. 119, no. 1, pp. 52–60, 2013.

[16] Y. Wan, J. Xu, F. Meng et al., "Cognitive decline following major surgery is associated with gliosis, $\beta$-amyloid accumulation, and $\tau$ phosphorylation in old mice," *Critical Care Medicine*, vol. 38, no. 11, pp. 2190–2198, 2010.

[17] X. Run, Z. Liang, L. Zhang, K. Iqbal, I. Grundke-Iqbal, and C.-X. Gong, "Anesthesia induces phosphorylation of tau," *Journal of Alzheimer's Disease*, vol. 16, no. 3, pp. 619–626, 2009.

[18] Y. Wang and E. Mandelkow, "Tau in physiology and pathology," *Nature Reviews Neuroscience*, vol. 17, no. 1, pp. 22–35, 2016.

[19] C. Tapia-Rojas, F. Cabezas-Opazo, C. A. Deaton, E. H. Vergara, G. V. W. Johnson, and R. A. Quintanilla, "It's all about tau," *Progress in Neurobiology*, vol. 175, pp. 54–76, 2019.

[20] S.-W. Min, X. Chen, T. E. Tracy et al., "Critical role of acetylation in tau-mediated neurodegeneration and cognitive deficits," *Nature Medicine*, vol. 21, no. 10, pp. 1154–1162, 2015.

[21] S.-W. Min, S.-H. Cho, Y. Zhou et al., "Acetylation of tau inhibits its degradation and contributes to tauopathy," *Neuron*, vol. 67, no. 6, pp. 953–966, 2010.

[22] T. E. Tracy, P. D. Sohn, S. S. Minami et al., "Acetylated tau obstructs KIBRA-mediated signaling in synaptic plasticity and promotes tauopathy-related memory loss," *Neuron*, vol. 90, no. 2, pp. 245–260, 2016.

[23] D. J. Irwin, T. J. Cohen, M. Grossman et al., "Acetylated tau, a novel pathological signature in Alzheimer's disease and other tauopathies," *Brain*, vol. 135, Part 3, pp. 807–818, 2012.

[24] P. D. Sohn, T. E. Tracy, H.-I. Son et al., "Acetylated tau destabilizes the cytoskeleton in the axon initial segment and is mislocalized to the somatodendritic compartment," *Molecular Neurodegeneration*, vol. 11, no. 1, p. 47, 2016.

[25] J. Yan, A. Luo, J. Gao et al., "The role of SIRT1 in neuroinflammation and cognitive dysfunction in aged rats after anesthesia and surgery," *American Journal of Translational Research*, vol. 11, no. 3, pp. 1555–1568, 2019.

[26] M. H. Keylor, B. S. Matsuura, and C. R. Stephenson, "Chemistry and biology of resveratrol-derived natural products," *Chemical Reviews*, vol. 115, no. 17, pp. 8976–9027, 2015.

[27] A. P. Singh, R. Singh, S. S. Verma et al., "Health benefits of resveratrol: evidence from clinical studies," *Medicinal Research Reviews*, vol. 35, pp. 1851–1891, 2019.

[28] H. Jeong, D. E. Cohen, L. Cui et al., "Sirt1 mediates neuroprotection from mutant huntingtin by activation of the TORC1 and CREB transcriptional pathway," *Nature Medicine*, vol. 18, no. 1, pp. 159–165, 2012.

[29] M. Jiang, J. Wang, J. Fu et al., "Neuroprotective role of Sirt1 in mammalian models of Huntington's disease through activation of multiple Sirt1 targets," *Nature Medicine*, vol. 18, no. 1, pp. 153–158, 2012.

[30] B. A. Q. Gomes, J. P. B. Silva, C. F. R. Romeiro et al., "Neuroprotective mechanisms of resveratrol in Alzheimer's disease: role of SIRT1," *Oxidative Medicine and Cellular Longevity*, vol. 2018, Article ID 8152373, 15 pages, 2018.

[31] K. B. Koronowski, K. R. Dave, I. Saul et al., "Resveratrol preconditioning induces a novel extended window of ischemic tolerance in the mouse brain," *Stroke*, vol. 46, no. 8, pp. 2293–2298, 2015.

[32] D. Della-Morte, K. R. Dave, R. A. DeFazio, Y. C. Bao, A. P. Raval, and M. A. Perez-Pinzon, "Resveratrol pretreatment protects rat brain from cerebral ischemic damage via a sirtuin 1-uncoupling protein 2 pathway," *Neuroscience*, vol. 159, no. 3, pp. 993–1002, 2009.

[33] F. Wang, N. Cui, L. Yang et al., "Resveratrol rescues the impairments of hippocampal neurons stimulated by microglial over-activation in vitro," *Cellular and Molecular Neurobiology*, vol. 35, no. 7, pp. 1003–1015, 2015.

[34] X. Zhang, H. Dong, N. Li et al., "Activated brain mast cells contribute to postoperative cognitive dysfunction by evoking microglia activation and neuronal apoptosis," *Journal of Neuroinflammation*, vol. 13, no. 1, p. 127, 2016.

[35] S.-Y. Li, L.-X. Xia, Y.-L. Zhao et al., "Minocycline mitigates isoflurane-induced cognitive impairment in aged rats," *Brain Research*, vol. 1496, pp. 84–93, 2013.

[36] X. Tang, Y. Zhao, Z. Zhou et al., "Resveratrol mitigates sevoflurane-induced neurotoxicity by the SIRT1-dependent regulation of BDNF expression in developing mice," *Oxidative Medicine and Cellular Longevity*, vol. 2020, Article ID 9018624, 18 pages, 2020.

[37] L. Tan, X. Chen, W. Wang et al., "Pharmacological inhibition of PTEN attenuates cognitive deficits caused by neonatal repeated exposures to isoflurane via inhibition of NR2B-mediated tau phosphorylation in rats," *Neuropharmacology*, vol. 114, pp. 135–145, 2017.

[38] S. Newman, J. Stygall, S. Hirani, S. Shaefi, and M. Maze, "Postoperative cognitive dysfunction after noncardiac surgery: a systematic review," *Anesthesiology*, vol. 106, no. 3, pp. 572–590, 2007.

[39] M. Cibelli, A. R. Fidalgo, N. Terrando et al., "Role of interleukin-1beta in postoperative cognitive dysfunction," *Annals of Neurology*, vol. 68, no. 3, pp. 360–368, 2010.

[40] J. Hu, X. Feng, M. Valdearcos et al., "Interleukin-6 is both necessary and sufficient to produce perioperative neurocognitive disorder in mice," *British Journal of Anaesthesia*, vol. 120, no. 3, pp. 537–545, 2018.

[41] I. B. Hovens, R. G. Schoemaker, E. A. van der Zee, A. R. Absalom, E. Heineman, and B. L. van Leeuwen, "Postoperative cognitive dysfunction: Involvement of neuroinflammation and neuronal functioning," *Brain, Behavior, and Immunity*, vol. 38, pp. 202–210, 2014.

[42] H. A. Rosczyk, N. L. Sparkman, and R. W. Johnson, "Neuroinflammation and cognitive function in aged mice following minor surgery," *Experimental Gerontology*, vol. 43, no. 9, pp. 840–846, 2008.

[43] N. Terrando, C. Monaco, D. Ma, B. M. J. Foxwell, M. Feldmann, and M. Maze, "Tumor necrosis factor-alpha triggers a cytokine cascade yielding postoperative cognitive decline," *Proceedings of the National Academy of Sciences*, vol. 107, no. 47, pp. 20518–20522, 2010.

[44] M. G. Spillantini and M. Goedert, "Tau pathology and neurodegeneration," *The Lancet Neurology*, vol. 12, no. 6, pp. 609–622, 2013.

[45] K. Iqbal, F. Liu, and C. X. Gong, "Tau and neurodegenerative disease: the story so far," *Nature Reviews Neurology*, vol. 12, no. 1, pp. 15–27, 2016.

[46] W. Liu, J. Xu, H. Wang et al., "Isoflurane-induced spatial memory impairment by a mechanism independent of amyloid-beta levels and tau protein phosphorylation changes in aged rats," *Neurological Research*, vol. 34, no. 1, pp. 3–10, 2012.

[47] C. Huang, J. M. Chu, Y. Liu, R. C. Chang, and G. T. Wong, "Varenicline reduces DNA damage, tau mislocalization and post surgical cognitive impairment in aged mice," *Neuropharmacology*, vol. 143, pp. 217–227, 2018.

[48] Y. Dong, X. Wu, Z. Xu, Y. Zhang, and Z. Xie, "Anesthetic isoflurane increases phosphorylated tau levels mediated by caspase activation and Abeta generation," *PLoS One*, vol. 7, no. 6, article e39386, 2012.

[49] S.-W. Min, P. D. Sohn, Y. Li et al., "SIRT1 deacetylates tau and reduces pathogenic tau spread in a mouse model of tauopathy," *The Journal of Neuroscience*, vol. 38, no. 15, pp. 3680–3688, 2018.

[50] T. J. Cohen, J. L. Guo, D. E. Hurtado et al., "The acetylation of tau inhibits its function and promotes pathological tau aggregation," *Nature Communications*, vol. 2, p. 252, 2011.

[51] A. Z. Herskovits and L. Guarente, "SIRT1 in neurodevelopment and brain senescence," *Neuron*, vol. 81, no. 3, pp. 471–483, 2014.

[52] J. Gao, W. Y. Wang, Y. W. Mao et al., "A novel pathway regulates memory and plasticity via SIRT1 and miR-134," *Nature*, vol. 466, no. 7310, pp. 1105–1109, 2010.

[53] I. B. Hovens, R. G. Schoemaker, E. A. van der Zee, E. Heineman, G. J. Izaks, and B. L. van Leeuwen, "Thinking through postoperative cognitive dysfunction: how to bridge the gap between clinical and pre-clinical perspectives," *Brain, Behavior, and Immunity*, vol. 26, no. 7, pp. 1169–1179, 2012.

[54] A. Alam, Z. Hana, Z. Jin, K. C. Suen, and D. Ma, "Surgery, neuroinflammation and cognitive impairment," *EBioMedicine*, vol. 37, pp. 547–556, 2018.

[55] A. L. Luo, J. Yan, X. L. Tang, Y. L. Zhao, B. Y. Zhou, and S. Y. Li, "Postoperative cognitive dysfunction in the aged: the collision of neuroinflammaging with perioperative neuroinflammation," *Inflammopharmacology*, vol. 27, no. 1, pp. 27–37, 2019.

[56] D. R. Skvarc, M. Berk, L. K. Byrne et al., "Post-operative cognitive dysfunction: an exploration of the inflammatory hypothesis and novel therapies," *Neuroscience & Biobehavioral Reviews*, vol. 84, pp. 116–133, 2018.

[57] H.-J. He, Y. Wang, Y. Le et al., "Surgery upregulates high mobility group box-1 and disrupts the blood-brain barrier causing cognitive dysfunction in aged rats," *CNS Neuroscience & Therapeutics*, vol. 18, no. 12, pp. 994–1002, 2012.

[58] S.-H. Cho, J. A. Chen, F. Sayed et al., "SIRT1 deficiency in microglia contributes to cognitive decline in aging and neurodegeneration via epigenetic regulation of IL-1$\beta$," *The Journal of Neuroscience*, vol. 35, no. 2, pp. 807–818, 2015.

[59] S. Michan, Y. Li, M. M.-H. Chou et al., "SIRT1 is essential for normal cognitive function and synaptic plasticity," *Journal of Neuroscience*, vol. 30, no. 29, pp. 9695–9707, 2010.

[60] R. Velagapudi, A. El-Bakoush, I. Lepiarz, F. Ogunrinade, and O. A. Olajide, "AMPK and SIRT1 activation contribute to inhibition of neuroinflammation by thymoquinone in BV2 microglia," *Molecular and Cellular Biochemistry*, vol. 435, no. 1-2, pp. 149–162, 2017.

[61] J. W. Hwang, H. Yao, S. Caito, I. K. Sundar, and I. Rahman, "Redox regulation of SIRT1 in inflammation and cellular senescence," *Free Radical Biology and Medicine*, vol. 61, pp. 95–110, 2013.

[62] L.-L. Qiu, M.-H. Ji, H. Zhang et al., "NADPH oxidase 2-derived reactive oxygen species in the hippocampus might contribute to microglial activation in postoperative cognitive dysfunction in aged mice," *Brain, Behavior, and Immunity*, vol. 51, pp. 109–118, 2016.

[63] P. Wei, F. Yang, Q. Zheng, W. Tang, and J. Li, "The potential role of the NLRP3 inflammasome activation as a link between mitochondria ROS generation and neuroinflammation in postoperative cognitive dysfunction," *Frontiers in Cellular Neuroscience*, vol. 13, p. 73, 2019.

[64] J.-S. Ye, L. Chen, Y.-Y. Lu, S.-Q. Lei, M. Peng, and Z.-Y. Xia, "Honokiol-mediated mitophagy ameliorates postoperative cognitive impairment induced by surgery/sevoflurane via inhibiting the activation of NLRP3 inflammasome in the hippocampus," *Oxidative Medicine and Cellular Longevity*, vol. 2019, Article ID 8639618, 13 pages, 2019.

[65] N. Pomara, D. Bruno, A. S. Sarreal et al., "Lower CSF amyloid beta peptides and higher F2-isoprostanes in cognitively intact elderly individuals with major depressive disorder," *American Journal of Psychiatry*, vol. 169, no. 5, pp. 523–530, 2012.

[66] Z. Xia, D. V. Godin, and D. M. Ansley, "Propofol enhances ischemic tolerance of middle-aged rat hearts: effects on 15-F2t-isoprostane formation and tissue antioxidant capacity," *Cardiovascular Research*, vol. 59, no. 1, pp. 113–121, 2003.

[67] A. V. Witte, L. Kerti, D. S. Margulies, and A. Floel, "Effects of resveratrol on memory performance, hippocampal functional connectivity, and glucose metabolism in healthy older adults," *Journal of Neuroscience*, vol. 34, no. 23, pp. 7862–7870, 2014.

[68] G. T. Diaz-Gerevini, G. Repossi, A. Dain, M. C. Tarres, U. N. Das, and A. R. Eynard, "Beneficial action of resveratrol: how and why?," *Nutrition*, vol. 32, no. 2, pp. 174–178, 2016.

[69] J. A. Baur and D. A. Sinclair, "Therapeutic potential of resveratrol: the _in vivo_ evidence," *Nature Reviews Drug Discovery*, vol. 5, no. 6, pp. 493–506, 2006.

[70] C. Lu, Y. Guo, J. Yan et al., "Design, synthesis, and evaluation of multitarget-directed resveratrol derivatives for the treatment of Alzheimer's disease," *Journal of Medicinal Chemistry*, vol. 56, no. 14, pp. 5843–5859, 2013.

Hindawi
Oxidative Medicine and Cellular Longevity
Volume 2020, Article ID 7635291, 11 pages
https://doi.org/10.1155/2020/7635291

*Research Article*

# Botanical Drug Puerarin Promotes Neuronal Survival and Neurite Outgrowth against MPTP/MPP$^+$-Induced Toxicity via Progesterone Receptor Signaling

**Yingke Zhao,[1] Jia Zhao,[1,2] Xiuying Zhang,[1] Yuanyuan Cheng,[1] Dan Luo,[1] Simon Ming-Yuen Lee,[3] Lixing Lao,[1,2] and Jianhui Rong[1,4]**

[1]*School of Chinese Medicine, Li Ka Shing Faculty of Medicine, The University of Hong Kong, Pokfulam, Hong Kong*
[2]*Department of Chinese Medicine, The University of Hong Kong Shenzhen Hospital, Shenzhen, China*
[3]*State Key Laboratory of Quality Research in Chinese Medicine, Institute of Chinese Medical Sciences, University of Macau, Macau, China*
[4]*The University of Hong Kong Shenzhen Institute of Research and Innovation (HKU-SIRI), Shenzhen, China*

Correspondence should be addressed to Jianhui Rong; jrong@hkucc.hku.hk

Received 3 July 2020; Revised 29 August 2020; Accepted 20 September 2020; Published 17 October 2020

Academic Editor: Shi Yuan Xu



*Background*. Progesterone receptor (PR) modulates neuroprotective and regenerative responses in Parkinson's disease and related neurological diseases. *Objectives*. The present study was designed to determine whether botanical drug puerarin could exhibit neuroprotective and neurorestorative activities via PR signaling. *Methods*. The neuroprotective and neurotrophic activities of puerarin were investigated in MPTP-lesioned mice and MPP$^+$-challenged primary rat midbrain neurons. Rotarod performance test and tail suspension test were used to assess motor functions. Tyrosine hydroxylase (TH) and PR were determined by immunostaining, Western blotting, and luciferase reporter assays. Neurite outgrowth was assessed by fluorescence staining and immunostaining. *Results*. Puerarin effectively ameliorated the MPTP-induced motor abnormalities in MPTP-lesioned mice and protected primary rat midbrain neurons against MPP$^+$-induced toxicity via PR signaling although progesterone exhibited the neuroprotection. PR antagonist mifepristone (RU486) diminished the neuroprotection of puerarin in MPTP-lesioned mice and MPP$^+$-induced primary rat midbrain neurons. Moreover, puerarin promoted the differentiation of primary rat midbrain neurons and potentiated NGF to induce neuritogenesis in PC12 cells. RU486 and PR-siRNA could inhibit the effect of puerarin. Puerarin and progesterone could enhance the PR promoter. *Conclusion*. Puerarin attenuated MPTP- and MPP$^+$-induced toxicity and potentiated neurite outgrowth via PR. These results suggested that puerarin may become an alternative hormone for suppressing MPTP- and MPP$^+$-induced toxicity in neurodegenerative diseases.

## 1. Introduction

Parkinson's disease (PD) is the second most common neurodegenerative disease worldwide and characterized by motor dysfunctions (e.g., tremor, rigidity, and dyskinesia) as well as some other nonmotor symptoms (e.g., cognition deficit and depression) [1]. The pathological change in PD patients is hallmarked by the progressive loss of dopaminergic neurons in substantia nigra compacta (SNpc) [2]. Levodopa is a commonly accepted drug for the treatment of PD although the unavoidable side effects and instability are documented after long-term use [3]. Therefore, it is pressingly needed to discover new neuroprotective and neuroregenerative small molecules to meet the clinical demand.

Clinical evidence shows that men suffer from higher prevalence and incidence of PD than women, suggesting the neuroprotective role of sex hormones in the brain [4, 5]. Estrogens (e.g., 17$\beta$-estradiol and estradiol) showed neuroprotective potential to diminish the nigrostriatal degeneration in mouse model of PD [6, 7]. However, the feminizing effects of estrogens limit its medical use in the treatment of PD. On the other hand, progesterone is free of feminizing

effects and could be available for both men and women [4]. Although progesterone is classically recognized as an endogenous steroid from ovary, Pomata et al. found that progesterone could be synthesized from cholesterol in the central nervous system [8]. Several studies showed that progesterone played the neuromodulatory and neuroprotective roles in PD [9, 10]. Presumably, progesterone exhibits neuroprotective effects via interacting progesterone receptor (PR) [11]. PR exists in two isoforms: PR-A and PR-B, which are transcribed from two different promoter regions of single gene and expressed in the brain [12]. PR-B is a stronger transcriptional activator compared with PR-A [13]. Interestingly, PRs are recognized as therapeutic target for the control of neurodegeneration [14].

Herbal medicines are well documented for the chemical compositions of stilbenoids, flavonoids, catechols, and terpenes and the potential activities against neurodegeneration [15, 16]. Puerarin (Figure 1(a)) is a unique C-glycosylated isoflavone from the herb *Radix Puerariae lobatae* [17]. We previously demonstrated that puerarin markedly reduced neurotoxicity of 6-hydroxydopamine (6-OHDA) and MPTP, *in vitro* and *in vivo*, respectively [18, 19]. As far as the mechanism is concerned, puerarin might mimic estrogen to protect the nigral neurons from apoptosis [20, 21]. On the other hand, puerarin could recover the decrease in progesterone levels in rats that suffered from chronic stress and post-traumatic stress disorder [22, 23]. Puerarin disrupted the implantation of the rat uterus by inhibiting PR [24]. Thus, the present study was designed to determine whether puerarin could exhibit neuroprotective and neurorestorative activities via PR signaling.

## 2. Materials and Methods

*2.1. Biochemical Reagents.* Antibody against tyrosine hydroxylase (TH) was purchased from Merck Millipore (Billerica, MA, USA). Antibodies against GAPDH and Alexa Fluor 594-conjugate anti-rabbit IgG antibody were purchased from Cell Signaling Technology (Boston, BA, USA). Mouse antigrowth-associated protein 43 (GAP43) antibody and rabbit anti-PR antibody were purchased from Santa Cruz Biotechnology Inc. (Santa Cruz, CA, USA). Protein assay dye reagent concentrate was purchased from Bio-Rad Labs (Hercules, CA, USA). Enhanced chemiluminescence (ECL) detection reagent was purchased from GE Healthcare (Uppsala, Sweden). 3,3-N-diaminobenzidine tetrahydrochloride (DAB) substrate kit was obtained from Dako Corporation (Carpintera, CA, USA). PR siRNA, HiPerFect transfection reagent, and Effectene Transfection Reagent were purchased from Qiagen (Hilden, Germany). The luciferase reporter vectors (i.e., 2xPRE-TK-Luc) were obtained from Addgene (Cambridge, MA, USA). pRL-TK vector encoding Renilla luciferase and dual-luciferase reporter assay system was purchased from Promega (Madison, USA). The neurite outgrowth staining kit was purchased from Invitrogen (Carlsbad, CA, USA). HRP-conjugated anti-rabbit IgG secondary antibody, MPTP, $MPP^+$ iodide, NGF-2.5S, Hoechst 33342, and propidium iodide (PI) were purchased from Sigma-Aldrich (St. Louis, MO, USA). Puerarin and RU486 (mifepristone) were purchased from Yick-Vic Chemicals & Pharmaceuticals (Shatin, Hong Kong).

*2.2. Animals and Drug Treatment.* The experimental procedures were approved by the Committee on the Use of Live Animal in Teaching and Research (CULATR No. 4046-16), University of Hong Kong. The animal experiments were outlined in Figure 1(b). C57BL/6N male mice (7-8 weeks old, 21-25 g) were provided by the Laboratory Animal Unit on the campus and housed under a controlled temperature (25 ± 2°C) and humidity (55 ± 10%) condition in a 12-12 h light/dark cycle at the animal unit. For drug treatment, puerarin and progesterone were dissolved in saline containing 50% 1,2-propylene glycol, and the solutions were sterilized via 0.22 $\mu$m filters from Pall Corporate (Port Washington, NY, USA). Prior to use, RU486 was freshly prepared in saline containing 1% Tween-80 with 30-second sonication, while MPTP was dissolved in saline. Following the regulation of the university safety office, when MPTP was used, mice were isolated in carcinogen suite for additional 3 days after the final treatment. Thereafter, mice were moved to the conventional facility for behavioral tests and bioassays.

*2.3. Animal Experimental Design.* The doses and delivery of different drugs were decided based on previous publications [9, 18, 25]. Briefly, mice were firstly randomly divided into five groups ($n = 10$): control, MPTP, MPTP+Puerarin, MPTP+Progesterone, and MPTP+Puerarin+RU486. Mice were treated with MPTP (25 mg/kg/day via intraperitoneal injection for 7 days while animals in the control group were injected the equal volume of saline. At the time point of 4 hours prior to daily MPTP injection, puerarin (120 mg/kg/day) or progesterone (8 mg/kg/day) was administered to the mice in the indicated group via oral gavage, while mice in the control and MPTP groups were injected the same volume of vehicle. For RU486 administration, mice were intraperitoneally injected with RU486 (3 mg/kg/day) or vehicle at 30 min prior to puerarin treatment for 7 days.

*2.4. Rotarod Performance Test.* Mice were evaluated for motor impairments with a rotarod apparatus (Harvard apparatus, Holliston, MA, USA) as described [26, 27]. In brief, at 3 days after last dosage of MPTP treatment, mice were subjected to behavioral assessments. On the day for behavioral tests, animals were firstly pretrained for 3 sessions prior to the assessment and placed on the lane (constant 15 rpm) for 5 min. The dropping time was automatically recorded for each mouse. Three independent tests were performed with each mouse at 1 h intervals.

*2.5. Tail Suspension Test.* Tail suspension test was carried out at 4 hours after rotarod test as described [26]. Briefly, mice were suspended by fixing the tail to the pole with adhesive tape. The distance between the mouse's nose and the bottom was 20-25 cm, and the test time was 6 min. Mice were monitored by video during the process, while the results were analyzed by the observers after the behavior tests. The immobility time of each mouse within 6 min was measured for assessing the motor functions.

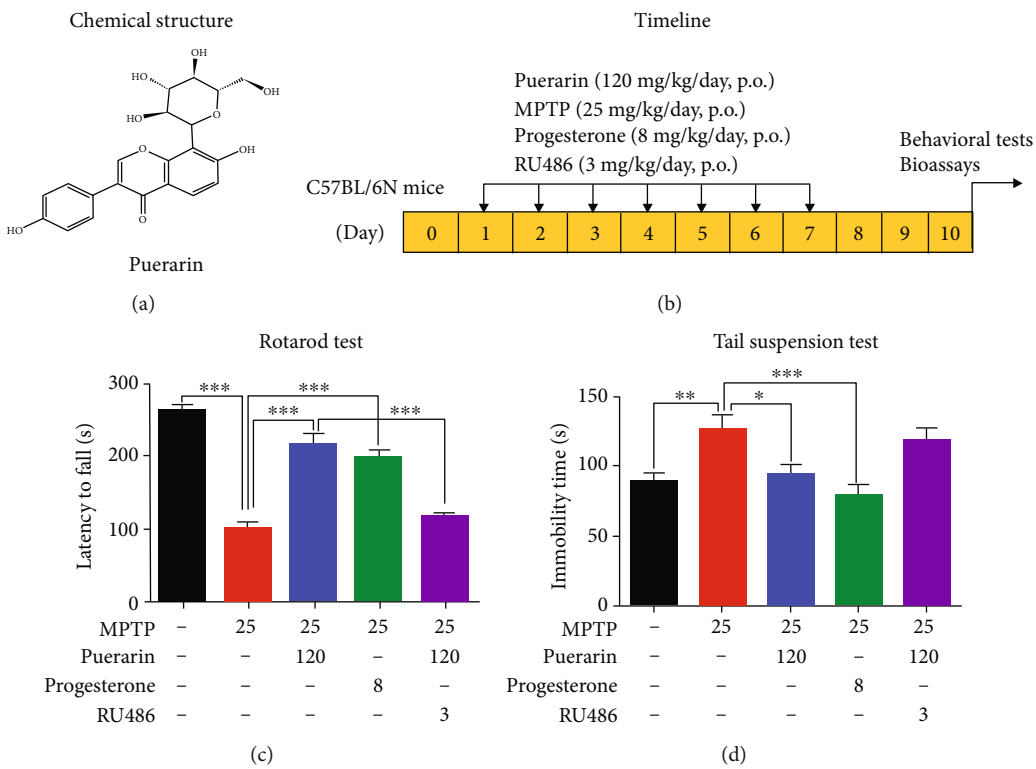


Figure 1: Puerarin ameliorated behavioral impairments in MPTP-lesioned mice. (a) Chemical structure of puerarin. Chemical structure was generated by ChemSketch (http://www.acdlabs.com/home/). (b) Design for animal experiments. C57BL/6N mice were randomly divided into five groups: control, MPTP, MPTP+Puerarin, MPTP+Progesterone, and MPTP+Puerarin+RU486. Following treatments, the mice were assessed for behavioral impairments and biomarker expression. (c) Rotarod performance test. Animals were evaluated for the riding time. (d) Tail suspension test. Animals were assessed for the immobility time. The results of behavioral tests were presented as mean ± SEM ($n = 10$) and analyzed by one-way ANOVA followed by Dunnett's test. $^{*}p < 0.05$, $^{**}p < 0.01$, $^{***}p < 0.001$.

*2.6. Immunohistochemistry Staining.* The expression of TH in the midbrain was detected by immunohistochemical staining as previously described [27]. In brief, mice were transcardially perfused sequentially with saline and 4% paraformaldehyde under anesthetic condition. The brains were collected and fixed in 4% paraformaldehyde overnight at 4°C. Following immersed in a 30% sucrose containing 4% paraformaldehyde, the brains were embedded in Tissue-Tek O.C.T. Compound (Sakura, USA) and stored at -80°C. The cryosections were cut into serial coronal sections at a thickness of 30 $\mu$m on a freezing microtome (Model CM-1850, Leica, Germany). After thawed at room temperature for 1 hour, the cryostat sections were heated in antigen retrieval buffer, immersed in 3% hydrogen peroxide solution to quench the endogenous peroxidase, and subsequently blocked with 5% goat serum to avoid nonspecific staining. For TH detection, the brain sections were probed with anti-TH primary antibody overnight at 4°C. After excessive wash, the bound antibodies were detected with HRP-conjugated goat anti-rabbit secondary antibody for 1 hour at room temperature. The horseradish peroxidase was then assayed with 3,3-N-diaminobenzidine tetrahydrochloride (DAB) substrate kit from Dako (Carpintera, CA, USA). The slices were counterstained with hematoxylin and imaged under an Olympus microscope (Olympus Corp, Tokyo, Japan). The number of $TH^{+}$ neurons in each section was counted within three nonoverlapping views at tenfold magnification.

*2.7. Western Blotting Analysis.* The expression of indicated biomarkers was examined by Western blotting as described [26]. Briefly, midbrain tissues, primary midbrain neurons, and PC12 cells were lysed in RIPA buffer containing 1x protease inhibitor cocktail. The proteins were recovered by centrifugation at 13,000 rpm for 15 min at 4°C. The concentration of proteins was determined with the protein assay dye reagent from Bio-Rad (Hercules, CA, USA). Proteins (70 $\mu$g for tissue, 30 $\mu$g for cells) were resolved on 10% SDS-polyacrylamide gels and transferred onto PVDF membranes. After 2-hour incubation in 5% BSA in Tris buffer containing 1% Tween-20 (TBS-T), the membranes were incubated with primary antibodies overnight at 4°C and then detected with HRP-conjugated goat anti-rabbit IgG secondary antibodies for another 3 hour at 4°C. The blots were visualized with Amersham™ ECT™ detection reagent from GE Healthcare (Uppsala, Sweden).

*2.8. PC12 Cell Culture.* Rat pheochromocytoma PC12 cell line was obtained from American Type Culture Collection (Manassas, VA, USA) and cultured in Dulbecco's modified Eagle's medium (DMEM) containing 10% horse serum (HS), 5% fetal bovine serum (FBS), and 1% penicillin/streptomycin (Invitrogen, Carlsbad, CA, USA) in incubators with 37°C and 5% $CO_2$ atmosphere. For drug treatment, the cells were cultured to the density of 70-80% and subsequently treated with indicated drugs.

*2.9. Primary Culture of Rat Midbrain Neurons.* Primary rat midbrain neurons were isolated from 17-day-old Sprague-Dawley (SD) rat embryos as previously described [27]. Briefly, 1 day before the isolation of the midbrain neurons, 6-well plates were precoated with poly-D-lysine. The midbrain neurons were dissociated by using trypsin and DNase. After centrifugation, freshly isolated neurons were seeded onto six-well plates at a density of 5 or $8 \times 100000$ cells/ml and cultured in Neurobasal® medium containing 2% B27 supplement from Thermo Fisher Scientific Inc. (Waltham, MA, USA) for 3 or 7 days prior to drug treatment.

*2.10. Hoechst 33342/Propidium Iodide Staining.* Freshly isolated midbrain neurons were seeded on 6-well-plate at the density of $1 \times 10^6$ cells/well and cultured for 7 days. The neurons were treated with puerarin, progesterone, RU486, and $MPP^+$, alone or in combination for 24 h. To stain the dead cells, 5 $\mu$M Hoechst 33342 and 5 $\mu$M PI were added to each well. The neurons were visualized under a Zeiss fluorescence microscope from Carl Zeiss Company (Jena, Germany).

*2.11. Immunofluorescence Staining.* The expression of PR in the brains was examined by the immunofluorescence staining as previously described [5, 26, 28]. Following antigen retrieval, the slides were immersed in 0.5% Triton X-100 in PBS for 30 mins and blocked in 5% goat serum for 2 h. The sections were probed with polyclonal antibody against PR overnight at 4°C, washed with PBS for 3 times, and detected with Alexa Fluor 594-conjugated rabbit IgG secondary antibody. The cell nuclei were stained with $4'$-6-diamidino-2-phenylindole (DAPI) for 10 min. After the slides were mounted with coverslips, the images were then acquired under a Zeiss LSM 780 confocal microscopy from Carl-Zeiss Company (Jena, Germany) with 20x objective lens.

On the other hand, GAP43 was detected by immunostaining as previously described [29]. After the drug treatment with puerarin and RU486, alone or in combination for 48 h, the neurons were fixed in 4% paraformaldehyde, incubated in 0.5% Triton X-100 for 30 min to permeabilize the cells, and then blocked in 5% normal goat serum for 2 h at room temperature. The cells were then incubated with anti-GAP43 primary antibodies at 4°C overnight, and the bound antibodies were detected with Alexa Fluor 594 anti-rabbit IgG secondary antibody for 2 h at room temperature. After the cells were washed with PBS for three times, the cell nuclei were then stained with DAPI for 10 min. The fluorescence images were visualized under fluorescence microscope (Carl Zeiss, Jena, Germany). The neurite length of $GAP\text{-}43^+$ neurons was automatically detected by ImageJ software (http://imagej.nih.gov).

*2.12. siRNA-Mediated Silencing of PR Expression.* The expression of PR in PC12 cells was transiently silenced with PR-specific siRNAs as previously described [28]. Briefly, PC12 cells were grown on poly-L-lysine precoated coverslips and then transfected with specific siRNAs using HiPerFect Transfection Reagent according to the manufacturer's protocol. After 24 h incubation, the transfected cells were treated with puerarin and NGF, alone or in combination, for 72 h. The cells were then stained with neurite outgrowth staining kit and analyzed for PR expression by Western blotting with specific antibodies.

*2.13. Assay of Neurite Outgrowth.* Neurite outgrowth was assessed by commercial neurite outgrowth assay kit as described [18]. In practice, PC12 cells were transfected with specific siRNAs and subsequently treated with puerarin and NGF, alone or in combination, for 72 h. The cells were stained by neurite outgrowth assay kit according to the manufacture's instruction. The neurites were imaged under a Zeiss fluorescence microscope. The average length of neurites was determined by Image J software (https://imagej.nih.gov/ij/).

*2.14. Transfection and Luciferase Reporter Assays.* The promoter activities of PR were assayed using promoter-reporter system as previously described [30]. Briefly, PC12 cells were seeded in 96-well plates at the density of $1 \times 10^5$ cells/well, cultured to the cell density of 70-80% and transiently transfected with 0.1 $\mu$g 2xPRE-TK-Luc and 0.05 $\mu$g pRL-TK. The transfection was continued for 6 h using Transfectene (Qiagen) according to the manufacturer's instruction. At 24 h after transfection, the cells were treated with puerarin and progesterone for 24 h. The promoter activity was then assayed with the Dual-Luciferase Reporter System according to the manufacturer's protocol while the luciferase activity was monitored on a Clariostar microplate reader from BMG Labtech (Ortenberg, Germany). The results were expressed as luciferase activity after normalization to Renilla activity.

*2.15. Molecular Docking.* The crystal structure (PDB: 3D90) of human PR was downloaded from RCSB PDB website (http://www.rcsb.org/pdb). The chemical structures of the ligand molecules (i.e., puerarin and progesterone) were generated by the ChemBioDraw Ultra 12.0 software. The protein-ligand interactions were simulated by the AutoDock Vina in PyRx-virtual screen tool package. Prior to docking, all water molecules were removed from PR structure. The docking results were analyzed by the Discovery Studio Visualizer software.

*2.16. Statistical Analysis.* The results were represented as mean ± SEM for behavioral tests and mean ± SD for other experiments. The statistical significance was determined by one-way analysis of variance (ANOVA) followed by Dunnett's test with GraphPad Prism 6 (La Jolla, CA, USA). A $p$ value of $<0.05$ was considered as statistically significant.

## 3. Results

*3.1. Puerarin Ameliorated Behavioral Impairments in MPTP-Lesioned Mice.* To validate the *in vivo* neuroprotective activity of puerarin, we firstly employed rotarod performance test and tail suspension test to determine the effects of puerarin on the behavioral deficits in MPTP-treated mice. In practice, the animals were sequentially evaluated for motor disability by rotarod performance test and the stress response by tail suspension test while two tests were performed in a 4-hour

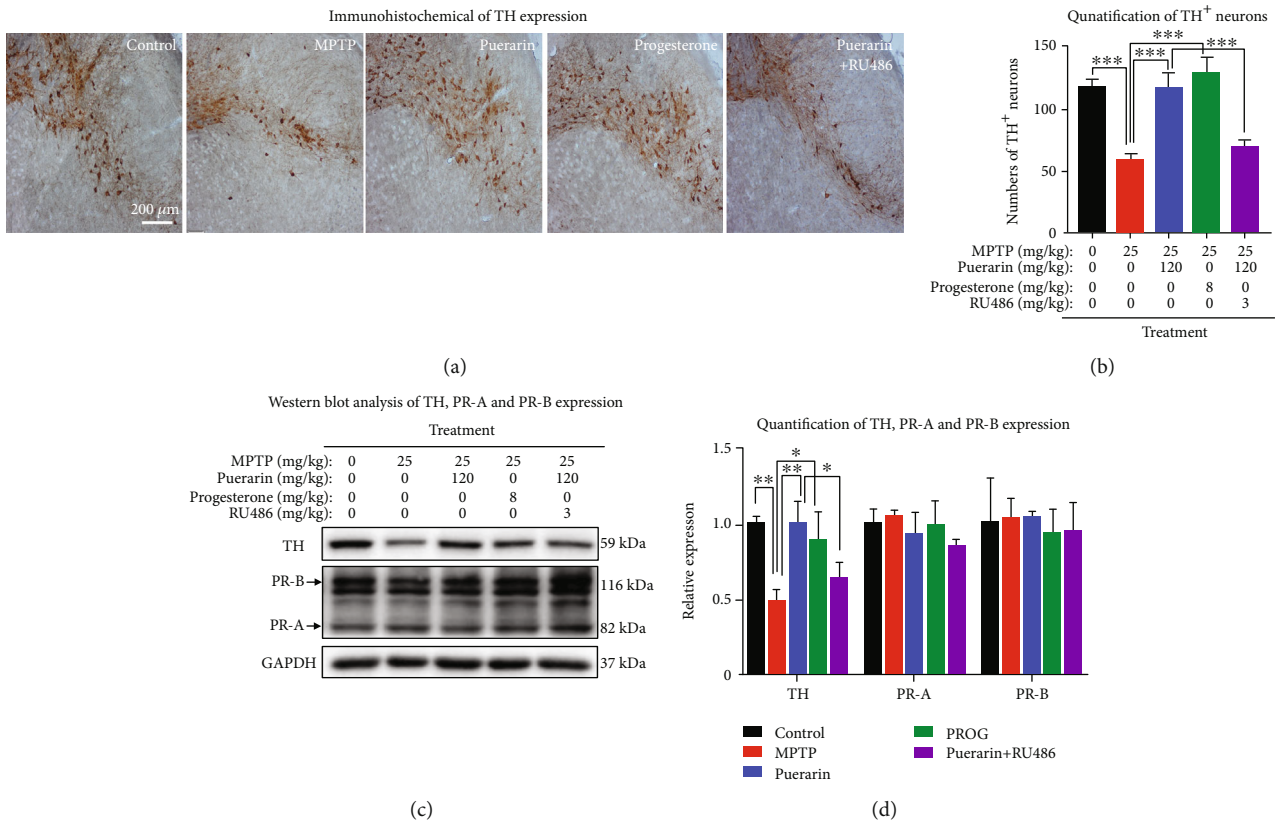


Figure 2: Puerarin protected dopaminergic neurons from MPTP-induced damage in mice. (a) Immunohistochemical staining of TH expression. The frozen brain sections were analyzed by immunohistochemical staining with anti-TH antibody. The images were captured under an Olympus microscope (Tokyo, Japan). (b) Quantification for $TH^+$ neurons. The number of $TH^+$ neurons in each group ($n = 3$) were counted. $^{***}p < 0.001$. (c) Western blot analysis of TH, PR-A, and PR-B expression. Midbrain tissues were collected and analyzed by Western blotting with antibodies against TH, PR-A, and PR-B, whereas GAPDH was analyzed as control. Representative blots for each group were shown. (d) Quantification of TH, PR-A, and PR-B expression. Western blots ($n = 3$) in (c) were determined by a densitometric method. $^{*}p < 0.05$, $^{**}p < 0.01$.

interval. As shown in Figure 1(c), MPTP reduced the time for mice to stay on the rod compared with control mice. Both puerarin and progesterone effectively helped mice to ride on the rotarod for longer time compared with untreated MPTP mice. PR inhibitor RU486 diminished the beneficial effects of puerarin in rotarod performance test. As shown in Figure 1(d), on the other hand, tail suspension test also confirmed that MPTP prolonged the immobility time of mice whereas puerarin and progesterone markedly reduced the immobility time of mice. RU486 reversed the beneficial effects of puerarin.

*3.2. Puerarin Enhanced the Survival of Dopaminergic Neurons against MPTP Neurotoxicity.* To evaluate the *in vivo* neuroprotective activity of puerarin, dopaminergic neurons was examined by detecting the expression of TH in MPTP-treated mice. As shown in Figures 2(a) and 2(b), MPTP dramatically reduced TH expression as the indicator for TH-positive dopaminergic neurons in SNpc, whereas both puerarin and progesterone effectively halted the loss of dopaminergic neuron. RU486 attenuated the beneficial effects of puerarin. On the other hand, the expression of TH was also assessed by Western blotting with specific antibody. The results in Figures 2(c) and 2(d) essentially verified the neuroprotective effects of puerarin on dopaminergic neurons against MPTP neurotoxicity and the inhibitory effects of RU486 on the activity of puerarin.

*3.3. Puerarin Did Not Change the Expression of PR in MPTP-Lesioned Mice.* To clarify why RU486 could antagonize puerarin, we employed Western blotting and fluorescence immunostaining techniques to determine the effect of puerarin on the expression of PR in the MPTP-treated mice. Western blotting results in Figures 2(c) and 2(d) did not show much difference in the levels of PR expression between different treatment groups. The immunofluorescence staining results in Figure 3 further confirmed that the levels of PR expression in the brain were not changed under the experimental conditions.

*3.4. Puerarin Exerted Neuroprotective Properties in Primary Midbrain Neurons.* To verify the *in vitro* neuroprotective activities of puerarin, we employed fluorescence dye PI to detect $MPP^+$-induced cell death in primary rat midbrain

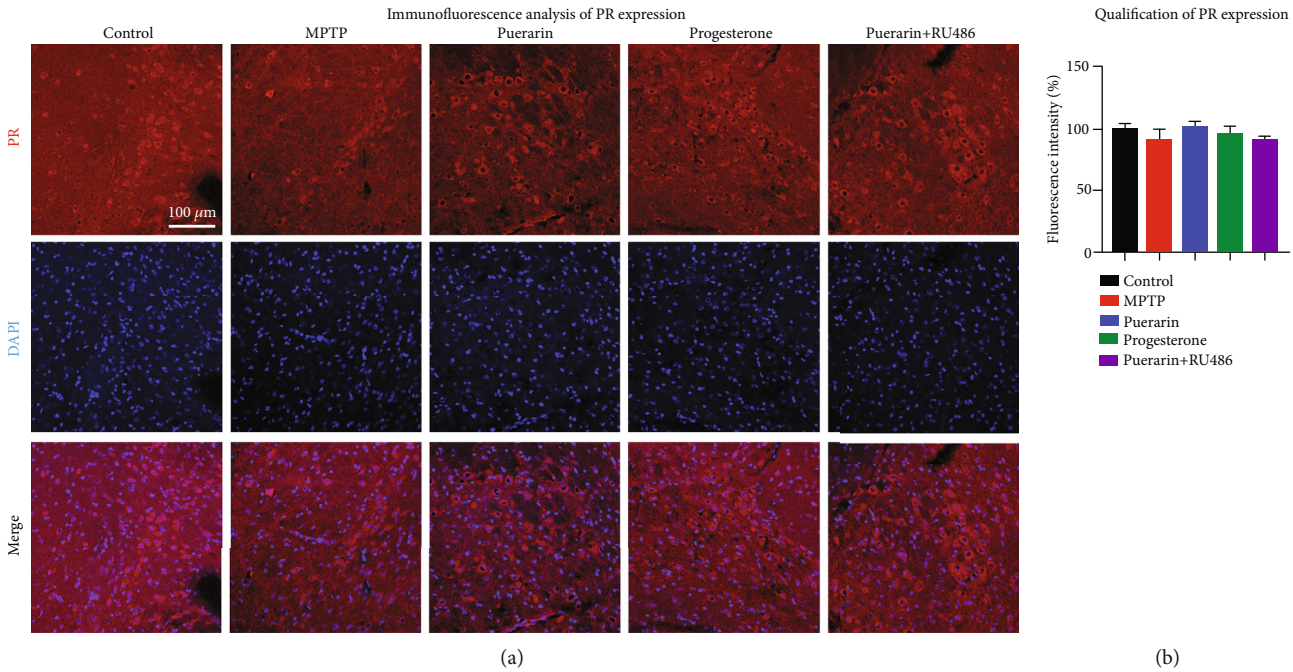


Figure 3: Immunofluorescence analysis of PR expression. (a) Detection of PR expression. The model of MPTP-induced parkinsonism was treated with puerarin (120 mg/kg/day), progesterone (8 mg/kg/day), or RU486 (3 mg/kg/day), as indicated. Midbrain cryosections were probed with primary anti-PR antibody and visualized with Alexa Fluor 594-conjugated secondary antibody, whereas the cell nuclei were stained with DAPI. The substantia nigra areas were examined under a Zeiss LSM 780 confocal microscopy. Representative images with 20x amplification were shown. Scale bar, 100 $\mu$m. (b) Quantitative analysis of PR levels. Fluorescence intensity of PR staining in the midbrain was quantified by a densitometric method and expressed in mean ± SD ($n = 3$).

neurons. Primary rat midbrain neurons were freshly isolated for each experiment. Following 7-day culture in complete growth medium, the neurons were challenged with $MPP^+$, and the neuronal viability was assessed by PI/Hoechst 33342 staining. As shown in Figures 4(a) and 4(b), 100 $\mu$M $MPP^+$ dramatically caused cell death, whereas puerarin (25 $\mu$M) and progesterone (10 nM or 100 nM) effectively enhanced the survival of neurons against $MPP^+$-induced neurotoxicity. RU486 effectively prohibited the neuroprotective activity of puerarin and, to a lesser extent, affected the activity of progesterone. On the other hand, the expression of PR in primary neurons was also determined by Western blot analysis. As shown in Figures 4(c) and 4(d), the expression of PR did not vary much between the treatment groups.

*3.5. Puerarin Promoted Neurite Outgrowth via PR Signaling.* To further determine whether puerarin exhibits neurotrophic activities in a PR-dependent manner, we evaluated the effects of puerarin on neurite outgrowth in primary midbrain neurons and PC12 cells. As shown in Figures 5(a) and 5(b), puerarin greatly promoted the neurite extension in primary midbrain neurons. RU486 abolished the neurotrophic effect of puerarin so that puerarin did not increase the neurite length in the presence of RU486 relative to the control group.

To determine the role of PR in the neurotrophic activities of puerarin, on the other hand, we successfully generated a PR-silenced PC12 cell model by transiently transfecting specific siRNAs for evaluating the effects of puerarin on neurite outgrowth. As shown in Figure 6(a), PR-specific siRNAs effectively downregulated PR expression whereas the negative control siRNAs did not alter PR expression. Upon transfection with PR siRNAs, as shown in Figures 6(b) and 6(c), the transfected cells failed to generate neurites in response to puerarin (10, 25, and 50 $\mu$M) whereas PC12 cell transfected with the negative control siRNA group responded to puerarin for neurite outgrowth in a highly similar fashion compared with the untransfected cells.

To clarify whether puerarin could activate PR-mediated transcriptional activity, we introduced the promoter-reporter construct carrying PR-binding DNA sequence into PC12 cells. In the experiments, PC12 cells were transfected with plasmid DNA construct 2xPRE-TK-Luc. As shown in Figure 6(d), puerarin and progesterone markedly increased the PR-mediated transcriptional activity. Based on molecular docking as shown in Figure 6(e), puerarin and progesterone bind to the different sites of PR with the binding energy of -8.2 kcal/mol for puerarin and -10.1 kcal/mol for progesterone, respectively. Puerarin appeared to be a moderate to strong binder, whereas progesterone is a high affinity ligand.

## 4. Discussion

Early diagnosis and early intervention are equally important to maintain the life quality of PD patients [31, 32]. While the efficacy of the existing clinical drugs is controversial, natural product flavonoids hold promise for halting the progression

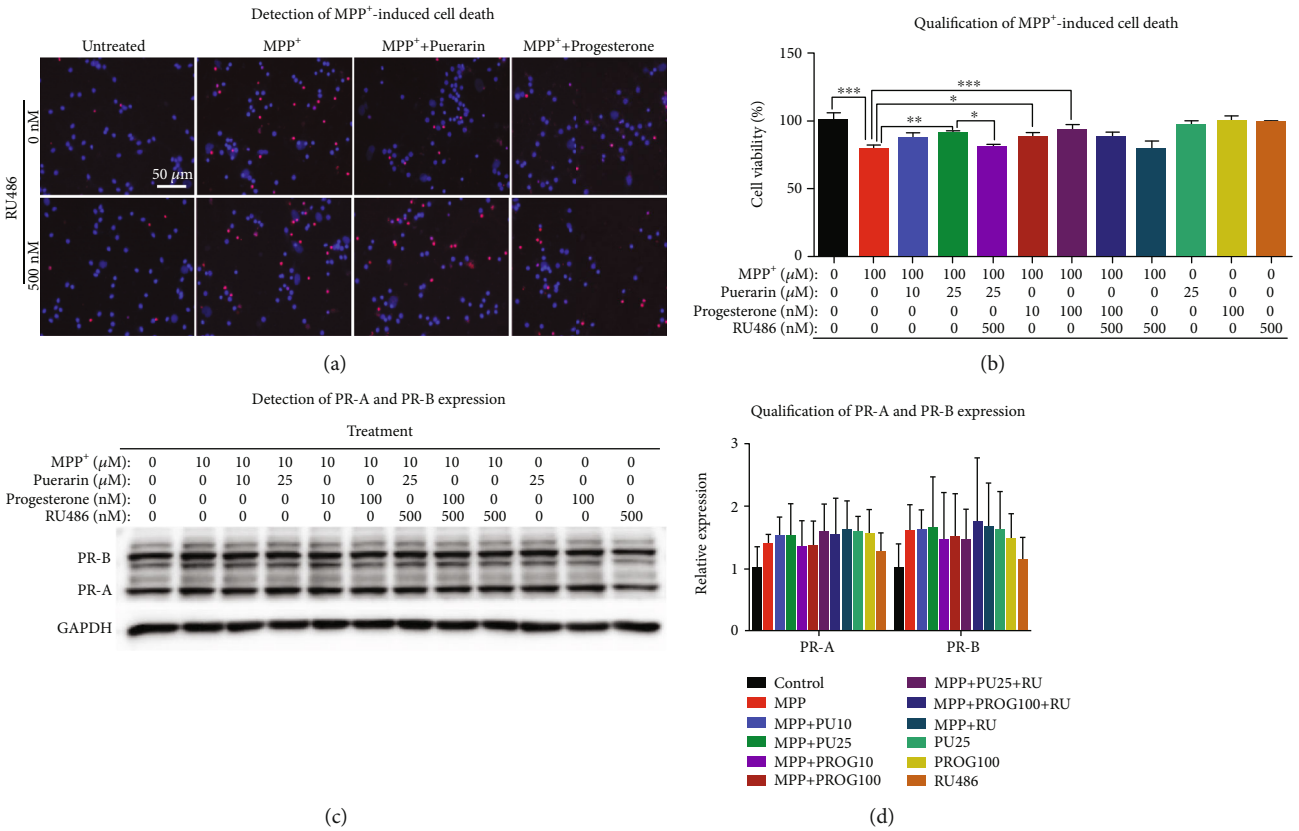


Figure 4: Puerarin enhanced the survival of primary midbrain neurons against $MPP^+$-induced neurotoxicity. (a) Detection of $MPP^+$-induced cell death. Primary midbrain neurons were treated with $MPP^+$, puerarin, progeresterone, and RU486 as indicated. Cell viability was assessed by Hoechst 33342 and PI staining. The representative images were shown. (b) Quantification of neuronal viability. Hoechst- and PI-positive cells were counted under a Zeiss fluorescence microscope (Carl Zeiss, Jena, Germany). $^*p < 0.05$; $^{**}p < 0.01$; $^{***}p < 0.001$. (c) Western blot analysis of PR-A and PR-B expression. Primary midbrain neurons were treated with $MPP^+$, puerarin, progeresterone, and RU486 as indicated. The expression of PRs was analyzed by Western blot analysis with specific antibodies, while GAPDH was analyzed as the loading control. Representative blot was shown. (d) Quantification of PR-A and PR-B expression. Western blots ($n = 3$) in (c) were determined by a densitometric method. $^*p < 0.05$.

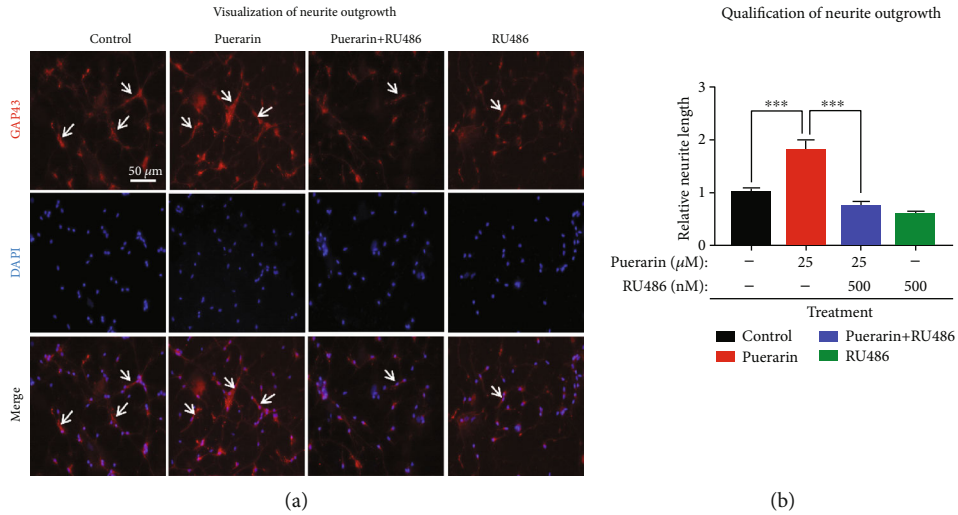


Figure 5: Puerarin promoted neurite outgrowth in primary midbrain neurons. (a) Visualization of neurite outgrowth. Primary midbrain neurons were treated with puearin and RU486 as indicated. Following immunofluorescence staining with anti-GAP43 antibody and DAPI, the cells were examined under a fluorescence microscope from Carl Zeiss (Jena, Germany). Scale bar, 50 μm. (b) Quantification of neurite outgrowth. The neurite length was quantified by using ImageJ (http://imageJ.nih.gov). Neurites from three nonoverlapping fields for each slice were recorded and analyzed for (a). $^{***}p < 0.001$.

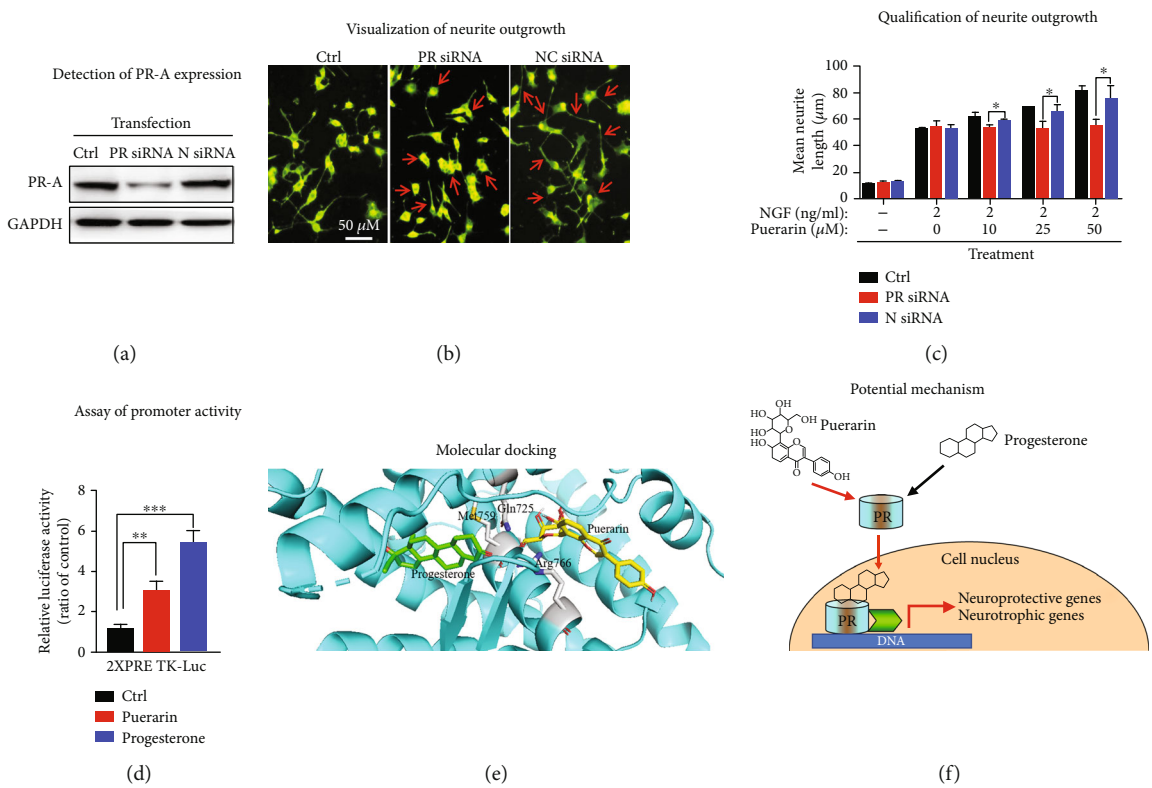


Figure 6: Puerarin promoted neurite outgrowth via PR signaling. (a) siRNA-mediated silencing of PR in PC12 cells. PC12 cells were transiently silenced by PR siRNAs and negative control siRNAs. The expression of PR was determined by Western blot analysis with anti-PR antibody. Representative blots were shown. (b) Visualization of neurite outgrowth. After siRNA transfection, PC12 cells were treated with puerarin and NGF for 72 h. Neurite outgrowth was determined by a commercial neurite staining kit and analyzed under a fluorescence microscope from Carl Zeiss (Jena, Germany). The representative images were shown. Scale bar, 50 $\mu$m. (c) Quantification of neurite outgrowth. Neurites from three nonoverlapping fields for each slice were recorded and analyzed. $^{*}p < 0.05$, $^{**}p < 0.01$, $^{***}p < 0.001$. (d) Luciferase assay for promoter activity. PC12 cells were transiently transfected with 2xPRE-TK-Luc and pRL-TK and cultured for 24 h. The cells were subsequently treated with puerarin and progesterone for 24 h. The promoter activity was assayed with the Dual-Luciferase Reporter System under a Clariostar microplate reader from BMG Labtech (Ortenberg, Germany). Results were expressed as luciferase activity and normalized to Renilla activity for three independent experiments. $^{**}p < 0.01$, $^{***}p < 0.001$. (e) Molecular docking of puerarin and progesterone. Puerarin and progesterone were docked into PR structure (PDB: 3D90) by AutoDock Vina. (f) Potential mechanism. Puerarin may interact with PR and activate the transcriptional factor activity of PR to induce neuroprotective genes and neurotrophic factors.

of the disease and restoring the neuronal functions in PD patients [17]. As a key example, puerarin is extensively evaluated for the neuroprotective effects in different PD models [33–35]. We previously demonstrated several indirect mechanisms underlying the neuroprotective and neurotrophic effects of puerarin [18, 19]. The present study focused on the question of whether puerarin could modulate PR signaling to exhibit neuroprotective and neurotrophic activity.

The progesterone-PR signaling pathway is initially known for its important regulatory role in female reproduction and the link to the progression of breast cancer [13]. Meanwhile, a few earlier studies reported that endogenous progesterone and PR could exhibit cerebroprotection in stroke [36]. Progesterone is now known as an important neurosteroid for its capacity of protecting neurons and promoting neuronal repair in PD and traumatic brain injury [9, 37]. The neuroprotective potential of progesterone was validated to be PR-dependent in MPTP-induced PD models [4, 38]. These results highlight that PR signaling is a potential therapeutic target for the treatment of neurodegeneration [14]. Progesterone induces genomic and nongenomic signals through classical intracellular PRs, the seven transmembrane domain 7TMPRb, and the membrane-associated PR component 1 (PGRMC1) [39]. Progesterone directly interacts with PR and promotes the translocation of PR into cell nuclei, whereas PR functions as a transcriptional factor to regulate the expression of genes for various functions including neuroprotection and neuronal restoration [40].

On the other hand, puerarin is classically tested for its estrogenic activity in the animal models [41]. In the present study, we found that puerarin (120 mg/kg) could reduce MPTP-induced motor dysfunctions to the similar extent to progesterone (8 mg/kg) (Figures 1(c) and 1(d)). RU486 effectively antagonized the beneficial effect of puerarin on MPTP-induced behavioral impairments. Based on the immunohistochemical analysis for TH expression, puerarin (120 mg/kg)

and progesterone (8 mg/kg) enhanced the survival of dopaminergic neurons against MPTP-induced neurotoxicity to a similar extent. Again, RU486 abolished the neuropotective effect of puerarin (Figures 2(a) and 2(b)). The assay of neuronal viability also confirmed the neuroprotective activity of puerarin and the antagonizing effect of RU486 (Figures 4(a) and 4(b)). Furthermore, puerarin effectively promoted neurite growth in primary rat midbrain neurons, whereas RU486 abolished the neurotrophic activity of puerarin. Importantly, puerarin did not alter the *in vivo* and *in vitro* expression of PR (Figures 2(c), 2(d), 3, 4(c), and 4(d)). Taken together, these results suggested that puerarin might be able to interact with PR or some signaling molecules in PR signaling pathway. In the present study, therefore, we examined the role of PR in the beneficial effects of puerarin. Our strategy was to transiently silence PR-A expression in dopaminergic PC12 cells by specific siRNAs and examine the neurite outgrowth in response to puerarin. Indeed, puerarin failed to induce neurite outgrowth in PR siRNA-transfected cells (Figures 6(a)–6(c)). These results suggest that PR is essential for puerarin to exhibit neurotrophic activity, suggesting that puerarin could potentiate neurite outgrowth via PR signaling. To clarify the dependence of PR, we employed the promoter-reporter system to assay the effects of puerarin on the transcriptional activities of PR. As a result, puerarin markedly induced the transcriptional activity of PR, whereas progesterone specifically induced the transcriptional activity of PR (Figure 6(d)). Moreover, the molecular docking software AutoDock Vina was employed to simulate the binding of the puerarin and progesterone to human PR structure (PDB: 3D90). As shown in Figure 6(e), puerarin and progesterone appeared to bind to the different sites of PR while the residues such as Gln725, Met759, and Arg766 might contribute to the binding. Puerarin and progesterone bind to PR at the binding energy of -8.2 kcal/mol and -10.1 kcal/mol, respectively. Collectively, these results suggested that puerarin attenuated MPTP- and $MPP^+$-induced neurotoxicity and potentiated neurite outgrowth via PR signaling.

## 5. Conclusion

The present study demonstrated that puerarin ameliorated MPTP- or $MPP^+$-induced neurotoxicity and promoted neurite outgrowth in mouse PD model and cultured primary rat midbrain neurons via PR-dependent mechanism. Our results for the first time suggest that puerarin may mimic progesterone to interact with PR at the cell surface, cytosol, or cell nucleus although the involvement of PGRMC1 is not excluded. Ultimately, puerarin could exhibit neuroprotective and neurotrophic activities via PR signaling (Figure 6(f)). We believe that puerarin may serve as lead compounds for the development of novel PR agonists to treat PD and other neurodegenerative diseases.

## Data Availability

The data were available from the corresponding author upon request.

## Conflicts of Interest

The authors declare that there is no competing interest.

## Authors' Contributions

Yingke Zhao, Jia Zhao, Xiuying Zhang, Yuanyuan Cheng, and Dan Luo performed the experiments. Simon Ming-Yuen Lee provided the instrument and reagents. Lixing Lao supervised the data analysis. Jianhui Rong designed the research and revised the article. Yingke Zhao and Jia Zhao contributed equally to this work.

## Acknowledgments

The authors are grateful to Mr. Wong Hei Kiu, Ms. Lee Wai Sin, and Mr. Shek Chun Shum for their technical assistance. This work was supported by General Research Fund (GRF) grants (17120915, 17146216, 17100317, and 17119619) from the Research Grants Council of Hong Kong, National Natural Science Foundation of China (Nos. 81703726 and 21778046), Health and Medical Research Fund (15161731, 16171751, and 17181231), Science, Technology and Innovation Commission of Shenzhen Municipality (Basic Research Program, Free Exploration Project JCYJ20180306173835901), Research and Cultivation Plan of High-Level Hospital Construction (HKUSZH201902040), Midstream Research Programme for Universities (MRP) (053/18X), and the Seed Funding (201611159156) for Basic Research Programme from University of Hong Kong.

## Supplementary Materials

Figure S1: simplification of Figure 4. Table S1: list of antibodies. *(Supplementary Materials)*

## References

[1] V. L. Feigin, A. A. Abajobir, K. H. Abate et al., "Global, regional, and national burden of neurological disorders during 1990-2015: a systematic analysis for the Global Burden of Disease Study 2015," *The Lancet Neurology*, vol. 16, no. 11, pp. 877–897, 2017.

[2] S. Przedborski, "The two-century journey of Parkinson disease research," *Nature Reviews Neuroscience*, vol. 18, no. 4, pp. 251–259, 2017.

[3] H. Kataoka and S. Ueno, "Can postural abnormality really respond to levodopa in Parkinson's disease?," *Journal of the Neurological Sciences*, vol. 377, pp. 179–184, 2017.

[4] M. Bourque, M. Morissette, and T. Di Paolo, "Repurposing sex steroids and related drugs as potential treatment for Parkinson's disease," *Neuropharmacology*, vol. 147, pp. 37–54, 2019.

[5] M. A. Tenkorang, B. Snyder, and R. L. Cunningham, "Sex-related differences in oxidative stress and neurodegeneration," *Steroids*, vol. 133, pp. 21–27, 2018.

[6] F. Siani, R. Greco, G. Levandis et al., "Influence of estrogen modulation on glia activation in a murine model of Parkinson's disease," *Frontiers in Neuroscience*, vol. 11, p. 306, 2017.

[7] H. Yi, X. Bao, X. Tang, X. Fan, and H. Xu, "Estrogen modulation of calretinin and BDNF expression in midbrain

dopaminergic neurons of ovariectomised mice," *Journal of Chemical Neuroanatomy*, vol. 77, pp. 60–67, 2016.

[8] P. E. Pomata, A. A. Colman-Lerner, J. L. Baranao, and M. L. Fiszman, "In vivo evidences of early neurosteroid synthesis in the developing rat central nervous system and placenta," *Developmental Brain Research*, vol. 120, no. 1, pp. 83–86, 2000.

[9] M. Bourque, M. Morissette, S. al Sweidi, D. Caruso, R. C. Melcangi, and T. di Paolo, "Neuroprotective effect of progesterone in MPTP-treated male mice," *Neuroendocrinology*, vol. 103, no. 3-4, pp. 300–314, 2016.

[10] S. Casas, F. Giuliani, F. Cremaschi, R. Yunes, and R. Cabrera, "Neuromodulatory effect of progesterone on the dopaminergic, glutamatergic, and GABAergic activities in a male rat model of Parkinson's disease," *Neurological Research*, vol. 35, no. 7, pp. 719–725, 2013.

[11] L. M. Rudolph, C. A. Cornil, M. A. Mittelman-Smith et al., "Actions of steroids: new neurotransmitters," *The Journal of Neuroscience*, vol. 36, no. 45, pp. 11449–11458, 2016.

[12] M. Schumacher, C. Mattern, A. Ghoumari et al., "Revisiting the roles of progesterone and allopregnanolone in the nervous system: resurgence of the progesterone receptors," *Progress in Neurobiology*, vol. 113, pp. 6–39, 2014.

[13] S. L. Grimm, S. M. Hartig, and D. P. Edwards, "Progesterone receptor signaling mechanisms," *Journal of Molecular Biology*, vol. 428, no. 19, pp. 3831–3849, 2016.

[14] A. F. de Nicola, M. C. Gonzalez Deniselle, L. Garay et al., "Progesterone protective effects in neurodegeneration and neuroinflammation," *Journal of Neuroendocrinology*, vol. 25, no. 11, pp. 1095–1103, 2013.

[15] P. Srivastava and R. S. Yadav, "Efficacy of natural compounds in neurodegenerative disorders," *Advances in Neurobiology*, vol. 12, p. 107, 2016.

[16] I. Solanki, P. Parihar, and M. S. Parihar, "Neurodegenerative diseases: from available treatments to prospective herbal therapy," *Neurochemistry International*, vol. 95, pp. 100–108, 2016.

[17] J. Zhao, M. Zhu, M. Kumar et al., "A pharmacological appraisal of neuroprotective and neurorestorative flavonoids against neurodegenerative diseases," *CNS & Neurological Disorders Drug Targets*, vol. 18, no. 2, pp. 103–114, 2019.

[18] J. Zhao, Y. Y. Cheng, W. Fan et al., "Botanical drug puerarin coordinates with nerve growth factor in the regulation of neuronal survival and neuritogenesis via activating ERK1/2 and PI3K/Akt signaling pathways in the neurite extension process," *CNS Neuroscience & Therapeutics*, vol. 21, no. 1, pp. 61–70, 2015.

[19] J. Zhao, Y. Cheng, C. Yang et al., "Botanical drug puerarin attenuates 6-hydroxydopamine (6-OHDA)-induced neurotoxicity via upregulating mitochondrial enzyme arginase-2," *Molecular Neurobiology*, vol. 53, no. 4, pp. 2200–2211, 2016.

[20] L. Li, Z. Xue, L. Chen, X. Chen, H. Wang, and X. Wang, "Puerarin suppression of A$\beta$ 1–42 -induced primary cortical neuron death is largely dependent on ER$\beta$," *Brain Research*, vol. 1657, pp. 87–94, 2017.

[21] Y. F. Cheng, G. Q. Zhu, Q. W. Wu et al., "GPR30 activation contributes to the puerarin-mediated neuroprotection in MPP+-induced SH-SY5Y cell death," *Journal of Molecular Neuroscience*, vol. 61, no. 2, pp. 227–234, 2017.

[22] Z. K. Qiu, G. H. Zhang, D. S. Zhong et al., "Puerarin ameliorated the behavioral deficits induced by chronic stress in rats," *Scientific Reports*, vol. 7, no. 1, article 6266, 2017.

[23] A. S. Su, J. W. Zhang, and J. Zou, "The anxiolytic-like effects of puerarin on an animal model of PTSD," *Biomedicine & Pharmacotherapy*, vol. 115, article 108978, 2019.

[24] P. Saha, G. Saraswat, P. Chakraborty, S. Banerjee, B. C. Pal, and S. N. Kabir, "Puerarin, a selective oestrogen receptor modulator, disrupts pregnancy in rats at pre-implantation stage," *Reproduction*, vol. 144, no. 5, pp. 633–645, 2012.

[25] A. C. Wulsin, J. P. Herman, and S. C. Danzer, "RU486 mitigates hippocampal pathology following status epilepticus," *Frontiers in Neurology*, vol. 7, 2016.

[26] Y. Zhao, D. Luo, Z. Ning, J. Rong, and L. Lao, "Electro-acupuncture ameliorated MPTP-induced parkinsonism in mice via TrkB neurotrophic signaling," *Frontiers in Neuroscience*, vol. 13, p. 496, 2019.

[27] D. Luo, J. Zhao, Y. Y. Cheng, S. M. Y. Lee, and J. H. Rong, "N-propargyl caffeamide (PACA) ameliorates dopaminergic neuronal loss and motor dysfunctions in MPTP mouse model of Parkinson's disease and in MPP+-induced neurons via promoting the conversion of proNGF to NGF," *Molecular Neurobiology*, vol. 55, no. 3, pp. 2258–2267, 2018.

[28] Y. Cheng, C. Yang, J. Zhao, H. F. Tse, and J. Rong, "Proteomic identification of calcium-binding chaperone calreticulin as a potential mediator for the neuroprotective and neuritogenic activities of fruit-derived glycoside amygdalin," *The Journal of Nutritional Biochemistry*, vol. 26, no. 2, pp. 146–154, 2015.

[29] D. Luo, Y. Guo, Y. Cheng, J. Zhao, Y. Wang, and J. Rong, "Natural product celastrol suppressed macrophage M1 polarization against inflammation in diet-induced obese mice via regulating Nrf2/HO-1, MAP kinase and NF-$\kappa$B pathways," *Aging*, vol. 9, no. 10, pp. 2069–2082, 2017.

[30] N. Purandare, M. Somayajulu, M. Huttemann, L. I. Grossman, and S. Aras, "The cellular stress proteins CHCHD10 and MNRR1 (CHCHD2): partners in mitochondrial and nuclear function and dysfunction," *Journal of Biological Chemistry*, vol. 293, no. 17, pp. 6517–6529, 2018.

[31] L. V. Kalia and A. E. Lang, "Parkinson's disease," *The Lancet*, vol. 386, no. 9996, pp. 896–912, 2015.

[32] L. F. Burbulla, S. Jeon, J. Zheng, P. Song, R. B. Silverman, and D. Krainc, "A modulator of wild-type glucocerebrosidase improves pathogenic phenotypes in dopaminergic neuronal models of Parkinson's disease," *Science Translational Medicine*, vol. 11, no. 514, article eaau6870, 2019.

[33] M. Jiang, Q. Yun, G. Niu, Y. Gao, F. Shi, and S. Yu, "Puerarin prevents inflammation and apoptosis in the neurocytes of a murine Parkinson's disease model," *Genetics and Molecular Research*, vol. 15, no. 4, 2016.

[34] R. Li, T. Liang, L. Xu, N. Zheng, K. Zhang, and X. Duan, "Puerarin attenuates neuronal degeneration in the substantia nigra of 6-OHDA-lesioned rats through regulating BDNF expression and activating the Nrf2/ARE signaling pathway," *Brain Research*, vol. 1523, pp. 1–9, 2013.

[35] G. Zhu, X. Wang, S. Wu, X. Li, and Q. Li, "Neuroprotective effects of puerarin on 1-methyl-4-phenyl-1,2,3,6-tetrahydropyridine induced Parkinson's disease model in mice," *Phytotherapy Research*, vol. 28, no. 2, pp. 179–186, 2014.

[36] X. Zhu, M. Frechou, P. Liere et al., "A role of endogenous progesterone in stroke cerebroprotection revealed by the neural-specific deletion of its intracellular receptors," *The Journal of Neuroscience*, vol. 37, no. 45, pp. 10998–11020, 2017.

[37] J. Wei and G. M. Xiao, "The neuroprotective effects of progesterone on traumatic brain injury: current status and future prospects," *Acta Pharmacologica Sinica*, vol. 34, no. 12, pp. 1485–1490, 2013.

[38] E. Brotfain, S. E. Gruenbaum, M. Boyko, R. Kutz, A. Zlotnik, and M. Klein, "Neuroprotection by estrogen and progesterone in traumatic brain injury and spinal cord injury," *Current Neuropharmacology*, vol. 14, no. 6, pp. 641–653, 2016.

[39] D. Garg, S. S. M. Ng, K. M. Baig, P. Driggers, and J. Segars, "Progesterone-mediated non-classical signaling," *Trends in Endocrinology and Metabolism*, vol. 28, no. 9, pp. 656–668, 2017.

[40] S. L. Gonzalez, M. F. Coronel, M. C. Raggio, and F. Labombarda, "Progesterone receptor-mediated actions and the treatment of central nervous system disorders: an update of the known and the challenge of the unknown," *Steroids*, vol. 153, article 108525, 2019.

[41] Y. X. Zhou, H. Zhang, and C. Peng, "Puerarin: a review of pharmacological effects," *Phytotherapy Research*, vol. 28, no. 7, pp. 961–975, 2014.

Hindawi
Oxidative Medicine and Cellular Longevity
Volume 2020, Article ID 6454281, 12 pages
https://doi.org/10.1155/2020/6454281

*Research Article*

# RiPerC Attenuates Cerebral Ischemia Injury through Regulation of miR-98/PIK3IP1/PI3K/AKT Signaling Pathway

**Dengwen Zhang,[1] Li Mei,[1] Ruichun Long,[1] Can Cui,[1] Yi Sun,[1] Sheng Wang,[1,2] and Zhengyuan Xia[3,4]**

[1]*Department of Anesthesiology, Guangdong Provincial People's Hospital, Guangdong Academy of Medical Sciences, Guangzhou, Guangdong Province, China*
[2]*Department of Anesthesiology, Linzhi People's Hospital, Linzhi, Tibet, China*
[3]*Department of Anesthesiology, The University of Hong Kong, Hong Kong, SAR, China*
[4]*Department of Anesthesiology, Affiliated Hospital of Guangdong Medical University, Zhanjiang, China*

Correspondence should be addressed to Yi Sun; sunnyuva2014@yahoo.com and Sheng Wang; shengwang_gz@163.com

Received 28 June 2020; Revised 11 September 2020; Accepted 19 September 2020; Published 6 October 2020

Academic Editor: Teresa I. Fortoul



*Background*. Cerebral ischemic stroke is a refractory disease which seriously endangers human health. Remote ischemic perconditioning (RiPerC) by which the sublethal ischemic stimulus is administered during the ischemic event is beneficial after an acute stroke. However, the regulatory mechanism of RiPerC that relieves cerebral ischemic injury is still not completely clear. *Methods*. In the present study, we investigated the regulatory mechanism of RiPerC in a rat model of ischemia induced by the middle cerebral artery occlusion (MCAO). Forty-eight adult male Sprague-Dawley (SD) rats were injected intracerebroventricularly with miR-98 agomir, miR-98 antagomir, or their negative controls (agomir-NC, antagomir-NC) 2 h before MCAO or MCAO+RiPerC followed by animal behavior tests and infraction volume measurement at 24 h after MCAO. The expression of miR-98, PIK3IP1, and tight junction proteins in rat hippocampus and cerebral cortex tissues was detected by quantitative polymerase chain reaction (qPCR) and Western blot (WB). Enzyme-linked immunosorbent assay (ELISA) was used to assess the IL-1$\beta$, IL-6, and TNF-$\alpha$ levels in the rat serum. *Results*. The results showed that in MCAO group, the expression of PIK3IP1 was upregulated, but decreased after RiPerC treatment. Then, we found that PIK3IP1 was a potential target of miR-98. Treatment with miR-98 agomir decreased the infraction volume, reduced brain edema, and improved neurological functions compared to control rats. But treating with miR-98 antagomir in RiPerC group, the protective effect on cerebral ischemia injury was canceled. *Conclusion*. Our finding indicated that RiPerC inhibited the MCAO-induced expression of PIK3IP1 through upregulated miR-98, thereby reducing the apoptosis induced by PIK3IP1 through the PI3K/AKT signaling pathway, thus reducing the cerebral ischemia-reperfusion injury.

## 1. Introduction

Cerebral ischemic stroke is a refractory disease which seriously endangers human health. It is characterized by high incidence, high disability, and high mortality. Cerebral ischemic injury is one of the serious perioperative complications, which can cause neurological dysfunction and is an important cause of death and disability of patients. Perioperative general anesthesia, postoperative dehydration, bed rest, and other factors can all increase the risk of cerebral ischemia. Statistical studies show that the risk of stroke in general surgical patients is up to 0.1-3%, and the risk of stroke in patients with complex heart surgery is up to 10% [1, 2]. Ischemic stroke is caused by insufficient blood supply to the brain and is characterized by hypoxia, excitotoxicity, and inflammation, which ultimately lead to neuronal cell death [3, 4]. Since neurons are difficult to regenerate, the research on how to reduce the death and apoptosis of neurons and

increase the tolerance of neurons to ischemia is the main direction of the current research on the treatment of cerebral ischemic injury.

Recent studies have found that during cerebral ischemia, transient ischemic reperfusion stimulation in the distal limb can also reduce cerebral ischemia reperfusion injury. This protective effect is known as remote ischemic perconditioning (RiPerC) [5, 6]. This is different from previously reported ischemic preconditioning (IPC) and drug preconditioning, including opioid agonists, inhaled anesthetics, and adenosine that can reduce ischemic reperfusion injury [7, 8]. Those preconditioning measures must be implemented before the occurrence of ischemia. However, the occurrence of clinical ischemia is often unpredictable, which restricts the clinical application of these preconditioning methods. The very important advantage of RiPerC is that it can be carried out during the occurrence of ischemia without the support of very complex technical conditions, so it should have a broader clinical application prospect [9, 10]. Therefore, the mechanism by which RiPerC operation alleviates cerebral ischemia injury deserves further investigation.

The phosphatidylinositol 3-kinase/protein kinase B (PI3K/Akt) signaling pathway, involved in the regulation of cell proliferation and differentiation, has been documented to protect neural stem cells (NSCs) against oxidative damage [11, 12]. Activation of the PI3K/Akt signaling pathway has been implicated in neuroprotective effects of various agents against ischemia reperfusion injury [13, 14]. In the light of the findings cited above, we hypothesized that the PI3K/Akt signaling pathway may account for the neuroprotective effects of RiPerC operation.

## 2. Materials and Methods

*2.1. Animals.* Forty-eight adult male Sprague-Dawley (SD) rats weighing 250-300 g were randomly divided into 7 groups: sham group (sham operated rats without other treatment; $n = 12$), MCAO group (modeled rats; $n = 6$), RiPerC group (modeled rats with RiPerC operation; $n = 6$), MCAO-NC agomir group (modeled rats with lateral cerebroventricular injection of NC agomir; $n = 6$), MCAO-miR-98 agomir group (modeled rats with lateral cerebroventricular injection of miR-98 agomir; $n = 6$), RiPerC-NC antagomir group (modeled rats with lateral cerebroventricular injection of NC antagomir; $n = 6$), and RiPerC-miR-98 antagomir group (modeled rats with lateral cerebroventricular injection of miR-98 antagomir; $n = 6$). The rats were housed in a clean animal room with room temperature at $22 \pm 2^{\circ}$C, the relative humidity at 60%, and 12 h day/night cycle. The litter was changed every day to avoid infection. All procedures involving animals were performed according to the USA Care and Use of Laboratory Animals. Animals were purchased from the Experimental Animal Center of Sun Yat-sen University (Guangzhou, China). This study was approved by the Animal Ethics Committee of Guangzhou Forevergen Medical Experimental Animal Center.

*2.2. Establishment of Rat MCAO Model.* Middle cerebral artery occlusion (MCAO) rat model was established according to the reference [15, 16]. Rats were deeply anesthetized with an intraperitoneal injection of chloralic hydras (0.4 g/kg, J1516063, Aladdin Biochemical Technology Co., Ltd. Shanghai, China). A blunt dissection was performed under a stereomicroscope (Stemi 2000, Carl Zeiss) to expose the left common carotid artery (CCA), then gradually expose CCA bifurcation, external carotid artery (ECA), and internal carotid artery (ICA), until near skull base, followed by ligation of the ipsilateral CCA proximal end and external carotid artery and clamping of the CCA and ICA with arterial clamp. This was followed by a small incision in the ECA between permanent and temporary sutures, in which a 5-0 surgical nylon filament with a round silica gel tip ($0.34 \pm 0.02$ mm in diameter) (L3400, Guangzhou Jialing Biotechnology Co., Ltd., Guangzhou Jialing Biotechnology Co. LTD, Guangzhou, China) was inserted into the ICA approximately 18-20 mm beyond the carotid bifurcation, thereby occluding the origin of the middle cerebral artery. Loosen the arteriole clip and suture the skin. The end of the occlusion line will be slightly exposed to the skin 1 cm. After 2 hours of MCAO, the rat was allowed to recover for 1 day. The sham operation group was performed with the same surgical procedure except for the ligation and the strand placement. Rectal temperature was maintained at 37.0°C during and after surgery with a temperature control heating pad.

RiPerC operation was carried out during MCAO ischemia. In RiPerC group, a tourniquet was applied around the right hind-limb just below the level of the inguinal ligament for $3 \times 10$ minutes with 10-minute intermittent reperfusion periods. This process was performed with MCAO at the same time.

*2.3. Intracerebroventricular Injection.* MiR-98 agomir (agomir-98, RiboBio, Guangzhou, China), which is a chemically modified double-stranded miRNA-98 that mimics the endogenous miR-98 was injected into hippocampus by intracerebroventricular (ICV) injection to establish the overexpression of miR-98 in the rat, whilst miR-98 antagomir (antagomir-98, RiboBio) is a chemically modified single-stranded miRNA and perfectly complementary to the miR-98 sequence. Through binding to the miR-98, miR-98 antagomir can inhibit the function of miR-98. To knockdown miR-98 expression in rat, miR-98 antagomir was injected into hippocampus by ICV injection according to the manufacturer's instructions. Briefly, agomir-98, antagomir-98, agomir-NC, and antagomir-NC (0.8 nmol dissolved in 4 $\mu$L PBS; RiboBio) were applied 3 days before MCAO. The injections were performed as previously described [17]. Rats were anesthetized and positioned lying prone in a stereotactic head frame (RWD Life Science, China). A scalp incision was made along the midline, and a burr hole was drilled into the right side of the skull (0.5 mm posterior and 1.0 mm lateral to the bregma). AgomiR-98, antagomiR-98, agomir-NC, and antagomir-NC were microinfused into right lateral ventricles through a Hamilton syringe (2.5 mm vertically), which was driven by a microinfusion pump (KDS 310, KD Scientific) with 0.2 $\mu$L/min. The needle was left in place for an additional 5 min after injection to prevent possible leakage and was slowly withdrawn within 4 min. After the needle was

removed, the burr hole was sealed with bone wax, the incision was closed with sutures, and the rats were allowed to recover.

*2.4. Rat Neurological Function Score.* According to Longa's 5-point scoring method [18], scoring was started from the time when the MCAO rat first recovered completely. 0 point, normal without neurological deficit; 1 point, unilateral forelimb cannot be straightened after rising; 2 points, the body tilted to one side when the rat was crawling forward; 3 points, the rat's crawling body fell to the side; 4 points, coma or cannot crawl spontaneously.

*2.5. 2,3,5-Triphenyltetrazolium Hydrochloride (TTC) Staining.* After 24 h reperfusion, animals were sacrificed by common carotid perfusion fixation with cold Tris-buffered saline under isoflurane anesthesia. The brain was immediately removed and sectioned into five coronal slices (2 mm in thickness) using a brain-cutting matrix. The brain slices were stained with 1% 2,3,5-triphenyltetrazolium chloride (TTC; Sigma-Aldrich Pty Ltd, Australia) at 37°C in the dark for 30 min. Noninfarcted tissues were stained (red), and infarct tissues were not stained (white). Then, brain sections were fixed in 2% paraformaldehyde and photographed with a digital camera (Canon IXUS175, Tokyo, Japan). The percentage of infarct volume was analysed using Image J software 1.50i by calculating the infarct volume ratio. Briefly, the infarct volume was calculated as a percentage of the entire brain adjusted for edema using modified Swanson calculation.

*2.6. Quantitative Polymerase Chain Reaction (PCR).* Total RNA was extracted by TRIzol (Invitrogen, Carlsbad, CA, USA) using an RNA extraction kit. Complementary deoxyribose nucleic acid (cDNA) was synthesized by reverse transcription. The levels of mature miR-98 were determined using a stem-loop real-time PCR system with TaqMan Universal Master Mix II (Ambion, CA, USA). The miR-98 levels were normalized to those of U6 snRNA. The level of PIK3IP1 expression was detected by quantitative PCR. The sequences of the primers are listed below: miRNA-98 (Forward) 5′-TGAGGTAGTAAGTTGTATTGTT-3′; U6 (Forward) 5′-GCAAATTCGTGAAGCGTTCC-3′; PIK3IP1 (Forward) 5′-AGAGACCACTTCCGGTGACA-3′; (Reverse) 5′-ACAC GTAGCCCAAAGTTCCC-3′; $\beta$-actin (Forward) 5′-AGAT CAAGATCATTGCTCCTCCT-3′; (Reverse) 5′-ACGCAG CTCAGTAACAGTCC-3′. The fold change in relative miRNA expression was determined using the $2^{-\Delta\Delta Ct}$ method, as described previously [19].

*2.7. Enzyme-Linked Immunosorbent Assay (ELISA).* Enzyme-linked immunosorbent assay (ELISA) was used to assess the IL-1$\beta$, IL-6, and TNF-$\alpha$ levels in the rat serum. IL-1$\beta$, IL-6, and TNF-$\alpha$ were measured with commercial ELISA kits (Boster Biosciences Co., Wuhan, China) according to the manufacturer's instructions. A microplate reader (Infinite M200 PRO, Tecan, Switzerland) was used to assess the OD value.

*2.8. Luciferase Reporter Assay.* The wild type of the 3′ untranslated region (3′UTR) of the PIK3IP1 gene (including miR-98 binding sites) and mutant 3′UTR of the PIK3IP1 gene were synthesized by Guangzhou HYY Biotechnology Co. LTD (Guangzhou, People's Republic of China) and cloned into the downstream portion of the psiCHECK-2 vector (Promega) to generate PIK3IP1–WT and mutant PIK3IP1 (PIK3IP1–MUT), which were confirmed by sequencing. For the luciferase reporter assay, 293T cells were seeded in 24-well plates at a density of $2 \times 10^4$ cells per well. When the cells reached 70% confluency, they were cotransfected with either PIK3IP1–WT (100 ng) or PIK3IP1–MUT (100 ng) and miR-98 mimics (100 nM) or miR-NC mimics (100 nM). Forty-eight hours later, cells were harvested and assayed using the Dual-Luciferase Reporter Assay System (LF005, FulenGen, Guangzhou, China) according to the manufacturer's instruction. Each experiment was independently repeated 3 times.

*2.9. Western Blot Assay.* Rats were sacrificed, and the cerebral cortex and hippocampus were collected. Whole-cell protein was prepared from the ischemic cortices divided from left cerebral hemisphere. In brief, brain tissues were homogenized in RIPA buffer (P1003B, Beyotime, Wuhan, China) containing PMSF (ST506, Beyotime, Wuhan, China) and then sonicated on ice. After centrifugation, the supernatant was collected for Western blot assay. An aliquot of 10 $\mu$g/mg protein from each sample was separated by SDS-PAGE and then transferred onto a nitrocellulose membrane. The membrane was blocked with 5% nonfat milk in TBST for 2 h (pH 7.4) and then incubated with primary antibodies against PI3KIP1 (1 : 1000; sc-365777, Santa Cruz), $\beta$-catenin (1 : 1000; BM0627, BOSTER), Bcl-2 (1 : 1000; ab32124, Abcam), Bax (1 : 1000; ab32503, Abcam), caspase 9 (1 : 1000, ab32539, Abcam), AKT (1 : 1000, 71632S, Cell Signaling Technology), p-AKT (1 : 1000, 9271S, Cell Signaling Technology), PI3K (1 : 1000, 4249S, Cell Signaling Technology), and p-PI3K (1 : 1000, 17366S, Cell Signaling Technology) at 4°C overnight. After incubation with secondary antibody for 2 h at room temperature, visualization was done with a chemiluminescence imaging analysis system (5200, Tanon, China). The gray value of PI3KIP1, $\beta$-catenin, Bcl-2, Bax, Caspase 9, AKT, p-AKT, PI3K, and p-PI3K was measured with Image-J software and normalized to that of $\beta$-actin as the relative protein expression.

*2.10. Terminal Deoxynu-Cleotidyl Trans/Erase- (TDT-) Mediated dUTP-Biotin Nick End-Labeling (TUNEL) Staining.* At 24 h after the operation, the brain tissue was fixed with 4% paraformaldehyde, routinely dehydrated, paraffin-embedded, and then sliced at a thickness of 3 $\mu$m. Afterward, the section was dewaxed and hydrated and boiled. The section was then treated with 0.01 mol/L citrate buffer (pH 6.0), and the DNA fragment labeling was performed. The staining was conducted according to the instructions of the TUNEL Kit (Bollingman, Beijing, China). The results of the experiment were shown as the number of cells with apoptotic nuclei and the cells' total number in each high-power field of view (six high-power fields per section). The

apoptotic index (AI) is the apoptotic nuclei's number out of 100 nuclei. The average value of AI was calculated as TUNEL positive cells/total cell number × 100%. Each experiment runs in triplicate.

*2.11. Statistical Analyses.* The analysis of the data was performed using the GraphPad Prism software. Multiple comparisons were statistically analyzed with one-way analysis of variance (ANOVA) followed by the Tukey method or nonparametric test. The data are presented as means ± SEM, and a $P$ value < 0.05 represents statistical significance.

## 3. Result

*3.1. RiPerC Protects Rat against Ischemic Brain Injury at the Structural and Functional Levels.* We investigated the effects of RiPerC on ischemic brain injury. The rat received a RiPerC operation during MCAO operation. Compared to the MCAO group alone, the combination of RiPerC and MCAO operation displayed lower neurological deficit score (Figure 1(b)) and infarct volume (Figures 1(b) and 1(c)).

Immunity and inflammation are key elements in the pathophysiology of stroke; we detected the inflammation factors by ELISA. Compared with the sham group, the expression of IL-1$\beta$, IL-6, and TNFa was all upregulated in MCAO group, while the expression of IL-1$\beta$, IL-6, and TNFa was downregulated with RiPerC treatment (Figure 1(d)).

Some studies have pointed out that the PI3K/Akt signalling pathway participates in neuronal injury [20, 21], which has been reported to suppress neuronal apoptosis [22]. Given the fact that PIK3IP1 downregulates PI3K activity, we detected the mRNA and protein levels of PIK3IP1. In MCAO group, the mRNA and protein expression of PIK3IP1 was upregulated in both hippocampus and cerebral cortex. However, the mRNA and protein expression of PIK3IP1 was decreased with RiPerC treatment (Figures 1(e) and 1(f)).

*3.2. PIK3IP1 Is a Potential Target of miR-98.* To explore the signaling pathway of PIK3IP1-modulated neuroinflammation, we identified the potential miRNA which targets of PIK3IP1 by using the computer algorithm (http://www.microrna.org/microrna/home.do). Among all of the predicted miRNA, miR-98 was chosen as a candidate because it is reported to be involved in MCAO. In addition, the seed sequence of miR-98 displays perfectly complementary matching with the 3′UTR of the PIK3IP1 gene (Figure 2(a)). To obtain direct evidence that PIK3IP1 was a target of miR-98, the fragment of the PIK3IP1 3′-UTR containing the nucleotides complementary to miR-98 was cloned into a luciferase reporter plasmid (psiCHECK-2), such that the PIK3IP1 3′-UTR was placed downstream of the luciferase reporter gene. Plasmids containing either the wild-type or mutant PIK3IP1 3′-UTR were then cotransfected with the miR-98 mimic in HEK 293T cells. The miR-98 mimic inhibited luciferase activity in the HEK 293T cells transfected with the wild-type PIK3IP1 3′-UTR, but such reduction of luciferase activity was cancelled when the miR-98 binding site was mutated, indicating that PIK3IP1 is a direct target gene of miR-98 (Figure 2(b)).

Considering that miR-98 plays an important regulatory role in cerebral ischemic injury, we used qRT-PCR to assess the expression levels of miR-98 in rat hippocampus tissue and cerebral cortex tissue of rats in MCAO group and RiPerC group. Compared to the sham-operated rat, rat receiving MCAO displayed a significant decrease in level of miR-98 in the hippocampus tissue at 24 h after reperfusion. Furthermore, relative to the MCAO-operated brain, miR-98 level was remarkably enhanced in the hippocampus tissue after RiPerC operation (Figure 2(c)). But the expression of miR-98 was not significantly different in cerebral cortex tissues (Figure 2(d)).

*3.3. miRNA-98 Expression in Hippocampus Tissue Play a Key Role in Cerebral Ischemic Injury.* To investigate the overexpression of miR-98 is the role of MCAO on cerebral ischemic injury. The rat received an ICV infusion of either the miR-98 agomir or control NC agomir 3 days prior to MCAO. Compared to the sham group, MCAO suppressed the level of miR-98, while the miR-98 agomir injection enhanced the level of miR-98 to similar extent with the sham group. The result showed that miR-98 agomir displayed significantly smaller infarct volumes (Figures 3(a) and 3(b)), lower neurological deficit (Figure 3(c)), and lower levels of inflammatory cytokines in serum when compared with NC-agomir group (Figures 3(f)–3(h)). The qPCR measurement confirmed that the miR-98 agomir injection increased postischemic induction of miR-98 expression in hippocampus, 24 h after reperfusion in MCAO rat. Compared to the NC-agomir, the expression of miR-98 was significantly upregulated 2.054 times ($P < 0.05$, Figure 3(e)), and the expression of PIK3IP1 was significantly downregulated 0.718 times ($P < 0.05$, Figure 3(d)). The protein expression of PIK3IP1 detected by WB showed the same results.

To investigate whether knockdown of miR-98 cancels the protective effect of RiPerC on cerebral ischemic injury, the rat received an ICV infusion of miR-98 antagomir and NC antagomir 3 days prior to MCAO and RiPerC operation. The results showed that miR-98 antagomir suppressed the RiPerC-mediated induction of miR-98. miR-98 antagomir canceled the protective effect of RiPerC, as evidenced by increased infarct volumes (Figures 3(a) and 3(b)), enhanced neurological deficit (Figure 3(c)), and greater levels of inflammatory cytokines (Figures 3(f)–3(h)), suggesting miR-98 mediates the effect of RiPerC on cerebral ischemic injury. The result of qPCR showed that the miR-98 expression in the RiPerC+miR-98 antagomir group was lower than that in the RiPerC+NC antagomir group ($P < 0.05$, Figure 3(e)), and the PIK3IP1 expression in the RiPerC+miR-98 antagomir group was higher than that in the RiPerC+NC antagomir group ($P < 0.05$, Figure 3(d)).

*3.4. miR-98 Mediates the Antiapoptotic Effect of RiPerC in MCAO Model.* TUNEL staining was then performed to determine apoptosis of hippocampus in each rat group, the results indicated that the apoptosis rate in the MCAO injected with miR-98 agomir was lower than the MCAO injected with NC agomir group (Figure 4(a)). Relative to the RiPerC injected with NC antagomir group, the apoptotic

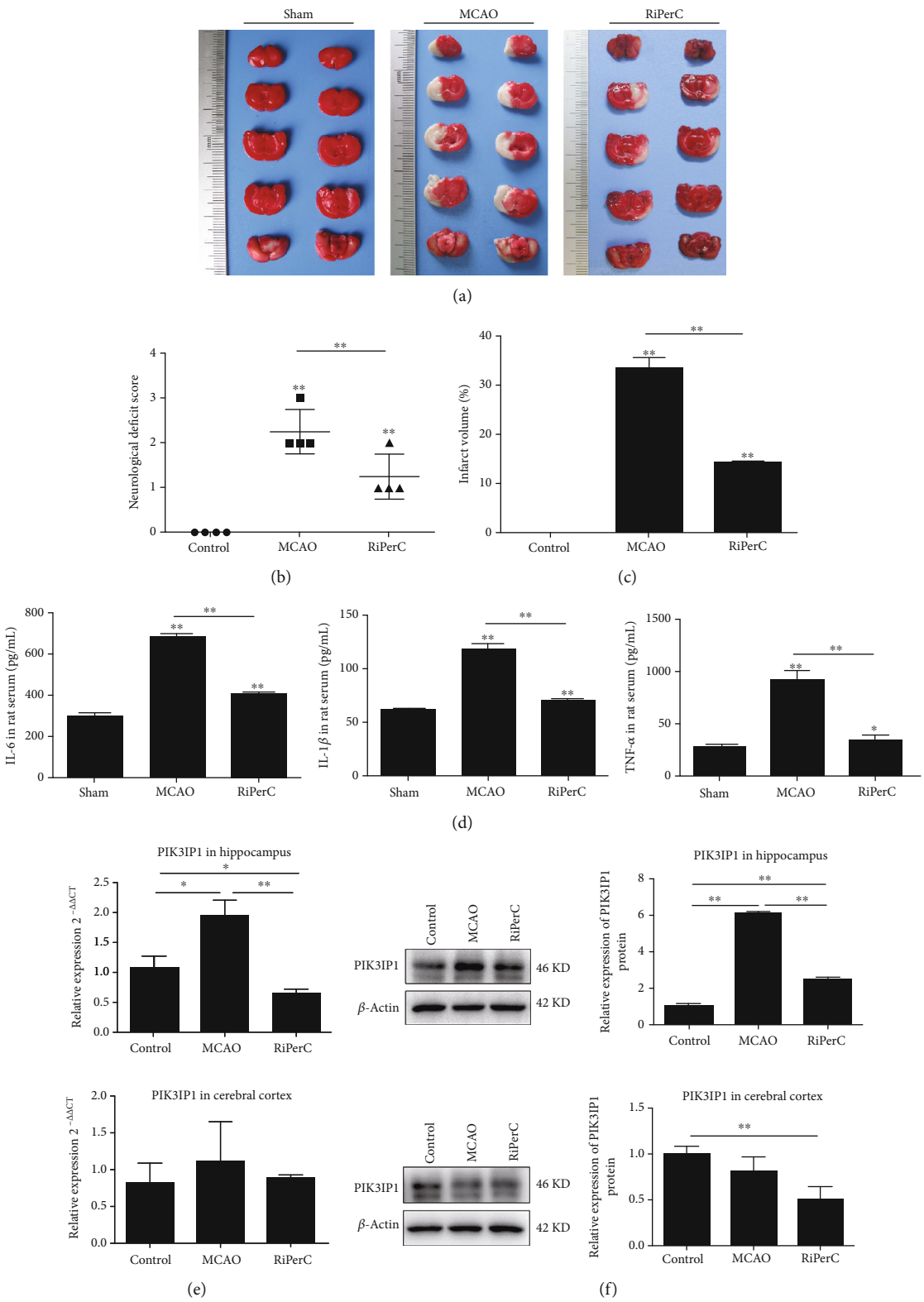


Figure 1: RiPerC reduced acute infarct damage in rat following MCAO. (a) Representative images of TTC staining in brain sections collected from rat receiving RiPerC operation at 1 day after reperfusion. (b) The neurological deficit score was assessed by the Longa scale scoring system at 1 day after reperfusion. (c) Quantitative data regarding the effects of the RiPerC operation on cerebral infarction as assessed by TTC histology at 1 day ($n = 4$ per group). (d) The expression of IL-1$\beta$, IL-6, and TNF-$\alpha$ in rat serum by ELISA. (e) The expression of PI3KIP1 in hippocampus and cerebral cortex by qPCR and WB.

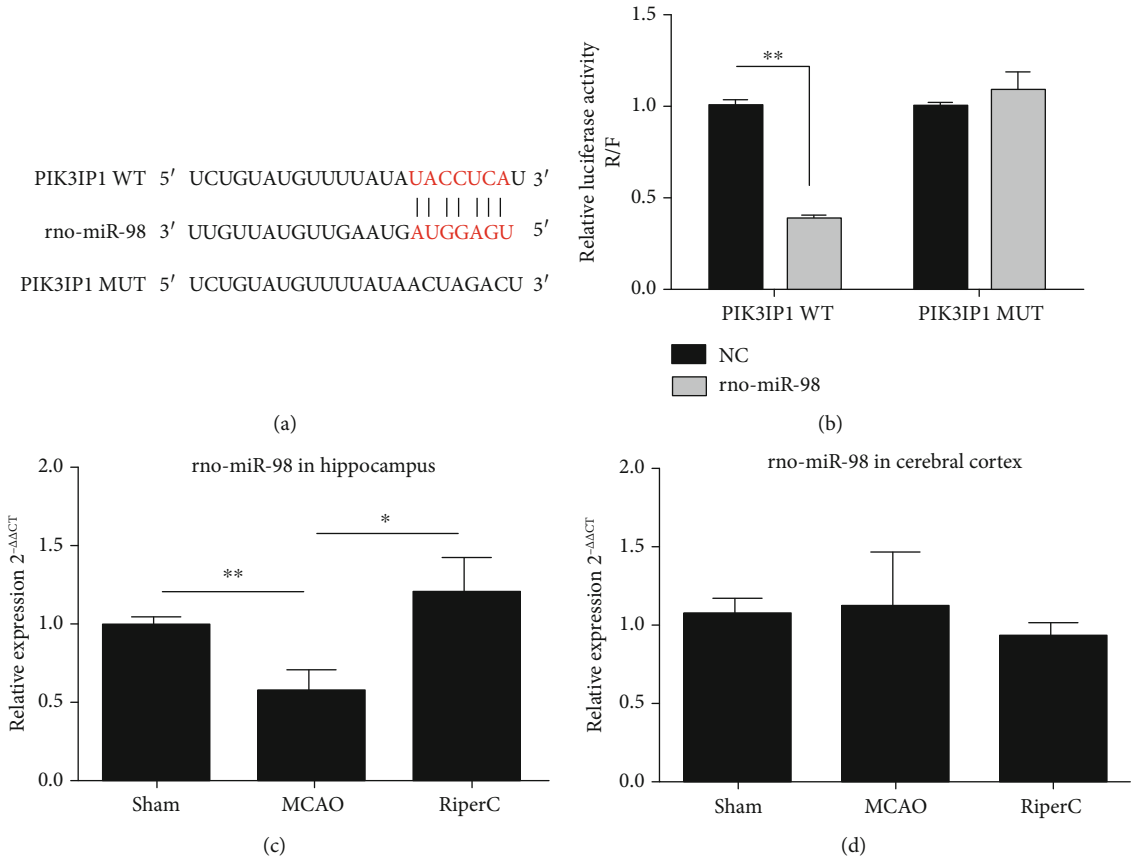


Figure 2: PIK3IP1 3′-UTR was directly targeted by miR-98. (a) Schema of the WT and mutated PIK3IP1 3′-UTR indicating the interaction sites between miR-98 and the 3′-UTR of PIK3IP1. (b) Dual luciferase assay in HEK293T cells cotransfected with the miR-98 mimic and reporter vectors containing either the wild-type or mutated 3′-UTR of PIK3IP1. (c) The miR-98 in rats hippocampus tissue detected by qPCR. (d) The miR-98 in rats cerebral cortex tissue detected by qPCR.

cells elevated in the RiPerC injected with miR-98 antagomir group (Figure 4(a)). Furthermore, Western blot assay was employed to detect the apoptosis-related proteins caspase-9, Bax, and Bcl-2 expression. The findings (Figure 4(b)) indicated that significant upregulation was detected in caspase-9 and Bax, and Bcl-2 was downregulation between the MCAO and the sham groups (all $P < 0.05$). In comparison to the MCAO injected with NC agomir group, caspase-9 and Bax reduced in the MCAO injected with miR-98 agomir group, accompanied by reduced Bcl-2 (all $P < 0.05$).

Compared with the RiPerC+NC antagomir group, TUNEL staining showed that the apoptosis rate in the RiPerC injected with miR-98 antagomir was significantly upregulated (Figure 4(a)). The protein expression of caspase 9, Bax, and Bcl-2 was detected by WB; the result showed that caspase 9 and Bax in RiPerC+miR-98 antagomir were upregulated, and Bcl-2 in RiPerC+miR-98 antagomir was downregulated when compare with RiPerC+NC antagomir.

*3.5. PI3K/Akt Signaling Pathway Was Modulated by miR-98/PIK3IP1 Axis in Cerebral Ischemic Injury In Vivo.* To further explore the molecular mechanism of miR-98 in regulating the development of cerebral ischemic injury, we investigated whether PI3K/Akt signaling pathway was involved in the progression of cerebral ischemic injury regulated by miR-98/PIK3IP1 axis. Western blot assay was carried out to detect the downstream genes of PI3K/Akt pathway in the cerebral ischemia injury, including PIK3IP1, PI3K, p-PI3K, Akt, and p-Akt (Figure 5(a)). The findings displayed that the phosphorylation of PI3K and Akt was decreased markedly after MCAO operation. Treatment with miR-98 agomir and RiPerC operation significantly increased the expression of p-PI3K and p-Akt. However, RiPerC operation group treatment with miR-98 antagomir decreased the expression of p-PI3K and p-Akt (Figures 5(b)–5(f)). These results revealed that miR-98 promoted, whereas PIK3IP1 inhibited the activation of PI3K/Akt pathway in rat hippocampus after cerebral ischemic injury, suggesting that miR-98 could activate the PI3K/Akt pathway by suppressing PIK3IP1 in cerebral ischemic injury.

## 4. Discussion

RiPerC by which the sublethal ischemic stimulus is administered during the ischemic event is beneficial after an acute stroke [23]. Both remote ischemic pre- and perconditioning have now been proven effective in animal models, and remote perconditioning was even found to be superior to

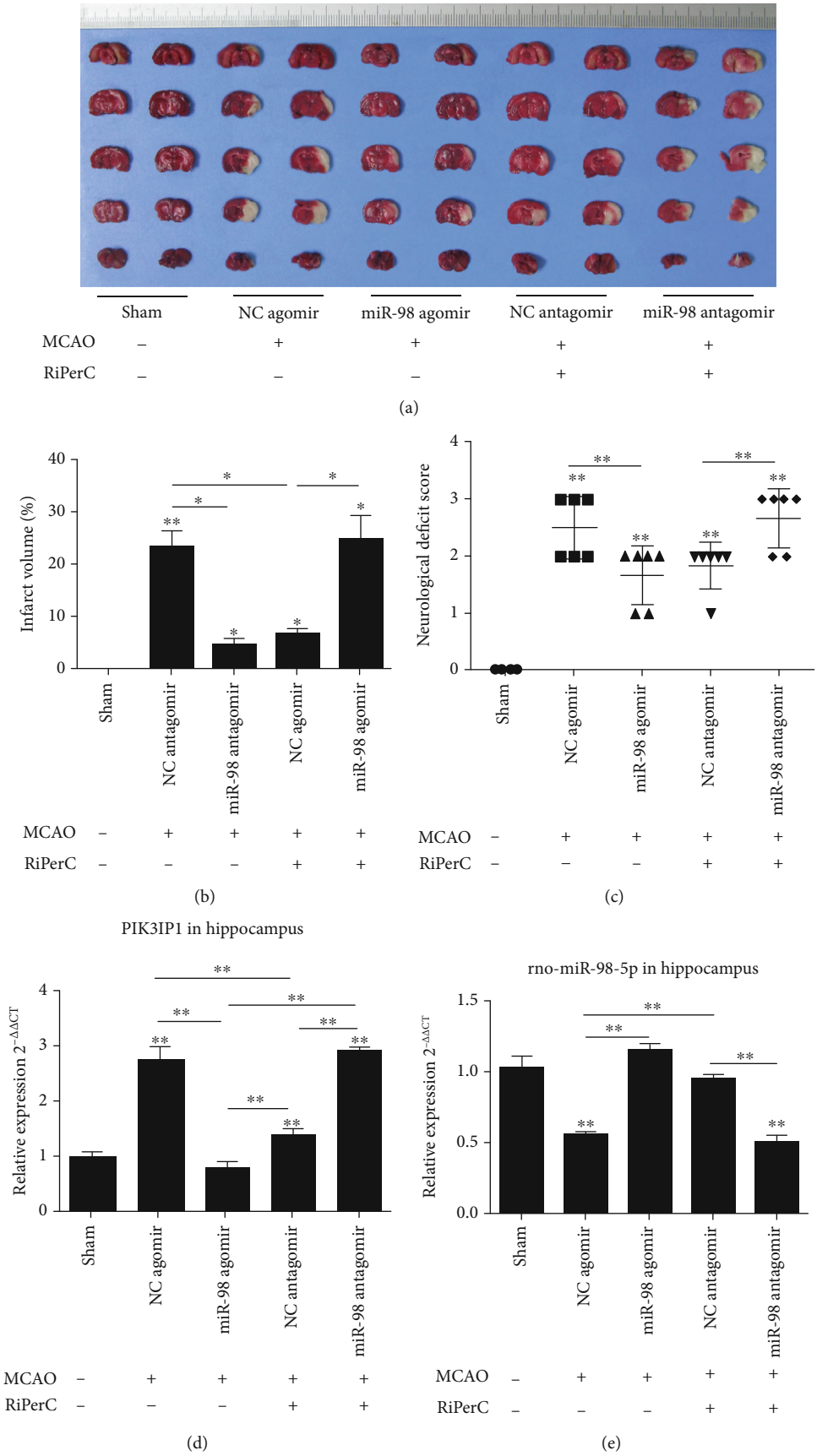


Figure 3: Continued.

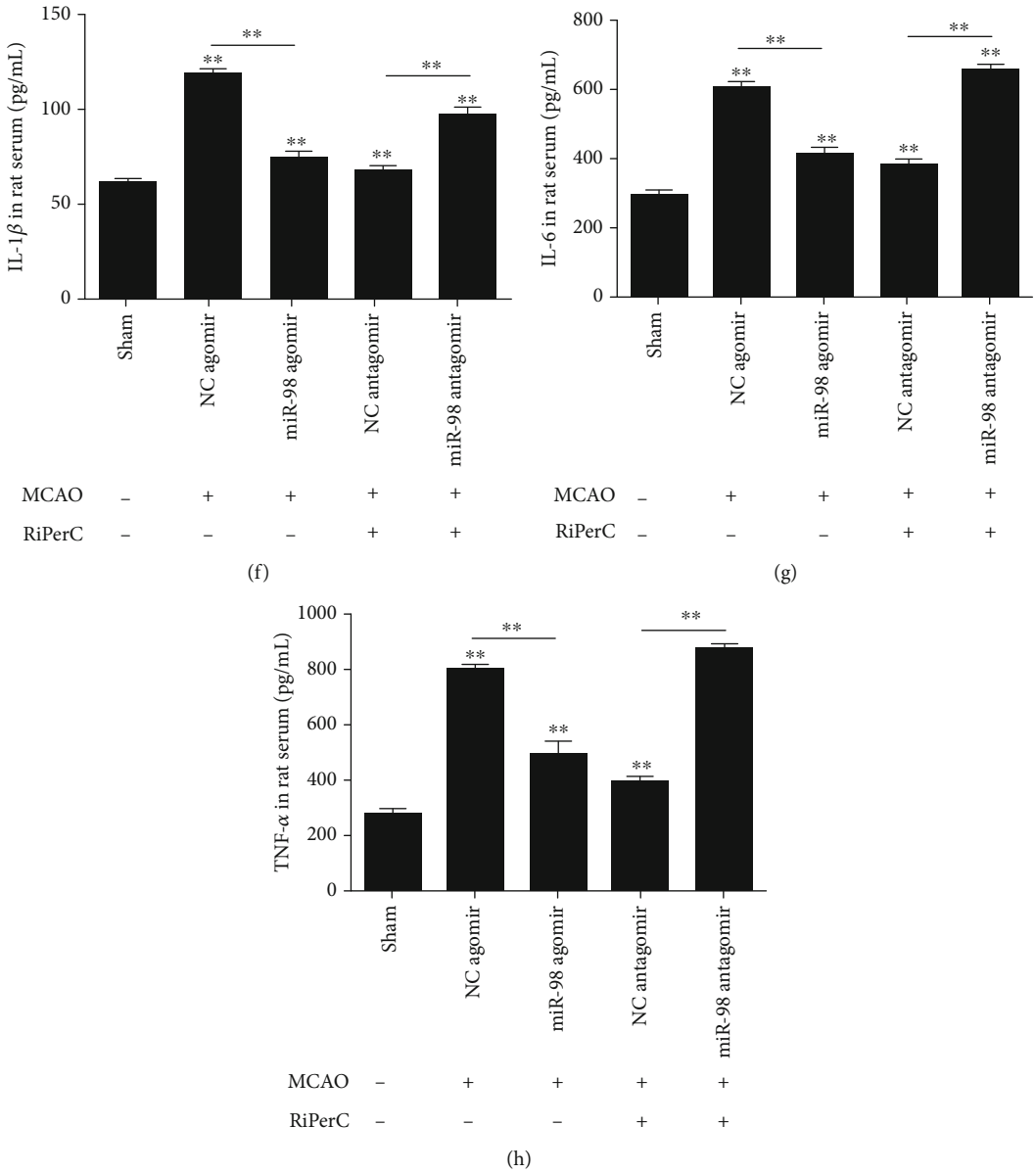


Figure 3: The miRNA-98 expression in hippocampus tissue plays a key role in cerebral ischemic injury. (a) Representative images of TTC staining in brain sections collected from rat receiving RiPerC operation or ICV injection at 1 day after reperfusion. (b) The neurological deficit score was assessed by the Longa scale scoring system at 1 day after reperfusion. (c) Quantitative data regarding the effects of the RiPerC operation on cerebral infarction as assessed by TTC histology at 1 day ($n = 4$ per group). (d, e) The expression of PI3KIP1 and miR-98 in hippocampus detected by qPCR. (f–h) The expression of IL-1$\beta$, IL-6, and TNF-$\alpha$ in rat serum by ELISA.

preconditioning [24, 25]. A potent endogenous protective mechanism of RiPerC is that ischemia induced in one organ leads to ischemic tolerance in other organs [26]. However, the regulatory mechanism of RiPerC relieve cerebral ischemic injury is still not completely clear.

PIK3IP1 is a transmembrane protein that possesses an intracellular domain homologous to the p85 regulatory subunit of PI3K, which downregulates PI3K activity by binding to a PI3K subunit through a specific domain [27]. It is abundantly expressed in many tissues, including the heart, liver, brain, and lung. It is reported that the overexpression of PIK3IP1 in mouse hepatocytes leads to a reduction in PI3K signaling and the suppression of hepatocyte carcinoma development [28]. PIK3IP1 participates in the PI3K pathway, which is in many cellular functions such as T cell activation, carcinogenesis, and apoptosis [29, 30]. Several studies have shown that silencing of PIK3IP1 increases PI3K activity in basal conditions [27]. In the present study, RiPerC significantly reduced neurobehavioral deficits and reduced the percentage of infarction volume, which is associated with downregulation of PI3KIP1 in ischemic perconditioning. The research of Shaurya et al. has been reported that let-7 represses PIK3IP1 in hypoxia myocytes in vitro [31]. Studies also showed that the expression patterns of a series of microRNAs in ischemic tissues had changed dramatically [32, 33]. To explore the signaling pathway of PIK3IP1-modulated

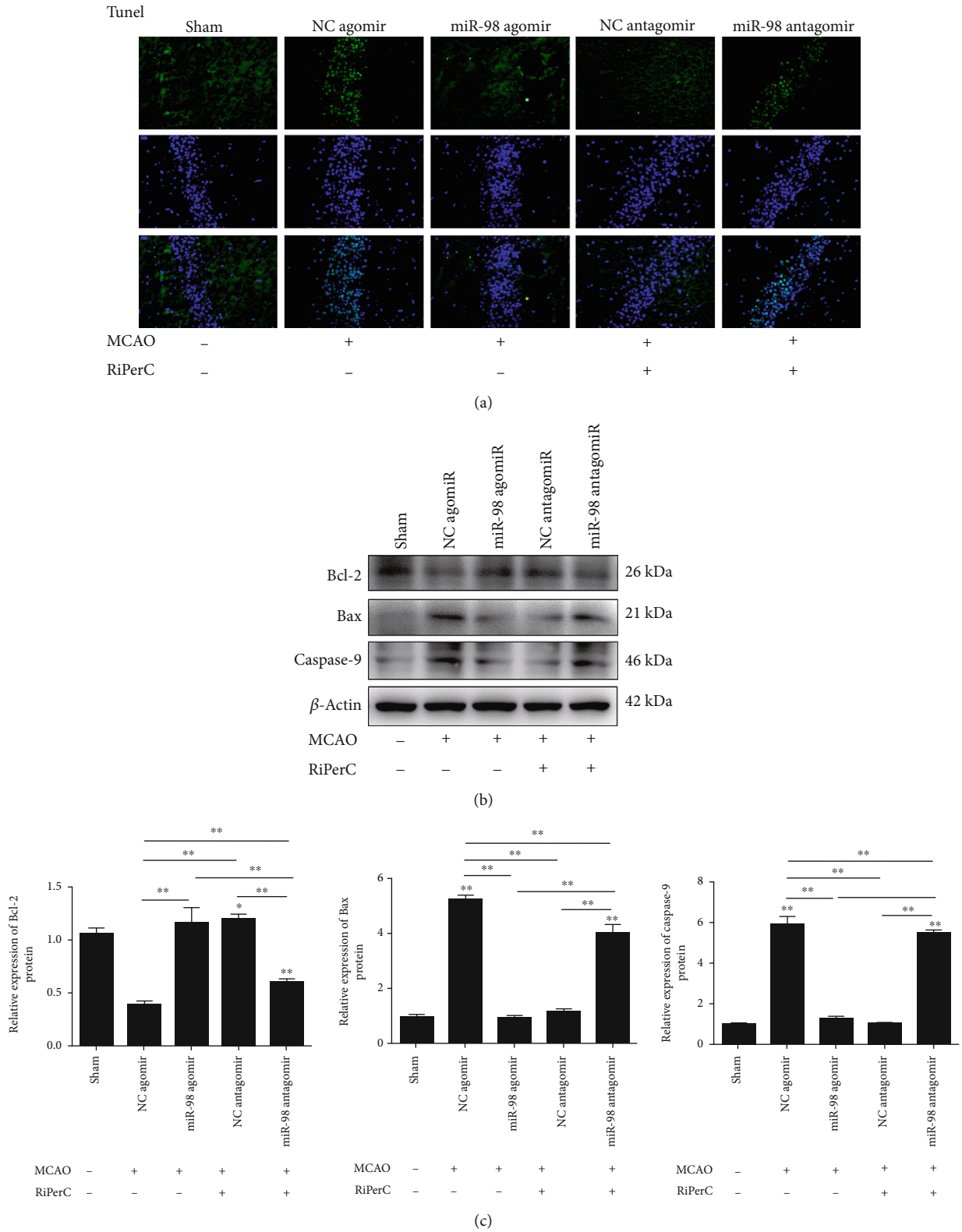


Figure 4: Suppression of miR-98 by decreased the neuronal apoptosis in RiPerC. (a) Brain cell apoptosis was detected by TUNEL assay. (b, c) The Western blot assay to measure the expression of apoptosis-related proteins in rat hippocampus tissue. $^{*}P < 0.05$, $^{**}P < 0.01$.

neuroinflammation, we identified the potential miRNA which targets PIK3IP1 by using the microRNA program (http://www.microrna.org/microrna/home.do). Among the predicted miRNAs, miR-98 was chosen as a candidate because it is reported to be involved in MCAO [34]. There have been several other studies reporting the altered

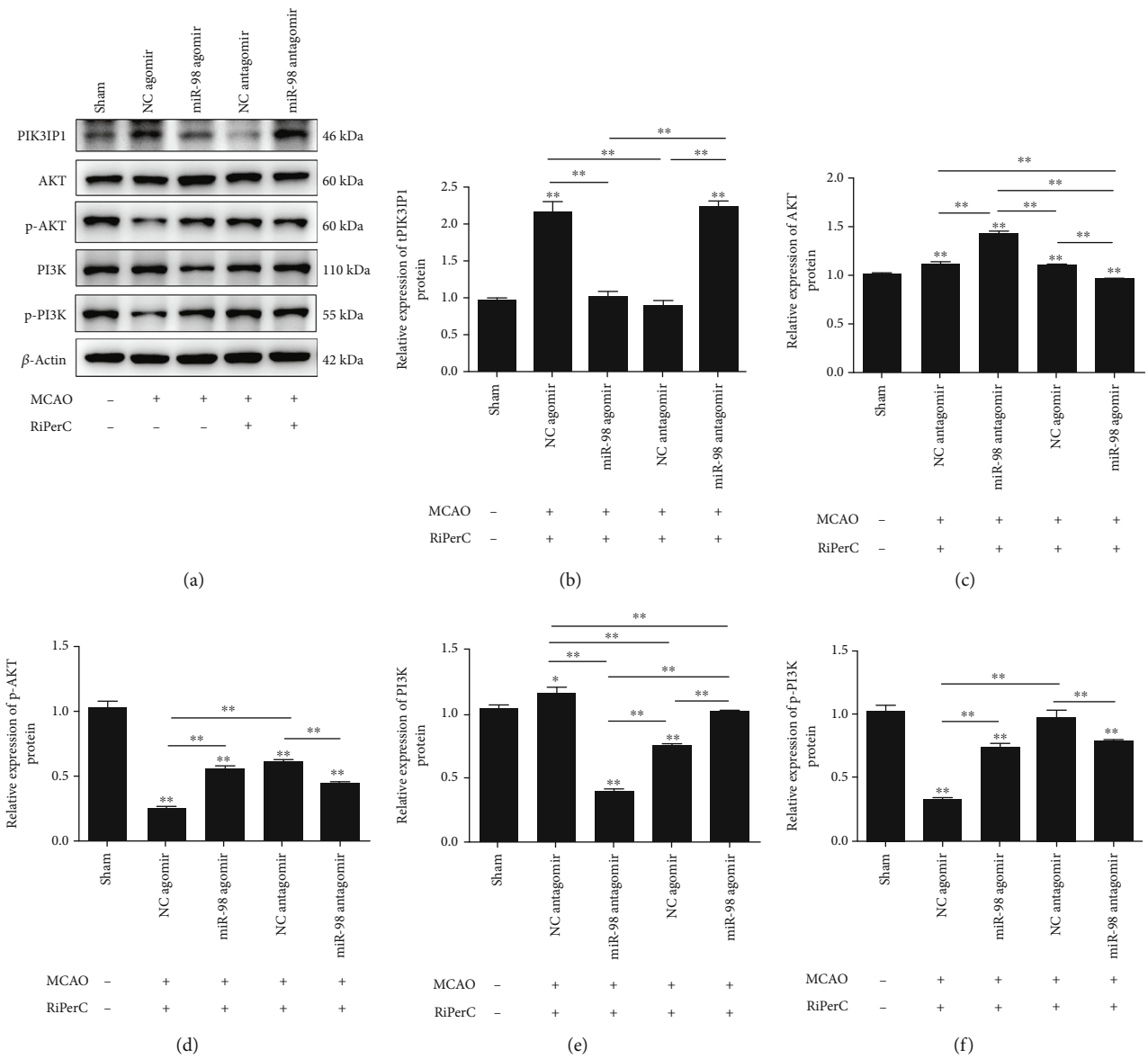


Figure 5: PI3K/Akt signaling pathway was modulated by miR-98/PIK3IP1 axis in cerebral ischemic injury in vivo. (a–f) The Western blot assay to measure the expression of PIK3IP1, AKT, p-AKT, PI3K, and p-PI3K proteins in rat hippocampus tissue. $^{*}P < 0.05$, $^{**}P < 0.01$.

expression of miR-98 during the ischemia injury [35, 36]. A study has shown that let-7/miR-98 regulated Fas expression and the sensitivity of Fas-mediated apoptosis [37]. In this study, we also found that miR-98 was downregulated in MCAO model group, then upregulated when rat received RiPerC operation. Meanwhile, our result indicated that RiPerC operation and the overexpression of miR-98 can reduce the apoptosis rate induced by cerebral ischemic injury in hippocampus tissue.

In order to explore whether miR-98 acts protective effects on cerebral ischemic injury, we made use of miR-98 agomir/-antagomir by ICV infusion to elevate miR-98 expression in rat hippocampus prior to MCAO/RiPerC+MCAO operation. As expected, overexpression of miR-98 significantly reduced the cerebral ischemic injury compared with the MCAO group, and inhibition of miR-98 significantly offsets the cerebral ischemic injury relief by RiPerC treatment. In addition, overexpression of miR-98 administration significantly decreased the number of TUNEL-positive cells in hippocampus tissue. These results indicated the protective effect of miR-98 in cerebral ischemic injury. Furthermore, the results showed that RiPerC relieve cerebral ischemic injury might be regulated through miR-98.

Studies have indicated that inflammatory response runs through the pathological development of cerebral ischemia-reperfusion and is one of the main causes of neuronal death [38]. Elevated proinflammatory cytokines aggregate a large number of inflammatory cells which secrete excessive inflammatory cytokines and aggravate brain damage [39]. Mo et al. found that OGD/R induced the expression of IL-1$\beta$, IL-6, and TNF-$\alpha$ in the supernatant of microglia [40]. In the results of Zhang et al., inflammatory factors, such as TNF-$\alpha$, IL-1$\beta$, IL-6, iNOS, CD32, and CD68, were markedly upregulated in the ischemic striatum at 24 h after reperfusion

in mice following MCAO [41]. In our study, we detected the proinflammatory cytokines IL-1$\beta$, IL-6, and TNF-$\alpha$ by ELISA. The results showed that IL-1$\beta$, IL-6, and TNF-$\alpha$ levels were increased in MCAO group, which is in line with the reports of Mo et al. and Zhang et al. Moreover, the levels of IL-1$\beta$, IL-6, and TNF-$\alpha$ were decreased when rats received RiPerC operation and miR-98 agomir injection.

The PI3K/AKT signaling pathway can inhibit apoptosis through the following pathways [42]: (1) increase the activity of antiapoptotic protein Bcl-2; (2) inhibition of the activation of aspartic acid-specific cysteine protease family members and inhibition of apoptosis induced by caspase-9; (3) inhibition of the expression of proapoptotic genes; (4) ATK activates IKK$\alpha$, leading to the degradation of NF-$\kappa$B inhibitor I$\kappa$B, which releases NF-$\kappa$B from the cytoplasm for nuclear translocation, activating its target genes and promoting cell survival. In our study, we find that miR-98 agomir and RiPerC operation significantly increased the expression of Bcl-2 and decreased the expression of Bax and caspase-9. When suppressing the expression of miR-98 in RiPerC group, the regulations of Bcl-2, Bax, and caspase-9 were all reversed. The results of apoptotic cell detected by TUNEL stain in each group were consistent with Bax and caspase-9 expression.

Studies have shown that PIK3IP1 can bind to PI3K, downregulate the activity of AKT, and inhibit the activation of AKT [28]. Our findings displayed that the phosphorylation of PI3K and AKT was decreased markedly after MCAO operation. Treatment with miR-98 agomir and RiPerC operation significantly decreased PIK3IP1 and increased the expression of p-PI3K and p-AKT. However, RiPerC operation group treatment with miR-98 antagomir decreased the expression of p-PI3K and p-AKT. Therefore, PIK3IP1 induce apoptosis by inhibiting the PI3K/AKT signaling pathway.

In conclusion, our results indicate that RiPerC operation significantly decreased the infarct volume; improved sensorimotor function; reduced the IL-1$\beta$, IL-6, and TNF-$\alpha$ level and PIK3IP1 expression; and improved the expression of miR-98. Furthermore, injected with miR-98 antagomir can offset the cerebral ischemia-reperfusion injury relief by RiPerC treatment. Therefore, our finding indicates that RiPerC inhibited the expression of PIK3IP1 by upregulated miR-98, thereby reducing the apoptosis induced by PIK3IP1 through the PI3K/AKT signaling pathway, thus reducing the cerebral ischemia-reperfusion injury.

## Data Availability

The data used to support the finding of this study are available from the corresponding author upon request.

## Conflicts of Interest

The authors declare that there is no conflict of interest regarding the publication of this article.

## Authors' Contributions

Dengwen Zhang and Li Mei contributed equally to this work.

## Acknowledgments

The authors research was supported by the project supported by the Natural Science Foundation of Guangdong, China (Grant no: 2018A0303130297); Science and Technology Program of Guangzhou, China (Grant no: 201904010080); and Foundation for Basic and Applied Basic Research of Guangdong Province (Grant no: 2019A1515110063).

## References

[1] D. C. Brooks and J. L. Schindler, "Perioperative stroke: risk assessment, prevention and treatment," *Current Treatment Options in Cardiovascular Medicine*, vol. 16, no. 2, p. 282, 2014.

[2] M. Sharifpour, L. E. Moore, A. M. Shanks, T. J. Didier, S. Kheterpal, and G. A. Mashour, "Incidence, predictors, and outcomes of perioperative stroke in noncarotid major vascular surgery," *Anesthesia and Analgesia*, vol. 116, no. 2, pp. 424–434, 2013.

[3] V. Carelli and D. C. Chan, "Mitochondrial DNA: impacting central and peripheral nervous systems," *Neuron*, vol. 84, no. 6, pp. 1126–1142, 2014.

[4] P. M. George and G. K. Steinberg, "Novel stroke therapeutics: unraveling stroke pathophysiology and its impact on clinical treatments," *Neuron*, vol. 87, no. 2, pp. 297–309, 2015.

[5] K. D. Hougaard, N. Hjort, D. Zeidler et al., "Remote ischemic perconditioning as an adjunct therapy to thrombolysis in patients with acute ischemic stroke: a randomized trial," *Stroke*, vol. 45, no. 1, pp. 159–167, 2014.

[6] J. Wang, D. Han, M. Sun, and J. Feng, "A combination of remote ischemic perconditioning and cerebral ischemic postconditioning inhibits autophagy to attenuate plasma HMGB1 and induce neuroprotection against stroke in rat," *Journal of Molecular Neuroscience*, vol. 58, no. 4, pp. 424–431, 2016.

[7] S. Y. Lim and D. J. Hausenloy, "Remote ischemic conditioning: from bench to bedside," *Frontiers in Physiology*, vol. 3, p. 27, 2012.

[8] W. Shi and J. Vinten-Johansen, "Endogenous cardioprotection by ischaemic postconditioning and remote conditioning," *Cardiovascular Research*, vol. 94, no. 2, pp. 206–216, 2012.

[9] J. Pan, X. Li, and Y. Peng, "Remote ischemic conditioning for acute ischemic stroke: dawn in the darkness," *Reviews in the Neurosciences*, vol. 27, no. 5, pp. 501–510, 2016.

[10] J. Ma, Y. Ma, B. Dong, M. V. Bandet, A. Shuaib, and I. R. Winship, "Prevention of the collapse of pial collaterals by remote ischemic perconditioning during acute ischemic stroke," *Journal of Cerebral Blood Flow and Metabolism*, vol. 37, no. 8, pp. 3001–3014, 2017.

[11] Y. H. Yan, S. H. Li, H. Y. Li, Y. Lin, and J. X. Yang, "Osthole protects bone marrow-derived neural stem cells from oxidative damage through PI3K/Akt-1 pathway," *Neurochemical Research*, vol. 42, no. 2, pp. 398–405, 2017.

[12] J. S. Yu and W. Cui, "Proliferation, survival and metabolism: the role of PI3K/AKT/mTOR signalling in pluripotency and cell fate determination," *Development*, vol. 143, no. 17, pp. 3050–3060, 2016.

[13] C. Lu, T. Ha, X. Wang et al., "The TLR9 ligand, CpG-ODN, induces protection against cerebral ischemia/ reperfusion injury via activation of PI3K/Akt signaling," *Journal of the American Heart Association*, vol. 3, article e000629, 2014.

[14] X. Xu, C. C. Chua, J. Gao et al., "Neuroprotective effect of humanin on cerebral ischemia/reperfusion injury is mediated by a PI3K/Akt pathway," *Brain Research*, vol. 1227, pp. 12–18, 2008.

[15] Zhiyan Wu, Y. Liang, and S. Yu, "Downregulation of microRNA-103a reduces microvascular endothelial cell injury in a rat model of cerebral ischemia by targeting AXIN2," *Journal of Cellular Physiology*, vol. 235, no. 5, pp. 4720–4733, 2020.

[16] X. K. Zuo, J. F. Lu, A. Manaenko et al., "MicroRNA-132 attenuates cerebral injury by protecting blood-brain-barrier in MCAO mice," *Experimental Neurology*, vol. 316, pp. 12–19, 2019.

[17] Q. Hu, A. Manaenko, H. Bian et al., "Hyperbaric oxygen reduces infarction volume and hemorrhagic trans-formation through ATP/NAD (+)/Sirt1 pathway in hyperglycemic middle cerebral artery occlusion rats," *Stroke*, vol. 48, no. 6, pp. 1655–1664, 2017.

[18] G. P. Morris, A. L. Wright, R. P. Tan, A. Gladbach, L. M. Ittner, and B. Vissel, "A comparative study of variables influencing ischemic injury in the Longa and Koizumi methods of intraluminal filament middle cerebral artery occlusion in rat," *PLoS One*, vol. 11, no. 2, article e0148503, 2016.

[19] T. D. Schmittgen and K. J. Livak, "Analyzing real-time PCR data by the comparative C(T) method," *Nature Protocols*, vol. 3, no. 6, pp. 1101–1108, 2008.

[20] Z. Lai, L. Zhang, J. Su, D. Cai, and Q. Xu, "Sevoflurane postconditioning improves long-term learning and memory of neonatal hypoxia-ischemia brain damage rats via the PI3K/Akt-mPTP pathway," *Brain Research*, vol. 1630, pp. 25–37, 2016.

[21] H. He, W. Liu, Y. Zhou et al., "Sevoflurane post-conditioning attenuates traumatic brain injury-induced neuronal apoptosis by promoting autophagy via the PI3K/AKT signaling pathway," *Drug Design, Development and Therapy*, vol. 12, pp. 629–638, 2018.

[22] Z. Zhuang, X. Zhao, Y. Wu et al., "The anti-apoptotic effect of PI3K-Akt signaling pathway after subarachnoid hemorrhage in rats," *Annals of Clinical and Laboratory Science*, vol. 41, no. 4, pp. 364–372, 2011.

[23] M. R. Schmidt, M. Smerup, I. E. Konstantinov et al., "Intermittent peripheral tissue ischemia during coronary ischemia reduces myocardial infarction through a KATP-dependent mechanism: first demonstration of remote ischemic perconditioning," *American Journal of Physiology. Heart and Circulatory Physiology*, vol. 292, no. 4, pp. H1883–H1890, 2007.

[24] C. D. Hahn, C. Manlhiot, M. R. Schmidt, T. T. Nielsen, and A. N. Redington, "Remote ischemic per-conditioning: a novel therapy for acute stroke?," *Stroke*, vol. 42, pp. 2960–2962, 2011.

[25] C. Ren, X. Gao, G. K. Steinberg, and H. Zhao, "Limb remote-preconditioning protects against focal ischemia in rats and contradicts the dogma of therapeutic time windows for preconditioning," *Neuroscience*, vol. 151, no. 4, pp. 1099–1103, 2008.

[26] K. Przyklenk, B. Bauer, M. Ovize, R. A. Kloner, and P. Whittaker, "Regional ischemic 'preconditioning' protects remote virgin myocardium from subsequent sustained coronary occlusion," *Circulation*, vol. 87, no. 3, pp. 893–899, 1993.

[27] Z. Zhu, X. He, C. Johnson et al., "PI3K is negatively regulated by PIK3IP1, a novel p110 interacting protein," *Biochemical and Biophysical Research Communications*, vol. 358, no. 1, pp. 66–72, 2007.

[28] X. He, Z. Zhu, C. Johnson et al., "PIK3IP1, a negative regulator of PI3K, suppresses the development of hepatocellular carcinoma," *Cancer Research*, vol. 68, no. 14, pp. 5591–5598, 2008.

[29] M. C. DeFrances, D. R. Debelius, J. Cheng, and L. P. Kane, "Inhibition of T-cell activation by PIK3IP1," *European Journal of Immunology*, vol. 42, no. 10, pp. 2754–2759, 2012.

[30] P. Gao, W. T. Zeng, W. W. Deng, N. Li, T. P. Shi, and D. L. Ma, "Both PIK3IP1 and its novel found splicing isoform, PIK3IP1-v1, are located on cell membrane and induce cell apoptosis," *Beijing Da Xue Xue Bao. Yi Xue Ban*, vol. 40, pp. 572–577, 2008.

[31] S. Joshi, J. Wei, and N. H. Bishopric, "A cardiac myocyte-restricted Lin28/let-7 regulatory axis promotes hypoxia-mediated apoptosis by inducing the AKT signaling suppressor PIK3IP1," *Biochimica et Biophysica Acta*, vol. 1862, no. 2, pp. 240–251, 2016.

[32] A. Dharap, K. Bowen, R. Place, L. C. Li, and R. Vemuganti, "Transient focal ischemia induces extensive temporal changes in rat cerebral microRNAome," *Journal of Cerebral Blood Flow and Metabolism*, vol. 29, no. 4, pp. 675–687, 2009.

[33] K. Jeyaseelan, K. Y. Lim, and A. Armugam, "MicroRNA expression in the blood and brain of rats subjected to transient focal ischemia by middle cerebral artery occlusion," *Stroke*, vol. 39, no. 3, pp. 959–966, 2008.

[34] D. L. Bernstein, V. Zuluaga-Ramirez, S. Gajghate et al., "miR-98 reduces endothelial dysfunction by protecting blood-brain barrier (BBB) and improves neurological outcomes in mouse ischemia/reperfusion stroke model," *Journal of Cerebral Blood Flow & Metabolism*, vol. 10, 2019.

[35] U. B. Hendgen-Cotta, D. Messiha, S. Esfeld, R. Deenen, T. Rassaf, and M. Totzeck, "Inorganic nitrite modulates miRNA signatures in acute myocardial in vivo ischemia/reperfusion," *Free Radical Research*, vol. 51, no. 1, pp. 91–102, 2017.

[36] J. Li, Z. Pierre Arany, and M. Eghbali, "Implication of miR-98 in the cardiac vulnerability of pregnancy to ischemia reperfusion injury," *Circulation Research*, vol. 115, article A342, 2014.

[37] S. Wang, Y. Tang, H. Cui et al., "Let-7/miR-98 regulate Fas and Fas-mediated apoptosis," *Genes and Immunity*, vol. 12, no. 2, pp. 149–154, 2011.

[38] L. Su, R. Zhang, Y. Chen, Z. Zhu, and C. Ma, "Raf kinase inhibitor protein attenuates ischemia induced microglia cell apoptosis and activation through nf-kappab pathway," *Cellular Physiology and Biochemistry*, vol. 41, no. 3, pp. 1125–1134, 2017.

[39] H. C. Koennecke, W. Belz, D. Berfelde et al., "Factors influencing in hospital mortality and morbidity in patients treated on a stroke unit," *Neurology*, vol. 77, pp. 965–972, 2011.

[40] Z. T. Mo, Y. L. Liao, J. Zheng, and W. N. Li, "Icariin protects neurons from endoplasmic reticulum stress-induced apoptosis after OGD/R injury via suppressing IRE1$\alpha$-XBP1 signaling pathway," *Life Sciences*, vol. 26, article 117847, 2020.

[41] Z. Yuan, S. Yi-Yun, and Y. Hai-Yan, "Triad3A displays a critical role in suppression of cerebral ischemic/reperfusion (I/R) injury by regulating necroptosis," *Biomedicine & Pharmacotherapy*, vol. 24, p. 128, 2020.

[42] H. K. Song, J. Kim, J. S. Lee et al., "Pik3ip1 modulates cardiac cypertrophy by inhibiting PI3K pathway," *Plos One*, vol. 10, no. 3, article e0122251, 2015.

Hindawi
Oxidative Medicine and Cellular Longevity
Volume 2020, Article ID 5780703, 15 pages
https://doi.org/10.1155/2020/5780703

*Research Article*

# Network Pharmacology Analysis and Molecular Characterization of the Herbal Medicine Formulation Qi-Fu-Yin for the Inhibition of the Neuroinflammatory Biomarker iNOS in Microglial BV-2 Cells: Implication for the Treatment of Alzheimer's Disease

**Fung Yin Ngo,[1] Weiwei Wang,[1,2] Qilei Chen,[3] Jia Zhao,[1] Hubiao Chen,[3] Jin-Ming Gao,[2] and Jianhui Rong[1,4]**

[1]*School of Chinese Medicine, The University of Hong Kong, Hong Kong 999077, China*
[2]*Shaanxi Key Laboratory of Natural Products & Chemical Biology, College of Chemistry & Pharmacy, Northwest A&F University, Yangling 712100, China*
[3]*School of Chinese Medicine, Hong Kong Baptist University, Hong Kong 999077, China*
[4]*Shenzhen Institute of Research and Innovation, The University of Hong Kong, Shenzhen 518057, China*

Correspondence should be addressed to Jin-Ming Gao; jinminggao@nwsuaf.edu.cn and Jianhui Rong; jrong@hkucc.hku.hk

Received 10 June 2020; Accepted 12 August 2020; Published 1 September 2020

Academic Editor: Shi Yuan Xu



Aberrant microglial activation drives neuroinflammation and neurodegeneration in Alzheimer's disease (AD). The present study is aimed at investigating whether the herbal formula Qi-Fu-Yin (QFY) could inhibit the inflammatory activation of cultured BV-2 microglia. A network pharmacology approach was employed to predict the active compounds of QFY, protein targets, and affected pathways. The representative pathways and molecular functions of the targets were analyzed by Gene Ontology (GO) and pathway enrichment. A total of 145 active compounds were selected from seven herbal ingredients of QFY. Targets (e.g., MAPT, APP, ACHE, iNOS, and COX-2) were predicted for the selected active compounds based on the relevance to AD and inflammation. As a validation, fractions were sequentially prepared by aqueous extraction, ethanolic precipitation, and HPLC separation, and assayed for downregulating two key proinflammatory biomarkers iNOS and COX-2 in lipopolysaccharide-(LPS-) challenged BV-2 cells by the Western blotting technique. Moreover, the compounds of QFY in 90% ethanol downregulated iNOS in BV-2 cells but showed no activity against COX-2 induction. Among the herbal ingredients of QFY, Angelicae Sinensis Radix and Ginseng Radix et Rhizoma contributed to the selective inhibition of iNOS induction. Furthermore, chemical analysis identified ginsenosides, especially Rg3, as antineuroinflammatory compounds. The herbal formula QFY may ameliorate neuroinflammation via downregulating iNOS in microglia.

## 1. Introduction

Alzheimer's disease (AD) is the major neurodegenerative cause of progressive dementia in the elderly [1]. The pathology of AD is hallmarked by the accumulation of extracellular $\beta$-amyloid (A$\beta$) and the formation of peptide plaques and intraneuronal tau lesions, resulting in impaired neurotransmission and neuronal death [2]. Among the existing pharmacological anti-AD interventions, acetylcholinesterase inhibitors are known to restore cholinergic neurotransmission, whereas *N*-methyl-D-aspartate (NMDA) receptor antagonists suppress the neuronal excitability towards NMDA [3]. However, some controversial results showed that these agents barely prevented the progression of AD and could cause adverse effects [4]. Nevertheless, neurotoxic peptide A$\beta$ activates microglia and exacerbates neuroinflammation, leading to

the onset and progression of AD [5, 6]. Indeed, the overexpression of proinflammatory enzymes such as inducible nitric oxide synthase (iNOS) and cyclooxygenase-2 (COX-2) jeopardizes the survival of neurons in brains [7]. Notably, excessive nitric oxide in the brain induced oxidative damage in neurons and led to the activation of apoptosis [8]. Therefore, effective inhibition of neuroinflammation represents a key strategy for the management of AD, but the in vivo efficacies of antineuroinflammatory and microglia-targeting agents remain uncertain [9].

Traditional herbal medicines may serve as alternative therapeutic strategies against various multifactorial and complex chronic diseases including AD [10]. The herbal formula Qi-Fu-Yin (QFY) was documented for managing dementia four hundred years ago [11]. The formula QFY is composed of seven herbal ingredients, namely, Atractylodis Macrocephalae Rhizoma (Baizhu, BZ), Angelicae Sinensis Radix (Danggui, DG), Glycyrrhizae Radix et Rhizoma (Gancao, GC), Ginseng Radix et Rhizoma (Renshen, RS), Rehmanniae Radix Preparata (Shudi, SD), Ziziphi Spinosae Semen (Suanzaoren, SZR), and Polygalae Radix (Yuanzhi, YZ). Previous studies showed that QFY improved learning and memory of AD rodents via increasing somatostatin in the hippocampus, reducing A$\beta$ accumulation and proinflammatory biomarkers in mouse brains [12–14]. Comprehensive chemical profiling of QFY and a modified QFY formula with two additional herbs identified active compounds that were neuroprotective or exhibited a therapeutic effect towards AD [15, 16]. Several other studies also suggested the antineuroinflammatory action of GC, RS, and YZ via modulating microglial activity [17–19]. However, effort is needed to elucidate the molecular mechanisms by which QFY modulates microglial activation within the context of AD.

The aim of the present study was to characterize the antineuroinflammatory activity of QFY. We employed a network pharmacology approach to analyze the compound-target interactions of QFY and the relevant signaling pathways. We further validated the antineuroinflammatory property in microglial BV-2 cell culture and identified the principal active compounds through a bioactivity-guided fractionation procedure.

## 2. Materials and Methods

*2.1. Chemicals and Reagents.* The dried aqueous extracts of seven QFY ingredients were manufactured by Nong's Pharmaceutical Ltd., Hong Kong. Dulbecco's modified Eagle's medium (DMEM), fetal bovine serum (FBS), and penicillin/streptomycin solution were purchased from Invitrogen (Carlsbad, CA, USA). Protein assay dye reagent concentrate was purchased from Bio-Rad (Hercules, CA, USA). Lipopolysaccharide (LPS), RIPA assay buffer, protease inhibitor cocktail, and anti-rabbit horseradish peroxidase- (HRP-) conjugated IgG secondary antibody were purchased from Sigma-Aldrich (St. Louis, MO, USA). An antibody against iNOS was purchased from Abcam (Cambridge, UK). Antibodies against COX-2 and GAPDH were purchased from Cell Signaling Technology (Boston, MA, USA). Anti-mouse HRP-conjugated IgG was purchased from Santa Cruz Biotechnology (Santa Cruz, CA, USA). An enhanced chemiluminescence (ECL) detection reagent was purchased from GE Healthcare (Uppsala, Sweden). Ginsenoside Rg3 with the purity of >98% was purchased from Nanjing Spring and Autumn Biological Engineering Company (Nanjing, China).

*2.2. Identification of the Active Compounds in the Formulation QFY.* The chemical compounds were selected from the herbs of QFY in the databases of TCMSP (https://tcmspw.com/) based on the oral bioavailability ($OB$) ≥ 30%, drug-likeness ($DL$) ≥ 0.18, and blood-brain barrier ($BBB$) ≥ −0.3. On the other hand, the compounds in the herbal ingredient not found in TCMSP were selected from the database of TCMID (http://www.megabionet.org/tcmid/) when the compounds possessed the blood-brain barrier (BBB) permeability of ≥-1 through checking pkCSM (http://biosig.unimelb.edu.au/pkcsm/) and did not violate more than one of the criteria stated in Lipinski's rule of five. In addition, the active compounds were collected by text mining.

*2.3. Prediction of Protein Targets.* The active compounds in the formulation QFY were loaded to the Similarity Ensemble Approach (SEA) at http://sea.bkslab.org, the Search Tool for Interactions of Chemicals (STITCH) at http://stitch.embl.de, and SwissTargetPrediction at http://swisstargetprediction.ch for the prediction of the corresponding biological targets. The AD-related targets after checking Molecule Annotation System 3 (MAS 3.0) at http://bioinfo.capitalbio.com/mas3, Therapeutic Targets Database (TTD) at http://bidd.nus.edu.sg/group/cjttd/, and Comparative Toxicogenomics Database (CTD) at http://ctdbase.org/ were retained for further study.

*2.4. Gene Ontology and Pathway Enrichment Analysis.* The selected targets were analyzed for the enriched Gene Ontology (GO) terms and the Kyoto Encyclopedia of Genes and Genomes (KEGG) pathway using the online bioinformatics tool DAVID 6.8 at http://david.ncifcrf.gov. The annotations with adjusted $p < 0.05$ were considered significantly enriched.

*2.5. Visualization of the Compound-Target Interaction and the Target-Pathway Relationship.* The interaction networks were visualized using the open software package Cytoscape (http://www.cytoscape.org/). For the compound-target interactions, the active compounds in QFY and the corresponding protein targets were presented in a compound-target (C-T) network. For the target-pathway interactions, the targets and the related pathways were presented in a target-pathway (T-P) network.

*2.6. Microglial BV-2 Cell Culture and Treatment.* The murine microglial cell line BV-2 was purchased from the American Type Culture Collection (Manassas, VA, USA) and cultured in DMEM supplemented with 10% heat-inactivated FBS and 1% penicillin/streptomycin solution. The cells were incubated at an atmosphere with 5% $CO_2$ at 37°C. For the indicated treatments, BV-2 cells were plated in 6-well plates at a density of $2 \times 10^5$/mL overnight. BV-2 cells were treated with herbal extracts as indicated and costimulated with 0.1 $\mu$g/mL LPS in DMEM supplemented with 3% FBS for 24 hours.

*2.7. Fractionation of Herbal Extracts.* QFY was prepared by mixing the dried aqueous extracts of seven herbal ingredients: BZ, 1.6 g; DG, 3 g; GC, 0.6 g; RS, 1.2 g; SD, 1.8 g; SZR, 1.2 g; and YZ, 1 g. Following extraction with distilled water at 80°C for 30 min, the mixture was cooled to room temperature and centrifuged at 13,000 rpm for 10 min. The supernatant was recovered and precipitated with ethanol at the final concentrations of 50%, 75%, and 90% overnight at 4°C. After centrifugation at 6,000 rpm for 30 min, the supernatant was collected to yield the corresponding ethanol solutions of QFY. The ethanolic materials were dried with a rotary evaporator, dissolved in DMSO, and sterilized by passing through a 0.22 $\mu$m syringe filter for bioassays. For HPLC separation, the compounds were separated on an ACE C18 HPLC column (250 × 4.6 mm, 5 $\mu$m) from Advanced Chromatography Technologies Ltd. (Aberdeen, Scotland, UK) under the control of the Waters Controller 600S HPLC system coupled with a photodiode array detector (Waters, Milford, MA, USA). The column temperature was maintained at 25°C. The mobile phases of (A) methanol and (B) 0.1% aqueous formic acid were pumped into the column at a flow rate of 1.0 mL/min to form the gradient as follows: 0-25 min, 5-50% A; 25-45 min, 50-70% A; 45-47 min, 70-95% A; and 47-53 min, 95% A. The fractions were collected, dried, and dissolved in DMSO for subsequent bioassays.

*2.8. Western Blot Analysis.* After drug treatment as indicated, BV-2 cells were washed twice with cold PBS and lysed with cold RIPA buffer to collect the cellular proteins. The cellular proteins (30 $\mu$g) from each sample were resolved by 12% SDS-polyacrylamide gel electrophoresis and transferred to a polyvinylidene difluoride (PVDF) membrane. After overnight blocking with 5% non-fat milk, the membranes were probed with primary antibodies against iNOS, COX-2, and GAPDH overnight. The bound antibodies were detected with the HRP conjugate of the corresponding anti-rabbit or anti-mouse secondary antibodies for 2 hours. The activity of HRP was detected with ECL detection reagents. The blots were quantified by a densitometric method using the NIH ImageJ software.

*2.9. Chemical Profiling by the LC-MS/MS System.* The Agilent 6540 Ultra High Definition (UHD) Accurate-Mass Q-TOF LC/MS system from Agilent Technologies (Santa Clara, CA, USA) was used for mass spectrometry analysis. The compounds in 10 $\mu$L were injected and separated on an ACE C18 HPLC column at a flow rate of 1.0 mL/min and column temperature of 40°C, by using the same gradient from the mobile phases of (A) 0.1% formic acid in water and (B) methanol as described for HPLC. The MS parameters were set as follows: electrospray ionization source (ESI) in a negative mode, nitrogen ($N_2$) as drying gas, flow rate at 8 L/min, gas temperature at 300°C, nebulizer at 40 psi, sheath gas temperature at 350°C, flow rate of sheath gas at 8 L/min, capillary voltage at 4.0 kV, end plate offset at -500 V, fragmentor at 150 V, skimmer at 65 V, Oct RF Vpp at 600 V, scan range of 100-1700 m/z, and collision energy at 25 V for MS and 45 V for MS/MS, respectively. The data was analyzed on Agilent MassHunter Qualitative Analysis B.06.00 and Agilent MassHunter Quantitative Analysis B.06.00 from Agilent Technologies (Santa Clara, CA, USA).

*2.10. Statistical Analysis.* Data was presented as *mean* ± *SD* of three replicates. The difference between two groups was analyzed by one-way ANOVA and Tukey's multiple comparison using the GraphPad Prism 7 software (La Jolla, CA, USA). A $p$ value of <0.05 was considered statistically significant.

## 3. Results

*3.1. QFY Targets Key Proteins in Inflammation and AD Pathogenesis.* To characterize the biological targets of QFY in a comprehensive manner, we employed a network pharmacology approach to dissect the complex multicompound and multitarget interaction. A total of 812 compounds in QFY were firstly retrieved from TCMSP and TCMID. Based on the pharmacokinetic or physiochemical properties, 126 active compounds were obtained while another 19 compounds were added by searching the PubMed database for the implications in the treatment of AD. The nomenclature of the active compounds was guided by PubChem, and the detailed information is listed in Supplementary Tables 1 and 2. The active compounds were further classified by the Medical Subject Headings (MeSH) classification system and text mining. The candidate compounds were chemically categorized into flavonoids, terpenoids, alkaloids, xanthones, phenylpropanoids, lipids, glycosides, carboxylic acids, phenolic compound, and amino acids. The protein targets were fished out using various predictive models (e.g., SEA, STITCH, and SwissTargetPrediction). As shown in Figure 1(a), 25 protein targets formed a total of 213 interactions with 96 active compounds. Specifically, MAPT as an important pathological target in AD showed the highest connectivity with 56 of the active compounds. Several active compounds in QFY showed interactions with other AD-relevant mediators (e.g., BACE1, APP, and SNCA), cholinergic neurotransmission (e.g., ACHE, CHRM1, CHRNA4, and CHRNB2), and inflammation (e.g., COX-2, eNOS, and iNOS). For the target-pathway network as shown in Figure 1(b), the protein targets were mapped to 14 different biological pathways or diseases in KEGG. Six protein targets (i.e., MAPT, BACE1, APP, SNCA, MAOA, and MAOB) were categorized in "Alzheimer's disease," and five targets (i.e., ACHE, CHRM1, CHRNA4, CHRNB2, and FOS) were grouped to "cholinergic synapse," while another three targets (i.e., CASP8, FOS, and COX-2) were grouped to "TNF signaling pathway".

To characterize the functional annotations of the protein targets, Gene Ontology (GO) and KEGG pathway enrichment analysis were carried out on the online bioinformatics tool DAVID. As shown in Figure 2, the inflammation- or AD-related GO terms appeared in the ten most significantly enriched GO terms from "biological process" and "molecular function," in particular, acetylcholinesterase activity (GO: 0003990), amyloid-beta binding (GO: 0001540), and response to lipopolysaccharide (GO: 0032496). The three most significantly enriched KEGG pathways were Alzheimer's disease (KEGG: hsa05010), cholinergic neurotransmission pathway

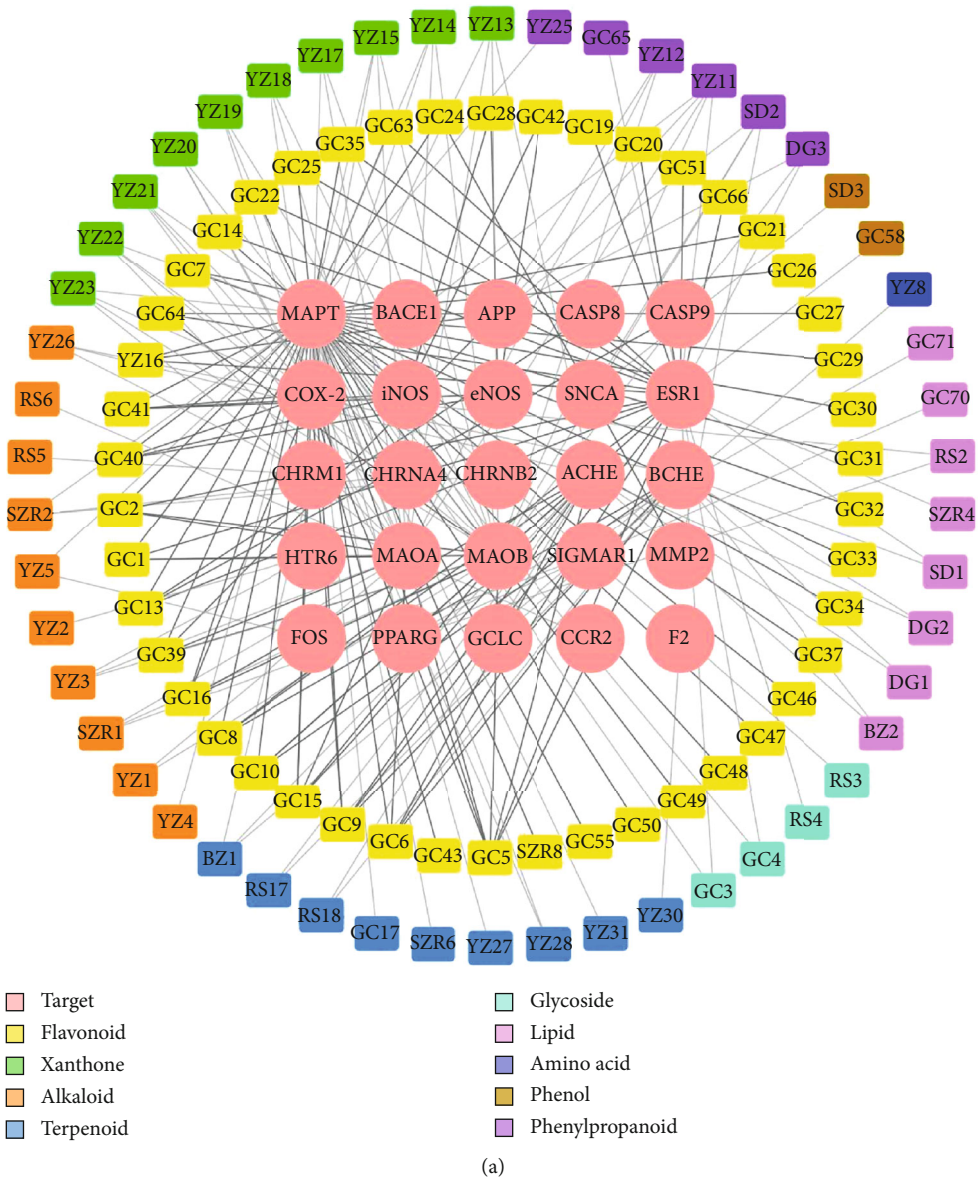


(a)

Figure 1: Continued.

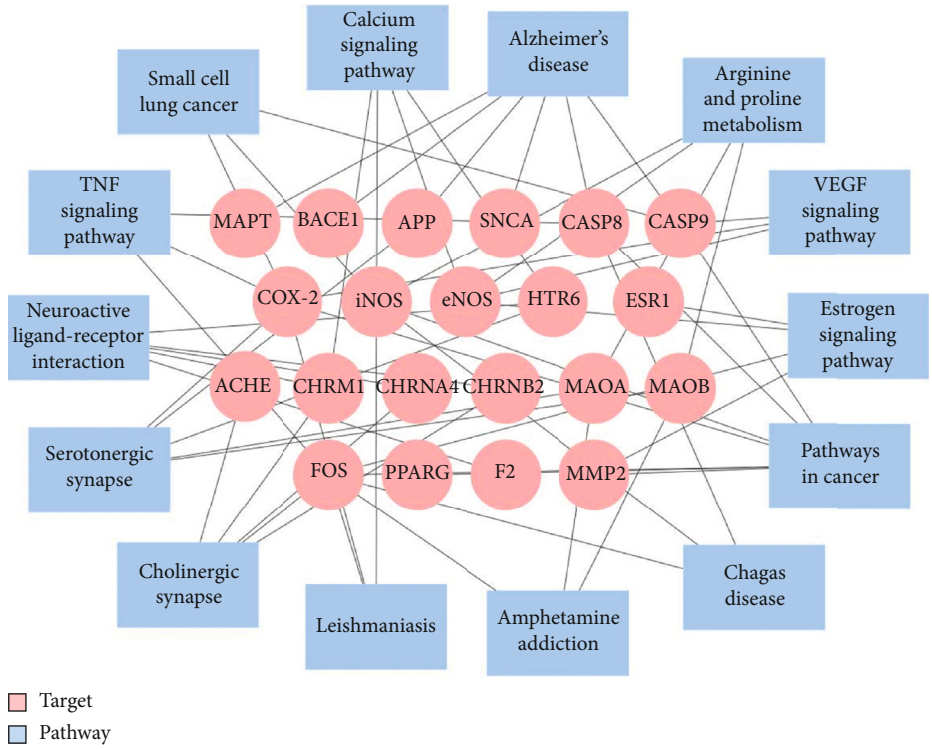


(b)

Figure 1: Network pharmacology analysis of QFY. (a) The compound-target (C-T) network. The grey lines indicate the interactions between the candidate active compounds (outer circles) from the individual herbal ingredients of QFY and the predicted protein targets at the center. (b) The target-pathway (T-P) network. The grey lines indicate the interactions between the protein targets at the center and the signaling pathways or diseases (outer circles).

(KEGG: hsa04725), and serotonergic neurotransmission pathway (KEGG: hsa04726).

*3.2. QFY Differentially Affected iNOS and COX-2 Expression against LPS Stimulation.* To validate the antineuroinflammatory action of QFY and identify the corresponding active compounds, we developed a bioactivity-guided fractionation approach involving ethanolic precipitation, HPLC separation, and *in vitro* assays (Figure 3(a)). The aqueous extract of QFY was firstly precipitated in 50%, 75%, and 90% ethanol. The ethanol solutions and aqueous extract of QFY were assayed for the effects on iNOS and COX-2 in LPS-stimulated BV-2 cells. As shown in Figure 3(b), LPS-induced iNOS expression was decreased by these ethanol solutions of QFY. The 90% ethanol solution of QFY (90% QFY) selectively suppressed LPS-induced iNOS expression in a concentration-dependent manner. In contrast, none of the four QFY preparations effectively suppressed LPS-induced COX-2 expression. To identify the specific compounds, 90% QFY preparation was separated into nine fractions by reverse-phase HPLC on a C18 column (Figure 3(c)). Based on the results of Western blot analysis in Figure 3(d), fractions 1, 2, and 9 showed strong activity to downregulate LPS-induced iNOS expression. Interestingly, these active fractions showed comparable activity with the parent 90% QFY preparation, whereas the other fractions did not show much activity.

*3.3. Ginsenosides in RS Were Identified as the Principal Active Compounds in QFY.* To identify the active ingredients, seven herbal ingredients in QFY were processed into 90% ethanol solutions and assayed for downregulating iNOS in microglia following the procedure described for the whole QFY formulation. As shown in Figure 4(a), 90% ethanol extracts of DG (90% DG) and RS (90% RS) abolished LPS-induced iNOS expression but showed no effect against COX-2 induction. The 90% RS preparation appeared to be more potent than the 90% DG preparation, although less RS was used in the formula than DG. For this reason, the 90% RS solution was selected for further bioactivity-guided fractionation. The compounds in the 90% RS preparation were separated by HPLC under the same conditions as described for the 90% QFY preparation (Figure 4(b)). The resulting fractions were assayed for the activity towards iNOS induction. As shown in Figure 4(c), fraction 9 (90% RS-F9) effectively and selectively suppressed LPS-induced iNOS expression to a greater extent than the parent 90% RS solution.

To identify the specific ginsenosides, the 90% RS preparation and 90% RS-F9 were separated on a C18 HPLC column and detected with a MALDI-TOF mass spectrometer. As shown in Figure 5(a), the 90% RS-F9 fraction showed identical distribution of base peaks compared with the parent 90% RS solution within the elution time interval. As listed in Table 1, a total of 18 ginsenosides and one notoginsenoside were identified in the 90% RS-F9 fraction in a negative ion

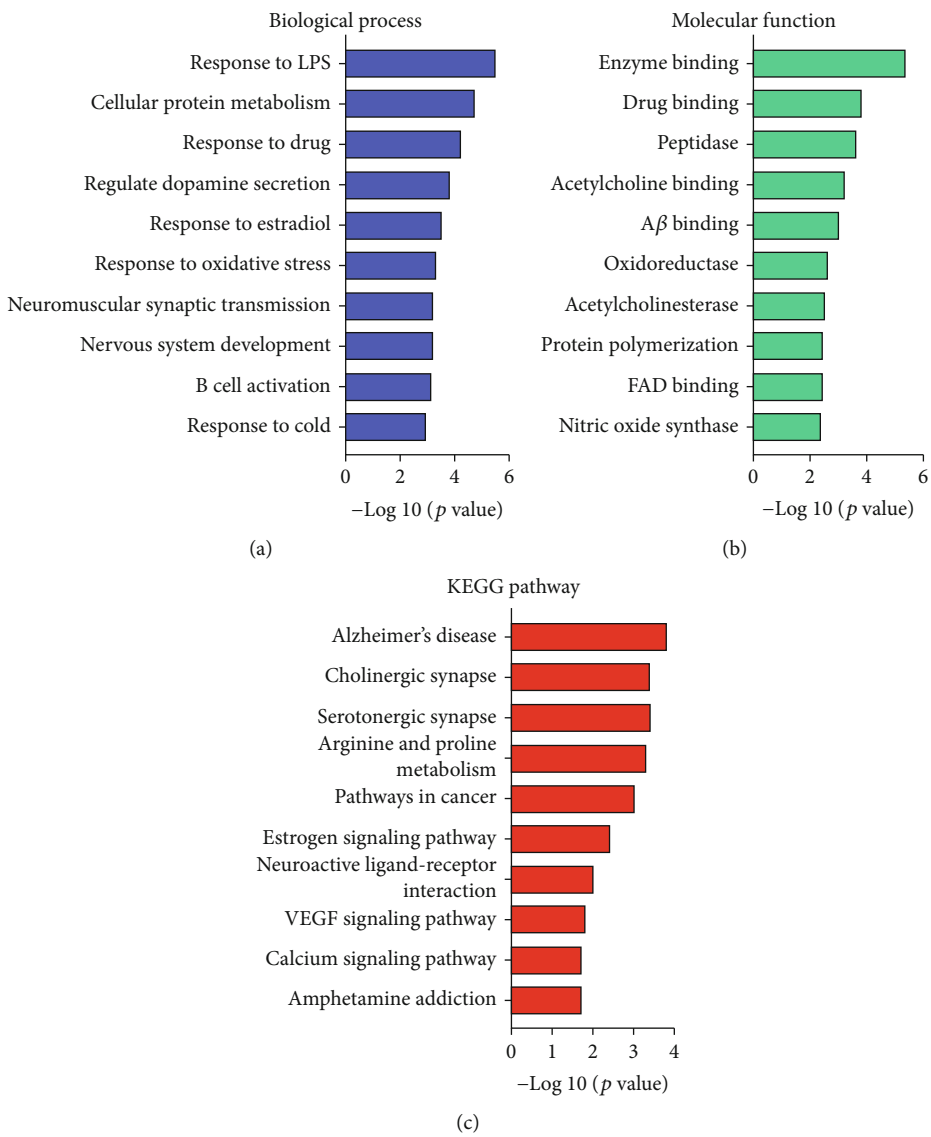


Figure 2: GO terms and KEGG pathway enrichment analysis of the protein targets. (a) The most significantly enriched GO terms were selected in terms of "biological process." (b) The most significantly enriched GO terms were selected in terms of "molecular function." (c) The most significantly enriched KEGG pathways were selected in terms of "KEGG pathways".

mode. In particular, peaks 19 and 20 were relatively prominent in the 90% RS-F9 fraction and detected as the stereoisomers of ginsenoside Rg3. 20($R$)-Ginsenoside Rg3 and 20($S$)-ginsenoside were mainly detected as formate ions at $m/z$ 829.4965 and 829.4971, respectively, while the deprotonated ions were also detected at $m/z$ 783.4906 and 783.7922, respectively. To compare the migration pattern with pure compounds, commercial ginsenoside Rg3 was spiked in the 90% RS-F9 fraction prior to LC-MS/MS analysis. As shown in Figure 5(b), ginsenoside Rg3 was verified by using the identical elution time and mass fragmentation pattern (data not shown). In addition, ginsenoside Rg3 was quantified from the acquired scan data using a target ion of 829.50. The calibration curve for ginsenoside Rg3 ($y = 62240.86x - 24991.72$, $R^2 = 0.9993$) was optimized over the concentration range of 3.9–125 $\mu$g/mL. The calculated amount of ginsenoside Rg3 in 90% RS and 90% RS-F9 was $2.11 \pm 0.02\,mg/g$ and $2.05 \pm 0.08\,mg/g$, respectively.

To examine the potency of different preparations to downregulate iNOS expression, ginsenoside Rg3 and the parent extracts (i.e., 90% QFY and 90% RS) were normalized based on quantification results in the assay of the *in vitro* effects. As shown in Figure 5(c), 90% QFY and 90% RS suppressed iNOS induction to an extent similar to 10 $\mu$M and 20 $\mu$M of ginsenoside Rg3, respectively.

## 4. Discussion

Microglial activation triggers neuroinflammation and neurodegeneration in the onset of AD [20]. Single-drug therapies such as nonsteroidal anti-inflammatory drugs (NSAIDs), TNF-$\alpha$ inhibitor, advanced glycation end product receptor

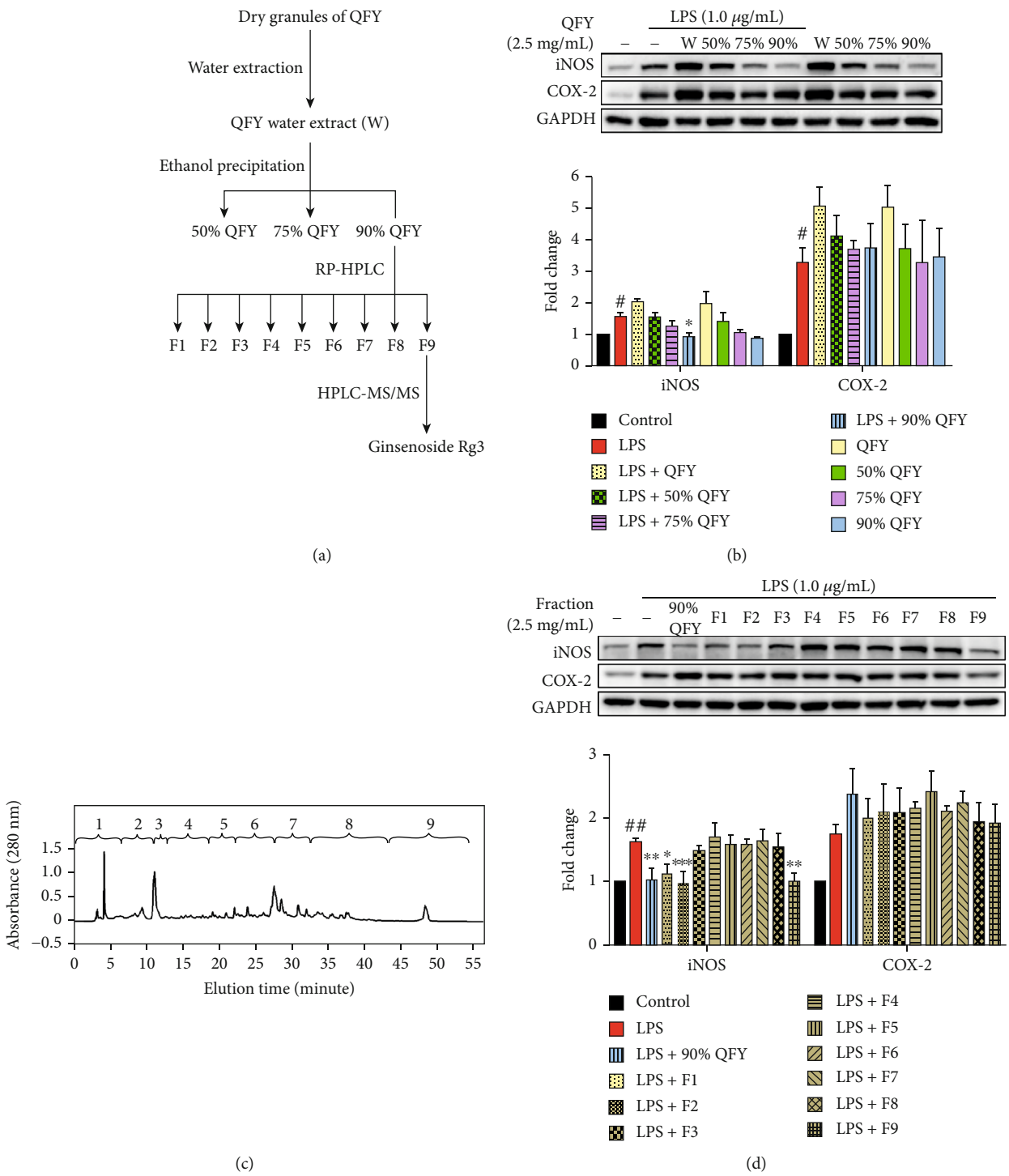


Figure 3: Bioactivity-guided fractionation of the herbal formulation QFY for potential active compounds. (a) Schematic illustration of the bioactivity-guided fractionation procedure. The fractions were prepared by sequential water extraction, ethanolic precipitation, and RP-HPLC separation on a C18 column. The fractions were sequentially analyzed by Western blot for the effects on LPS-induced expression of iNOS and COX-2 in BV-2 cells. (b) Bioassays of the QFY water extract and the fractions from ethanolic precipitation. BV-2 cells were treated with the indicated QFY extract with or without simultaneous stimulation with LPS for 24 h. The expression of iNOS and COX-2 was detected by Western blot using specific antibodies. Representative blots were shown. The blots ($n = 3$) were quantified by a densitometric method using the ImageJ software. The results were expressed as *mean* ± *SD*. $^{\#}p < 0.05$ (LPS vs. untreated control); $^{*}p < 0.05$ (treatment+LPS vs. LPS). (c) HPLC separation of the 90% QFY fraction. The compounds were separated into nine fractions by RP-HPLC on a C18 column. (d) Bioassays of the QFY-derived HPLC fractions. BV-2 cells were treated with the indicated concentration of different HPLC fractions or 90% QFY together with LPS stimulation. The cellular proteins were analyzed by Western blot, and the blots were quantified as previously described. $^{\#\#}p < 0.01$ (LPS vs. untreated control); $^{*}p < 0.05$, $^{**}p < 0.01$, and $^{***}p < 0.001$ (treatment+LPS vs. LPS).

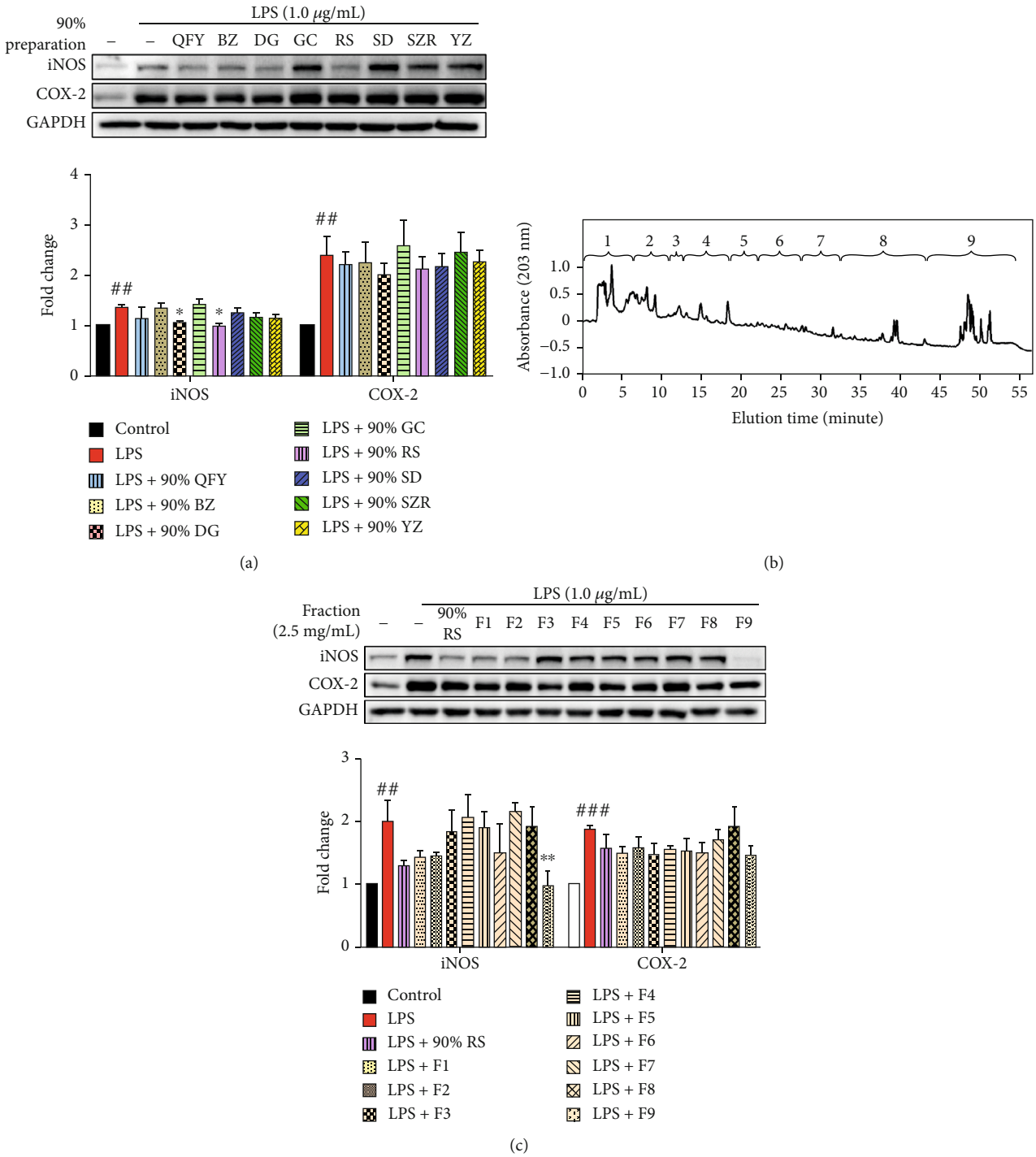


Figure 4: Identification of the active ingredients for the downregulation of iNOS expression. (a) Bioassays of the QFY extract and individual herbal extracts. QFY and individual herbal ingredients were extracted with water and precipitated with 90% ethanol. BV-2 cells were treated with 90% ethanol solutions of herbal extracts for 24 h with LPS stimulation. The expression of specific markers was detected by Western blot, and the blots were quantified as previously described. $^{\#\#}p < 0.01$ (LPS vs. untreated control); $^{*}p < 0.05$ (treatment+LPS vs. LPS). (b) HPLC separation of the 90% RS fraction. The 90% RS solution was separated into nine fractions by RP-HPLC on a C18 column using the same gradient and elution time as described for the 90% QFY fraction. (c) Bioassays of the 90% RS-derived HPLC fractions. BV-2 cells were treated with the indicated concentration of HPLC fractions or 90% RS for 24 h with LPS stimulation. The expression of specific markers was detected by Western blot, and the blots were quantified as previously described. $^{\#\#}p < 0.01$, $^{\#\#\#}p < 0.001$ (LPS vs. untreated control); $^{**}p < 0.01$ (treatment+LPS vs. LPS).

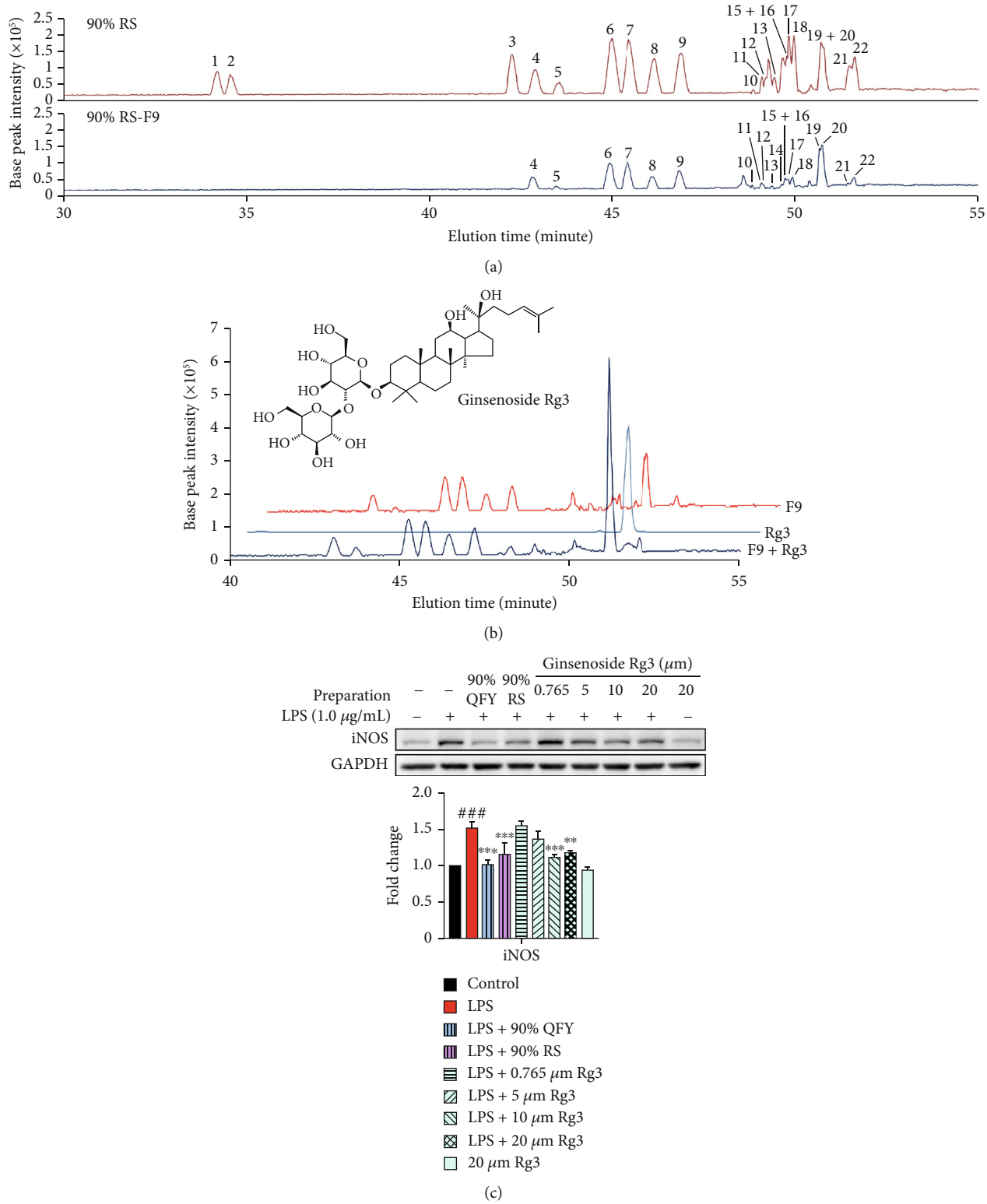


Figure 5: Chemical characterization of fraction 9 derived from 90% RS. (a) Chromatographic profiles of the parent 90% RS solution and the derived fraction 9. (b) Verification of ginsenoside Rg3 in the 90% RS-derived fraction 9. Fraction 9 and ginsenoside Rg3, alone or in combination, were analyzed by HPLC-MS/MS on a C18 column under the same conditions. (c) Bioassays of ginsenoside Rg3 for suppressing iNOS induction. BV-2 cells were treated with the indicated concentration of 90% QFY, 90% RS, and commercial ginsenoside Rg3 for 24 h. The expression of iNOS was detected by Western blot, and the blots were quantified as previously described. $^{###}p < 0.001$ (LPS vs. untreated control); $^{**}p < 0.01$, $^{***}p < 0.001$ (treatment+LPS vs. LPS).

Table 1: Chemicals identified from HPC chromatograms of 90% RS (from 30 to 55 min) and 90% RS-F9.

| Peak | $t_R$ (min) | Identification | Molecular formula | Theoretical $m/z$ | Major fragment Experimental $m/z$ | Error (ppm) | Adduct ion | Other fragments | Possible source |
|---|---|---|---|---|---|---|---|---|---|
| 1 | 34.149 | Ginsenoside Re | $C_{48}H_{82}O_{18}$ | 991.5483 | 991.5512 | 2.92 | $[M+HCOO]^-$ | 945.544 $[M-H]^{-799.4846}$ $[M-H-(Rha-H_2O)]^{-475.3788}$ $[M-H-(Rha-H_2O)-2(Glc-H_2O)]^-$ | Roots |
| 2 | 34.530 | Ginsenoside Rg1 | $C_{42}H_{72}O_{14}$ | 845.4904 | 845.4911 | 0.83 | $[M+HCOO]^-$ | 799.5847 $[M-H]^{-637.4322}$ $[M-H-(Glc-H_2O)]^{-475.3792}$ $[M-H-2(Glc-H_2O)]^-$ | Roots |
| 3 | 42.229 | Gomisin P isomer | $C_{23}H_{28}O_8$ | 431.1711 | 431.1720 | 2.09 | $[M-H]^-$ | 384.9360 $[M-H-(CHO)-(H_2O)]^-$ | Metabolite |
| 4 | 42.847 | Ginsenoside Rf | $C_{42}H_{72}O_{14}$ | 845.4904 | 845.4911 | 0.83 | $[M+HCOO]^-$ | 799.4680 $[M-H]^{-637.4319}$ $[M-H-(Glc-H_2O)]^{-475.3799}$ $[M-H-2(Glc-H_2O)]^-$ | Roots |
| 5 | 43.490 | Notoginsenoside R2 | $C_{41}H_{70}O_{13}$ | 815.4798 | 815.4802 | 0.49 | $[M+HCOO]^-$ | 769.4750 $[M-H]^{-637.4325}$ $[M-H-(Ara/Xyl-H_2O)]^{-475.3795}$ $[M-H-(Ara/Xyl-H_2O)-(Glc-H_2O)]^-$ | Roots |
| 6 | 44.903 | 20(*S*)-Ginsenoside Rg2 | $C_{42}H_{72}O_{13}$ | 829.4955 | 829.4969 | 1.69 | $[M+HCOO]^-$ | 783.4918 $[M-H]^{-637.4321}$ $[M-H-(Rha-H_2O)]^{-475.3800}$ $[M-H-(Rha-H_2O)-(Glc-H_2O)]^-$ | Roots |
| 7 | 45.431 | 20(*S*)-Ginsenoside Rh1 | $C_{36}H_{62}O_9$ | 683.4376 | 683.4383 | 1.02 | $[M+HCOO]^-$ | 637.4325 $[M+cl]^{-475.3789}$ $[M-H-(Glc-H_2O)]^-$ | Roots |
| 8 | 46.106 | 20(*R*)-Ginsenoside Rg2 | $C_{42}H_{72}O_{13}$ | 829.4955 | 829.4969 | 1.69 | $[M+HCOO]^-$ | 783.4916 $[M-H]^{-637.4325}$ $[M-H-(Rha-H_2O)]^{-475.3798}$ $[M-H-(Rha-H_2O)-(Glc-H_2O)]^-$ | Roots |
| 9 | 46.868 | 20(*R*)-Ginsenoside Rh1 | $C_{36}H_{62}O_9$ | 683.4376 | 683.4383 | 1.02 | $[M+HCOO]^-$ | 637.4322 $[M+cl]^{-475.3796}$ $[M-H-(Glc-H_2O)]^-$ | Roots |
| 10 | 48.833 | Ginsenoside Ro | $C_{48}H_{76}O_{19}$ | 955.4908 | 955.4914 | 0.63 | $[M-H]^-$ | 793.4452 $[M-H-(Glc-H_2O)]^-$ | Roots |
| 11 | 49.094 | Ginsenoside Rb1 | $C_{54}H_{92}O_{23}$ | 1153.6011 | 1153.6010 | 0.26 | $[M+HCOO]^-$ | 1107.5979 $[M-H]^{-945.5461}$ $[M-H-(Glc-H_2O)]^{-783.4906}$ $[M-H-2(Glc-H_2O)]^-$ | Roots |
| 12 | 49.180 | Ginsenoside Rc | $C_{53}H_{90}O_{22}$ | 1123.5906 | 1123.5920 | 0.80 | $[M+HCOO]^-$ | 1077.5878 $[M-H]^{-945.5437}$ $[M-H-(Ara(f)-H_2O)]^{-783.4902}$ $[M-H-(Glc-H_2O)-(Ara(f)-H_2O)]^-$ | Roots |
| 13 | 49.419 | Ginsenoside Rb2 | $C_{53}H_{90}O_{22}$ | 1123.5906 | 1123.5920 | 0.80 | $[M+HCOO]^-$ | 1077.5878 $[M-H]^{-945.5437}$ $[M-H-(Ara(p)-H_2O)]^{-783.4902}$ $[M-H-(Glc-H_2O)-(Ara(p)-H_2O)]^-$ | Roots |
| 14 | 49.654 | Ginsenoside Rg6 | $C_{42}H_{70}O_{12}$ | 811.4849 | 811.4868 | 2.34 | $[M+HCOO]^-$ | 765.4806 $[M-H]^{-619.4227}$ $[M-H-(Rha-H_2O)]^{-457.3683}$ $[M-H-(Glc-H_2O)-(Rha-H_2O)]^-$ | Steamed roots |
| 15 | 49.742 | Ginsenoside Rd | $C_{48}H_{82}O_{18}$ | 991.5483 | 991.5506 | 2.32 | $[M+HCOO]^-$ | 945.5441 | Steamed roots |
| 16 | 49.771 | Ginsenoside Rk3 | $C_{36}H_{60}O_8$ | 665.4270 | 665.4280 | 1.50 | $[M+HCOO]^-$ | 619.4262 $[M-H]^-$ | Steamed roots |
| 17 | 49.801 | Ginsenoside F4 | $C_{42}H_{70}O_{12}$ | 811.4849 | 811.4855 | 0.74 | $[M+HCOO]^-$ | 765.4807 $[M-H]^{-619.4224}$ $[M-H-(Rha-H_2O)]^{-457.3696}$ $[M-H-(Glc-H_2O)-(Rha-H_2O)]^-$ | Leaves |
| 18 | 49.947 | Ginsenoside Rh4 | $C_{36}H_{60}O_8$ | 665.4270 | 665.4280 | 1.50 | $[M+HCOO]^-$ | 619.4205 $[M-H]^-$ | Steamed roots |

Table 1: Continued.

| Peak | $t_R$ (min) | Identification | Molecular formula | Theoretical $m/z$ | Major fragment Experimental $m/z$ | Error (ppm) | Adduct ion | Other fragments | Possible source |
|---|---|---|---|---|---|---|---|---|---|
| 19 | 50.681 | 20(*S*)-Ginsenoside Rg3 | $C_{42}H_{72}O_{13}$ | 829.4955 | 829.4971 | 1.93 | $[M+HCOO]^-$ | 783.7922 $[M-H]^{-621.4373}$ $[M-H-(Glc-H_2O)]^{-459.3856}$ $[M-H-(Glc-H_2O)]^-$ | Steamed roots |
| 20 | 50.768 | 20(*R*)-Ginsenoside Rg3 | $C_{42}H_{72}O_{13}$ | 829.4955 | 829.4965 | 1.21 | $[M+HCOO]^-$ | 783.4906 $[M-H]^{-621.4386}$ $[M-H-(Glc-H_2O)]^{-459.3847}$ $[M-H-(Glc-H_2O)]^-$ | Steamed roots |
| 21 | 51.472 | Ginsenoside Rk1 | $C_{42}H_{70}O_{12}$ | 811.4849 | 811.4848 | -0.12 | $[M+HCOO]^-$ | 765.4803 $[M-H]^{-603.4266}$ $[M-H-(Glc-H_2O)]^-$ | Steamed roots |
| 22 | 51.619 | Ginsenoside Rg5 | $C_{42}H_{70}O_{12}$ | 811.4849 | 811.4868 | 2.34 | $[M+HCOO]^-$ | 765.4806 $[M-H]^{-603.4276}$ $[M-H-(Glc-H_2O)]^-$ | Steamed roots |

Rha: $\alpha$-L-rhamnose; Glc: $\beta$-D-glucose; Ara(p): $\alpha$-L-arabinose (pyranose); Ara(f): $\alpha$-L-arabinose (furanose); Xyl: $\beta$-D-xylose.

inhibitor, and PPAR$\gamma$ receptor agonist show varying efficacies in the treatment of AD [21]. Recent effort is directed to the discovery of multitarget drugs by a systems biology approach [22]. Many herbal formulas are well documented for the clinical treatment of dementia in traditional Chinese medicine, thereby representing a rich source for drug discovery [23]. The present study investigated the classical herbal formula QFY for the active compounds and protein targets and hence the molecular mechanisms for the management of AD. We firstly employed a network pharmacology approach to predict the biological targets of QFY and the relevant signaling pathways. We further identified the active compounds from QFY for targeting the neuroinflammatory biomarker iNOS.

Network pharmacology encompasses systems biology, pharmacology, and computational algorithms to robustly study the complex drug-target relationships [24, 25]. Several herbal medicines including RS and YZ were previously studied for the molecular targets against AD by a network pharmacology approach [26]. In the present study, we employed a network pharmacology approach to study the action of the comprehensive anti-AD herbal formula QFY. Firstly, we shortlisted the active compounds with satisfactory bioavailability and BBB penetration based on the common pharmacokinetic or physiochemical parameters curated in databases. We secondly predicted 25 protein targets for these active compounds by target fishing. The C-T network in Figure 1(a) demonstrated that multiple compounds interacted with each protein, whereas the T-P network in Figure 1(b) also vividly depicted that the protein targets were involved in different pathways. Finally, the selected targets were subjected to GO and KEGG enrichment analysis. QFY may exert the pharmacological effect against AD by modulating A$\beta$ aggregation, acetylcholinesterase activity, nitric oxide synthase activity, and cholinergic neurotransmission (Figure 2).

Neuroinflammation is well known to cause extensive damage to the central nervous system, leading to the disruption of synaptic function and the exacerbation of A$\beta$ pathology [27]. Along this line, the present study focused on the antineuroinflammatory activity of QFY and selected two key proinflammatory biomarkers iNOS and COX-2 from the prediction of network pharmacology. It was previously demonstrated that both iNOS and COX-2 were overexpressed in the activated microglia and contributed to neurodegeneration [28]. To investigate the effect of QFY on the expression of iNOS and COX-2, we adopted a bioactivity-guided fractionation approach to separate QFY into different fractions by water extraction, ethanolic precipitation, and HPLC fractionation. We prepared the QFY formulation from the dried, concentrated granules of different herbal ingredients, which facilitated the extraction process and produced a similar chemical profile to regular decoction [29]. We assayed all fractions for the activity to suppress LPS-induced expression of iNOS and COX-2 in microglial BV-2 cells. Based on Western blot analysis, the aqueous QFY extract potentiated the stimulatory effect of LPS on the expression of iNOS and COX-2. The stimulatory effect on microglia could be attributed to the water-soluble active immunopolysaccharide in the herbal ingredients [30]. On the other hand, alcoholic precipitation removed charged small molecules and polysaccharides from the aqueous herbal extracts that could stimulate the cells [31, 32]. Indeed, the 90% QFY preparation selectively suppressed LPS-induced iNOS expression in microglial BV-2 cells.

A bioactivity-guided fractionation approach is widely used to separate complex chemical mixture into different fractions, facilitating the identification of active compounds for specific biological entities [33–35]. In the present study, we firstly prepared a water extract and 50%, 75%, and 90% QFY ethanol extracts. Based on the bioassay results, the 90% QFY preparation appeared to be the active fraction. Therefore, the 90% QFY preparation was subsequently separated into 9 fractions by HPLC (Figure 3(c)). Western blot analysis suggested that fractions 1, 2, and 9 effectively suppressed LPS-induced iNOS expression, although different chemicals might contribute to the activity (Figure 3(d)). For the identification of the active compounds, we screened seven herbal ingredients in the formulation QFY and identified that 90% DG and 90% RS preparations selectively suppressed iNOS induction in LPS-challenged BV-2 cells (Figure 4(a)). We selected the 90% RS preparation for further identification of the active compounds since RS-derived active compounds better met the requirements for an orally active drug in network pharmacology analysis. Thus, the 90% RS preparation was separated into 9 fractions by HPLC using the same gradient and fractionation as described for the 90% QFY preparation. Western blot analysis suggested that fraction 9 derived from 90% RS best suppressed LPS-induced iNOS expression (Figures 4(b) and 4(c)). The 90% RS and 90% QFY preparations showed similar efficacy of inhibiting iNOS expression. In fact, previous studies demonstrated that RS exhibited excellent antineuroinflammatory and anti-A$\beta$ potency [17, 36]. Based on the LC-MS/MS profile, fraction 9 might contain several antineuroinflammatory ginsenosides such as Rh1, Rb2, Rd, Rg3, and Rg5 [37–40]. In particular, ginsenoside Rg3 could downregulate iNOS against LPS stimulation in macrophages and promote the phenotypic switch of macrophages towards a proresolving M2 subtype [41, 42]. Indeed, LC-MS/MS analysis confirmed the presence of ginsenoside Rg3 in 90% RS-derived fraction 9 since ginsenoside Rg3 spike-in comigrated with the endogenous ginsenoside Rg3 (Figure 5(b)). Furthermore, 10 $\mu$M ginsenoside Rg3 appeared to achieve the same potency of 90% QFY and 90% RS for suppressing iNOS induction, although ginsenoside Rg3 failed to exhibit similar activity at the concentration in 90% RS as deduced by the UPLC quantification (Figure 5(c)). Presumably, other compounds may act on iNOS induction in synergy with ginsenoside Rg3. As for the differential effects of QFY fractions on LPS-induced expression of iNOS and COX-2, we previously found that the concomitant activation of the antioxidant Nrf2/HO-1 pathway was a potential mechanism to support the selective suppression of iNOS over COX-2 in macrophages [43]. As elevation of iNOS resulted in oxidative damage in neurons, activation of the Nrf2/HO-1 pathway could effectively inhibit inflammation and oxidative stress, which restored cellular function to the physiological state [44]. Previous studies reported that ginseng and ginsenoside Rg3 could activate the Nrf2/HO-1 pathway [45, 46]. We speculate that ginsenoside Rg3

selectively suppressed iNOS induction in microglia due to the concomitant activation of the Nrf2/HO-1 pathway.

## 5. Conclusions

The present study demonstrated that the active compounds of the herbal formulation QFY could target several protein targets and signaling pathways in the pathogenesis of AD. Ginsenoside Rg3 was identified for potential activity to suppress LPS-induced iNOS expression in BV-2 microglial cells. Ultimately, the present study confirmed the possibility to identify the active compounds for targeting the most important anti-neuroinflammatory biomarkers against microglial activation and towards the development of anti-AD therapeutics.

## Data Availability

The data supporting the findings of this study are available in the article and its supplementary materials.

## Conflicts of Interest

The authors declare no conflict of interest.

## Authors' Contributions

Fung Yin Ngo performed the *in vitro* experiments and drafted the manuscript. Weiwei Wang conducted the network pharmacology analysis. Qilei Chen conducted the mass spectrometry identification. Jin-Ming Gao and Hubiao Chen supervised the data analysis. Jia Zhao and Jianhui Rong designed the research. Jianhui Rong supervised the data analysis, secured the funds to support this study, and finalized the manuscript. All authors revised the manuscript and approved the submitted version. Fung Yin Ngo and Weiwei Wang contributed equally to this work.

## Acknowledgments

This work was supported by General Research Fund (GRF) grants (17120915, 17146216, 17100317, and 17119619) from the Research Grants Council of Hong Kong, National Natural Science Foundation of China (nos. 81703726 and 21778046), Health and Medical Research Fund (15161731, 16171751, and 17181231), Science, Technology and Innovation Commission of Shenzhen Municipality (Basic Research Program, Free Exploration Project JCYJ20180306173835901), Research and Cultivation Plan of High-Level Hospital Construction (HKUSZH201902040), Midstream Research Programme for Universities (MRP) (053/18X), and Seed Funding for Basic Research Programme from the University of Hong Kong (201611159156).

## Supplementary Materials

Table S1: Candidate compounds obtained from the TCMSP database and their pharmacokinetic parameters. Table S2: Candidate compounds obtained from the TCMID database and their Lipinski's rule of five parameters. *(Supplementary Materials)*

## References

[1] M. W. Bondi, E. C. Edmonds, and D. P. Salmon, "Alzheimer's disease: past, present, and future," *Journal of the International Neuropsychological Society*, vol. 23, no. 9-10, pp. 818–831, 2017.

[2] M. Goedert, "Alzheimer's and Parkinson's diseases: the prion concept in relation to assembled A$\beta$, tau, and $\alpha$-synuclein," *Science*, vol. 349, no. 6248, p. 1255555, 2015.

[3] C. G. Parsons, W. Danysz, A. Dekundy, and I. Pulte, "Memantine and cholinesterase inhibitors: complementary mechanisms in the treatment of Alzheimer's disease," *Neurotoxicity Research*, vol. 24, no. 3, pp. 358–369, 2013.

[4] K. G. Yiannopoulou and S. G. Papageorgiou, "Current and future treatments for Alzheimer's disease," *Therapeutic Advances in Neurological Disorders*, vol. 6, no. 1, pp. 19–33, 2012.

[5] M. T. Heneka, M. J. Carson, J. E. Khoury et al., "Neuroinflammation in Alzheimer's disease," *The Lancet Neurology*, vol. 14, no. 4, pp. 388–405, 2015.

[6] S. Hickman, S. Izzy, P. Sen, L. Morsett, and J. El Khoury, "Microglia in neurodegeneration," *Nature Neuroscience*, vol. 21, no. 10, pp. 1359–1369, 2018.

[7] M. L. Block and J. S. Hong, "Microglia and inflammation-mediated neurodegeneration: multiple triggers with a common mechanism," *Progress in Neurobiology*, vol. 76, no. 2, pp. 77–98, 2005.

[8] T. Wei, C. Chen, J. Hou, W. Xin, and A. Mori, "Nitric oxide induces oxidative stress and apoptosis in neuronal cells," *Biochimica et Biophysica Acta (BBA) - Molecular Cell Research.*, vol. 1498, no. 1, pp. 72–79, 2000.

[9] W.-Y. Fu, X. Wang, and N. Y. Ip, "Targeting neuroinflammation as a therapeutic strategy for Alzheimer's disease: mechanisms, drug candidates, and new opportunities," *ACS chemical neuroscience.*, vol. 10, no. 2, pp. 872–879, 2019.

[10] L. Lin, Z. Lan, and Y. Cui-cui, "Multi-target strategy and experimental studies of traditional Chinese medicine for Alzheimer's disease therapy," *Current Topics in Medicinal Chemistry*, vol. 16, no. 5, pp. 537–548, 2016.

[11] W.-Y. Ong, Y.-J. Wu, T. Farooqui, and A. A. Farooqui, "Qi Fu Yin-a Ming dynasty prescription for the treatment of dementia," *Molecular Neurobiology*, vol. 55, no. 9, pp. 7389–7400, 2018.

[12] S. Y. Wang, J. P. Liu, W. W. Ji et al., "Qifu-Yin attenuates AGEs-induced Alzheimer-like pathophysiological changes through the RAGE/NF-$\kappa$B pathway," *Chinese journal of natural medicines.*, vol. 12, no. 12, pp. 920–928, 2014.

[13] G. H. Xing, C. R. Lin, N. Hu, Y. C. Niu, and Y. R. Sun, "Effect of Qifuyin on ability of learning and memory and expression of somatostatin in hippocampus on model rats of Alzheimer's disease induced by $\beta$-amyloid 1-42," *Chinese Journal of Information on Traditional Chinese Medicine*, vol. 17, pp. 34–36, 2010.

[14] J. P. Liu, Q. Q. Wang, Z. M. Hu, S. Y. Wang, and S. P. Ma, "Effect the AGEs/AGE/NF-$\kappa$B pathway in Alzheimer's disease model rats of Qifu Yin," *Pharmacology and Clinics of Chinese Materia Medica*, vol. 31, pp. 9–11, 2015.

[15] M.-N. Li, X. Dong, W. Gao et al., "Global identification and quantitative analysis of chemical constituents in traditional Chinese medicinal formula Qi-Fu-Yin by ultra-high performance liquid chromatography coupled with mass spectrometry,"

*Journal of Pharmaceutical and Biomedical Analysis*, vol. 114, pp. 376–389, 2015.

[16] H.-M. An, D.-R. Huang, H. Yang et al., "Comprehensive chemical profiling of Jia-Wei-Qi-Fu-Yin and its network pharmacology-based analysis on Alzheimer's disease," *Journal of Pharmaceutical and Biomedical Analysis*, vol. 189, p. 113467, 2020.

[17] J. H. Kim, Y.-S. Yi, M.-Y. Kim, and J. Y. Cho, "Role of ginsenosides, the main active components of Panax ginseng, in inflammatory responses and diseases," *Journal of Ginseng Research*, vol. 41, no. 4, pp. 435–443, 2017.

[18] M. H. Cheong, S. R. Lee, H. S. Yoo et al., "Anti-inflammatory effects of Polygala tenuifolia root through inhibition of NF-κB activation in lipopolysaccharide-induced BV2 microglial cells," *Journal of Ethnopharmacology*, vol. 137, no. 3, pp. 1402–1408, 2011.

[19] J. Y. Yu, J. Y. Ha, K. M. Kim, Y. S. Jung, J. C. Jung, and S. Oh, "Anti-inflammatory activities of licorice extract and its active compounds, glycyrrhizic acid, liquiritin and liquiritigenin, in BV2 cells and mice liver," *Molecules*, vol. 20, no. 7, pp. 13041–13054, 2015.

[20] M. L. Block, L. Zecca, and J.-S. Hong, "Microglia-mediated neurotoxicity: uncovering the molecular mechanisms," *Nature Reviews Neuroscience*, vol. 8, no. 1, pp. 57–69, 2007.

[21] Y. Dong, X. Li, J. Cheng, and L. Hou, "Drug development for Alzheimer's disease: microglia induced neuroinflammation as a target?," *International Journal of Molecular Sciences*, vol. 20, no. 3, p. 558, 2019.

[22] A. L. Hopkins, "Network pharmacology: the next paradigm in drug discovery," *Nature Chemical Biology*, vol. 4, no. 11, pp. 682–690, 2008.

[23] Z.-K. Sun, H.-Q. Yang, and S.-D. Chen, "Traditional Chinese medicine: a promising candidate for the treatment of Alzheimer's disease," *Translational Neurodegeneration*, vol. 2, no. 1, p. 6, 2013.

[24] X. Liang, H. Li, and S. Li, "A novel network pharmacology approach to analyse traditional herbal formulae: the Liu-Wei-Di-Huang pill as a case study," *Molecular BioSystems*, vol. 10, no. 5, pp. 1014–1022, 2014.

[25] S. Li and B. Zhang, "Traditional Chinese medicine network pharmacology: theory, methodology and application," *Chinese Journal of Natural Medicines*, vol. 11, no. 2, pp. 110–120, 2013.

[26] J. Fang, L. Wang, T. Wu et al., "Network pharmacology-based study on the mechanism of action for herbal medicines in Alzheimer treatment," *Journal of Ethnopharmacology*, vol. 196, pp. 281–292, 2017.

[27] F. L. Heppner, R. M. Ransohoff, and B. Becher, "Immune attack: the role of inflammation in Alzheimer disease," *Nature Reviews Neuroscience*, vol. 16, no. 6, pp. 358–372, 2015.

[28] M. N. Catorce and G. Gevorkian, "LPS-induced murine neuroinflammation model: main features and suitability for preclinical assessment of nutraceuticals," *Current Neuropharmacology*, vol. 14, no. 2, pp. 155–164, 2016.

[29] L. Chen, Q. Wang, and J. Liu, "Simultaneous analysis of nine active components in Gegen Qinlian preparations by high-performance liquid chromatography with diode array detection," *Journal of Separation Science*, vol. 29, no. 14, pp. 2203–2210, 2006.

[30] Y. Ji, R. Wang, Y. Peng, C. Peng, and X. Li, "Purification, preliminary characterization, and immunological activity of polysaccharides from crude drugs of Sijunzi formula," *Evidence-Based Complementary and Alternative Medicine*, vol. 2017, Article ID 2170258, 8 pages, 2017.

[31] G. Y. Koh, G. Chou, and Z. Liu, "Purification of a water extract of Chinese sweet tea plant (Rubus suavissimus S. Lee) by alcohol precipitation," *Journal of Agricultural and Food Chemistry*, vol. 57, no. 11, pp. 5000–5006, 2009.

[32] X. Yang, Y. Zhao, Y. Yang, and Y. Ruan, "Isolation and characterization of immunostimulatory polysaccharide from an herb tea, Gynostemma pentaphyllum Makino," *Journal of Agricultural and Food Chemistry*, vol. 56, no. 16, pp. 6905–6909, 2008.

[33] M. G. Weller, "A unifying review of bioassay-guided fractionation, effect-directed analysis and related techniques," *Sensors*, vol. 12, no. 7, pp. 9181–9209, 2012.

[34] H. Qi, S. O. Siu, Y. Chen et al., "Senkyunolides reduce hydrogen peroxide-induced oxidative damage in human liver HepG2 cells via induction of heme oxygenase-1," *Chemico-Biological Interactions*, vol. 183, no. 3, pp. 380–389, 2010.

[35] C. Yang, J. Zhao, Y. Cheng, X. Li, and J. Rong, "Bioactivity-guided fractionation identifies amygdalin as a potent neurotrophic agent from herbal medicine Semen Persicae extract," *BioMed Research International*, vol. 2014, Article ID 306857, 10 pages, 2014.

[36] W.-Y. Ong, T. Farooqui, H.-L. Koh, A. A. Farooqui, and E.-A. Ling, "Protective effects of ginseng on neurological disorders," *Frontiers in Aging Neuroscience*, vol. 7, no. 129, 2015.

[37] J. S. Jung, J. A. Shin, E. M. Park et al., "Anti-inflammatory mechanism of ginsenoside Rh1 in lipopolysaccharide-stimulated microglia: critical role of the protein kinase A pathway and hemeoxygenase-1 expression," *Journal of Neurochemistry*, vol. 115, no. 6, pp. 1668–1680, 2010.

[38] C. F. Wu, X. L. Bi, J. Y. Yang et al., "Differential effects of ginsenosides on NO and TNF-α production by LPS-activated N9 microglia," *International Immunopharmacology*, vol. 7, no. 3, pp. 313–320, 2007.

[39] S. S. Joo, Y. M. Yoo, B. W. Ahn et al., "Prevention of inflammation-mediated neurotoxicity by Rg3 and its role in microglial activation," *Biological & Pharmaceutical Bulletin*, vol. 31, no. 7, pp. 1392–1396, 2008.

[40] S. Chu, J. Gu, L. Feng et al., "Ginsenoside Rg5 improves cognitive dysfunction and beta-amyloid deposition in STZ-induced memory impaired rats via attenuating neuroinflammatory responses," *International Immunopharmacology*, vol. 19, no. 2, pp. 317–326, 2014.

[41] S. Kang, S.-J. Park, A.-Y. Lee, J. Huang, H.-Y. Chung, and D.-S. Im, "Ginsenoside Rg3 promotes inflammation resolution through M2 macrophage polarization," *Journal of Ginseng Research*, vol. 42, no. 1, pp. 68–74, 2018.

[42] S.-J. Yoon, J.-Y. Park, S. Choi et al., "Ginsenoside Rg3 regulates S-nitrosylation of the NLRP3 inflammasome via suppression of iNOS," *Biochemical and Biophysical Research Communications*, vol. 463, no. 4, pp. 1184–1189, 2015.

[43] Y. Cheng, C. Yang, D. Luo, and X. Li, "N-Propargyl caffeamide skews macrophages towards a resolving M2-like phenotype against myocardial ischemic injury via activating Nrf2/HO-1 pathway and inhibiting NF-κB pathway," *Cellular Physiology and Biochemistry*, vol. 47, no. 6, pp. 2544–2557, 2018.

[44] J.-F. Luo, X.-Y. Shen, C. K. Lio et al., "Activation of Nrf2/HO-1 pathway by nardochinoid C inhibits inflammation and oxidative stress in lipopolysaccharide-stimulated macrophages," *Frontiers in Pharmacology*, vol. 9, p. 911, 2018.

[45] G. Carota, M. Raffaele, V. Sorrenti, L. Salerno, V. Pittalà, and S. Intagliata, "Ginseng and heme oxygenase-1: the link between an old herb and a new protective system," *Fitoterapia*, vol. 139, p. 104370, 2019.

[46] C. K. Lee, K.-K. Park, A.-S. Chung, and W.-Y. Chung, "Ginsenoside Rg3 enhances the chemosensitivity of tumors to cisplatin by reducing the basal level of nuclear factor erythroid 2-related factor 2-mediated heme oxygenase-1/NAD(P)H quinone oxidoreductase-1 and prevents normal tissue damage by scavenging cisplatin-induced intracellular reactive oxygen species," *Food and Chemical Toxicology*, vol. 50, no. 7, pp. 2565–2574, 2012.

Hindawi
Oxidative Medicine and Cellular Longevity
Volume 2020, Article ID 9524635, 13 pages
https://doi.org/10.1155/2020/9524635

*Review Article*

# Understanding Diabetic Neuropathy: Focus on Oxidative Stress

**Lei Pang,[1] Xin Lian,[2] Huanqiu Liu,[1] Yuan Zhang,[1] Qian Li,[3] Yin Cai,[4] Haichun Ma,[1] and Xin Yu[5]**

[1]*Department of Anesthesiology, The First Hospital of Jilin University, Jilin, China*
[2]*Department of Urology, The First Hospital of Jilin University, Jilin, China*
[3]*Department of Ophthalmology, The First Hospital of Jilin University, Jilin, China*
[4]*Department of Anaesthesiology, The University of Hong Kong, Hong Kong SAR, China*
[5]*Department of Hand Surgery, The First Hospital of Jilin University, Jilin, China*

Correspondence should be addressed to Haichun Ma; mahaichun2003@163.com and Xin Yu; yoson911@yeah.net

Received 14 June 2020; Accepted 22 July 2020; Published 3 August 2020

Guest Editor: Wei Zhao



Diabetic neuropathy is one of the clinical syndromes characterized by pain and substantial morbidity primarily due to a lesion of the *somatosensory nervous system*. The burden of diabetic neuropathy is related not only to the complexity of diabetes but also to the poor outcomes and difficult treatment options. There is no specific treatment for diabetic neuropathy other than glycemic control and diligent foot care. Although various metabolic pathways are impaired in diabetic neuropathy, enhanced cellular oxidative stress is proposed as a common initiator. A mechanism-based treatment of diabetic neuropathy is challenging; a better understanding of the pathophysiology of diabetic neuropathy will help to develop strategies for the new and correct diagnostic procedures and personalized interventions. Thus, we review the current knowledge of the pathophysiology in diabetic neuropathy. We focus on discussing how the defects in metabolic and vascular pathways converge to enhance oxidative stress and how they produce the onset and progression of nerve injury present in diabetic neuropathy. We discuss if the mechanisms underlying neuropathy are similarly operated in type I and type II diabetes and the progression of antioxidants in treating diabetic neuropathy.

## 1. Introduction

Diabetic late complications are described as macrovascular complications comprising cardiovascular diseases and microvascular complications, including retinopathy, nephropathy, and neuropathy [1]. Diabetic neuropathy, one of the clinical syndromes, is characterized by pain and substantial morbidity primarily due to a lesion of the *somatosensory nervous system* [2, 3]. The most common clinical pattern is the neuropathy of the feet and the hands with a distal-to-proximal gradient of severity [1–3]. Currently, the only treatment for diabetic neuropathy is glucose control and foot care [2–5].

There are two major predictors of diabetic neuropathy: the duration of diabetes and the levels of haemoglobin A1c [6]. The latter is commonly associated with metabolic factors, genetic risk factors, environmental factors, common cardiovascular risk factors, and poor glycemic control [7–9]. The question, as to by what molecular mechanisms that diabetes mellitus could target sensory neurons, remains unclear [10]. However, a novel concept involving oxidative stress as a potent causative factor of diabetic neuropathy has been put forward [9, 10].

Oxidative stress is caused by an imbalance between production of reactive oxygen species (ROS) and antioxidant systems. It modulates functions of nerve cells through many molecular signalling pathways [10, 11]. Impaired glucose metabolism in diabetes is a critical mechanism to induce oxidative stress as a result of shunting excess glucose to other metabolic or nonmetabolic pathways [7, 8]. This causes accumulation of the toxic metabolites and overconsumption of nicotinic acid adenine dinucleotide phosphate (NADPH). These converge to increase intracellular redox stress and abnormal modifications on protein [12], lipid [13], and DNA [14], thereby adding mitochondrial injury and causing overproduction of ROS. This damages the peripheral nervous system, as indicated by loss of Schwann cells, myelinated

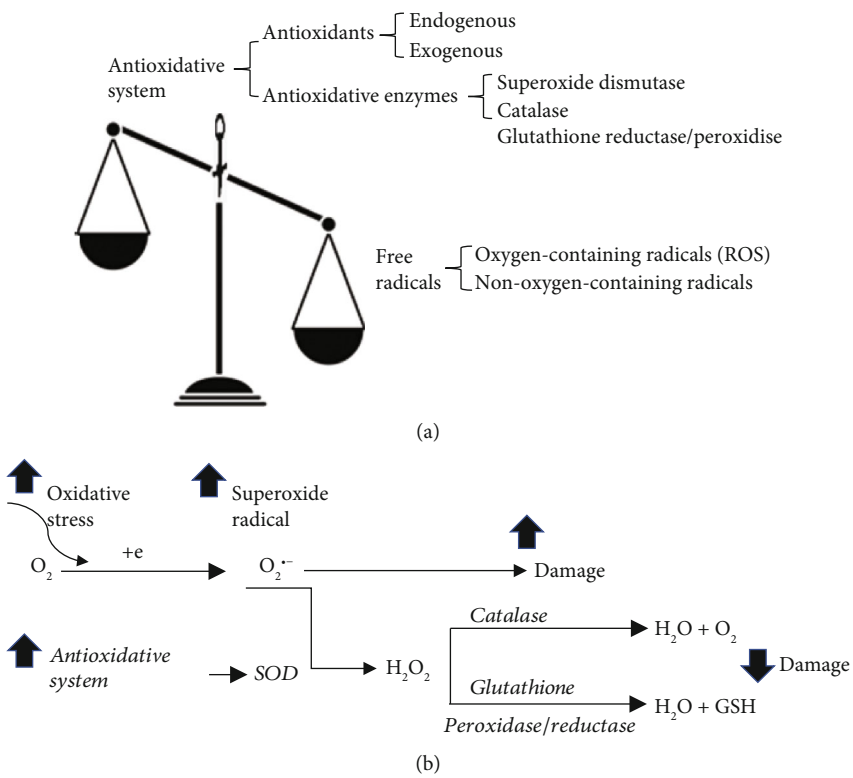


Figure 1: Components of oxidative stress and working mechanism of antioxidative system. (a) Oxidative stress consists of two components as the free radicals and the antioxidative system. The term of oxidative stress describes a condition when the generation of free radicals and the antioxidative system is imbalanced. Free radicals can be the radicals with or without reactivity of oxygen. Antioxidative system consist of antioxidants, that are derived either endogenous or exogenous, and antioxidative enzymes, such as superoxide dismutase, glutathione reductase/peroxidise, and catalase. (b) Antioxidative system works through mechanisms suppressing and scavenging not only free radicals but also *de novo* antioxidant. Superoxide ($O_2^{\bullet-}$) is the major ROS produced in the mitochondria with increased oxidative stress. However, conversion of $O_2^{\bullet-}$ to $H_2O$ by coupled reactions of superoxide dismutase (SOD), catalase, and glutathione reductase/peroxidise is accompanied by the formation of GSH and elimination of the detrimental effect of $O_2^{\bullet-}$ on damage the cells.

axons, and sensory neurons located in the dorsal root ganglia [10, 15, 16]. Meanwhile, insufficient mitochondrial energy production loses the ability to traffic down axons, thereby further promoting axonal injury [17], causing many chronic degenerative diseases, including diabetic neuropathy [7, 8, 18–20].

In this review, we discuss the following points. Firstly, how impaired pathway(s) of glucose metabolism in diabetes lead to oxidative stress, thereby producing the onset and progression of nerve injury present in diabetic neuropathy. The altered pathways include polyol pathway, the hexosamine pathway, the advanced glycation end products (AGE), and protein kinase C (PKC) pathway. Secondly, are the mechanisms underlying neuropathy in type I and type II diabetes distinct? Thirdly, is any antioxidative drug specific and effective for relieving painful diabetic neuropathy? Finally, to highlight areas of research needed for improving the fate of patients with painful diabetic neuropathy.

## 2. General Concept of Oxidative Stress

The term of oxidative stress describes a condition (Figure 1(a)) when the balance between the generation of free radical and antioxidant system is unfavorable [21, 22]. A free radical can be defined as any molecular species capable of either donating or accepting an electron therefore behaving as oxidants [22], while antioxidants are the molecules stable enough to neutralize the free radicals, thereby maintaining a balance. Despite the chemical structural differences, free radicals share similar mechanisms for damage at the level of biomolecules [23].

Among the free radicals, ROS are the oxygen-containing free radicals as the natural by-products of the metabolism of oxygen, including hydroxyl radical, superoxide anion radical, hydrogen peroxide, oxygen singlet, hypochlorite, nitric oxide radical, and peroxynitrite radical. They are derived within organelles including peroxisomes, endoplasmic reticulum, and mitochondria, the major site of ROS production.

Antioxidant system consists of antioxidants and antioxidative enzymes (Figure 1(a)). The resources of antioxidants can be endogenous and exogenous. Glutathione is the most abundant endogenous antioxidant in most cell types with the reduced form (GSH) as biologically active [24]. The exogenous antioxidants are derived from either diet or supplement, such as vitamin A, C, and E [21, 25] and antioxidant minerals (copper, zinc, manganese, selenium). The major antioxidative enzymes, including superoxide dismutase, glutathione reductase/peroxidise, and catalase, metabolize free radicals to nontoxic intermediates. They work in synergy

(Figure 1(b)) through mechanisms not only suppressing and scavenging free radicals before they can damage cells, but also repairing *de novo* antioxidants [24, 26].

## 3. Diabetic Neuropathy

*3.1. General Aspects.* Diabetic neuropathy, a damage occurred in sensory neurons, causes neuropathic pain with either central or peripheral syndromes in different patterns (e.g., pain and numbness) [7, 9]. Clinically, the most common pattern is the distal symmetric polyneuropathy of the feet and hands, with a distal-to-proximal gradient of severity [1, 9, 10, 27]. Of note, pain is reported by approximately one third of patients with diabetes, regardless of associated neurological deficits [27].

The cause of diabetic neuropathy has been attributed to diabetes [8, 9], which is a metabolic disorder characterized by impaired glucose metabolism with chronic hyperglycaemia and dysfunction of endogenous insulin (insufficiency of secretion as type I or action as type II). Based on the large clinical studies in patients with type I or type II diabetes, a strong correlation between chronic hyperglycaemia and diabetic microvascular complications has been established [28–33]. At least 50% of individuals with diabetes develop diabetic neuropathy with time [34].

Increased glucose levels in diabetes affect primarily those cells that have a limited capacity to regulate their glucose intake, including vascular cells, Schwann cells, and neurons of the peripheral and central nervous systems [35, 36]. It is unclear whether high glucose triggers axonal degeneration by promoting intrinsic programmes within axons [36–38], nor is whether peripheral axons or their associated Schwann cells, the first target. Clinical findings have demonstrated that Schwann cells are targeted in patients with diabetic neuropathy [39]. Experimental studies in diabetic rodents have associated endoplasmic reticulum stress with diabetes-mediated peripheral nerve damage [40]. At the early stage of diabetes, hyperglycaemia causes abnormalities in blood flow and in vascular permeability [7]. With time, impaired glucose metabolism reduces intracellular levels of NADPH and decreases the synthesis of myo-inositol that is particularly required for the normal function of nerves [41, 42]. Collectively, diabetic neuropathy might be caused by a direct effect of hyperglycaemia on damaging cells [43, 44] and an indirect effect on affecting cellular functions [7, 45]. Loss of microvascular cell occurs, in parallel with reduced production of endothelial and neuronal cells, which leads to degeneration of peripheral nerves [46].

*3.2. Diabetic Neuropathy in Type I and Type II Diabetes.* The major predictors of diabetic neuropathy are the duration of diabetes and the blood levels of haemoglobin A1c (HbA1c) [6]. The severity of diabetic complications correlates with the severity of hyperglycaemia, suggesting that the complications are triggered by the elevation in glucose levels [28]. However, rapid glucose control significantly increased the risk of severe hypoglycemic episodes [47] and resulted in treatment-induced neuropathy in both type I and type II diabetes [48–50].

Diabetic neuropathy can be found late in type I diabetes but early in type II diabetes, and the cause of this occurrence remains unclear. As the consistent feature between type I and type II is hyperglycaemia, one would assume that controlling hyperglycaemia would be the best preventive treatment for diabetic neuropathy regardless the diabetic type. Of interest, the incidence of neuropathy is higher in diabetic patients with type II than those with type I [51–54], whereas the prevalence of diabetic neuropathy was similar in type II diabetic patients [55–57] as seen in type I [6, 58]. Clinically, efficient glucose control significantly reduced or delayed the incidence of developing neuropathy in type I diabetic patients [59, 60], whereas it remains elusive with type II diabetes [29, 47, 61–63]. In addition, lowing haemoglobin A1c in type II diabetic patients has little effect on diabetic neuropathy [64], whereas a greater improvement has been observed in type I diabetic patients after 18 months of glycemic control [48]. Collectively, it suggests that hyperglycaemia is not the prime driving cause of all complications [35, 65], and mechanisms underlying diabetic neuropathy in type I and type II diabetes could be fundamentally different [47].

The most recent findings with alterations in DNA methylation have been suggested as a contributor to diabetic neuropathy in type I and type II diabetic patients [14, 66]. Of interest, spliceosome dysregulation has been proposed as a key neurodegenerative mechanism underlying diabetic neuropathy in type I diabetic patients [67]. Spliceosome is a complex assembled from small nuclear RNA and proteins in nucleus and required to catalyze pre-mRNA splicing in nuclear speckles [68]. Whether splicing abnormalities are identifiable in type II diabetes remains unexplored.

The current approaches to managing diabetic neuropathy focus on improving glycaemic control, mainly in type I diabetic patients, and lifestyle modifications, mainly in type II diabetic patients [35, 69]. Although diabetic neuropathy is the strongest predictor of mortality in type II diabetes, it remains the only microvascular complication of diabetes without a specific treatment owing to our lack of basic understanding of this disease.

## 4. Oxidative Stress in Diabetic Neuropathy

*4.1. Main Sources of ROS Production in Diabetic Neuropathy.* The main proof of oxidative stress involvement in diabetic neuropathy was the accumulation of free radicals and reduced activity of antioxidant enzymes in the diabetic animals with diabetic neuropathy, and the effect was ameliorated, in parallel with the alleviation of symptoms, upon antioxidant treatment [70]. Ample evidence strongly support that hyperglycaemia leads to increased oxidative stress that plays a pivotal role in the development of diabetic neuropathy [7] by damaging the cells including endothelial, retinal, mesangial, and neural cells [2, 8].

Impaired mitochondrial glucose oxidation is believed as a main source of ROS production in diabetes [7, 8]. To understand how hyperglycaemia increases ROS production, a brief overview of glucose metabolism is helpful (Figure 2(a)). Under a physiological condition, after being taken-up, intracellular glucose is converted to glucose-6-phosphate, then

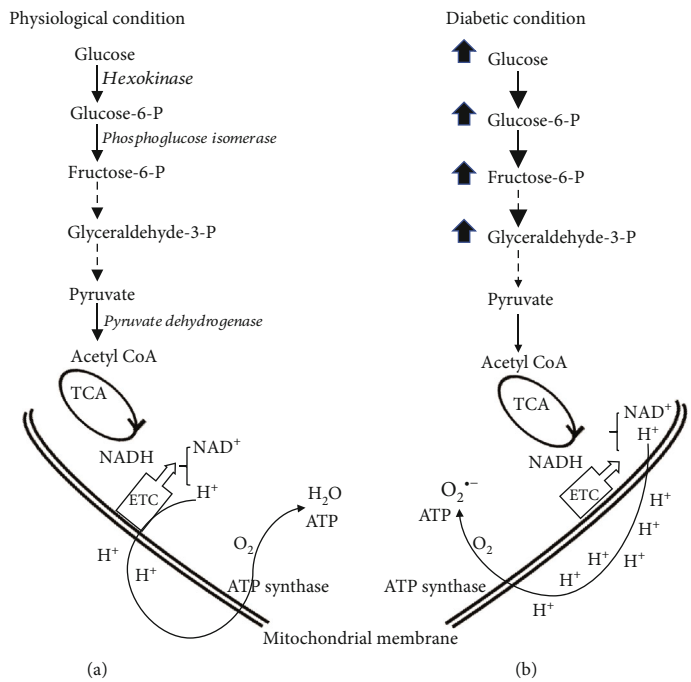


Figure 2: Major glucose metabolism pathway under physiological condition and diabetic condition. (a) Under a physiological condition, intracellular glucose is converted to glucose-6-phosphate, via hexokinase, then following isomerization to fructose-6-phosphate. Along glycolysis pathway, glyceraldehyde-3-phosphate travels down to pyruvate and acetyl CoA via pyruvate dehydrogenase, which then enters tricarboxylic acid (TCA) cycle. NADH, as electron carrier and generated during the process of glycolysis and glucose oxidation, can donate reducing equivalents to the mitochondrial electron transport chain (ETC), thereby creating a proton gradient that is used by ATP synthase to produce ATP and converting $O_2$ to $H_2O$. (b) Under diabetic condition, glucose metabolism is impaired, causing accumulation of glucose and the glycolytic intermediates, resulting mitochondrial injury, thereby converting $O_2$ to superoxide radical ($O_2^{\bullet-}$) instead of $H_2O$. As a result, ATP production is reduced.

followed by glycolysis and oxidation to produce NADH and acetyl CoA. Electrons carried by NADH are transferred to oxygen following mitochondrial electron transport chain (ETC), along with pumping protons out of the mitochondrial matrix thereby creating a proton gradient that is used by ATP synthase to produce ATP (Figure 2(a)). Under normal condition, there are only 0.2-2% of the electrons in the ETC leaking out to produce ROS [71], and neurons have sufficient capacity to remove ROS by innate cellular antioxidants (Figure 1(b)) [72]. Under a diabetic condition, however, impaired glucose metabolism shunts glucose or intermediates of glycolysis to other metabolic and nonmetabolic pathways (Figure 2(b)), which causes mitochondrial injury with higher rates of protons returning to the mitochondria without generating ATP and an overwhelming production of ROS in a neuron [11]. Axons are rich of mitochondria, having a direct access to nerve blood supply. The inability of the neuron to detoxify the excess ROS together with insufficient ATP production leave axons being more susceptible to ROS-mediated damage in hyperglycaemia [11], in part because of their dependence on local mitochondria for energy, which in turn precipitates axonal degeneration [11].

*4.2. Molecular Mechanisms of ROS Production in Diabetic Neuropathy.* There are four damaging pathways (Figure 3) that can explain the detrimental effects of ROS in hyperglycaemia-induced diabetic neuropathy, including polyol pathway and hexosamine pathway that have been consistently observed in patients with diabetic neuropathy [73–76]. The AGE and PKC pathway modify proteins, lipids, and DNAs via a direct [77–80] or an indirect effect of glucose [81, 82]. All of which are linked to diabetic neuropathy by a single event: overproduction of ROS [7], which is a consistent differentiating feature common to all cell types that are damaged by hyperglycaemia [8].

*4.2.1. Activated Polyol Pathway.* The polyol pathway is a two-step metabolic process (Figure 3), promoted by a mass action of excess glucose to activate aldose reductase. Aldose reductase, a cytosolic protein, normally has low affinity to glucose, and function for reducing toxic aldehydes in tissues such as nerve, retina, lens, glomerulus, and vascular cells [83, 84]. In many of which, glucose moves freely across the cell membrane independent of insulin, and intracellular levels of glucose rise with hyperglycaemia in parallel with an increased affinity of aldose reductase for glucose. This favors the excess glucose to generate sorbitol, instead of down to glycolysis, with consumption of nicotinamide adenine dinucleotide phosphate (NADPH) to $NADP^+$ (Figure 3). Sorbitol is subsequently oxidized to fructose through sorbitol dehydrogenase, with $NAD^+$ as a cofactor. To note, compared to glucose, glyceraldehyde 3-phosphate, a glycolytic intermediate, has been

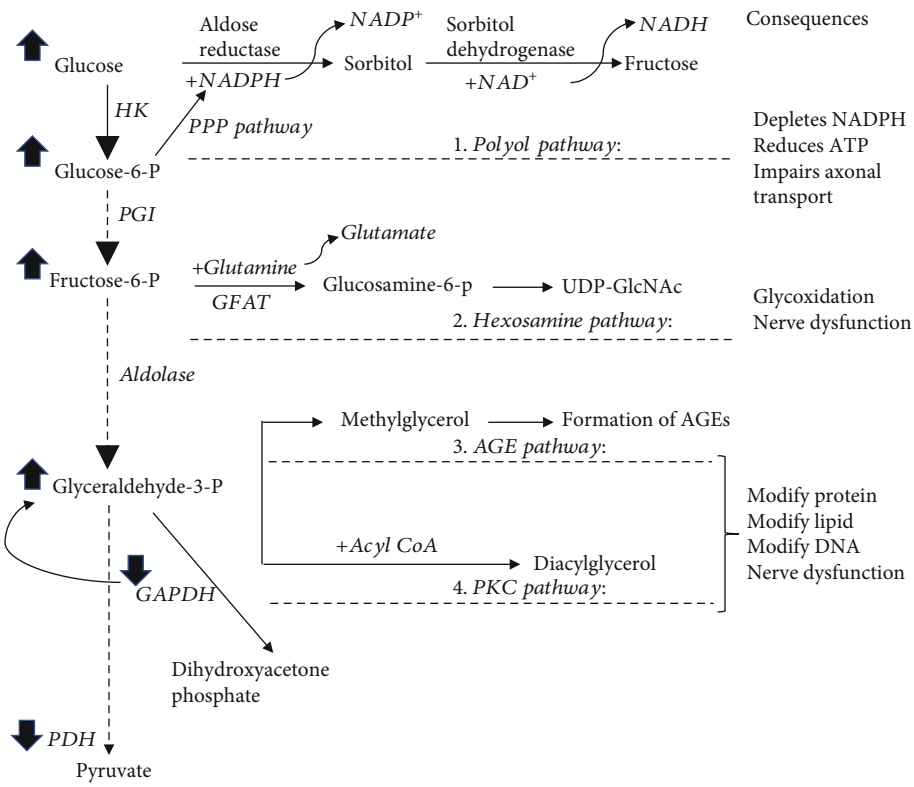


Figure 3: Four damaging pathways that can explain the detrimental effects of ROS in hyperglycaemia-induced diabetic neuropathy. The impaired glucose metabolism in diabetic condition causes an accumulation of glucose and glycolytic intermediates, which, instead of travel along glycolysis pathway, shunts to other metabolic or nonmetabolic pathways, resulting activation of the polyol pathway, hexosamine pathway, and AGE and PKC pathway. Superoxide inhibits glyceraldehyde-3-phosphate dehydrogenase (GAPDH) activity, which is proposed to be a reason causing accumulation of all the glycolytic intermediates. Pentose phosphate pathway (PPP pathway) is to generate NADPH, which is used in polyol pathway. GFAT: glutamine-fructose-6-phosphate aminotransferase; GAPDH: glyceraldehyde-3 phosphate dehydrogenase; PDH: pyruvate dehydrogenase.

suggested as a relevant substrate for aldose reductase, owing to its higher affinity to aldose reductase under pathological conditions [85].

The well accepted mechanism for hyperglycaemia-induced polyol pathway is the increased redox stress due to the consumption of NADPH, which is derived from pentose phosphate pathway for generating GSH from glutathione (Figure 3). This notion is further supported by the observation that overexpression of human aldose reductase in diabetic mice reduced the expression of regulatory genes for regenerating glutathione [86]. Meanwhile, excess fructose, as a product, promotes glycation and further depletion of NADPH thereby causing and exacerbating intracellular oxidative stress.

Relevant to diabetic neuropathy, accumulation of sorbitol and fructose were observed in the peripheral nerves of diabetic rats [87], while shunting glycolytic intermediates to polyol pathway also promotes glycation and formation of diacylglycerol in dorsal root ganglia of the diabetic mice [88]. Inhibiting aldose reductase prevented accumulation of sorbitol and fructose in peripheral nerves of the diabetic rats [89, 90] and restored diabetes-induced defect in nerve conduction velocity in diabetic dogs [91]. In addition, patients with a high aldose reductase expression are commonly having an early diabetic neuropathy relative to the patients with a low aldose reductase expression [92, 93]. Thus, inhibiting the polyol pathway continues to be a drug target in the treatment of diabetic neuropathy.

*4.2.2. Activated Hexosamine Pathway.* The well accepted mechanism that hexosamine pathway contributes to diabetic neuropathy is the effect of intracellular UDP-GlcNAc on modification of proteins [94, 95]. Under physiological condition, hexosamine pathway is a minor branch of the glycolytic pathway [96, 97] with only 2-5% [97] of fructose-6-phosphate being converted to glucosamine-6-phosphate by glutamine-fructose-6-phosphate aminotransferase (GFAT), the rate limiting enzyme. Under hyperglycaemia condition, however, the increased production of mitochondrial ROS inhibits glyceraldehyde-3 phosphate dehydrogenase activity, a glycolytic enzyme (Figure 3), thereby blocking fructose-6-phosphate flow through glycolysis [98]. Subsequently, glucosamine-6-phosphate along with acetyl-CoA and uridine-5′-triphosphate are used to produce the amino sugar uridine-5′-diphosphat-N-acetylglucosamine (UDP-GlcNAc) [97], which controls activity of O-linked N-acetylglucosamine transferase [99]. The latter is a cytosolic and nuclear enzyme, catalyzing a reversible posttranslational protein modification by

transferring GlcNAc to specific serine and threonine residues on proteins [99, 100]. Of particular interest at proteins modified by O-GlcNAcylation are insulin receptor substrates-1 and 2 [101, 102] as well as glucose transporter 4 [103].

Relevant to diabetic neuropathy, an increase in GFAT activity and UDP-GlcNAc concentrations was evident in muscle of ob/ob mice [104]. Conversely, a reduced UDP-GlcNAc concentration was observed, in parallel with improved insulin sensitivity in muscles of the rats with chronic caloric restriction [104]. Clinically, GFAT activity is increased in muscle biopsies obtained from insulin resistant patients with type II diabetes [105], while insulin resistance is improved markedly by insulin treatment in patients with severely insulin resistant, uncontrolled, obese, type II diabetes, concomitant with 40% increase in the levels of UDP-GlcNAc in muscle [106]. In contrary, a positive correlation among UDP-GlcNAc circulating levels of FFA and leptin was found in adipocytes, but not in muscle of type II diabetic patients relative to nondiabetic control [107]. Hyperglycaemia-induced overmodification of proteins by glucosamine results in pathological changes in gene expression, especially transcription factors, which contribute to the pathogenesis of diabetic complications with the strongest evidence for the role in diabetic complications [102, 108]. However, it is not yet clear what kind of peripheral nerve proteins can be modified by activated hexosamine pathway following diabetes, nor is the causal connection. Thus, the contribution of hexosamine pathway to diabetic neuropathy remains to be further explored.

*4.2.3. Activated AGE and PKC Pathway.* The common feature of both pathways is the modification of proteins thereby modulating diabetic complications via activating transcription factors. Activation of hexosamine pathway causes an elevated level of glyceraldehyde-3 phosphate, which upon conjugation with fatty acid, produces diacylglycerol [109, 110] to activate PKC. Thus, both activated polyol pathway and hexosamine pathway in diabetes can activate AGE and PKC pathway.

*(1) Activation of AGE Pathway.* AGEs are intracellular and extracellular adducts formed by covalent linking reducing sugars or its metabolites to lysine or arginine on proteins [111–113]. Hyperglycaemia is recognized as the primary initiating event in the formation of AGEs [78]. There are two forms of AGEs precursors, glyoxal and methylglyoxal, which can be generated through three major pathways: autooxidation of glucose to form glyoxal, a smallest dialdehyde [80]; abnormal metabolism of glyceraldehyde-3 phosphate from glycolysis to form methylglyoxal; and degradation of glyceraldehyde and glycolaldehyde (fructose-lysine adducts) to form both glyoxal and methylglyoxal. Compared to glyoxal, methylglyoxal is highly reactive and causing vascular endothelial cells to be more sensitive to damage [114].

Relevant to diabetic neuropathy, the well accepted mechanism is that extracellular AGEs interact with a specific AGE receptor: known as RAGE on the cell surface [115], causing overproduction of ROS, thereby activating nuclear factor kappa B (NF-$\kappa$B) to initiate multiple pathological changes in gene expression [116]. Activation of AGE-RAGE-NF-$\kappa$B axis appears to be sustained in both clinical [117] and laboratory settings [112, 117]. In the streptozotocin-induced diabetic mice, knockdown of RAGE gene significantly improved electrophysiological and anatomical markers of diabetic neuropathy [112] as well as restored pain perception in sciatic nerves [117], in parallel with a decreased expression of NF-$\kappa$B in peripheral nerves [117], and particularly in Schwann cells [112]. Clinically, activated NF-$\kappa$B was colocalized with RAGE within the vasa nervorum in the sural nerve biopsies from the patients with diabetic neuropathy [117]. In relevant, diabetic patients have increased expression of endothelia RAGE and less collateral vessels, compared with nondiabetic controls, which contributes to increased rates of lower limb amputation [118]. Thus, AGE-RAGE-NF-$\kappa$B axis might promote diabetic neuropathy through its impact on microvessels within the sensory neurons. Up to date, effective treatment modalities of AGE-induced nerve injury is not available clinically [67].

*(2) Activation of Protein Kinase C.* Activation of classic PKC is dependent on both $Ca^{2+}$ ions and phosphatidylserine and is greatly enhanced by diacylglycerol [119]. The primary function of PKC is phosphorylating targeted proteins, which in turn operating on gene expression in diabetes, thereby mediating abnormalities of blood flow and permeability via inhibiting NO production [120] or activating NF-$\kappa$B [121] and microvascular matrix proteins [122] in both diabetic patients [123] and animal models [124].

Of relevance, the PKC $\beta$-isoform in particular has been linked to the development of diabetic nephropathy in the diabetic animal models, such as in the streptozotocin-induced diabetic rats; PKC$\beta$ inhibitors actually improve motor nerve conduction velocity and endoneurial blood flow [125, 126]. However, clinical studies using ruboxistaurin, a selective PKC$\beta$ inhibitor, for treatment of painful diabetic neuropathy did not achieve significance [127]. Based on six randomized controlled trials, it was concluded that PKC$\beta$ inhibitor offered no benefit in the treatment of diabetic neuropathy [128]. Up to date, the role for PKC activation in diabetic neuropathy remains unclear.

## 5. Management of Treating Diabetic Neuropathy in Relation to Oxidative Stress

*5.1. Assessment.* There are two newer techniques, besides a number of other tools [65], for clinician to assess diabetic neuropathy, including the visual quantification of intraepidermal nerve fibers through skin biopsy for peripheral vs. MR imaging for central neuropathy, which allows noninvasive *in vivo* imaging of corneal nerves [129, 130].

*5.2. Newest Approach in Pain Medicine.* The newest approach was released on May 2020 by Vienna University of Technology that chronic pain can be reduced by stimulating the vagus nerve in the ear with a tiny electrodes, in which a 3D computer model is created to calculate the optimal stimulation of nerve branches [131, 132]. The approach has now been successfully tested on patients [132]. Although this is not specifically for treatment of diabetic neuropathy, it is an important step forward.

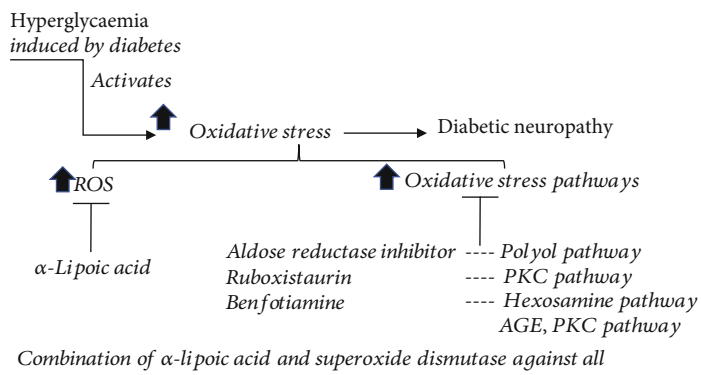


Figure 4: Strategies of antioxidative drugs in treating diabetic neuropathy include directly against ROS and against individual oxidative stress pathways. The listed drugs showed effect on improving symptoms of diabetic neuropathy. However, none of them have been FDA-approved due to the lack of clinical significance.

In clinical practice, the assessment with combination pharmacotherapy is often applied for managing diabetic neuropathy. Of interest, pharmacological approaches aiming at targeting antioxidative stress are the few strategies that reduce pain in diabetic neuropathy patients in clinical trials [133–138].

*5.3. Targeting Oxidative Stress.* Several strategies aiming at antioxidative stress have been employed (Figure 4) to combat nerve dysfunction in diabetes, including directly against ROS, against individual oxidative stress pathways, or targeted at mitochondria.

*5.4. Targeting ROS.* Including $\alpha$-lipoic acid (ALA), vitamins A, C, and E, acetyl L-carnitine, taurine, and melatonin, taurine, acetyl L-carnitine, and N-acetylcysteine have been demonstrated to reduce the progression of diabetic neuropathy [139], whereas the effect of vitamins A, C, and E in diabetic neuropathy needs more research to ascertain [9, 21]. ALA is thought to be a valuable therapeutic option for diabetic neuropathy as the treatment ameliorated the symptoms of diabetic neuropathy in the clinical trials [135, 137, 138]. ALA is a water- and fat-soluble compound known to reduce oxidative stress by inhibiting hexosamine and AGEs pathways [140]. The combination of ALA and superoxide dismutase has improved symptoms and electroneurographic parameters in the patients with diabetic neuropathy [141]. Currently, ALA has been licensed in Germany to treat symptomatic diabetic neuropathy with 600 mg daily dosage [142].

*5.5. Targeting Individual Oxidative Stress Pathways.* Including aldose reductase inhibitors, anti-AGE agents, and PKC inhibitors, in contrast to ruboxistaurin, a specific PKC$\beta$ inhibitor failed to achieve its clinical significance; aldose reductase inhibitors and anti-AGE agents have shown the therapeutic effect.

Aldose reductase inhibitors are used to reduce the flux of glucose into the polyol pathway. The positive effect of inhibiting aldose reductase on diabetic neuropathy includes enhancing sural motor and sensory nerve conduction velocities, improving wrist and ankle *F*-wave latency together with and alleviating neuropathic pain [143], which have been observed in diabetic mice [143] and in diabetic patients [144]. However, its efficacy needs further investigation [145].

Anti-AGE agents are used to prevent the formation and accumulation of AGEs. Benfotiamine, a lipid-soluble analogue of vitamin $B_1$, has the effect on preventing the activation of the hexosamine pathway and the AGE and PKC pathway induced by diabetes [7, 8]. Importantly, benfotiamine has shown the therapeutic efficacy in the patients with diabetic neuropathy [134, 146, 147] and in diabetic rats [8, 133], which suggests that benfotiamine may extend the treatment option for diabetic neuropathy based on causal influence on impaired glucose metabolism [134].

The clinical translation is challenging, as none of these drugs are currently FDA-approved yet, in part, due to the failure in clinical trials [148, 149]. One of the common contributors to the failure in the clinical trials is the irreproducibility of the improvement in the treated animal models vs. in humans, for example, sorbinil (an aldose reductase inhibitor), which was shown to inhibit diabetes-induced nerve conduction deficit in streptozotocin-induced diabetic rats [150]; however, it did not produce similar results in humans [151]. Another concern is the side effect, such as photosensitive skin rash, discouraging the further usage [152]. Extensive preclinical research is still on going to investigate further mechanisms and new targets with improved efficacy and safety for treating diabetic neuropathy.

## 6. Conclusion

Although considerable research has been devoted to understanding mechanisms of diabetic neuropathy in general, treatment options to eliminate the initial causes are still ``lacking. There have been disparities between the results obtained from animals and human studies. Currently, genetic- or diet-induced animal models are commonly used to investigate neuropathy in type II diabetes, while high-dose streptozotocin-induced diabetic animal models are used to mimic the metabolic phenotype of type I diabetes. However, no single rodent model accurately mimics human diabetic neuropathy [153] with the major problems not only in pain assessment that is hard to measure in rodents [154] but also in the knowledge about the molecular mechanisms.

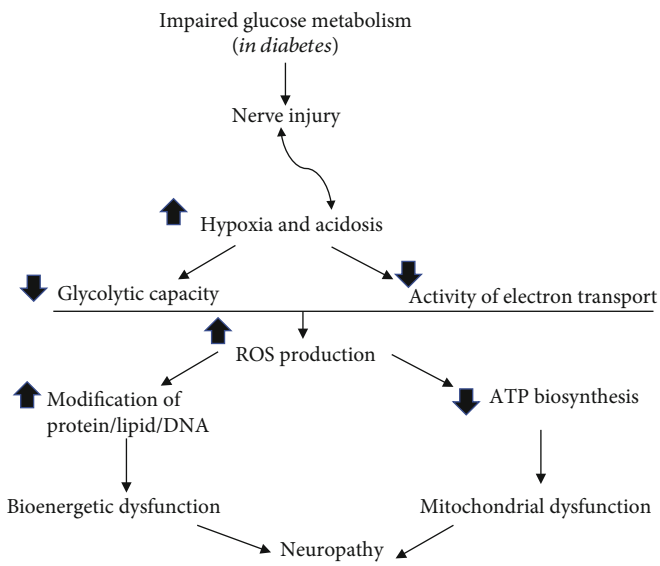


Figure 5: Summary of the major contributors to diabetic neuropathy. Diabetes-induced impairment of glucose metabolism causes hypoxia and acidosis, which contributes to and exacerbates the nerve injury. As a result, both glycolytic capacity and activity of electron transport chain are reduced, leading to overproduction of ROS, which, not only reducing ATP production but also initiating various modifications on protein/lipid and DNA. Thus, mitochondrial and bioenergetic dysfunction leads to neuropathy.

Most knowledge about mechanisms of diabetic neuropathy was gained in genetically homogenous male rodents, while patients vary in sex, ethnicity and genetic background, age, and duration of diabetes. Thus, these factors should be considered in designing the individualized treatment plans for patients with diabetic neuropathy.

Hyperglycaemia-induced oxidative stress remains the most accepted mechanism for the progression of diabetes to diabetic neuropathy (Figure 5). The impaired glucose metabolism in diabetes leads to hypoxia and acidosis, which trigger other abnormalities responsible for mitochondrial and bioenergetic dysfunction by increasing ROS production to cause membrane hyperexcitability and reduction of ATP production. Treatment options with antioxidants have been investigated; none are satisfactory. Treatment which repairs nerves, in patients with diabetic neuropathy, has yet to be translated into clinical trials. Thus, future research must establish the most efficacious drug combinations on combating hyperglycaemia and oxidative stress for the prevention/treatment of diabetic neuropathy, in addition to explore the new mechanisms. Clinically, predictors and biomarkers need to be validated for both clinical trials and clinical practice.

## Conflicts of Interest

The authors declare that they have no conflicts of interest.

## Authors' Contributions

Lei Pang and Xin Lian contributed equally to this work.

## Acknowledgments

The authors' research was supported by the National Natural Science Foundation of Jilin Province (nos. 20190201061JC and 20200201321JC), the National Natural Science Foundation (no. 81970228), and the Educational Commission of Jilin Province of China (JJKH20201085KJ and JJKH20201047KJ).

## References

[1] B. C. Callaghan, H. T. Cheng, C. L. Stables, A. L. Smith, and E. L. Feldman, "Diabetic neuropathy: clinical manifestations and current treatments," *Lancet Neurology*, vol. 11, no. 6, pp. 521–534, 2012.

[2] A. J. Boulton, A. I. Vinik, J. C. Arezzo et al., "Diabetic neuropathies: a statement by the American Diabetes Association," *Diabetes Care*, vol. 28, no. 4, pp. 956–962, 2005.

[3] A. A. Little, J. L. Edwards, and E. L. Feldman, "Diabetic neuropathies," *Practical Neurology*, vol. 7, no. 2, pp. 82–92, 2007.

[4] A. I. Vinik, R. E. Maser, B. D. Mitchell, and R. Freeman, "Diabetic autonomic neuropathy," *Diabetes Care*, vol. 26, no. 5, pp. 1553–1579, 2003.

[5] A. I. Vinik and A. Mehrabyan, "Diabetic neuropathies," *The Medical Clinics of North America*, vol. 88, no. 4, pp. 947–999, 2004, xi.

[6] S. Tesfaye, N. Chaturvedi, S. E. Eaton et al., "Vascular risk factors and diabetic neuropathy," *The New England Journal of Medicine*, vol. 352, no. 4, pp. 341–350, 2005.

[7] M. Brownlee, "Biochemistry and molecular cell biology of diabetic complications," *Nature*, vol. 414, no. 6865, pp. 813–820, 2001.

[8] M. Brownlee, "The pathobiology of diabetic complications: a unifying mechanism," *Diabetes*, vol. 54, no. 6, pp. 1615–1625, 2005.

[9] E. L. Feldman, B. C. Callaghan, R. Pop-Busui et al., "Diabetic neuropathy," *Nature Reviews Disease Primers*, vol. 5, no. 1, 2019.

[10] E. L. Feldman, K. A. Nave, T. S. Jensen, and D. L. H. Bennett, "New horizons in diabetic neuropathy: mechanisms, bioenergetics, and pain," *Neuron*, vol. 93, no. 6, pp. 1296–1313, 2017.

[11] P. Fernyhough and J. McGavock, "Mechanisms of disease: mitochondrial dysfunction in sensory neuropathy and other complications in diabetes," *Handbook of Clinical Neurology*, vol. 126, pp. 353–377, 2014.

[12] M. Ott, V. Gogvadze, S. Orrenius, and B. Zhivotovsky, "Mitochondria, oxidative stress and cell death," *Apoptosis*, vol. 12, no. 5, pp. 913–922, 2007.

[13] A. M. Vincent, J. M. Hayes, L. L. McLean, A. Vivekanandan-Giri, S. Pennathur, and E. L. Feldman, "Dyslipidemia-induced neuropathy in mice: the role of oxLDL/LOX-1," *Diabetes*, vol. 58, no. 10, pp. 2376–2385, 2009.

[14] K. Guo, S. Elzinga, S. Eid et al., "Genome-wide DNA methylation profiling of human diabetic peripheral neuropathy in subjects with type 2 diabetes mellitus," *Epigenetics*, vol. 14, no. 8, pp. 766–779, 2019.

[15] S. K. R. Chowdhury, D. R. Smith, and P. Fernyhough, "The role of aberrant mitochondrial bioenergetics in diabetic neuropathy," *Neurobiology of Disease*, vol. 51, pp. 56–65, 2013.

[16] P. Fernyhough, "Mitochondrial dysfunction in diabetic neuropathy: a series of unfortunate metabolic events," *Current Diabetes Reports*, vol. 15, no. 11, 2015.

[17] A. E. Rumora, S. I. Lentz, L. M. Hinder et al., "Dyslipidemia impairs mitochondrial trafficking and function in sensory neurons," *The FASEB Journal*, vol. 32, no. 1, pp. 195–207, 2017.

[18] A. M. Vincent, J. L. Edwards, M. Sadidi, and E. L. Feldman, "The antioxidant response as a drug target in diabetic neuropathy," *Current Drug Targets*, vol. 9, no. 1, pp. 94–100, 2008.

[19] A. M. Vincent and E. L. Feldman, "New insights into the mechanisms of diabetic neuropathy," *Reviews in Endocrine & Metabolic Disorders*, vol. 5, no. 3, pp. 227–236, 2004.

[20] A. M. Vincent, J. W. Russell, P. Low, and E. L. Feldman, "Oxidative stress in the pathogenesis of diabetic neuropathy," *Endocrine Reviews*, vol. 25, no. 4, pp. 612–628, 2004.

[21] C. L. Rock, R. A. Jacob, and P. E. Bowen, "Update on the biological characteristics of the antioxidant Micronutrients," *Journal of the American Dietetic Association*, vol. 96, no. 7, pp. 693–702, 1996, quiz 703-704.

[22] K. H. Cheeseman and T. F. Slater, "An introduction to free radical biochemistry," *British Medical Bulletin*, vol. 49, no. 3, pp. 481–493, 1993.

[23] B. Halliwell and M. Whiteman, "Measuring reactive species and oxidative damage in vivo and in cell culture: how should you do it and what do the results mean?," *British Journal of Pharmacology*, vol. 142, no. 2, pp. 231–255, 2004.

[24] H. Shi, N. Noguchi, and E. Niki, "Comparative study on dynamics of antioxidative action of alpha-tocopheryl hydroquinone, ubiquinol, and alpha-tocopherol against lipid peroxidation," *Free Radical Biology & Medicine*, vol. 27, no. 3-4, pp. 334–346, 1999.

[25] M. Levine, S. C. Rumsey, R. Daruwala, J. B. Park, and Y. Wang, "Criteria and recommendations for vitamin C intake," *JAMA*, vol. 281, no. 15, pp. 1415–1423, 1999.

[26] A. C. Maritim, R. A. Sanders, and J. B. Watkins, "Diabetes, oxidative stress, and antioxidants: a review," *Journal of Biochemical and Molecular Toxicology*, vol. 17, no. 1, pp. 24–38, 2003.

[27] G. Sloan, P. Shillo, D. Selvarajah et al., "A new look at painful diabetic neuropathy," *Diabetes Research and Clinical Practice*, vol. 144, pp. 177–191, 2018.

[28] Diabetes Control and Complications Trial Research Group, "The effect of intensive treatment of diabetes on the development and progression of long-term complications in insulin-dependent diabetes mellitus," *The New England Journal of Medicine*, vol. 329, no. 14, pp. 977–986, 1993.

[29] UK Prospective Diabetes Study (UKPDS) Group, "Intensive blood-glucose control with sulphonylureas or insulin compared with conventional treatment and risk of complications in patients with type 2 diabetes (UKPDS 33)," *Lancet*, vol. 352, no. 9131, pp. 837–853, 1998.

[30] D. M. Nathan, "Long-term complications of diabetes mellitus," *The New England Journal of Medicine*, vol. 328, no. 23, pp. 1676–1685, 1993.

[31] N. B. Ruderman, J. R. Williamson, and M. Brownlee, "Glucose and diabetic vascular disease1," *The FASEB Journal*, vol. 6, no. 11, pp. 2905–2914, 1992.

[32] C. M. Clark Jr. and D. A. Lee, "Prevention and treatment of the complications of diabetes mellitus," *The New England Journal of Medicine*, vol. 332, no. 18, pp. 1210–1217, 1995.

[33] F. N. Ziyadeh, "The extracellular matrix in diabetic nephropathy," *American Journal of Kidney Diseases*, vol. 22, no. 5, pp. 736–744, 1993.

[34] B. C. Callaghan, K. A. Kerber, L. L. Lisabeth et al., "Role of neurologists and diagnostic tests on the management of distal symmetric polyneuropathy," *JAMA Neurology*, vol. 71, no. 9, pp. 1143–1149, 2014.

[35] D. C. Rosenberger, V. Blechschmidt, H. Timmerman, A. Wolff, and R. D. Treede, "Challenges of neuropathic pain: focus on diabetic neuropathy," *Journal of Neural Transmission (Vienna)*, vol. 127, no. 4, pp. 589–624, 2020.

[36] J. Scholz, D. C. Broom, D. H. Youn et al., "Blocking caspase activity prevents transsynaptic neuronal apoptosis and the loss of inhibition in lamina II of the dorsal horn after peripheral nerve injury," *The Journal of Neuroscience*, vol. 25, no. 32, pp. 7317–7323, 2005.

[37] J. N. Campbell and R. A. Meyer, "Mechanisms of neuropathic pain," *Neuron*, vol. 52, no. 1, pp. 77–92, 2006.

[38] A. May, "Chronic pain may change the structure of the brain," *Pain*, vol. 137, no. 1, pp. 7–15, 2008.

[39] S. K. Dunnigan, H. Ebadi, A. Breiner et al., "Conduction slowing in diabetic sensorimotor polyneuropathy," *Diabetes Care*, vol. 36, no. 11, pp. 3684–3690, 2013.

[40] S. Lupachyk, P. Watcho, R. Stavniichuk, H. Shevalye, and I. G. Obrosova, "Endoplasmic reticulum stress plays a key role in the pathogenesis of diabetic peripheral neuropathy," *Diabetes*, vol. 62, no. 3, pp. 944–952, 2013.

[41] R. S. Clements Jr., B. Vourganti, T. Kuba, S. J. Oh, and B. Darnell, "Dietary myo-inositol intake and peripheral nerve function in diabetic neuropathy," *Metabolism*, vol. 28, no. 4, pp. 477–483, 1979.

[42] J. G. Salway, L. Whitehead, J. A. Finnegan, A. Karunanayaka, D. Barnett, and R. B. Payne, "Effect of myo-inositol on peripheral-nerve function in diabetes," *Lancet*, vol. 2, no. 8103, pp. 1282–1284, 1978.

[43] D. Trachootham, W. Lu, M. A. Ogasawara, N. R. D. Valle, and P. Huang, "Redox regulation of cell survival," *Antioxidants & Redox Signaling*, vol. 10, no. 8, pp. 1343–1374, 2008.

[44] H. E. Poulsen, E. Specht, K. Broedbaek et al., "RNA modifications by oxidation: a novel disease mechanism?," *Free Radical Biology & Medicine*, vol. 52, no. 8, pp. 1353–1361, 2012.

[45] F. Giacco and M. Brownlee, "Oxidative stress and diabetic complications," *Circulation Research*, vol. 107, no. 9, pp. 1058–1070, 2010.

[46] B. Williams, "Angiotensin II, VEGF, and diabetic retinopathy," *Lancet*, vol. 351, no. 9105, pp. 837-838, 1998.

[47] B. C. Callaghan, A. A. Little, E. L. Feldman, and R. A. Hughes, "Enhanced glucose control for preventing and treating diabetic neuropathy," *Cochrane Database of Systematic Reviews*, vol. 6, no. 6, article CD007543, 2012.

[48] C. H. Gibbons and R. Freeman, "Treatment-induced diabetic neuropathy: a reversible painful autonomic neuropathy," *Annals of Neurology*, vol. 67, no. 4, pp. 534–541, 2010.

[49] C. H. Gibbons, "Treatment-induced neuropathy of diabetes," *Current Diabetes Reports*, vol. 17, no. 12, p. 127, 2017.

[50] Y. T. Hwang and G. Davies, "'Insulin neuritis' to 'treatment-induced neuropathy of diabetes': new name, same mystery," *Practical Neurology*, vol. 16, no. 1, pp. 53–55, 2016.

[51] R. Pop-Busui, A. J. M. Boulton, E. L. Feldman et al., "Diabetic neuropathy: a position statement by the American Diabetes Association," *Diabetes Care*, vol. 40, no. 1, pp. 136–154, 2016.

[52] L. Ang, M. Jaiswal, C. Martin, and R. Pop-Busui, "Glucose control and diabetic neuropathy: lessons from recent large clinical trials," *Current Diabetes Reports*, vol. 14, no. 9, p. 528, 2014.

[53] C. L. Martin, J. W. Albers, R. Pop-Busui, and for the DCCT/EDIC Research Group, "Neuropathy and related findings in the diabetes control and complications trial/epidemiology of diabetes interventions and complications study," *Diabetes Care*, vol. 37, no. 1, pp. 31–38, 2013.

[54] R. Pop-Busui, J. Lu, M. M. Brooks et al., "Impact of glycemic control strategies on the progression of diabetic peripheral neuropathy in the Bypass Angioplasty Revascularization Investigation 2 Diabetes (BARI 2D) Cohort," *Diabetes Care*, vol. 36, no. 10, pp. 3208–3215, 2013.

[55] G. M. Franklin, L. B. Kahn, J. Baxter, J. A. Marshall, and R. F. Hamman, "Sensory neuropathy in non-insulin-dependent diabetes mellitus. The San Luis Valley Diabetes Study," *American Journal of Epidemiology*, vol. 131, no. 4, pp. 633–643, 1990.

[56] J. Partanen, L. Niskanen, J. Lehtinen, E. Mervaala, O. Siitonen, and M. Uusitupa, "Natural history of peripheral neuropathy in patients with non-insulin-dependent diabetes mellitus," *The New England Journal of Medicine*, vol. 333, no. 2, pp. 89–94, 1995.

[57] P. J. Dyck, K. M. Kratz, J. L. Karnes et al., "The prevalence by staged severity of various types of diabetic neuropathy, retinopathy, and nephropathy in a population-based cohort: the Rochester Diabetic Neuropathy Study," *Neurology*, vol. 43, no. 4, pp. 817–824, 1993.

[58] A. J. M. Boulton, G. Knight, J. Drury, and J. D. Ward, "The prevalence of symptomatic, diabetic neuropathy in an insulin-treated population," *Diabetes Care*, vol. 8, no. 2, pp. 125–128, 1985.

[59] B. Fullerton, K. Jeitler, M. Seitz, K. Horvath, A. Berghold, and A. Siebenhofer, "Intensive glucose control versus conventional glucose control for type 1 diabetes mellitus," *Cochrane Database of Systematic Reviews*, vol. 2014, no. 2, article CD009122, 2014.

[60] J. W. Albers, W. H. Herman, R. Pop-Busui et al., "Effect of prior intensive insulin treatment during the Diabetes Control and Complications Trial (DCCT) on peripheral neuropathy in type 1 diabetes during the Epidemiology of Diabetes Interventions and Complications (EDIC) Study," *Diabetes Care*, vol. 33, no. 5, pp. 1090–1096, 2010.

[61] K. M. Pantalone, A. D. Misra-Hebert, T. M. Hobbs et al., "Effect of glycemic control on the Diabetes Complications Severity Index score and development of complications in people with newly diagnosed type 2 diabetes," *Journal of Diabetes*, vol. 10, no. 3, pp. 192–199, 2018.

[62] F. Ismail-Beigi, T. Craven, M. A. Banerji et al., "Effect of intensive treatment of hyperglycaemia on microvascular outcomes in type 2 diabetes: an analysis of the ACCORD randomised trial," *Lancet*, vol. 376, no. 9739, pp. 419–430, 2010.

[63] J. Calles-Escandon, L. C. Lovato, D. G. Simons-Morton et al., "Effect of intensive compared with standard glycemia treatment strategies on mortality by baseline subgroup characteristics: the Action to Control Cardiovascular Risk in Diabetes (ACCORD) trial," *Diabetes Care*, vol. 33, no. 4, pp. 721–727, 2010.

[64] The Action to Control Cardiovascular Risk in Diabetes Study Group, "Effects of intensive glucose lowering in type 2 diabetes," *The New England Journal of Medicine*, vol. 358, no. 24, pp. 2545–2559, 2008.

[65] S. Tesfaye, A. J. M. Boulton, P. J. Dyck et al., "Diabetic neuropathies: update on definitions, diagnostic criteria, estimation of severity, and treatments," *Diabetes Care*, vol. 33, no. 10, pp. 2285–2293, 2010.

[66] D. Roshandel, DCCT/EDIC Research Group, Z. Chen et al., "DNA methylation age calculators reveal association with diabetic neuropathy in type 1 diabetes," *Clinical Epigenetics*, vol. 12, no. 1, p. 52, 2020.

[67] M. Kobayashi and D. W. Zochodne, "Diabetic neuropathy and the sensory neuron: new aspects of pathogenesis and their treatment implications," *Journal of Diabetes Investigation*, vol. 9, no. 6, pp. 1239–1254, 2018.

[68] C. Girard, C. L. Will, J. Peng et al., "Post-transcriptional spliceosomes are retained in nuclear speckles until splicing completion," *Nature Communications*, vol. 3, no. 1, article 994, 2012.

[69] A. Qaseem, T. J. Wilt, D. Kansagara et al., "Hemoglobin A1cTargets for glycemic control with pharmacologic therapy for nonpregnant adults with type 2 diabetes mellitus: a guidance statement update from the American College of Physicians," *Annals of Internal Medicine*, vol. 168, no. 8, pp. 569–576, 2018.

[70] N. E. Cameron, M. A. Cotter, V. Archibald, K. C. Dines, and E. K. Maxfield, "Anti-oxidant and pro-oxidant effects on nerve conduction velocity, endoneurial blood flow and oxygen tension in non-diabetic and streptozotocin-diabetic rats," *Diabetologia*, vol. 37, no. 5, pp. 449–459, 1994.

[71] J. F. Turrens, "Mitochondrial formation of reactive oxygen species," *The Journal of Physiology*, vol. 552, no. 2, pp. 335–344, 2003.

[72] T. Nishikawa, D. Edelstein, X. L. du et al., "Normalizing mitochondrial superoxide production blocks three pathways of hyperglycaemic damage," *Nature*, vol. 404, no. 6779, pp. 787–790, 2000.

[73] D. A. Greene, J. C. Arezzo, and M. B. Brown, "Effect of aldose reductase inhibition on nerve conduction and morphometry

in diabetic neuropathy," *Neurology*, vol. 53, no. 3, pp. 580–591, 1999.

[74] T. Behl, I. Kaur, and A. Kotwani, "Implication of oxidative stress in progression of diabetic retinopathy," *Survey of Ophthalmology*, vol. 61, no. 2, pp. 187–196, 2016.

[75] J. M. Forbes, M. T. Coughlan, and M. E. Cooper, "Oxidative stress as a major culprit in kidney disease in diabetes," *Diabetes*, vol. 57, no. 6, pp. 1446–1454, 2008.

[76] S. Javed, I. N. Petropoulos, U. Alam, and R. A. Malik, "Treatment of painful diabetic neuropathy," *Therapeutic Advances in Chronic Disease*, vol. 6, no. 1, pp. 15–28, 2014.

[77] S. P. Wolff and R. T. Dean, "Glucose autoxidation and protein modification. The potential role of 'autoxidative glycosylation' in diabetes," *The Biochemical Journal*, vol. 245, no. 1, pp. 243–250, 1987.

[78] K. J. Wells-Knecht, D. V. Zyzak, J. E. Litchfield, S. R. Thorpe, and J. W. Baynes, "Mechanism of autoxidative glycosylation: identification of glyoxal and arabinose as intermediates in the autoxidative modification of proteins by glucose," *Biochemistry*, vol. 34, pp. 3702–3709, 2002.

[79] M. X. Fu, K. J. Wells-Knecht, J. A. Blackledge, T. J. Lyons, S. R. Thorpe, and J. W. Baynes, "Glycation, glycoxidation, and cross-linking of collagen by glucose. Kinetics, mechanisms, and inhibition of late stages of the Maillard reaction," *Diabetes*, vol. 43, no. 5, pp. 676–683, 1994.

[80] S. Chetyrkin, M. Mathis, V. Pedchenko et al., "Glucose autoxidation induces functional damage to proteins via modification of critical arginine residues," *Biochemistry*, vol. 50, no. 27, pp. 6102–6112, 2011.

[81] A. W. Stitt, Y. M. Li, T. A. Gardiner, R. Bucala, D. B. Archer, and H. Vlassara, "Advanced glycation end products (AGEs) co-localize with AGE receptors in the retinal vasculature of diabetic and of AGE-infused rats," *The American Journal of Pathology*, vol. 150, no. 2, pp. 523–531, 1997.

[82] K. Horie, T. Miyata, K. Maeda et al., "Immunohistochemical colocalization of glycoxidation products and lipid peroxidation products in diabetic renal glomerular lesions. Implication for glycoxidative stress in the pathogenesis of diabetic nephropathy," *The Journal of Clinical Investigation*, vol. 100, no. 12, pp. 2995–3004, 1997.

[83] R. Ramasamy and I. J. Goldberg, "Aldose reductase and cardiovascular diseases, creating human-like diabetic complications in an experimental model," *Circulation Research*, vol. 106, no. 9, pp. 1449–1458, 2010.

[84] H. G. Hers, "The mechanism of the transformation of glucose in fructose in the seminal vesicles," *Biochimica et Biophysica Acta*, vol. 22, no. 1, pp. 202-203, 1956.

[85] K. M. Bohren, C. E. Grimshaw, and K. H. Gabbay, "Catalytic effectiveness of human aldose reductase. Critical role of C-terminal domain," *The Journal of Biological Chemistry*, vol. 267, no. 29, pp. 20965–20970, 1992.

[86] R. K. Vikramadithyan, Y. Hu, H. L. Noh et al., "Human aldose reductase expression accelerates diabetic atherosclerosis in transgenic mice," *The Journal of Clinical Investigation*, vol. 115, no. 9, pp. 2434–2443, 2005.

[87] M. A. Stewart, W. R. Sherman, M. M. Kurien, G. I. Moonsammy, and M. Wisgerhof, "Polyol accumulations in nervous tissue of rats with experimental diabetes and galactosaemia," *Journal of Neurochemistry*, vol. 14, no. 11, pp. 1057–1066, 1967.

[88] K. Uehara, S. I. Yamagishi, S. Otsuki, S. Chin, and S. Yagihashi, "Effects of polyol pathway hyperactivity on protein kinase C activity, nociceptive peptide expression, and neuronal structure in dorsal root ganglia in diabetic mice," *Diabetes*, vol. 53, no. 12, pp. 3239–3247, 2004.

[89] J. H. Mayer and D. R. Tomlinson, "Prevention of defects of axonal transport and nerve conduction velocity by oral administration of myo-inositol or an aldose reductase inhibitor in streptozotocin-diabetic rats," *Diabetologia*, vol. 25, no. 5, pp. 433–438, 1983.

[90] D. Finegold, S. A. Lattimer, S. Nolle, M. Bernstein, and D. A. Greene, "Polyol pathway activity and myo-inositol metabolism. A suggested relationship in the pathogenesis of diabetic neuropathy," *Diabetes*, vol. 32, no. 11, pp. 988–992, 1983.

[91] R. L. Engerman, T. S. Kern, and M. E. Larson, "Nerve conduction and aldose reductase inhibition during 5 years of diabetes or galactosaemia in dogs," *Diabetologia*, vol. 37, no. 2, pp. 141–144, 1994.

[92] A. G. Demaine, "Polymorphisms of the aldose reductase gene and susceptibility to diabetic microvascular complications," *Current Medicinal Chemistry*, vol. 10, no. 15, pp. 1389–1398, 2003.

[93] K. Thamotharampillai, A. K. F. Chan, B. Bennetts et al., "Decline in neurophysiological function after 7 years in an adolescent diabetic cohort and the role of aldose reductase gene polymorphisms," *Diabetes Care*, vol. 29, no. 9, pp. 2053–2057, 2006.

[94] D. A. McClain, "Hexosamines as mediators of nutrient sensing and regulation in diabetes," *Journal of Diabetes and its Complications*, vol. 16, no. 1, pp. 72–80, 2002.

[95] D. A. McClain, W. A. Lubas, R. C. Cooksey et al., "Altered glycan-dependent signaling induces insulin resistance and hyperleptinemia," *Proceedings of the National Academy of Sciences of the United States of America*, vol. 99, no. 16, pp. 10695–10699, 2002.

[96] M. G. Buse, "Hexosamines, insulin resistance, and the complications of diabetes: current status," *American Journal of Physiology. Endocrinology and Metabolism*, vol. 290, no. 1, pp. E1–E8, 2006.

[97] S. Marshall, V. Bacote, and R. R. Traxinger, "Discovery of a metabolic pathway mediating glucose-induced desensitization of the glucose transport system. Role of hexosamine biosynthesis in the induction of insulin resistance," *The Journal of Biological Chemistry*, vol. 266, pp. 4706–4712, 1991.

[98] X.-L. Du, D. Edelstein, L. Rossetti et al., "Hyperglycemia-induced mitochondrial superoxide overproduction activates the hexosamine pathway and induces plasminogen activator inhibitor-1 expression by increasing Sp1 glycosylation," *Proceedings of the National Academy of Sciences of the United States of America*, vol. 97, no. 22, pp. 12222–12226, 2000.

[99] L. K. Kreppel, M. A. Blomberg, and G. W. Hart, "Dynamic glycosylation of nuclear and cytosolic proteins. Cloning and characterization of a unique O-GlcNAc transferase with multiple tetratricopeptide repeats," *The Journal of Biological Chemistry*, vol. 272, no. 14, pp. 9308–9315, 1997.

[100] W. A. Lubas, D. W. Frank, M. Krause, and J. A. Hanover, "O-linked GlcNAc transferase is a conserved nucleocytoplasmic protein containing tetratricopeptide repeats," *The Journal of Biological Chemistry*, vol. 272, no. 14, pp. 9316–9324, 1997.

[101] F. Andreozzi, C. D'Alessandris, M. Federici et al., "Activation of the hexosamine pathway leads to phosphorylation of insulin receptor substrate-1 on Ser307 and Ser612 and impairs the phosphatidylinositol 3-kinase/Akt/mammalian target of rapamycin insulin biosynthetic pathway in RIN pancreatic

beta-cells," *Endocrinology*, vol. 145, no. 6, pp. 2845–2857, 2004.

[102] M. Federici, R. Menghini, A. Mauriello et al., "Insulin-dependent activation of endothelial nitric oxide synthase is impaired by O-linked glycosylation modification of signaling proteins in human coronary endothelial cells," *Circulation*, vol. 106, no. 4, pp. 466–472, 2002.

[103] M. G. Buse, K. A. Robinson, B. A. Marshall, R. C. Hresko, and M. M. Mueckler, "Enhanced O-GlcNAc protein modification is associated with insulin resistance in GLUT1-overexpressing muscles," *American Journal of Physiology. Endocrinology and Metabolism*, vol. 283, no. 2, pp. E241–E250, 2002.

[104] M. G. Buse, K. A. Robinson, T. W. Gettys, E. G. McMahon, and E. A. Gulve, "Increased activity of the hexosamine synthesis pathway in muscles of insulin-resistant ob/ob mice," *The American Journal of Physiology*, vol. 272, 6 Part 1, pp. E1080–E1088, 1997.

[105] H. Yki-Jarvinen, M. C. Daniels, A. Virkamaki, S. Makimattila, R. A. DeFronzo, and D. McClain, "Increased glutamine:fructose-6-phosphate amidotransferase activity in skeletal muscle of patients with NIDDM," *Diabetes*, vol. 45, no. 3, pp. 302–307, 1996.

[106] M. J. J. Pouwels, P. N. Span, C. J. Tack et al., "Muscle uridine diphosphate-hexosamines do not decrease despite correction of hyperglycemia-induced insulin resistance in type 2 diabetes," *The Journal of Clinical Endocrinology and Metabolism*, vol. 87, no. 11, pp. 5179–5184, 2002.

[107] M. J. J. Pouwels, C. J. Tack, P. N. Span et al., "Role of hexosamines in insulin resistance and nutrient sensing in human adipose and muscle tissue," *The Journal of Clinical Endocrinology and Metabolism*, vol. 89, no. 10, pp. 5132–5137, 2004.

[108] V. Kolm-Litty, U. Sauer, A. Nerlich, R. Lehmann, and E. D. Schleicher, "High glucose-induced transforming growth factor beta1 production is mediated by the hexosamine pathway in porcine glomerular mesangial cells," *The Journal of Clinical Investigation*, vol. 101, no. 1, pp. 160–169, 1998.

[109] T. Inoguchi, R. Battan, E. Handler, J. R. Sportsman, W. Heath, and G. L. King, "Preferential elevation of protein kinase C isoform beta II and diacylglycerol levels in the aorta and heart of diabetic rats: differential reversibility to glycemic control by islet cell transplantation," *Proceedings of the National Academy of Sciences of the United States of America*, vol. 89, no. 22, pp. 11059–11063, 1992.

[110] T. Shiba, T. Inoguchi, J. R. Sportsman, W. F. Heath, S. Bursell, and G. L. King, "Correlation of diacylglycerol level and protein kinase C activity in rat retina to retinal circulation," *American Journal of Physiology-Endocrinology and Metabolism*, vol. 265, no. 5, pp. E783–E793, 1993.

[111] N. Ahmed, "Advanced glycation endproducts–role in pathology of diabetic complications," *Diabetes Research and Clinical Practice*, vol. 67, no. 1, pp. 3–21, 2005.

[112] C. Toth, L. L. Rong, C. Yang et al., "Receptor for advanced glycation end products (RAGEs) and experimental diabetic neuropathy," *Diabetes*, vol. 57, no. 4, pp. 1002–1017, 2008.

[113] X. Gallet, B. Charloteaux, A. Thomas, and R. Brasseur, "A fast method to predict protein interaction sites from sequences," *Journal of Molecular Biology*, vol. 302, no. 4, pp. 917–926, 2000.

[114] D. Yao, T. Taguchi, T. Matsumura et al., "High glucose increases angiopoietin-2 transcription in microvascular endothelial cells through methylglyoxal modification of mSin3A," *The Journal of Biological Chemistry*, vol. 282, no. 42, pp. 31038–31045, 2007.

[115] R. Ramasamy, S. F. Yan, and A. M. Schmidt, "Arguing for the motion: yes, RAGE is a receptor for advanced glycation end-products," *Molecular Nutrition & Food Research*, vol. 51, no. 9, pp. 1111–1115, 2007.

[116] A. Goldin, J. A. Beckman, A. M. Schmidt, and M. A. Creager, "Advanced glycation end products: sparking the development of diabetic vascular injury," *Circulation*, vol. 114, no. 6, pp. 597–605, 2006.

[117] A. Bierhaus, K. M. Haslbeck, P. M. Humpert et al., "Loss of pain perception in diabetes is dependent on a receptor of the immunoglobulin superfamily," *The Journal of Clinical Investigation*, vol. 114, no. 12, pp. 1741–1751, 2004.

[118] A. Abaci, A. Oguzhan, S. Kahraman et al., "Effect of diabetes mellitus on formation of coronary collateral vessels," *Circulation*, vol. 99, no. 17, pp. 2239–2242, 1999.

[119] P. Geraldes and G. L. King, "Activation of protein kinase C isoforms and its impact on diabetic complications," *Circulation Research*, vol. 106, no. 8, pp. 1319–1331, 2010.

[120] G. Pugliese, F. Pricci, F. Pugliese et al., "Mechanisms of glucose-enhanced extracellular matrix accumulation in rat glomerular mesangial cells," *Diabetes*, vol. 43, no. 3, pp. 478–490, 1994.

[121] K. K. Yerneni, W. Bai, B. V. Khan, R. M. Medford, and R. Natarajan, "Hyperglycemia-induced activation of nuclear transcription factor kappaB in vascular smooth muscle cells," *Diabetes*, vol. 48, no. 4, pp. 855–864, 1999.

[122] P. A. Craven, R. K. Studer, J. Felder, S. Phillips, and F. R. DeRubertis, "Nitric oxide inhibition of transforming growth factor-beta and collagen synthesis in mesangial cells," *Diabetes*, vol. 46, no. 4, pp. 671–681, 1997.

[123] J. S. Christiansen, J. Gammelgaard, M. Frandsen, and H. H. Parving, "Increased kidney size, glomerular filtration rate and renal plasma flow in short-term insulin-dependent diabetics," *Diabetologia*, vol. 20, no. 4, pp. 451–456, 1981.

[124] T. H. Hostetter, J. L. Troy, and B. M. Brenner, "Glomerular hemodynamics in experimental diabetes mellitus," *Kidney International*, vol. 19, no. 3, pp. 410–415, 1981.

[125] J. Nakamura, K. Kato, Y. Hamada et al., "A protein kinase C-beta-selective inhibitor ameliorates neural dysfunction in streptozotocin-induced diabetic rats," *Diabetes*, vol. 48, no. 10, pp. 2090–2095, 1999.

[126] N. E. Cameron, M. A. Cotter, A. M. Jack, M. D. Basso, and T. C. Hohman, "Protein kinase C effects on nerve function, perfusion, Na(+), K(+)-ATPase activity and glutathione content in diabetic rats," *Diabetologia*, vol. 42, no. 9, pp. 1120–1130, 1999.

[127] A. I. Vinik, V. Bril, P. Kempler et al., "Treatment of symptomatic diabetic peripheral neuropathy with the protein kinase C $\beta$-inhibitor ruboxistaurin mesylate during a 1-year, randomized, placebo-controlled, double-blind clinical trial," *Clinical Therapeutics*, vol. 27, no. 8, pp. 1164–1180, 2005.

[128] D. Bansal, Y. Badhan, K. Gudala, and F. Schifano, "Ruboxistaurin for the treatment of diabetic peripheral neuropathy: a systematic review of randomized clinical trials," *Diabetes and Metabolism Journal*, vol. 37, no. 5, pp. 375–384, 2013.

[129] M. Tavakoli, I. N. Petropoulos, and R. A. Malik, "Corneal confocal microscopy to assess diabetic neuropathy: an eye on the foot," *Journal of Diabetes Science and Technology*, vol. 7, no. 5, pp. 1179–1189, 2013.

[130] G. Lauria, D. R. Cornblath, O. Johansson et al., "EFNS guidelines on the use of skin biopsy in the diagnosis of peripheral neuropathy," *European Journal of Neurology*, vol. 12, no. 10, pp. 747–758, 2005.

[131] B. Dabiri, S. Kampusch, S. H. Geyer et al., "High-resolution episcopic imaging for visualization of dermal arteries and nerves of the auricular cymba conchae in humans," *Frontiers in Neuroanatomy*, vol. 14, 2020.

[132] Technology VUo, *Novel electric impulses relieve the pain*, ScienceDaily, 2020.

[133] G. M. Sanchez-Ramirez, N. L. Caram-Salas, H. I. Rocha-Gonzalez et al., "Benfotiamine relieves inflammatory and neuropathic pain in rats," *European Journal of Pharmacology*, vol. 530, no. 1-2, pp. 48–53, 2006.

[134] H. Stracke, W. Gaus, U. Achenbach, K. Federlin, and R. G. Bretzel, "Benfotiamine in diabetic polyneuropathy (BENDIP): results of a randomised, double blind, placebo-controlled clinical study," *Experimental and Clinical Endocrinology & Diabetes*, vol. 116, no. 10, pp. 600–605, 2008.

[135] D. Ziegler, A. Ametov, A. Barinov et al., "Oral treatment With -Lipoic Acid Improves Symptomatic Diabetic Polyneuropathy: The SYDNEY 2 trial," *Diabetes Care*, vol. 29, no. 11, pp. 2365–2370, 2006.

[136] D. Ziegler, L. Movsesyan, B. Mankovsky, I. Gurieva, Z. Abylaiuly, and I. Strokov, "Treatment of symptomatic polyneuropathy with actovegin in type 2 diabetic patients," *Diabetes Care*, vol. 32, no. 8, pp. 1479–1484, 2009.

[137] A. S. Ametov, A. Barinov, P. J. Dyck et al., "The sensory symptoms of diabetic polyneuropathy are improved with alpha-lipoic acid: the SYDNEY trial," *Diabetes Care*, vol. 26, no. 3, pp. 770–776, 2003.

[138] N. Papanas and D. Ziegler, "Efficacy of $\alpha$-lipoic acid in diabetic neuropathy," *Expert Opinion on Pharmacotherapy*, vol. 15, no. 18, pp. 2721–2731, 2014.

[139] A. Negre-Salvayre, C. Coatrieux, C. Ingueneau, and R. Salvayre, "Advanced lipid peroxidation end products in oxidative damage to proteins. Potential role in diseases and therapeutic prospects for the inhibitors," *British Journal of Pharmacology*, vol. 153, no. 1, pp. 6–20, 2008.

[140] X. Du, D. Edelstein, and M. Brownlee, "Oral benfotiamine plus alpha-lipoic acid normalises complication-causing pathways in type 1 diabetes," *Diabetologia*, vol. 51, no. 10, pp. 1930–1932, 2008.

[141] F. Bertolotto and A. Massone, "Combination of alpha lipoic acid and superoxide dismutase leads to physiological and symptomatic improvements in diabetic neuropathy," *Drugs in R&D*, vol. 12, no. 1, pp. 29–34, 2012.

[142] J. Shakher and M. J. Stevens, "Update on the management of diabetic polyneuropathies," *Diabetes, Metabolic Syndrome and Obesity: Targets and Therapy*, vol. 4, pp. 289–305, 2011.

[143] S. Yagihashi, S. I. Yamagishi, R. Wada Ri et al., "Neuropathy in diabetic mice overexpressing human aldose reductase and effects of aldose reductase inhibitor," *Brain*, vol. 124, no. 12, pp. 2448–2458, 2001.

[144] T. Kawai, I. Takei, M. Tokui et al., "Effects of epalrestat, an aldose reductase inhibitor, on diabetic peripheral neuropathy in patients with type 2 diabetes, in relation to suppression of Nε-carboxymethyl lysine," *Journal of Diabetes and its Complications*, vol. 24, no. 6, pp. 424–432, 2010.

[145] A. J. M. Boulton, P. Kempler, A. Ametov, and D. Ziegler, "Whither pathogenetic treatments for diabetic polyneuropathy?," *Diabetes/Metabolism Research and Reviews*, vol. 29, no. 5, pp. 327–333, 2013.

[146] G. Winkler, B. Pal, E. Nagybeganyi, I. Ory, M. Porochnavec, and P. Kempler, "Effectiveness of different benfotiamine dosage regimens in the treatment of painful diabetic neuropathy," *Arzneimittel-Forschung*, vol. 49, no. 3, pp. 220–224, 1999.

[147] E. Haupt, H. Ledermann, and W. Kopcke, "Benfotiamine in the treatment of diabetic polyneuropathy–a three-week randomized, controlled pilot study (BEDIP study)," *International Journal of Clinical Pharmacology and Therapeutics*, vol. 43, no. 2, pp. 71–77, 2005.

[148] S. Dewanjee, S. Das, A. K. Das et al., "Molecular mechanism of diabetic neuropathy and its pharmacotherapeutic targets," *European Journal of Pharmacology*, vol. 833, pp. 472–523, 2018.

[149] A. S. Grewal, S. Bhardwaj, D. Pandita, V. Lather, and B. S. Sekhon, "Updates on aldose reductase inhibitors for management of diabetic complications and non-diabetic diseases," *Mini Reviews in Medicinal Chemistry*, vol. 16, no. 2, pp. 120–162, 2015.

[150] N. E. Cameron, Z. Tuck, L. McCabe, and M. A. Cotter, "Effect of the hydroxyl radical scavenger, dimethylthiourea, on peripheral nerve tissue perfusion, conduction velocity and nociception in experimental diabetes," *Diabetologia*, vol. 44, no. 9, pp. 1161–1169, 2001.

[151] J. L. Edwards, A. M. Vincent, H. T. Cheng, and E. L. Feldman, "Diabetic neuropathy: mechanisms to management," *Pharmacology & Therapeutics*, vol. 120, no. 1, pp. 1–34, 2008.

[152] A. A. F. Sima, V. Bril, V. Nathaniel et al., "Regeneration and repair of myelinated fibers in sural-nerve biopsy specimens from patients with diabetic neuropathy treated with sorbinil," *The New England Journal of Medicine*, vol. 319, no. 9, pp. 548–555, 1988.

[153] P. D. O'Brien, S. A. Sakowski, and E. L. Feldman, "Mouse models of diabetic neuropathy," *ILAR Journal*, vol. 54, no. 3, pp. 259–272, 2014.

[154] A. Tappe-Theodor and R. Kuner, "Studying ongoing and spontaneous pain in rodents–challenges and opportunities," *The European Journal of Neuroscience*, vol. 39, no. 11, pp. 1881–1890, 2014.